



**SZKOŁA DOKTORSKA
BioMedChem**

Uniwersytetu Łódzkiego
i Instytutów Polskiej
Akademii Nauk w Łodzi



Mateusz Maksymilian Urbaniak

Praca doktorska:

**Proregeneracyjne,
przeciwdrobnoustrojowe
i immunomodulujące właściwości
piomelaniny *Pseudomonas aeruginosa***

Doctoral thesis:

Pro-regenerative, antimicrobial and
immunomodulatory properties of
Pseudomonas aeruginosa pyomelanin

- Promotor/Supervisor
prof. dr hab. Magdalena Mikołajczyk-Chmiela
Katedra Immunologii i Biologii Infekcyjnej
Wydział Biologii i Ochrony Środowiska
Uniwersytet Łódzki
- Promotor pomocniczy/Assistant Supervisor
dr Karolina Rudnicka, prof. Uł
Katedra Immunologii i Biologii Infekcyjnej
Wydział Biologii i Ochrony Środowiska
Uniwersytet Łódzki

Łódź, 2024

SPIS TREŚCI

Źródła finansowania	4
Wykaz publikacji będących podstawą rozprawy doktorskiej	6
Wykaz pozostałych publikacji.....	8
Wykaz zgłoszeń patentowych.....	11
Udział w projektach badawczych	13
Stáže badawcze	16
Streszczenie w języku polskim.....	18
Streszczenie w języku angielskim.....	21
Wykaz stosowanych skrótów	24
Wprowadzenie	28
Charakterystyka bakterii <i>Pseudomonas aeruginosa</i> oraz biomedyczny potencjał barwników i metabolitów tych drobnoustrojów	29
Charakterystyka piomelaniny produkowanej przez bakterie <i>Pseudomonas aeruginosa</i>	36
<i>Helicobacter pylori</i> – fizjologia, czynniki wirulancji i patogeneza.....	46
Biologia tkanki kostnej i poszukiwanie nowych stymulatorów procesów osteoindukcyjnych.....	52
Założenia i cele pracy.....	56
Materiały i metody.....	59
Materiały.....	60
Metody.....	61
Publikacje wchodzące w skład rozprawy doktorskiej.....	64
Podsumowanie prac wchodzących w skład rozprawy doktorskiej.....	65
Dyskusja.....	75
Wnioski szczegółowe i wniosek końcowy	82
Literatura	84
Oświadczenia współautorów o udziale w publikacjach	105

Źródła finansowania



Projekt "Wielofunkcyjne kompozyty aktywne biologicznie do zastosowań w medycynie regeneracyjnej układu kostnego" (POIR.04.04.00-00-16D7/18) realizowany w ramach programu TEAM - NET Fundacji na rzecz Nauki Polskiej finansowanego przez Unię Europejską z Europejskiego Funduszu Rozwoju Regionalnego.



Projekt „PioMelaCure – piomelaninowy preparat wspomagający terapię powszechnych zakażeń *H. pylori*” prowadzony w ramach konkursu „Inkubator Innowacyjności +” realizowany w ramach projektu pozakonkursowego „Wsparcie zarządzania badaniami naukowymi i komercjalizacja wyników prac B+R w jednostkach naukowych i przedsiębiorstwach” w ramach Programu Operacyjnego Inteligentny Rozwój 2014-2020 (Działanie 4.4).



Projekt „PyoBattery - piomelaniowe elektrolity i elektrody do zastosowań w bateriach elektrycznych” prowadzony w ramach konkursu „Inkubator Innowacyjności 4.0” realizowany w ramach projektu pozakonkursowego „Wsparcie zarządzania badaniami naukowymi i komercjalizacja wyników prac B+R w jednostkach naukowych i przedsiębiorstwach” w ramach Programu Operacyjnego Inteligentny Rozwój 2014-2020 (Działanie 4.4).

**Wykaz publikacji
będących podstawą
rozprawy doktorskiej**

- P.I. *In Vitro* and *In Vivo* Biocompatibility of Natural and Synthetic *Pseudomonas aeruginosa* Pyomelanin for Potential Biomedical Applications**
Urbaniak M. M., Gazińska M., Rudnicka K., Płociński P., Nowak M., Chmiela M.
International Journal of Molecular Sciences, 2023, 24, 7846.
DOI: 10.3390/ijms24097846
IF₂₀₂₃/MNiSW = 5,6/140
- P.II. Can Pyomelanin Produced by *Pseudomonas aeruginosa* Promote the Regeneration of Gastric Epithelial Cells and Enhance *Helicobacter pylori* Phagocytosis?**
Urbaniak M. M., Rudnicka K., Gościński G., Chmiela M.
International Journal of Molecular Sciences, 2023, 24, 13911.
DOI: 10.3390/ijms241813911
IF₂₀₂₃/MNiSW = 5,6/140
- P.III. Exploring the Osteoinductive Potential of Bacterial Pyomelanin Derived from *Pseudomonas aeruginosa* on Human Osteoblasts Model**
Urbaniak M. M., Rudnicka K., Płociński P., Chmiela M.
International Journal of Biological Macromolecules, 2024.
Manuskrypt w recenzji
- P.IV. Bioactive Materials for Bone Regeneration: Biomolecules and Delivery Systems**
Szwed-Georgiou A., Płociński P., Kupikowska-Stobba B., Urbaniak M. M., Rusek-Wala P., Szustakiewicz K., Piszko P., Krupa A., Biernat M., Gazińska M., Kasprzak M., Nawrotek K., Mira N. P., Rudnicka K.
ACS Biomaterials Science & Engineering, 2023, 9, 5222–5254.
DOI: 10.1021/acsbmaterials.3c00609
IF₂₀₂₃/MNiSW = 5,8/140

Łączny IF oraz sumaryczna liczba punktów MNiSW:

17/420

Wykaz pozostałych publikacji

- 1. Measurement Methodology toward Determination of Structure-Property Relationships in Acrylic Hydrogels with Starch and Nanogold Designed for Biomedical Applications**
Drabczyk A., Kudłacik-Kramarczyk S., Tyliczszak B., Rudnicka K., Urbaniak M. M., Michlewska S., Królczyk J. B., Gajda P., Pielichowski K.
Measurement, 2020, 156, 107608.
DOI: 10.1016/j.measurement.2020.107608
IF₂₀₂₀/MNiSW = 3,927/200
- 2. Composites Based on Hydroxyapatite and Whey Protein Isolate for Applications in Bone Regeneration**
Słota D., Głąb M., Tyliczszak B., Douglas T., Rudnicka K., Miernik K., Urbaniak M. M., Rusek-Wala P., Sobczak-Kupiec A.
Materials, 2021, 14, 2317.
DOI: 10.3390/ma14092317
IF₂₀₂₁/MNiSW = 3,748/140
- 3. Dual Modification of Porous Ca-P/PLA Composites with APTES and Alendronate Improves Their Mechanical Strength and Cytobiocompatibility towards Human Osteoblasts**
Biernat M., Szwed-Georgiou A., Rudnicka K., Płociński P., Pagacz J., Tymowicz-Grzyb P., Woźniak A., Włodarczyk M., Urbaniak M. M., Krupa A., Rusek-Wala P., Karska N., Rodziewicz-Motowidło S.
International Journal of Molecular Sciences, 2022, 23, 14315.
DOI: 10.3390/ijms232214315
IF₂₀₂₂/MNiSW = 5,6/140
- 4. Physicochemical and Biological Analysis of Composite Biomaterials Containing Hydroxyapatite for Biological Applications**
Bańkosz M., Urbaniak M. M., Szwed A., Rudnicka K., Włodarczyk M., Drabczyk A., Kudłacik-Kramarczyk S., Tyliczszak B., Sobczak-Kupiec A.
Journal of Biomedical Materials Research Part B: Applied Biomaterials, 2023, 12, 2077-2088.
DOI: 10.1002/jbm.b.35309
IF₂₀₂₃/MNiSW = 3,4/140

- 6. Effect of Calcination and Ion Substitution on Physicochemical and Biological Properties of Nanohydroxyapatite for Bone Tissue Engineering Applications**
Tymowicz-Grzyb P., Gerle A., Szterner P., Włodarczyk M., Płociński P., Urbaniak M. M., Rudnicka K., Biernat M.
Scientific Reports, 2023, 13, 15384.
DOI: 10.1038/s41598-023-42271-2
IF₂₀₂₃/MNiSW = 4,6/140
- 7. Clindamycin-Loaded Nanosized Calcium Phosphates Powders as a Carrier of Active Substances**
Słota D., Pięta K., Florkiewicz W., Jampilek J., Tomala A., Urbaniak M. M., Tomaszewska A., Rudnicka K., Sobczak-Kupiec A.
Nanomaterials, 2023, 13, 1469.
DOI: 10.3390/nano13091469
IF₂₀₂₃/MNiSW = 5,3/100
- 8. Crosslinked Hybrid Polymer/Ceramic Composite Coatings for Controlled Release of Clindamycin**
Słota D., Niziołek K., Urbaniak M. M., Tomaszewska A., Florkiewicz W., Sobczak-Kupiec A.
Biomaterials Science
Manuskrypt w recenzji

Łączny IF oraz sumaryczna liczba punktów MNiSW wszystkich publikacji:

43,575/1280

Wykaz zgłoszeń patentowych

1. Podłoże minimalne PMM d o hodowli bakterii *Pseudomonas aeruginosa* i izolacji piomelaniny

Urbaniak M. M., Rudnicka K., Płociński P., Chmiela M.

Nr zgłoszenia: P.438865

Data zgłoszenia: 2 września 2021

2. Sposób otrzymywania piomelaniny izolowanej z bakterii *Pseudomonas aeruginosa* metodą chloroformową oraz zastosowanie piomelaniny izolowanej z bakterii *Pseudomonas aeruginosa* metodą chloroformową jako środka immunomodulującego, bakteriobójczego, proregeneracyjnego oraz jako suplementu diety i żywności specjalnego przeznaczenia medycznego w celu ograniczenia zakażenia bakteriami *Helicobacter pylori*

Urbaniak M. M., Rudnicka K., Płociński P., Gonciarz W., Chmiela M.

Nr zgłoszenia: P.438866

Data zgłoszenia: 2 września 2021

Udział w projektach badawczych

- 1.** **Tytuł:** PyoBattery - piomelaniowe elektrolity i elektrody do zastosowań w bateriach elektrycznych
Rodzaj projektu: B+R
Rola w projekcie: kierownik naukowy, wykonawca
Okres realizacji: 01.10.2022 – 31.07.2023 r.
Jednostka finansująca: Inkubator Innowacyjności 4.0, Konsorcjum Uniwersytetu Łódzkiego, Uniwersytetu Medycznego w Łodzi i Uniwersytetu Warmińsko-Mazurskiego w Olsztynie w ramach środków Ministerstwa Nauki i Edukacji.
- 2.** **Tytuł:** PioMelaCure – piomelaninowy preparat wspomagający terapię powszechnych zakażeń *H. pylori*
Rodzaj projektu: B+R
Rola w projekcie: kierownik
Okres realizacji: 01.07.2019 – 01.04.2020 r.
Jednostka finansująca: Inkubator Innowacyjności +, Konsorcjum Uniwersytetu Łódzkiego, Uniwersytetu Medycznego w Łodzi i Uniwersytetu Warmińsko-Mazurskiego w Olsztynie w ramach środków Ministerstwa Nauki i Szkolnictwa Wyższego.
- 3.** **Tytuł:** Piomelaniowe baterie elektryczne – PyoBattery
Rodzaj projektu: Proof of concept
Rola w projekcie: kierownik
Okres realizacji: 15.03.2022 – 01.01.2023 r.
Jednostka finansująca: Nowa Ziemia Obiecana Seed Fund, RDS Fund sp. z o.o w ramach konkursu Narodowego Centrum Badań i Rozwoju.
- 4.** **Tytuł:** Wielofunkcyjne kompozyty aktywne biologicznie do zastosowań w medycynie regeneracyjnej układu kostnego
Konsorcjanci: Politechnika Wrocławska, Politechnika Krakowska, Uniwersytet Łódzki, Sieć Badawcza Łukasiewicz
Rodzaj projektu: B+R
Rola w projekcie: doktorant – stypendysta
Okres realizacji: 01.10.2019 – 30.09.2023 r.
Jednostka finansująca: Fundacja na Rzecz Nauki Polskiej, konkurs TEAM-NET finansowany z środków Unii Europejskiej (Działanie 4.4 POIR - Zwiększanie potencjału kadrowego, sektora B+R, Inteligentny Rozwój).
- 5.** **Tytuł:** Kompleksowa ocena biogodności i bioaktywności piomelaniny wspierającej procesy regeneracji i unaczyniania kośćca
Rodzaj projektu: B+R
Rola w projekcie: doktorant – stypendysta
Okres realizacji: 16.10.2020 – 30.09.2023 r.

Jednostka finansująca: Fundacja na Rzecz Nauki Polskiej, konkurs TEAM-NET finansowany z środków Unii Europejskiej (Działanie 4.4 POIR - Zwiększanie potencjału kadrowego, sektora B+R, Inteligentny Rozwój).

6. **Tytuł:** Badanie wpływu biomasy i składników komórek drożdży *Yarrowia lipolytica* Novel Food na odporność i stymulację komórek układu immunologicznego

Rodzaj projektu: komercyjny B+R

Rola w projekcie: wykonawca

Okres realizacji: 01.01.2023 – 15.04.2023 r.

Jednostka finansująca: SKOTAN S.A.

Staż badawcze

- 1. Rodzaj wyjazdu:** staż badawczy
Kraj: Polska, Wrocław
Instytucja: Katedra Inżynierii i Technologii Polimerów, Politechnika Wrocławska
Termin: 09 – 30.09.2022 r.
- 2. Rodzaj wyjazdu:** staż badawczy
Kraj: Polska, Warszawa
Instytucja: Łukasiewicz - Instytut Ceramiki i Materiałów Budowlanych
Termin: 28.03 – 05.04.2022 r.
- 3. Rodzaj wyjazdu:** staż badawczy
Kraj: Polska, Wrocław
Instytucja: Katedra Inżynierii i Technologii Polimerów, Politechnika Wrocławska
Termin: 22.02 – 02.03.2021 r.
- 4. Rodzaj wyjazdu:** staż badawczy
Kraj: Polska, Kraków
Instytucja: Instytut Inżynierii Materiałowej, Politechnika Krakowska
Termin: 17 – 25.02.2020 r.

**Streszczenie
w języku polskim**

Metabolity bakteryjne stanowią jedno z głównych źródeł pozyskiwania szerokiej gamy substancji bioaktywnych o potencjalnych zastosowaniach biomedycznych. Piomelanina (PyoM) wytwarzana przez bakterie *Pseudomonas aeruginosa* (*P. aeruginosa*) będąca czarno-brązowym polimerem kwasu homogentyzynowego (HGA) z racji swoich unikalnych właściwości fizykochemicznych i biologicznych, jest rozważana jako substancja o działaniu przeciwoksydacyjnym, cytoprotekcyjnym, przeciwbakteryjnym, a także stymulującym regenerację uszkodzonych tkanek i aktywującą komórki odpornościowe.

W niniejszej rozprawie doktorskiej scharakteryzowano właściwości fizykochemiczne i biologiczne dwóch wariantów naturalnej PyoM: rozpuszczalnej (PyoM_{sol}) lub nierozpuszczalnej w wodzie (PyoM_{insol}), a także syntetycznego odpowiednika tego polimeru (sPyoM). Zoptymalizowano sposób ich wytwarzania. W pracy wykazano przydatność podłoży minimalnych PMM I i PMM II do hodowli *P. aeruginosa* i izolacji PyoM_{sol} i PyoM_{insol}. W naturalnej i syntetycznej PyoM wykazano obecność hydroksylowych i karboksylowych grup charakterystycznych dla związków melaninowych pochodnych HGA oraz wysoką termoodporność badanych PyoM. Bakteryjne PyoM w przeciwieństwie do wariantu syntetycznego cechowały się wysoką cytokompatybilnością względem fibroblastów myszy (L-929), monocytów (THP-1), komórek nabłonka żołądka (AGS) i osteoblastów człowieka (hFOB 1.19) oraz bezpieczeństwem *in vivo* na modelu *Galleria mellonella*.

Na modelu *in vitro* komórek nabłonkowych żołądka wykazano działanie przeciwbakteryjne naturalnych PyoM wobec pałeczek *Helicobacter pylori* (*H. pylori*) wywołujących zapalenie błony śluzowej żołądka lub dwunastnicy, zarówno wobec szczepów wzorcowych jak i klinicznych, a także zdolność PyoM do neutralizacji wzbudzanego przez te bakterie stresu oksydacyjnego, ograniczenia apoptozy i przywracania barierowości komórek. Ponadto wykazano, że PyoM_{sol} nasila aktywność fagocytarną monocytów zahamowaną przez komponenty *H. pylori* i aktywuje czynnik transkrypcyjny NF-κB. Uzyskane wyniki wskazują na potencjał PyoM w ograniczaniu zakażenia *H. pylori* i jego negatywnych skutków dla nabłonka żołądka.

PyoM jako bezpieczny biomimetyk złogów ochronotycznych odpowiedzialnych za nadmierną mineralizację tkanki chrzęstnej w alkaptonurii może stanowić potencjalny stymulator dojrzewania osteoblastów, a w konsekwencji przyczyniać się do regeneracji uszkodzonej tkanki kostnej. W przeprowadzonych badaniach wykazano bowiem istotną rolę bakteryjnej PyoM we wspomaganie migracji komórek kościotwórczych, a także ograniczaniu

apoptozy tych komórek indukowanej dokсорubicyną. W środowisku osteoblastów bakteryjne PyoM nasilały aktywność fosfatazy alkalicznej i sekrecję osteokalcyny, interleukiny (IL)-6, IL-10 oraz czynnika martwicy guza (TNF)- α , które stanowią kluczowe markery osteoindukcji i osteokondukcji. W pracy wykazano także przeciwbakteryjne właściwości PyoM przeciwko klinicznemu szczepom *Staphylococcus* sp. wyizolowanym z zakażonej tkanki kostnej.

Prezentowane wyniki stanowią przesłankę do dalszych badań *in vivo* na dedykowanych modelach zwierzęcych z indukowanym zapaleniem nabłonka żołądka w następstwie zakażenia *H. pylori* lub z ubytkami kostnymi, z użyciem PyoM wolnej lub związanej z kompozytami. Wyniki tych badań pozwolą na ukierunkowane zastosowanie bakteryjnej PyoM jako substancji bioaktywnej będącej składnikiem żywności specjalnego przeznaczenia lub komponentem wyrobów medycznych do regeneracji tkanki kostnej.

**Streszczenie
w języku angielskim**

Bacterial metabolites are one of the primary sources of obtaining a wide range of bioactive substances with potential biomedical applications. Pyomelanin (PyoM) produced by *Pseudomonas aeruginosa* (*P. aeruginosa*), which is a black-brown polymer of homogentisic acid (HGA) due to its unique physicochemical and biological properties, has been considered an attractive stimulator of tissue regeneration and an immunomodulator, as well as an antibacterial, antioxidant, and cytoprotective biomolecule.

This doctoral dissertation characterizes the physicochemical and biological properties of two variants of natural PyoM: soluble (PyoM_{sol}) or water-insoluble (PyoM_{insol}), as well as the synthetic form of this polymer (sPyoM). The study demonstrated the usefulness of PMM I and PMM II minimal media for the cultivation of *P. aeruginosa* and the isolation of PyoM_{sol} and PyoM_{insol}. Also, it revealed the presence of hydroxyl and carboxyl groups in PyoM_{sol}, PyoM_{insol} and sPyoM molecules, which are representative of melanin compounds derived from HGA. Moreover, the thermogravimetric analysis showed high heat resistance of the tested PyoM. Bacterial PyoM, unlike the synthetic variant, exhibited high cytocompatibility against L-929 fibroblasts, THP-1 monocytes, AGS gastric epithelial cells and hFOB 1.19 osteoblasts and *in vivo* safety in the *Galleria mellonella* model.

In an *in vitro* model of gastric epithelial cells, the antibacterial effect of natural PyoM against *Helicobacter pylori* (*H. pylori*) strains causing gastritis or duodenitis, including the reference and clinical strains was showed, as well as the ability of PyoM to neutralize the oxidative stress induced by these bacteria, limit apoptosis and restore the gastric cell barrier. Moreover, it was demonstrated that bacterial PyoM improve the phagocytic activity of monocytes inhibited by *H. pylori* components and activate the NF- κ B transcription factor. These results indicate the potential of natural PyoM in eliminating *H. pylori* and reversing negative effects driven by these bacteria in the gastric mucosa.

PyoM, as a safe biomimetic of ochronotic deposits responsible for excessive mineralization of cartilage tissue in alkaptonuria, may be a potential stimulator of osteoblast maturation and contribute to the regeneration of damaged bone tissue. The studies demonstrated the important role of bacterial PyoM in supporting the migration of bone-forming cells and limiting apoptosis induced by doxorubicin. In the cell cultures of osteoblasts, bacterial PyoM increased the activity of alkaline phosphatase and the secretion of osteocalcin, interleukin (IL)-6, IL-10 and tumour necrosis factor (TNF)- α , which are the key markers of osteoinduction and osteoconduction. The study also presented the antibacterial

properties of PyoM against clinical strains of *Staphylococcus* sp. isolated from infected bone tissue.

The presented results constitute a premise for further *in vivo* research on dedicated animal models with *H. pylori* induced gastritis or with bone defects, using PyoM alone or as a part of a biocomposite. The results of the above research will allow for the future targeted use of PyoM as a bioactive substance in food for special medical purposes or as a stimulator in medical devices for the regeneration of bone tissue.

Wykaz stosowanych skrótów

4-HPP	<i>4-hydroxyphenylpyruvic acid</i>	kwask 4-hydroksyfenylopirogronianowy
AHC	<i>acyl-homoserine lactone</i>	lakton acylohomoseryny
AKU	<i>alkaptonuria</i>	alkaptonuria
ALP	<i>alkaline phosphatase</i>	fosfataza alkaliczna
ATP	<i>adenosine-5'-triphosphate</i>	adenozyno-5'-trifosforan
BabA	<i>blood group antigen-binding adhesin</i>	adhezyna wiążąca antygen grupowy krwi
Bax	<i>B-cell lymphoma-2 associated X</i>	białko Bax
Bcl-2	<i>B-cell lymphoma 2</i>	białko Bcl-2
BMP	<i>bone morphogenetic protein</i>	białko morfogenetyczne kości
BQA	<i>benzoquinone acetate</i>	benzochinon kwasu octowego
CagA	<i>cytotoxin-associated gene A protein</i>	białko cytotoksyczne CagA
cAMP	<i>cyclic adenosine monophosphate</i>	cykliczny adenozynomonofosforan
CLR	<i>clarithromycin</i>	klarytromycyna
COL1	<i>type I collagen</i>	kolagen typu I
COX-2	<i>cyclooxygenase-2</i>	cyklooksygenaza 2
CtsK	<i>cathepsin K</i>	katepsyna K
DSC	<i>differential scanning calorimetry</i>	skaningowa kalorymetria różnicowa
DNA	<i>deoxyribonucleic acid</i>	kwask deoksyrybonuleinowy
DOX	<i>doxorubicin</i>	doksorubicyna
eDNA	<i>extracellular deoxyribonucleic acid</i>	zewnątrzkomórkowy kwask deoksyrybonuleinowy
ELISA	<i>enzyme-linked immunosorbent assay</i>	immunoenzymatyczny test fazy stałej
FTIR	<i>Fourier-transform infrared spectroscopy</i>	spektroskopia w podczerwieni z transformacją Fouriera
G	<i>α-L-guluronic acid</i>	kwask α -L-guluronowy
HA	<i>hydroxyapatite</i>	hydroksyapatyt
HGA	<i>homogentisic acid</i>	kwask homogentyzynowy
HISS	<i>Health Index Scoring System</i>	system punktacji indeksu zdrowia <i>Galleria mellonella</i>
IL	<i>interleukin</i>	interleukina
JAK-STAT	<i>Janus kinase-signals transducer and activator of transcription</i>	kinaza Janus – przekaźnik sygnałów i aktywator transkrypcji

LEV	<i>levofloxacin</i>	lewofloksacyna
LPS	<i>lipopolysaccharide</i>	lipopolisacharyd
L-Tyr	<i>L-tyrosine</i>	L-tyrozyna
M	<i>β-D-mannuronic acid</i>	kwask β -D-mannuronowy
MALT	<i>mucosa associated lymphoid tissue lymphoma</i>	chłoniak tkanki limfatycznej związanej z błoną śluzową
MAPK	<i>mitogen-activated protein kinase</i>	kinaza aktywowana mitogenami
Mbp	<i>mega base pair</i>	mega par zasad
M-CSF	<i>macrophage colony-stimulating factor</i>	czynnik stymulujący tworzenie kolonii makrofagów
MET	<i>metronidazole</i>	metronidazol
MIC	<i>minimum inhibitory concentration</i>	minimalne stężenie hamujące
MMP9	<i>matrix metalloproteinase 9</i>	metaloproteinaza macierzy pozakomórkowej 9
NADH	<i>nicotinamide adenine dinucleotide</i>	dinukleotyd nikotyno-amidoadeninowy
NF-κB	<i>nuclear factor kappa-light-chain-enhancer of activated B cells</i>	transkrypcyjny czynnik jądrow κ B
NK	<i>natural killer</i>	naturalna komórka zabijająca
OC	<i>ostoecalcin</i>	osteokalcyna
ON	<i>osteonectin</i>	osteonektyna
OPN	<i>osteopontin</i>	osteopontyna
PAI	<i>pathogenicity island</i>	wyspa patogeniczności
PI3K/Akt	<i>phosphoinositide-3-kinase/Akt</i>	kinaza 3-fosfatydyloinozytolu i kinaza białkowa Akt
PMM	<i>pyomelanin minimal medium</i>	podłoża minimalne PMM do otrzymania piomelaniny
PQS	<i>Pseudomonas quinolone signal</i>	chinolonowy sygnał <i>Pseudomonas</i>
PyoC	<i>pyocyanin</i>	piocyjanina
PyoM	<i>pyomelanin</i>	piomelanina
PyoR	<i>pyorubin</i>	piorubina
PyoV	<i>pyoverdine</i>	piowerdyna
RANKL	<i>receptor activator of nuclear factor κB ligand</i>	ligand aktywatora receptora jądrowego czynnika κ B
RNA	<i>ribonucleic acid</i>	kwask rybonukleinowy

ROS	<i>reactive oxygen species</i>	reaktywne formy tlenu
SabA	<i>sialic acid-binding adhesin</i>	adhezyna wiążąca kwas sialowy
TGA	<i>thermogravimetry</i>	termograwimetria
TGF-β	<i>transforming growth factor β</i>	transformujący czynnik wzrostu β
TNF-α	<i>tumor necrosis factor-α</i>	czynnik martwicy nowotworu- α
TLR	<i>Toll-like receptor</i>	receptor Toll-podobny
TNSALP	<i>tissue-nonspecific alkaline phosphatase</i>	niespecyficzna tkankowo fosfataza alkaliczna
TRAP	<i>tartrate-resistant acid phosphatase</i>	kwaśna fosfataza oporna na winian
UV	<i>ultraviolet radiation</i>	promieniowanie nadfioletowe
VacA	<i>vacuolating cytotoxin A</i>	toksyna wakuolizująca A
VEGF	<i>vascular endothelial growth factor</i>	czynnik wzrostu śródbłonka naczyniowego
WHO	<i>World Health Organization</i>	Światowa Organizacja Zdrowia

Wprowadzenie

Charakterystyka bakterii *Pseudomonas aeruginosa* oraz biomedyczny potencjał barwników i metabolitów tych drobnoustrojów

Rodzaj *Pseudomonas* jest jednym z najbardziej licznych i zróżnicowanych rodzajów bakterii Gram-ujemnych, obejmującym 259 gatunków z wyłączeniem podgatunków i gatunków synonimicznych opisanych w bazie *List of Prokaryotic Names with Standing in Nomenclature*.¹ Bakterie *Pseudomonas aeruginosa* (*P. aeruginosa*) zostały po raz pierwszy wyizolowane przez francuskiego farmaceutę Louis-Carle'a Gessarda w 1882 r. z rany żołnierza, którego bandażę były zabarwione na charakterystyczny niebiesko-zielony kolor. Rodzaj *Pseudomonas* został opisany przez niemieckiego botanika Waltera Migula w 1894 r., który uznał *P. aeruginosa* jako gatunek typowy dla tej grupy taksonomicznej.² Nazwa rodzajowa *Pseudomonas* pochodzi od dwóch greckich słów: *pseudo* oznaczający „fałszywy” i *monas* oznaczający „jednostkę”, natomiast *aeruginosa* wywodzi się z łacińskiego *aerūgō* tłumaczonego jako „zardzewiała miedź, grynszpan” i odwołuje się do niebiesko-zielonego podłoża wzrostowego po namnożeniu bakterii, który przypomina barwę hydroksyoctanu miedzi (II) powstającego na skutek korozji płyt miedzianych.³ Warto zwrócić uwagę, że najprawdopodobniej Migula nie posiłkował się w pełni greckim rodowodem nazwy *Pseudomonas*, ale stworzył ją inspirując się wielkością i ruchliwością tych pałeczek i ich podobieństwem w tym zakresie do komórek glonów z rodzaju *Monas*. Być może pierwotnym zamiarem Miguli było nazwanie bakterii „fałszywymi *Monas*”, a nie jak często przyjęło się tłumaczyć „fałszywymi jednostkami”.²

Bakterie *P. aeruginosa* to szeroko rozpowszechnione heterotroficzne, oksydazododatnie, niefermentujące Gram-ujemne pałeczki należące do klasy *Gammaproteobacteria*, będące patogenem oportunistycznym powodującym zakażenia szpitalne oraz infekcje u osób z obniżoną odpornością.⁴ Bakterie te należą do względnie dużych pałeczek o długości około 1–5 μm i szerokości 0,5–1,0 μm posiadających zdolność do ruchu w środowisku płynnym dzięki jednej umieszczonej biegunowo rzęście oraz możliwość poruszania się na powierzchniach stałych dzięki polarnym pilom typu IV.^{5,6} *P. aeruginosa* dobrze rosną na podłożach hodowlanych w temperaturze 37°C, ale mogą przetrwać i namnażać się w szerokim zakresie temperatur, od 4°C do 42°C. Temperatura hodowli może wpływać na zjadliwość tych bakterii, ponieważ poniżej 30°C niektóre szlaki metaboliczne odpowiedzialne za syntezę czynników wirulencji nie są aktywne.⁷

P. aeruginosa to jedno z najbardziej różnorodnych i łatwo przystosowujących się do zmian środowiska gatunków bakterii.⁸ Mikroorganizmy te wykazują doskonałą zdolność do wzrostu w zróżnicowanych niszach ekologicznych tj. gleba, woda, środowiska o niskich temperaturach, tkanki roślinne i zwierzęce, a także kolonizacji szerokiej gamy organizmów, w tym roślin, nicieni, owadów i kręgowców.^{8,9} Zdolność adaptacji i plastyczność metabolizmu *P. aeruginosa* pozwalają przetrwać tym bakteriom na suchych, abiotycznych powierzchniach nawet do 6 miesięcy, przyczyniając się do sukcesu kolonizacyjnego.¹⁰ Kliniczne izolaty *P. aeruginosa* często wykazują heterogeniczność fenotypową występując w postaci gładkich, śluzowatych lub małych kolonii na podłożach stałych.¹¹

Pałeczki *P. aeruginosa* należące do fakultatywnych tlenowców angażują do produkcji energii w postaci adenozy-5'-trifosforanów (ATP) różnorodne donory i akceptory elektronów, w związku z czym charakteryzują się złożonymi i elastycznymi ścieżkami przenoszenia elektronów w łańcuchu oddechowym.¹² W warunkach beztlenowych *P. aeruginosa*, dzięki obecności reduktazy azotanowej, wykorzystują alternatywne zewnętrzne akceptory elektronów w postaci azotanów (III) i azotanów (IV).¹³ Wykorzystując argininę jako źródło energii *P. aeruginosa* mogą rosnąć bez dostępu tlenu i azotanów, jednakże wzrost ten jest bardzo powolny. Ponadto, fermentacja pirogronianowa warunkuje długotrwałe beztlenowe przeżycie *P. aeruginosa* jednakże nie umożliwia wzrostu bakterii w takich warunkach.¹² *P. aeruginosa* bytują w środowiskach, w których powstają nisze beztlenowe, takich jak podmokłe gleby, torfowiska i osady rzeczne. W takich ekosystemach często tworzą biofilmy bakteryjne z gradientem stężeń tlenu i kieszeniami beztlenowymi.¹⁴ Ponadto alginian, wydzielany przez bakterie rosnące w formie śluzowatych kolonii, ogranicza dyfuzję tlenu i przyczynia się do tworzenia środowisk mikrotlenowych lub beztlenowych.¹⁵ Bakterie te mogą wykorzystywać ponad 100 organicznych źródeł węgla i energii, a jako drobnoustroje prototroficzne wzrastają na podłożach o minimalnej zawartości soli i substancji odżywczych.¹⁶

P. aeruginosa posiadają stosunkowo duży genom (5,5 – 7 Mbp), w porównaniu z innymi bakteriami i charakteryzują się dużą plastycznością genetyczną, która umożliwia im łatwość adaptacji do zmieniających się warunków środowiskowych, wytwarzanie różnorodnych czynników wirulencji oraz oporność na większość obecnie stosowanych antybiotyków.¹⁷ Pałeczki *P. aeruginosa* szybko przystosowują się do niedoboru żelaza i fosforanów, nagłych zmian temperatury i stresu oksydacyjnego. Skutecznie konkurują z innymi drobnoustrojami o niszę i przewyciężają działanie wybranych mechanizmów

odpornościowych gospodarza.¹⁸ Główne zmiany morfologiczne u szczepów *P. aeruginosa* izolowanych z zakażeń górnych dróg oddechowych, m.in. w przebiegu mukowiscydozy, obejmują konwersję do wariantów śluzowatych, nadprodukcję alginianu i egzopolimerów, zwiększoną syntezę barwników i tworzenie małych kolonii, w konsekwencji czego powstaje mikrośrodowisko stanowiące barierę dla antybiotyków i komórek odpornościowych.¹⁹

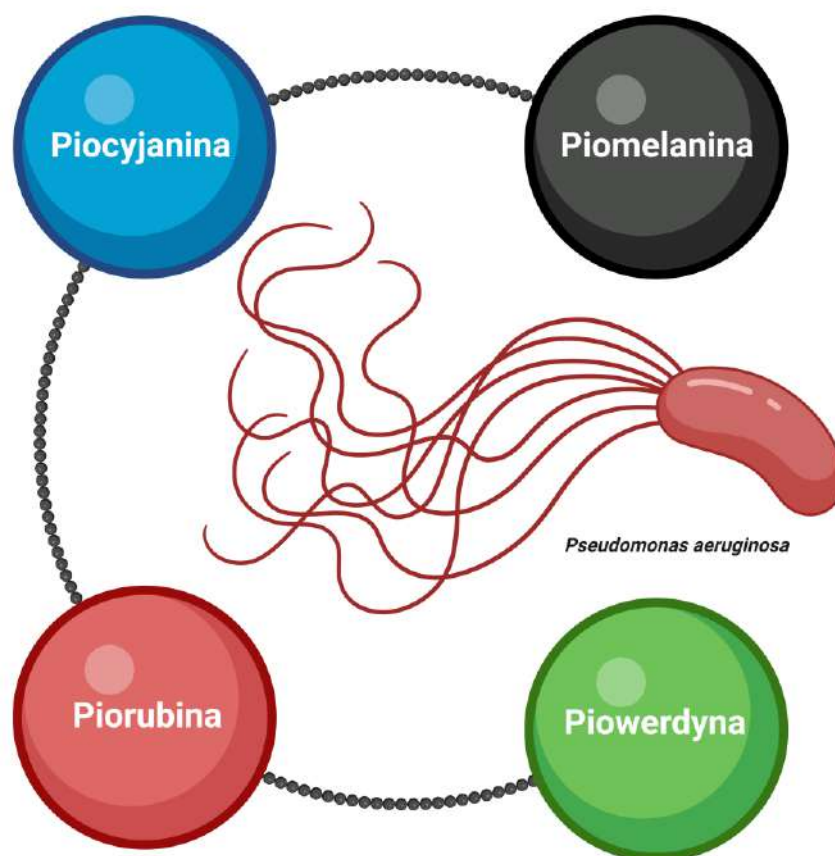
Jednym z kluczowych metabolitów *P. aeruginosa* jest alginian - wysokocząsteczkowy liniowy, organiczny heteropolisacharyd składający się z kwasu β -D-mannuronowego (M) i kwasu α -L-guluronowego (G) połączonych wiązaniami 1 \rightarrow 4 glikozydowymi.²⁰ Za polimeryzację, modyfikację i wydzielanie alginianu odpowiada wielobiałkowy kompleks zlokalizowany w przestrzeni peryplazmatycznej i błonie zewnętrznej. Białka tworzące ten kompleks ulegają ekspresji w operonie alginianu, który zawiera 12 sekwencji kodujących (*algD*, *alg8*, *alg44*, *algK*, *algE*, *algG*, *algX*, *algL*, *algI*, *algJ*, *algF* i *algA*), a także jeden gen (*algC*) zlokalizowany poza operonem. Wyżej wymienione geny są wysoce konserwatywne u alginiano-twórczych szczepów *P. aeruginosa*.²¹ Produkcja alginianu jest jedną ze strategii *P. aeruginosa* umożliwiającą adaptację i przeżycie tych bakterii w zmieniających się warunkach środowiskowych. Alginian zapewnia komórkom bakteryjnym zwiększoną tolerancję na wysychanie i działanie czynników utleniających oraz ochronę przed reakcjami odpornościowymi gospodarza. W szczepach śluzowatych, izolowanych od chorych na mukowiscydozę, alginian wydzielany jest do otaczającego bakterie środowiska i nie jest kowalencyjnie związany z ich powierzchnią.²² Alginian uczestniczy w tworzeniu, stabilizacji i zapobieganiu erozji biofilmu, jak również ogranicza przenikanie antybiotyków do komórek bakteryjnych, przyczyniając się do sukcesu kolonizacyjnego *P. aeruginosa*.²³

Bakteryjne alginiany dzięki wysokiej biokompatybilności, biodegradowalności, braku immunogenności, niskim kosztom biosyntezy i możliwości ich modyfikacji znalazły szerokie zastosowanie w medycynie regeneracyjnej i inżynierii tkankowej. W środowisku płynnym alginian tworzy hydrożele, dzięki czemu polisacharyd ten jest powszechnie używany jako stabilizator, zagęszczacz, środek żelujący, materiał opatrunkowy i składnik biokompozytów.²⁴ Masa cząsteczkowa alginianu waha się od 32 do 400 kDa, natomiast wraz ze wzrostem masy cząsteczkowej wzrasta także lepkość żelu alginianowego. Alginiany o wysokiej zawartości kwasu G tworzą sztywniejsze hydrożele, podczas gdy alginiany o wysokiej zawartości kwasu M tworzą hydrożele bardziej miękkie i elastyczne.²⁵ Hydrożele alginianowe, dzięki utrzymaniu wilgotnego środowiska o optymalnym pH i przyspieszaniu procesów gojenia tkanek, stanowią surowiec do produkcji opatrunków na rany skóry.

Wilgotne środowisko rany pod hydrożelem alginianowym przyczynia się do efektu hemostatycznego i pomaga w opanowaniu krwawienia, natomiast wysoka chłonność pozwala na absorbowanie wysięku.²⁶ Alginian jest powszechnie stosowanym polimerem do projektowania i wytwarzania systemów dostarczania leków lub substancji bioaktywnych. Obecność aktywnych grup funkcyjnych (karboksylowych i hydroksylowych) w jego strukturze stwarza szerokie możliwości modyfikacji biochemicznych, chemicznych lub strukturalnych. Łączenie bakteryjnego alginianu z innymi polimerami umożliwia zaprojektowanie komponentów o określonych cechach, takich jak biokompatybilność, porowatość, wytrzymałość mechaniczna, szybkość pęcznienia, czas i stopień degradacji, ładunek elektryczny oraz profil uwalniania cząsteczek bioaktywnych.²⁷ Właściwości przeciwbakteryjne biomateriałów alginianowych są efektem modyfikacji antybiotykami (klindamycyną, wankomycyną, gentamycyną, aminoglikozydami), nanocząstkami metali (tj. srebro, cynk, miedź, złoto, magnez) lub bakteriobójczymi olejkami eterycznymi. Pośród stosowanych modyfikatorów aktywności biologicznej kompozytów alginianowych, ukierunkowanej na przyspieszenie regeneracji tkanek, należy uwzględnić także czynniki wzrostowe, substancje przeciwutleniające i przeciwzapalne.²⁵

Jednym z przykładów wykorzystania alginianu wydzielanego przez *P. aeruginosa* w medycynie regeneracyjnej jest jego sprzężanie z białkami morfogenetycznymi kości (BMP, *bone morphogenetic protein*)-2 i BMP-7, co zwiększa potencjał różnicowania komórek macierzystych pochodzących ze szpiku kostnego do osteoblastów. Natomiast jednoczesne uwolnienie do obszaru gojenia BMP-2 i czynnika wzrostu śródbłonka naczyniowego (VEGF, *vascular endothelial growth factor*) z żeli alginianowych, znacząco poprawia rekonstrukcję ubytków kostnych.²⁸

Do cech fenotypowych *P. aeruginosa* umożliwiających wstępną identyfikację tego gatunku zalicza się charakterystyczny zapach jaśminu lub soku winogronowego, za który odpowiada 2-aminoacetofenon, a także β -hemolizę, obecność dużych, śluzowatych kolonii i zabarwienie agarowego podłoża hodowlanego pod wzrostem kolonii.²⁹ Głównymi rozpuszczalnymi barwnikami wytwarzanymi przez te mikroorganizmy są niebieska piocyjanina, żółto-zielona piowerdyna, czerwona piorubina oraz brązowo-czarna piomelanina (Ryc. 1). *P. aeruginosa* stanowią jedno z najcenniejszych bakteryjnych źródeł pozyskania barwników o potencjale biomedycznym i przemysłowym.³⁰



Ryc. 1. Barwniki produkowane przez bakterie *P. aeruginosa*.

Piocyjanina (PyoC, *pyocyanin*) jest niebieskim, fenazynewym, rozpuszczalnym w wodzie barwnikiem syntetyzowanym w późnej stacjonarnej fazie wzrostu przez około 90–95% szczepów *P. aeruginosa*. Jej wytwarzanie podlega regulacji w procesie *quorum sensing* przez autoinduktory: lakton acylohomoseryny (AHC, *acyl-homoserine lactone*) i 2-heptyl-3-hydroksy-4-chinolon, zwany chinolonowym sygnałem *Pseudomonas* (PQS, *Pseudomonas quinolone signal*).^{31–33} PyoC *P. aeruginosa* jest elektrochemicznie aktywnym metabolitem spełniającym funkcję nośnika elektronów, dzięki czemu wspiera oddychanie komórkowe i wytwarzanie energii w warunkach niedoboru tlenu.³⁴ Ponadto, PyoC kontroluje ekspresję genów, interakcje między komórkami bakteryjnymi oraz wielkość kolonii na podłożach stałych, a także grubość i stabilność biofilmu tworzonego przez *P. aeruginosa*.³⁵ Ten termolabilny barwnik ma znaczący wpływ na adhezję *P. aeruginosa* do różnych powierzchni poprzez tworzenie kompleksu z zewnątrzkomórkowym kwasem deoksyrybonuleinowym (eDNA, *extracellular deoxyribonucleic acid*), dzięki czemu zaburza hydrofobowość komórek

bakteryjnych i sprzyja tworzeniu stabilnych biofilmów.^{36,37} Ekspresja czynników wirulencji u *P. aeruginosa* jest wzmacniana przez syntezę PyoC, a szczepy wytwarzające piocyjanieę charakteryzują się wysoką zjadliwością i opornością na antybiotyki.³⁸ PyoC uważana jest za jeden z głównych czynników wirulencji *P. aeruginosa*. Ekspozycja komórek eukariotycznych na PyoC powoduje powstawanie wewnątrzkomórkowych reaktywnych form tlenu (ROS, *reactive oxygen species*), co prowadzi do oksydacyjnego uszkodzenia DNA, zmniejszenia syntezy dinukleotydu nikotynoamidoadeninowego (NADH, *nicotinamide adenine dinucleotide*) i hamowania aktywności enzymów, a w konsekwencji wzbudzenia procesu apoptozy.^{39,40} Jedną z głównych funkcji PyoC jest hamowanie reakcji odpornościowych gospodarza. Wykazano, że PyoC zmniejsza sekrecję interleukiny (IL, *interleukin*)-2 i ekspresję jej receptorów na powierzchni limfocytów T, prowadząc do zahamowania proliferacji tych komórek, a także zaburza wydzielanie przeciwciał przez limfocyty B. Oprócz negatywnego wpływu na limfocyty, PyoC wykazuje także toksyczne działanie względem neutrofilów, indukując szybką i selektywną apoptozę zależną od wzrostu ROS i zmniejszenia stężenia wewnątrzkomórkowego cyklicznego adenozynomonofosforanu (cAMP, *cyclic adenosine monophosphate*).^{41,42} PyoC w środowisku lipopolisacharydu (LPS, *lipopolysaccharide*) *P. aeruginosa* znacząco pobudza sekrecję IL-1 i czynnika martwicy nowotworu- α (TNF- α , *tumor necrosis factor- α*) przez monocyty, prowadząc do rozwoju silnej reakcji zapalnej oraz postępującej kolonizacji tkanek gospodarza.⁴³ PyoC odpowiada także za pozyskiwanie żelaza ze środowiska zewnątrzkomórkowego oraz odgrywa istotną rolę w metabolizmie tego pierwiastka. Właściwości redukujące tego barwnika ułatwiają uwalnianie żelaza z transferyny i jego transport do komórki bakteryjnej.⁴⁴ PyoC jest badana pod kątem wykorzystania jako alternatywnego środka przeciwbakteryjnego i przeciwgrzybiczego, a także barwnika ograniczającego stres oksydacyjny i hamującego rozwój komórek nowotworowych. Liczne doniesienia wskazują na zdolność PyoC do ograniczenia żywotności bakterii patogennych tj. *Staphylococcus aureus*, w tym szczepów metycylinoopornych, *Escherichia coli*, *Klebsiella pneumoniae*, *Enterococcus faecalis*, *Salmonella enterica* i *Bacillus cereus* oraz grzybów patogennych, w tym *Aspergillus niger*, *A. fumigatus*, *Cryptococcus neoformans*, *Candida albicans* i *C. tropicalis*.^{31,45-47} Ponadto wykazano, że PyoC skutecznie redukuje biofilm bakteryjny i wspomaga *P. aeruginosa* w zasiedlaniu nabłonka płuc pacjentów z mukowiscydozą konkurując z *S. aureus*.³¹ Badania wskazują także na hamowanie przez PyoC wzrostu komórek nowotworowych m. in. komórek mięśniakomięśaka prążkowanokomórkowego, raka wątrobowokomórkowego, kostniakomięśaka, raka okrężnicy, czerniaka i raka trzustki.^{31,48-50} Mechanizmy

ograniczające wzrost komórek nowotworowych przez PyoC obejmują zwiększenie przepuszczalności błony komórkowej, interkalację barwnika z DNA i hamowanie topoizomerazy, a ponadto indukcję stresu oksydacyjnego i w następstwie uszkodzenie DNA oraz aktywację kaspazy 3, co w konsekwencji prowadzi komórki nowotworowe na szlak apoptozy.^{48,51} Wykazano również hamowanie przez PyoC acetylocholinoesterazy, której nadmierna aktywność jest ściśle powiązana z genezą wielu chorób neurodegeneracyjnych.⁵²

Innym charakterystycznym barwnikiem syntetyzowanym i wydzielanym przez *P. aeruginosa* jest fluorescencyjna piowerdyna (PyoV, *pyoverdine*), która stanowi główny siderofor umożliwiający rozpuszczanie żelaza ze źródeł nieorganicznych oraz pozyskiwanie tego pierwiastka z ferroprotein gospodarza.⁵³ Szczepy *P. aeruginosa* wytwarzają trzy różne typy PyoV (PyoV I, PyoV II i PyoV III) składające się z peptydu o długości od 6 do 12 aminokwasów połączonego z chromoforem będącym pochodną 2,3-diamino-6,7-dihydroksychinoliny. Sekwencja aminokwasów i długość łańcucha peptydowego PyoV jest zróżnicowana.⁵⁴ PyoV jest kluczowym czynnikiem wirulencji, a jej produkcja jest konieczna dla uzyskania pełnej zjadliwości *P. aeruginosa*. Oprócz roli jaką pełni w pozyskiwaniu żelaza, PyoV kontroluje tworzenie biofilmu, komunikację między komórkami bakteryjnymi oraz reguluje ekspresję czynników zjadliwości, w tym egzotoksyny A i egzoproteazy PrpL.⁵⁵ PyoV jest jednym z czynników nasilających antybiotykooporność *P. aeruginosa*, a szczepy piowerdyno-twórcze cechują się wyższym poziomem oporności na ampicylinę, cefsulodynę, gentamycynę, norfloksacynę, ofloksacynę, tobramycynę i tygecyklinę.^{56,57} Aktualne badania nad biomedycznym wykorzystaniem PyoV skupiają się na zastosowaniu tzw. „strategii konia trojańskiego” polegającej na wykorzystaniu skoniugowanych barwników z antybiotykami, w celu zwalczania infekcji wywołanych przez wielolekooporne szczepy *P. aeruginosa*.⁵⁸

Bakterie *P. aeruginosa* produkują także rozpuszczalną w wodzie piorubinę (PyoR, *pyorubin*), a częstość występowania szczepów wydzielających ten czerwony barwnik szacuje się na 2–3%. PyoR jako siderofor chelatuje jony żelaza umożliwiając ich translokację poprzez bakteryjną błonę zewnętrzną i błonę cytoplazmatyczną.⁵⁹ Potwierdzone zostały także fotoprotekcyjne i przeciwutleniające właściwości PyoR oraz jej zdolność do utrzymywania równowagi redoks w komórkach bakteryjnych.^{60,61}

Ostatnim znanym barwnikiem wydzielanym przez *P. aeruginosa* jest piomelanina stanowiąca główny obiekt badań poniższej rozprawy doktorskiej.

Charakterystyka piomelaniny produkowanej przez bakterie *Pseudomonas aeruginosa*

Związki melaninowe stanowią szeroko rozpowszechnioną w przyrodzie heterogenną grupę amorficznych biopolimerów powstających w wyniku polimeryzacji fenoli lub indoli wywodzących się z tyrozyny. Greckie słowo *melanós* oznacza „czarny” lub „bardzo ciemny” i odzwierciedla obserwowalną właściwość melanin. Charakterystyczną cechą tych związków jest ich ciemnobrązowy lub czarny kolor, choć znane są także melaniny o czerwonym lub żółtym zabarwieniu.^{62,63} Związki melaninowe należą do polimerów o wysokiej odporności na działanie stężonych kwasów i środków redukujących, ponadto charakteryzują się wyjątkowo wysoką fotostabilnością i termoodpornością, nawet do temperatury 300°C.⁶⁴ Biorąc pod uwagę brak rozpuszczalności lub niską rozpuszczalność melanin w wodzie, interesujące wydają się ich właściwości higroskopijne. Melaniny są w stanie zaabsorbować cząsteczki wody nawet do 20% swojej własnej masy.⁶⁵ Pojedyncze monomery melanin są wysoce reaktywne chemicznie i niestabilne, natomiast ich polimery charakteryzują się stabilnością i niższym stopniem reaktywności wynikającym z zawady przestrzennej i interakcji wewnątrzcząsteczkowych.^{66,67}

Melaniny występują u organizmów wszystkich trzech domen taksonomicznych: *Archaea*, *Bacteria* i *Eucarya*. Barwniki te u mikroorganizmów pełnią różnorodne funkcje związane z przetrwaniem i adaptacją gatunków w ich naturalnym środowisku. Odpowiadają za ochronę przed promieniowaniem nadfioletowym (UV, *ultraviolet radiation*), termoregulację i termoprotekcję, usuwanie wolnych rodników i utrzymanie równowagi redoks, chelatowanie i sekwestrację jonów metali i substancji toksycznych. Ponadto pełnią funkcję cząsteczki sygnałowej oraz przenośnika elektronów w szlakach metabolicznych oraz chronią przed konkurencyjnymi i drapieżnymi drobnoustrojami.⁶⁸⁻⁷⁰

Obecnie przyjęta klasyfikacja związków melaninowych dzieli je na pięć głównych typów, uwzględniając strukturę monomeru, prekursor barwnika oraz obecności azotu i siarki w cząsteczce. Do melanin zalicza się eumelaninę, feomelaninę, allomelaninę, neuromelaninę i piomelaninę (Tabela 1).^{68,69,71}

Tabela. 1. Klasyfikacja melanin ze względu na prekursor oraz zawartość azotu i siarki.^{68,69,71}

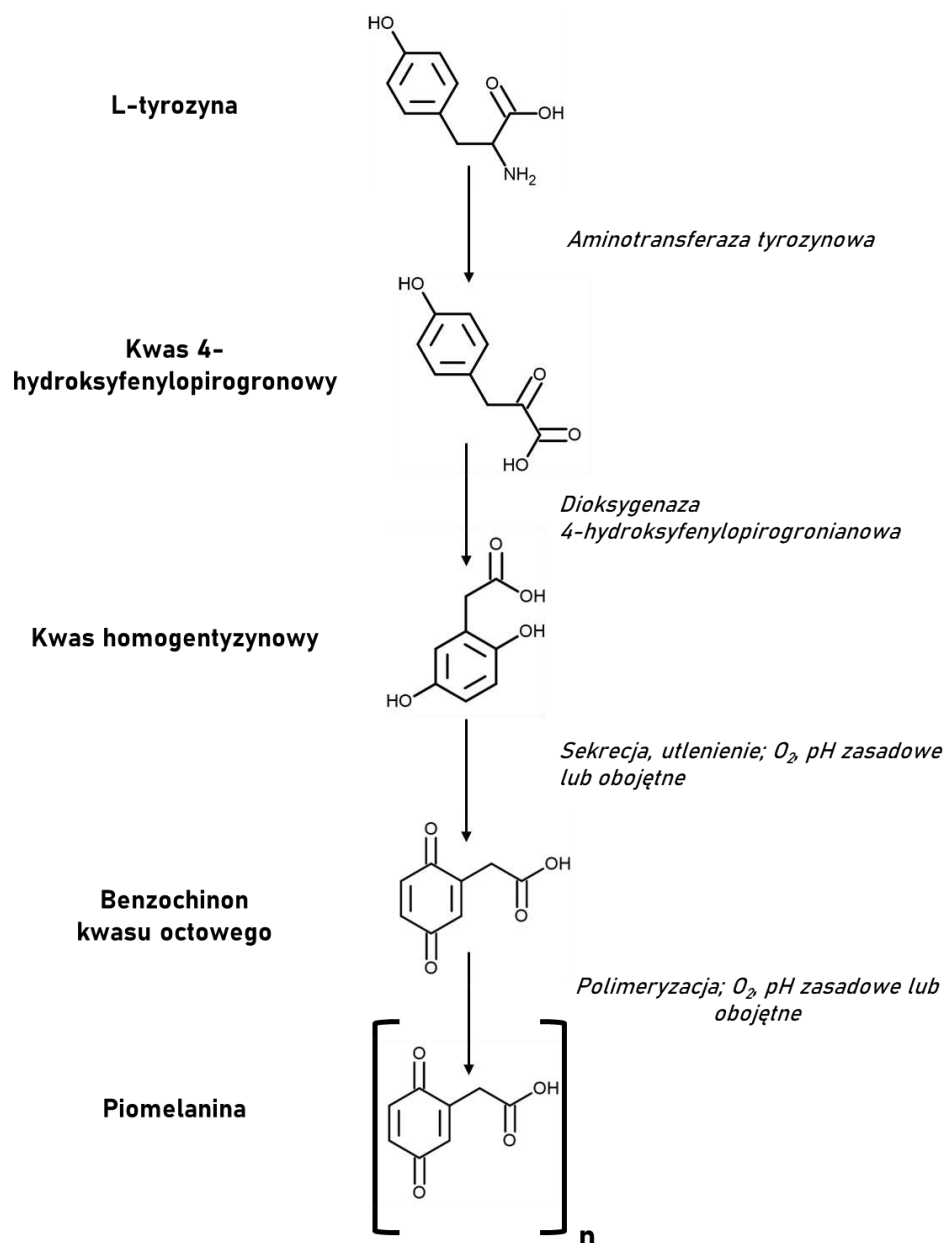
Typ melanin	Prekursor melaniny	Azot	Siarka
Eumelanina	Tyrozyna, lewodopa, 5,6-dihydroksyindole	+	+/-
Feomelanina	Cysteinyldopa, benzotiazyny	+	+
Neuromelanina	Dopamina, katecholaminy	+	-
Allomelanina	1,8-dihydroksynaftalen, katechole, kwas kawowy	-	-
Piomelanina	Kwas homogentyzynowy	-	-

(+) - obligatoryjna obecność, (+/-) – niska częstość występowania, (-) – brak obecności

Struktura indolowa lub aktywne grupy fenolowe w cząsteczkach melanin nadają im nie tylko charakterystyczne właściwości fizyczne i chemiczne, ale odpowiadają za wiele aktywności biologicznych o potencjalnym zastosowaniu w biologii i medycynie. Aktualne biomedyczne kierunki badań nad bakteryjnymi melaninami obejmują wykorzystanie tych barwników jako substancji przeciwutleniających, przeciwbakteryjnych, przeciwwirusowych, fotoprotekcyjnych, immunomodulujących i przeciwnowotworowych, a także jako nośników leków, modulatorów regeneracji tkanek, czy środków kontrastowych do obrazowania metodą rezonansu magnetycznego.^{68,72,73} Warty uwagi są możliwości zastosowania melanin bakteryjnych w przemyśle, rolnictwie, ochronie środowiska i bioelektrotechnice, gdzie związki te mogą pełnić rolę adsorbentów metali ciężkich, barwników spożywczych i przemysłowych, chemosensorów, jak również bioelektrolitów i fotouczulaczy przekształcających energię świetlną w barwnikowych ogniwach słonecznych.^{64,74-77}

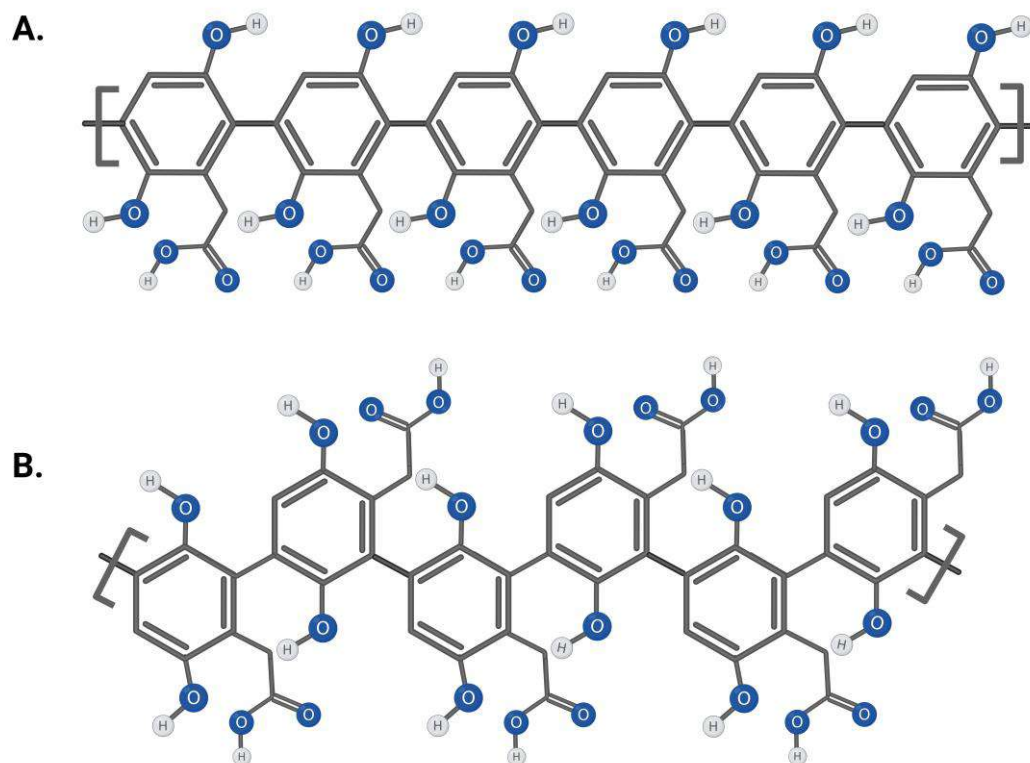
Jednym z najlepiej poznanych bakteryjnych związków melaninowych jest piomelanina (PyoM) wytwarzana przez *P. aeruginosa*. PyoM jest ujemnie naładowanym polimerem kwasu homogentyzynowego (HGA, *homogentisic acid*) syntetyzowanym w metabolicznym szlaku przemian L-tyrozyny (L-Tyr).^{60,78} Termin „*piomelanina*” został po raz pierwszy zastosowany dla brązowo-czarnego barwnika melaniowego, niezawierającego w swojej strukturze azotu, wyizolowanego z hodowli *P. aeruginosa* przez Yabuuchiego i Ohyamę w 1972 roku. Nazwa ta podtrzymała konwencję terminologiczną dodania przedrostka „*pio-*”, charakterystyczną dla pozostałych barwników produkowanych przez te bakterie.⁷⁹

PyoM powstaje na szlaku degradacji L-Tyr, jednakże w sytuacji braku lub niskiej podaży tego aminokwasu, L-feniloalanina może być przekształcana przez hydroksylazę L-feniloalaniny do L-Tyr. Biosynteza PyoM zaczyna się od konwersji L-Tyr przez aminotransferazę tyrozynową do kwasu 4-hydroksyfenylopirogronianowego (4-HPP, *4-hydroxyphenylpyruvic acid*) w obecności 2-oksoglutaranu jako kofaktora. Następnie 4-HPP jest przekształcany do HGA przez dioksygenazę 4-hydroksyfenylopirogronianu zależną od Fe^{2+} .⁸⁰ Znacząca większość PyoM powstaje abiotycznie na zewnątrz komórki bakteryjnej, gdy kwas HGA wydzielany przy udziale transporterów HatABCDE ABC ulega samoutlenieniu, tworząc kwas benzochinooctowy (BQA, *benzoquinone acetate*) w obecności tlenu i pH od obojętnego do zasadowego. W ostatnim etapie następuje spontaniczna samoorganizacja BQA w strukturę polimerową tworząc końcowy produkt – PyoM. Na tym etapie PyoM, podobnie jak chemicznie syntetyzowane polimery HGA, jest rozpuszczalnym w wodzie barwnikiem, który może ponownie wniknąć do komórki bakteryjnej, gdzie podlega dalszym modyfikacjom. Translokacja PyoM do wnętrza komórki oraz jej adsorpcja na powierzchni ściany komórkowej przyczynia się do brązowego zabarwienia komórek *P. aeruginosa*.⁸¹⁻⁸⁴ Schemat biosyntezy PyoM przedstawiono na Ryc. 2.



Ryc. 2. Schemat biosyntezy piomelaniny u *P. aeruginosa*.

Postulowana masa cząsteczkowa PyoM waha się od 10 do 14 kDa i jest mniejsza w porównaniu do innych związków melaninowych. Realna wielkość cząsteczek PyoM może być większa, gdyż zależy ona od aktywności metabolicznej szczepów *P. aeruginosa*, dostępności prekursorów tego związku oraz fazy wzrostu drobnoustroju.^{63,85} Struktura chemiczna PyoM nie jest dobrze scharakteryzowana, jednakże dotychczasowe badania wskazują na występowanie polimerowych struktur liniowych w łańcuchu tego barwnika (Ryc. 3).⁶³



Ryc. 3. Prawdopodobne struktury piomelaniny. A. Postulowana struktura chemiczna. B. Struktura chemiczna zaproponowana na podstawie modelowania matematycznego.⁶³

Dodatkowe trudności w scharakteryzowaniu struktury chemicznej PyoM wynikają z możliwości przyłączania się innych grup funkcyjnych do szkieletu cząsteczki wskutek metabolizmu bakterii, aniżeli wynikłoby to z polimeryzacji jej prekursora.⁸³ Analizy z wykorzystaniem spektroskopii w podczerwieni z transformacją Fouriera (FTIR, *Fourier-transform infrared spectroscopy*) pozwoliły zidentyfikować w strukturze PyoM obecność grup funkcyjnych charakterystycznych dla HGA, takich jak grupy hydroksylowe –OH, alifatyczne wiązania C–H oraz aromatyczne wiązania C=C sprzężone z grupami C=O i/lub COO[–]. Najprawdopodobniej grupa –CH₂COOH pozostaje nienaruszona podczas polimeryzacji, a sprzężenie oksydacyjne zachodzi w pozycji *orto* pierścienia fenolowego.^{63,86} Występowanie struktur chinonowych zapewnia cząsteczce PyoM zdolność przenoszenia elektronów i odwracalną aktywność redoks, co potwierdzają badania z wykorzystaniem cyklicznej woltamperometrii.⁸⁷

PyoM *P. aeruginosa* zapewnia bakteriom korzyści związane z dostosowaniem się do szkodliwych i zmiennych warunków środowiska oraz pełni istotne adaptacyjne role fizjologiczne (Ryc. 4).^{80,83}



Ryc. 4. Fizjologiczne funkcje piomelaniny *P. aeruginosa*.

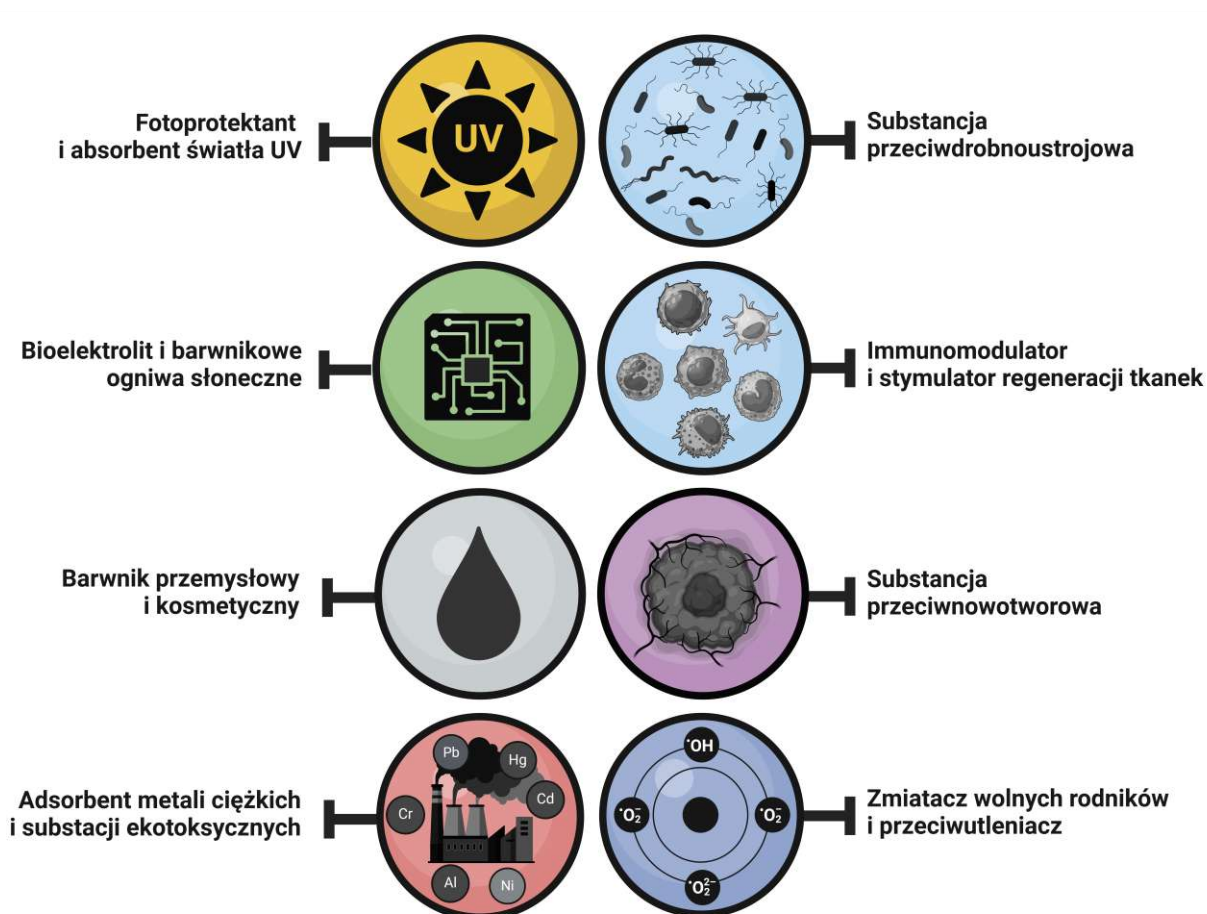
Głównym zadaniem PyoM jest ochrona bakterii przed promieniowaniem UV poprzez ograniczenie wytwarzania toksycznych ROS oraz zwiększenie odporności na światło. PyoM zmniejsza stres oksydacyjny w komórkach bakteryjnych wywołany toksycznymi substancjami utleniającymi znajdującymi się w środowisku wzrostu *P. aeruginosa*, a także ogranicza negatywne działanie ROS wytwarzanych przez komórki gospodarza w przebiegu zakażenia, zapewniając wysoką tolerancję na nadtlenek wodoru (H_2O_2), anionorodnik ponadtlenkowy ($O_2^{\cdot-}$) i rodnik hydroksylowy (OH^{\cdot}).^{88,89} Unikalne właściwości elektrochemiczne i neutralizacja ROS przez PyoM wynikają z jej zdolności do stabilizowania układów redoks, magazynowania i przenoszenia elektronów i protonów ($2e^-/2H^+$) na jednostkach chinonowych tworzących układ chinon–semichinon–hydrochinon.⁹⁰

Uwzględniając charakterystykę cykli redoks, PyoM służy jako transporter i końcowy akceptor elektronów, zapewniając wysoką podaż energetyczną zarówno w komórce, jak i biofilmie bakteryjnym. Co więcej, biosynteza PyoM może być mechanizmem mobilizacji kationów metali biogennych ze środowiska zewnętrznego i pozwala na ich magazynowanie. Wykazano, że PyoM bierze udział w przenoszeniu elektronów poprzez redukcję nierozpuszczalnego żelaza (Fe), umożliwiając przejście tego pierwiastka w formę rozpuszczalną oraz zapewniając homeostazę i odpowiedni stosunek Fe^{2+}/Fe^{3+} dla prawidłowego metabolizmu bakterii.^{91–93} Ponadto aktywne grupy hydroksylowe i karbohydroksylowe w strukturze PyoM odpowiadają za chelatowanie i udostępnianie komórkom bakteryjnym jonów pierwiastków biogennych tj. Na^+ , K^+ , Mg^{2+} , Ca^{2+} , Zn^{2+} , Fe^{3+} , Cu^{2+} , Mn^{2+} oraz sekwestrowanie toksycznych metali ciężkich (Gd^{3+} , La^{2+} , Al^{3+} , Pb^{2+}).^{94–96}

Ponadto, bakteryjne PyoM wykazują także zdolność do wiązania się z antybiotykami należącymi do aminoglikozydów, tetracyklin, fluorochinolonów, penicylin i cefalosporyn, ograniczając ich biodostępność i zwiększając szanse bakterii na przeżycie.⁹⁷

Sekrecja PyoM stanowi także ważny ewolucyjny mechanizm obronny bakterii piomelanio-twórczych przed „drapieżnymi” bakteriami i pierwotniakami, przyczyniając się do stabilizacji ich niszy kolonizacyjnej.⁹⁸ Kolejną istotną funkcją PyoM jest zwiększenie adhezji *P. aeruginosa* do powierzchni stałych, stabilizowanie biofilmu bakteryjnego oraz jego ochrona przed degradacją i działaniem enzymów proteo- i hydrolitycznych.^{99,100} Ponadto, PyoM pełni funkcję termoprotekcyjną, chroniąc komórki bakteryjne przed nagłymi zmianami temperatury i szokiem termicznym oraz zwiększając ich przeżywalność w chłodnych i zimnych środowiskach.¹⁰¹

Bakteryjna PyoM, z racji pełnienia wielu funkcji biologicznych i przewagi nad melaninami pozyskiwanymi z innych źródeł, na co składają się niskie koszty uzyskania, łatwość technologiczna biosyntezy i izolacji, biokompatybilność, biodegradowalność i możliwość modyfikacji chemicznych, jest szeroko badana pod kątem aplikacyjnym. Wraz z nową wiedzą i postępem technologii, bakteryjna PyoM może znaleźć zastosowanie w medycynie, biologii, kosmetologii, inżynierii materiałowej, bioremediacji i ochronie środowiska, przemyśle spożywczym i farbiarskim, a także elektrotechnice (Ryc. 5).^{70,72,102,103}



Ryc. 5. Aktualne kierunki badań nad zastosowaniem piomelaniny *P. aeruginosa* w różnych sektorach gospodarki i przemysłu.

W dobie narastającej lekooporności bakteryjne PyoM mogą stanowić alternatywny środek przeciwdrobnoustrojowy wspomagający eradykację mikroorganizmów chorobotwórczych. PyoM wykazuje właściwości przeciwbakteryjne przeciwko patogenom człowieka tj. *Staphylococcus aureus*, *Escherichia coli*, *Aeromonas* sp., *Citrobacter* sp., *Edwardsiella* sp., *Vibrio parahaemolyticus*, *Klebsiella pneumoniae*, *Enterococcus faecalis*, *Listeria monocytogenes*, *Shigella dysenteriae* i *Bacillus cereus*, jak również ogranicza żywotność fitopatogenów: *Erwinia chrysanthemi*, *E. cartovora* i *Pseudomonas fluorescens*.^{103–107} Ponadto, wykazano przeciwgrzybiczą aktywność PyoM przeciwko *C. albicans*, *Trichophyton rubrum* i *T. simii*.^{103,108} Ograniczenie wzrostu *in vitro* komórek raka skóry, komórek naskórkowego raka krtani, raka okrężnicy, gruczolakoraka piersi i raka wątrobowokomórkowego przez bakteryjną PyoM, czyni ten barwnik wartym uwagi w opracowywaniu alternatywnych terapii przeciwnowotworowych.^{103,108,109}

Właściwości PyoM sprawiają, że jest obiektem badań nad opracowaniem nowych systemów dostarczania leków. Jej biokompatybilność, biodegradowalność, wysoka

wydajność łączenia z innymi związkami oraz możliwość modyfikacji chemicznej PyoM pozwalają na uzyskanie optymalnych warunków wiązania i uwalniania substancji terapeutycznych. Aktywne leki lub proleki mogą być połączone z PyoM przez wiązania kowalencyjne lub zamykane w piomelaninowej matrycy polimerowej poprzez wiązania niekowalencyjne.¹¹⁰ Ze względu na tak unikalne cechy PyoM można stać się biomimetycznym nośnikiem antygenów szczepionkowych i leków przeciwnowotworowych, jak również pełnić rolę adjuwanta i immunomodulatora.¹¹¹ Wpływ PyoM na działanie komórek układu odpornościowego jest nadal słabo poznany, co stanowi przesłankę do dalszych, wielokierunkowych badań. Kuriana i wsp. potwierdzili, że bakteryjna PyoM wykazuje aktywność przeciwzapalną poprzez hamowanie aktywności trzech kluczowych enzymów zaangażowanych w rozwój reakcji zapalnej – cyklooksygenazy, lipoksygenazy i mieloperoksydazy.¹¹²

PyoM, jako związek naturalny, biodegradowalny i silnie koloryzujący związek chemiczny z powodzeniem może stanowić alternatywę dla ekotoksycznych barwników syntetycznych stosowanych w przemyśle tekstylnym. Bakteryjna PyoM efektywnie barwi tkaniny wełniane, zapewniając ich wyrazisty kolor, wysoką odporność na spieranie, oraz działanie potu i światła, a także aktywność przeciwdrobnoustrojową.^{113,114} Dzięki właściwościom barwiącym, fotoprotekcyjnym i przeciwutleniającym PyoM może być rozważana jako składnik filtrów UV, preparatów koloryzujących lub kosmetyków przeznaczonych do regeneracji skóry.^{115,116}

Rozwój urbanizacji i industrializacji naraził środowisko na działanie licznych substancji ekotoksycznych odkładających się w glebie i wodzie. Produkcja przemysłowa, jak również stosowanie nawozów, pestycydów i herbicydów w sektorze rolnym generują zanieczyszczenie środowiska glinem, miedzią, cynkiem, nikiel, ołowiem i arsenem. Podobnie, nieoczyszczone ścieki z przemysłu rolno-spożywczego, odprowadzane do kanałów rzecznych i zbiorników wodnych, mają szkodliwy wpływ na środowisko.^{117,118} Metody powszechnie stosowane do usuwania metali ciężkich ze środowiska tj. ekstrakcja, sorpcja, ługowanie kwasem i elektrokultywacja są kosztowne i wymagają dużych zasobów energetycznych.¹¹⁹ Właściwości chelatujące związków melaniowych, w tym PyoM, zapewniają wysoką zdolność wiązania i powinowactwo do różnych jonów metali ciężkich (Zn^{3+} , Cd^{2+} , U^{4+} , Mn^{2+}) poprzez interakcję z licznymi grupami funkcyjnymi, prowadząc do ich immobilizacji i umożliwiając zastosowanie w bioremediacji zanieczyszczonej wody i gleby.^{103,120,121}

Rozwój zrównoważonych i wydajnych technologii przetwarzania i magazynowania energii ma kluczowe znaczenie dla ograniczenia antropogenicznego wpływu na zmiany klimatyczne i zapobiegania możliwym niedoborom energii związanym ze wzrostem liczby ludności na świecie.⁷⁷ PyoM, z racji zdolności do absorpcji fotonów, przewodzenia prądu, biodegradowalności i niskich kosztów produkcji, może być wykorzystana jako bioelektrolit lub fotouczulacz w barwnikowych ogniwach słonecznych przekształcających energię słoneczną na energię elektryczną, stając się jednym z biologicznych odnawialnych źródeł energii elektrycznej.⁷⁵

Biorąc pod uwagę właściwości biologiczne PyoM, związek ten jest ciekawym obiektem do badań nad jego wykorzystaniem do zastosowań medycznych, w eliminacji przewlekłych zakażeń z towarzyszącą reakcją zapalną wywoływanych przez patogeny lekooporne na powszechnie stosowane antybiotyki lub w medycynie regeneracyjnej.

Helicobacter pylori – fizjologia, czynniki wirulancji i patogeneza

Bakterie *Helicobacter pylori* (*H. pylori*) to Gram-ujemne ruchliwe, mikroaerofilne, katalazo- i oksydazododatnie pałeczki o spiralnym kształcie zdolne do przeżycia w środowisku żołądka i dwunastnicy oraz kolonizacji tych narządów. Częstość występowania zakażenia *H. pylori* w populacji ludzi osiąga od 30% do 70%, w zależności od regionu świata, przy czym odsetek zakażeń bezobjawowych szacuje się nawet na 67%. Kolonizacja tymi bakteriami prowadzi do przewlekłego stanu zapalnego związanego z uszkodzeniem błony śluzowej żołądka, a długotrwałe zakażenie może skutkować schorzeniami klinicznymi.^{122–124} Większość zakażeń *H. pylori* przebiega bezobjawowo, jednak długo utrzymujące się i nieleczone infekcje zwiększają ryzyko rozwoju pełnoobjawowej choroby wrzodowej żołądka (10–15%), wrzodów dwunastnicy (95%) lub wrzodów żołądka (80%).¹²⁵ Zakażenie *H. pylori* jest także czynnikiem zwiększającym 3–6 krotnie ryzyko rozwoju nowotworów żołądka, w tym gruczolakoraka żołądka lub chłoniaka tkanki limfatycznej związanego z błoną śluzową (MALT, *mucosa associated lymphoid tissue lymphoma*).¹²⁶ Szacuje się, że choroba nowotworowa żołądka rozwija się u 1–3% zakażonych osób, w związku z czym bakterie te zostały zaklasyfikowane jako kancerogen grupy I przez Światową Organizację Zdrowia (WHO, *World Health Organization*).¹²⁷

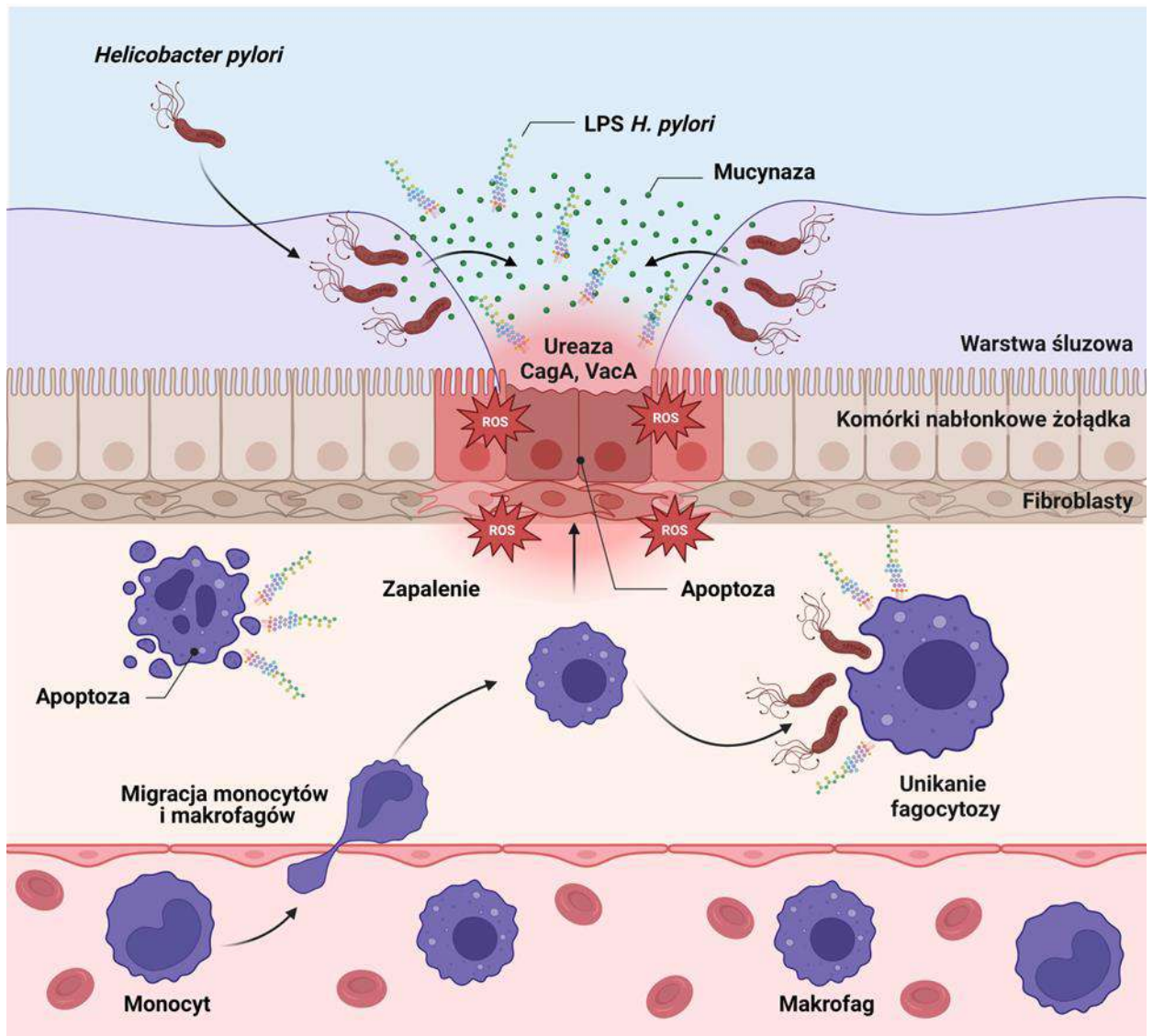
Koewolucja człowieka i *H. pylori* przez tysiąclecia umożliwiła tym pałeczkom adaptację do niszy kolonizacyjnej w żołądku i unikania odpowiedzi odpornościowej gospodarza.^{128,129} W 1983 r. australijscy badacze Robin Warren i Barry Marshall potwierdzili zależność pomiędzy zakażeniem *H. pylori* a rozwojem zapalenia błony śluzowej żołądka. Badacze za to odkrycie zostali uhonorowani w 2005 r. Nagrodą Nobla w dziedzinie medycyny i fizjologii.^{130,131}

Pałeczki *H. pylori* są małymi spiralnie skręconymi, ruchliwymi Gram-ujemnymi drobnoustrojami o długości od 2 do 4 μm i szerokości od 0,5 do 1 μm wyposażonymi w 2–6 rzęsek zlokalizowanych na jednym biegunie, które zapewniają szybki ruch w lepkim środowisku śluzu pokrywającym komórki nabłonka żołądka.^{132–134} Bakterie te należą do wymagających mikroorganizmów pod względem warunków hodowli. Do wzrostu na podłożach mikrobiologicznych wymagają warunków mikroaerofilnych, przy optymalnym stężeniu 2–5% O_2 , 5–10% CO_2 i wysokiej wilgotności. Wzrost bakterii następuje w temperaturze od 34°C do 40°C, optymalnie w 37°C. *H. pylori* zaliczane są do bakterii neutrofilnych, pomimo, iż naturalnym środowiskiem ich bytowania jest kwaśne środowisko

żołądka o pH 1–2. Pałeczki *H. pylori* zdolne są przetrwać krótką ekspozycję na pH poniżej 4 w warunkach hodowlanych, ale ich namnażanie zachodzi wyłącznie w wąskim zakresie pH (5,5–8,0).^{135,136} Podłoża stałe do hodowli *H. pylori* poza agarem Columbia lub Brucella zawierają odwłóknioną krew końską lub owczą, lub surowicą płodów cielęcych. W rutynowej hodowli stosuje się mieszaniny selektywnych antybiotyków zmniejszające ryzyko rozrostu mikroflory towarzyszącej.^{135–137}

Pałeczki *H. pylori* wykształciły szereg procesów adaptacyjnych, w tym mechanizmy regulujące ekspresję genów oraz odwracalne lub nieodwracalne zmiany w genomie, wskutek mutacji punktowych, inwersji, transpozycji, translokacji, duplikacji, insercji, delecji, fuzji lub podziału genów.^{138,139}

H. pylori kolonizując powierzchnie błon śluzowych żołądka lub dwunastnicy penetrują barierę śluzu, gdzie lokalizują się w mikroniszach i miejscowo alkalizują pH. W takich warunkach bakterie namnażają się i wchodzi w interakcje z komórkami nabłonka żołądka lub komórkami odpornościowymi gospodarza (Ryc. 6). Większość pałeczek *H. pylori* pozostaje w warstwie śluzowej żołądka, ale średnio 20% bakterii jest związanych z komórkami nabłonkowymi żołądka.¹⁴⁰ Kluczowymi czynnikami umożliwiającymi *H. pylori* przetrwanie w warstwie śluzowej i rozkład jej komponentów są zdolność ruchu i produkcja mucynazy zależnej od jonów cynku, a także tropizm do cząsteczek chemotaktycznych tj. wodorowęglan sodu, mocznik, chlorek sodu i niektórych aminokwasów.¹⁴¹



Ryc. 6. Przebieg zakażenia *H. pylori* i interakcji tych bakterii z komórkami gospodarza.

Aby uchronić się przed działaniem kwasu żołądkowego, bakterie *H. pylori* wytwarzają ureazę, która hydrolizuje mocznik do amoniaku (NH_3) i dwutlenku węgla (CO_2), co w konsekwencji prowadzi do miejscowej neutralizacji kwaśnego środowiska i utworzenia warstwy buforującej wokół bakterii. Ureaza zmniejsza także lepkość śluzu żołądkowego.^{142,143} W kolejnym etapie kolonizacji *H. pylori* przylegają do komórek nabłonka żołądka, łącząc się adhezynami z receptorami komórek gospodarza. Do najlepiej zbadanych adhezyn *H. pylori* należy adhezyna BabA (*blood group antigen-binding adhesin*) wiążąca fukozylowane antygeny grupowe krwi Lewis^b na komórkach nabłonka żołądka, oraz adhezyna SabA (*sialic acid-binding adhesin*), wiążąca sialowane antygeny Lewis^x gospodarza, których ekspresja w stanach zapalnych jest nasiloną na powierzchni komórek nabłonkowych.^{144,145}

Do głównych białkowych czynników wirulencji *H. pylori* należą białko cytotoksyczne CagA (*cytotoxin-associated gene A protein*) oraz cytotoksyna wakuolizująca VacA (*vacuolating cytotoxin A*).¹⁴⁶ CagA jest białkiem o masie 128–145 kDa kodowanym na wyspie patogeniczności *cag* (*cag PAI, cag pathogenicity island*), gdzie zlokalizowane są geny dla systemu sekrecji typu IV, który umożliwia wstrzyknięcie CagA do komórek gospodarza. Białko CagA po wnikięciu do komórek nabłonka żołądka przyczynia się do rozregulowania wielu szlaków sygnałowych, takich jak szlak kinazy aktywowanej mitogenami MAPK (MAPK, *mitogen-activated protein kinases*), szlak kinazy 3-fosfatydyloinozytolu i kinazy białkowej AKT (PI3K/Akt, *phosphoinositide-3-kinase/Akt*), ścieżka sygnałowa czynnika jądrowego κ B (NF- κ B, *nuclear factor kappa-light-chain-enhancer of activated B cells*), ścieżka Wnt/ β -kateniny oraz szlak JAK-STAT (*Janus kinase-Signals transducer and activator of transcription*). W efekcie dochodzi do patologicznych zmian w morfologii komórek gospodarza, ich nadmiernej proliferacji oraz zaburzeń adhezji i polarności.^{147,148} Ponadto CagA jest prozapalnym białkiem immunogennym, które stymuluje produkcję IL-8 przez komórki nabłonka żołądka, co skutkuje naciekiem neutrofilów i makrofagów do obszaru objętego stanem zapalnym, wytwarzaniem przez te komórki nadmiernej ilości ROS, co z kolei zwiększa ryzyko uszkodzenia DNA.¹⁴⁹ Interakcje CagA z komórkami nabłonkowymi żołądka mogą prowadzić do indukcji procesów związanych z nowotworzeniem, do których należą: nadmierna proliferacja komórek, unikanie supresorów wzrostu, nasilenie inwazyjności, odporność na apoptozę, niestabilność i zmienność genomu, a także utrwalenie zapalenia.^{150,151} Innym kluczowym czynnikiem wirulencji większości szczepów *H. pylori* jest wydzielnicza cytotoksyna VacA o masie 88 kDa zwiększająca przepuszczalność błony komórkowej komórek nabłonka żołądka, co skutkuje zaburzeniem osmozy i wpływem anionów oraz małych cząsteczek, w tym chlorków, mocznika i wodorowęglanów do przestrzeni zewnątrzkomórkowej. Negatywny wpływ VacA na komórki obejmuje powstawanie dużych wakuoli wewnątrzkomórkowych, indukcję apoptozy i autofagii, hamowanie proliferacji limfocytów T i B, hamowanie aktywności makrofagów, eozynofików, mastocytów oraz komórek dendrytycznych przez co osłabione zostają reakcje odpornościowe gospodarza.^{152–154} Ingerencja w przebieg szlaków przekazywania sygnału i zaburzenie funkcji mitochondriów przez VacA prowadzą do apoptozy makrofagów i monocytów. Kumulatywne efekty wywołane przez VacA hamują zdolność tych komórek do pochłaniania i niszczenia *H. pylori*. Oprócz działania immunosupresyjnego, VacA stymuluje ekspresję prozapalnej cyklooksygenazy 2 (COX-2, *cyclooxygenase-2*) w makrofagach i neutrofilach.^{154,155}

Pałeczki *H. pylori* wytwarzają LPS o unikalnych właściwościach biologicznych, wynikających z obniżonej acylacji i fosforylacji lipidu A, w porównaniu do typowych enterobakteryjnych lipopolisacharydów. Zaburzenie rozpoznawania LPS *H. pylori* przez receptory Toll-podobne (TLR, *toll-like receptors*) typu 4 skutkuje ograniczoną zdolnością do indukowania wytwarzania cytokin, tlenku azotu i prostaglandyny E₂ przez makrofagi, osłabieniem fagocytozy oraz aktywności cytotoksycznej limfocytów T i naturalnych komórek zabijających (NK, *natural killer*) w związku z hamowaniem prezentacji antygeny przez dojrzałe makrofagi.¹⁵⁶⁻¹⁵⁸ Uwalnianie LPS z powierzchni *H. pylori* do niszy kolonizacyjnej może odgrywać ważną rolę we wzbudzaniu zarówno miejscowej, jak i ogólnoustrojowej odpowiedzi zapalnej poprzez bezpośrednie interakcje LPS-komórka, za pośrednictwem innych receptorów lub pośrednio poprzez cytokiny.^{159,160} LPS *H. pylori* stymuluje aktywację szlaku NF-κB i wydzielanie prozapalnej, chemotaktycznej IL-8 zarówno w komórkach nabłonkowych, jak i odpornościowych, w sposób niezależny od CagA.¹⁶¹ LPS *H. pylori* zwiększa aktywność oksydazy fosforanu dinukleotydu nikotynamidoadeninowego i ekspresję TLR4 na powierzchni komórek nabłonka żołądka, co prowadzi do podwyższenia i utrwalenia toksycznego dla komórek gospodarza stresu oksydacyjnego. Ponadto LPS stymuluje makrofagi do wytwarzania poliamin poprzez indukcję arginazy i dekarboksylazy ornityny, prowadząc do ich apoptozy.¹⁶² Znana jest także aktywność proapoptotyczna LPS *H. pylori* względem komórek nabłonka żołądka i fibroblastów zależna od wzrostu aktywności kaspazy 3 i białka Bax (*B-cell lymphoma-2 associated X*), obniżenia wytwarzania przeciwapoptotycznych białek Bcl-xL i Bcl-2 (*B-cell lymphoma 2*), a także zahamowania wytwarzania IL-33.¹⁶³

W świetle powikłań zdrowotnych wynikających z zakażenia *H. pylori* niepokój budzi rosnąca oporność izolatów na powszechnie stosowane antybiotyki tj. klarytromycyna (CLR), metronidazol (MET), lewofloksacyna (LEV) i amoksycylina.¹⁶⁴ Profil oporności *H. pylori* na antybiotyki jest uzależniony od regionu zamieszkania i wieku osoby zakażonej. W Polsce odsetek szczepów lekoopornych na CLR, MTZ i LEV izolowanych od dorosłych wynosi odpowiednio 30,6%, 46,9% i 18,4%, natomiast u izolatów pochodzących od dzieci 54,5%, 31,8% i 9,1%.¹⁶⁵

Rosnąca antybiotykooporność *H. pylori*, w świetle poważnych konsekwencji zdrowotnych zakażeń wywoływanych przez te bakterie, stanowi przesłankę do poszukiwania i badania alternatywnych substancji bioaktywnych, w tym metabolitów bakteryjnych, do wspomaganie eradykacji *H. pylori*, odwracania efektów immunosupresyjnych

i cytotoksycznych wywoływanych przez te bakterie i ich komponenty, jak również wspomaganie procesów naprawczych nabłonka żołądka.¹⁶⁶⁻¹⁶⁸ Dotychczasowe wyniki badań nad aktywnością biologiczną bakteryjnych melanin pozwalają przypuszczać, że PyoM *P. aeruginosa* może spełniać powyższe wymagania. Nie mniej, aktualne doniesienia literaturowe nie dostarczają pełnych dowodów dla modelu zakażenia *H. pylori*. W związku z powyższym stawiane tezy wymagają potwierdzenia w badaniach eksperymentalnych.

Biologia tkanki kostnej i poszukiwanie nowych stymulatorów procesów osteoindukcyjnych

Kość to zmineralizowana tkanka łączna odpowiadająca za kluczowe funkcje i procesy fizjologiczne w organizmie, takie jak kształt ciała i poruszanie, podtrzymywanie i ochrona narządów oraz tkanek miękkich, funkcje syntetyczne związane z erytropoezą i limfopoezą, a także funkcje metaboliczne, w tym magazynowanie związków mineralnych, regulacja metabolizmu wapnia i fosforanów oraz utrzymanie homeostazy hormonalnej.^{169,170} Głównymi komórkami budującymi tkankę kostną są osteoblasty, osteocyty oraz osteoklasty. Pomimo litej i solidnej budowy, tkanka kostna ulega niezwykle dynamicznym procesom przebudowy zachodzącym z udziałem kościotwórczych osteoblastów i resorbujących osteoklastów.¹⁷¹ W remodelingu kości konieczne są stałe interakcje osteoblastów i osteoklastów, które muszą być skoordynowane w czasie i przestrzeni, aby utrzymać równowagę przebudowy tkanki kostnej. W wyniku przebudowy, stara lub uszkodzona kość zostaje zastąpiona nową tkanką kostną, bez jakiegokolwiek zmiany jej kształtu.¹⁷²

Osteoblasty wywodzące się z mezenchymalnych komórek macierzystych stanowią 4–6% całej puli komórek kostnych, które w głównej mierze odpowiadają za tworzenie nowej tkanki kostnej. Osteoblasty wykazują cechy morfologiczne charakterystyczne dla komórek syntetyzujących białka, posiadają obfitą szorstką siateczkę śródplazmatyczną i rozbudowany aparat Golgiego. Komórki kościotwórcze wytwarzają szeroką gamę pęcherzyków wydzielniczych odpowiadających za sekrecję organicznej substancji międzykomórkowej – osteoidu, zapewniającej elastyczność i wytrzymałość kości.¹⁷³

Cykl życiowy komórek kościotwórczych może prowadzić do ich przekształcenia w osteocyty lub komórki wyściółkowe, lub apoptozy. Druga ścieżka uruchamiana jest gdy osteoblasty nie spełniają kryteriów różnicowania i dotyczy 50–70% populacji komórek kościotwórczych.^{171,174} Zewnątrzkomórkowa macierz kostna produkowana jest w dwóch etapach: sekrecji niezmineralizowanego, gęstego i silnie usieciowanego osteoidu, a następnie jego mineralizacji poprzez akumulację fosforanu wapnia w postaci hydroksyapatytu (HA, *hydroxyapatite*).¹⁷⁵ Osteoblasty wytwarzają szereg białek zewnątrzkomórkowych, w tym kolagen typu I (COL1, *type I collagen*), który stanowi ponad 90% białek macierzy kostnej oraz białka niekolagenowe tj. osteokalcynę (OC, *ostoecalcin*), osteonektynę (ON, *osteonectin*), osteopontynę (OPN, *osteopontin*), fosfatazę alkaliczną (ALP, *alkaline phosphatase*), sialoproteinę kostną i ligand aktywatora receptora jądrowego czynnika κ B

(RANKL, *receptor activator of nuclear factor κ B ligand*). Białka te pełnią rolę stelaża dla osteocytów, jak również odpowiadają za interakcję i sygnalizację międzykomórkową, modyfikując aktywność metaboliczną osteoblastów, osteoklastów i osteocytów.¹⁷⁶ OC reguluje tworzenie kości, zapewnia wysoką gęstość tkanki kostnej oraz moduluje aktywność osteoklastów i ich prekursorów. ON i OPN modułują aktywność czynników wzrostowych, wpływają na adhezję komórek oraz uczestniczą w procesie mineralizacji i depozycji HA. Sialoproteina kostna wiąże jony wapnia biorąc bezpośredni udział w mineralizacji kości, natomiast ALP katalizuje hydrolizę estrów fosforanowych w środowisku zasadowym, uwalniając nieorganiczne fosforany będące prekursorami w mineralizacji macierzy kostnej.^{174,177} Osteoblasty odpowiedzialne są także za wydzielanie i odkładanie w macierzy zewnątrzkomórkowej białek BMP należących do nadrodziny transformujących czynników wzrostu β (TGF- β , *transforming growth factor β*), które regulując proliferację, różnicowanie i śmierć komórek osteoprogenitorowych, osteoblastów, osteoklastów oraz chondrocytów.¹⁷⁸

Drugą, istotną subpopulacją komórek kostnych biorących udział w procesie przebudowy i regeneracji tkanki kostnej są osteoklasty, będące wielojądrzastymi komórkami pochodzącymi z komórki macierzystej hemopoety, które ulegają różnicowaniu pod wpływem czynnika stymulującego tworzenie kolonii makrofagów (M-CSF, *macrophage colony-stimulating factor*), uwalnianego przez komórki osteoprogenitorowe i osteoblasty, a także czynnika RANKL wydzielanego przez osteoblasty, osteocyty i komórki wyściółkowe. Istotną rolę w inicjowaniu działania resorpcyjnego osteoklastów pełnią także IL-1 i TNF- α .^{179,180} Mimo, że osteoklasty stanowią stosunkowo niewielki procent ogółu komórek kostnych to odgrywają istotną rolę w procesach fizjologicznych kości. Osteoklasty biorą udział w resorpcji tkanki kostnej, procesie który przyczynia się do jej przebudowy w adaptacyjnej odpowiedzi na wzrost lub zmieniające się obciążenie mechaniczne kości, a także uczestniczą w utrzymaniu homeostazy wapnia we krwi.¹⁸¹ Osteoklasty, jako wielojądrzaste komórki fagocytarne, charakteryzują się metabolizmem, który ułatwia demineralizację i degradację macierzy kostnej. Resorpcja kości zależy od wydzielanych przez osteoklasty jonów wodorowych (H^+) i chlorkowych (Cl^-), a także katepsyny K (CtsK, *cathepsin K*), kwaśnej fosfatazy odpornej na winian (TRAP, *tartrate-resistant acid phosphatase*) i metaloproteinazy macierzy pozakomórkowej 9 (MMP9, *matrix metalloproteinases 9*). Jony H^+ i Cl^- zakwaszają przedział resorpcyjny w środowisku osteoklastów rozpuszczając hydroksyapatyt, podczas gdy CtsK, TRAP i MMP9 trawią macierz białkową.^{180,182}

Kość, jako tkanka podlegająca ciągłej przebudowie dzięki precyzyjnym procesom tworzenia i resorpcji kości wykazuje wysoką zdolność do regeneracji, która zapewnia ciągłość strukturalną i wytrzymałość mechaniczną po urazie.^{183,184} Naturalna zdolność do regeneracji kości może zostać zaburzona przez zabiegi chirurgiczne, choroby nowotworowe, osteopenię, osteoporozę, infekcję tkanki kostnej, a także podeszły wiek, nieodpowiednią dietę lub zmiany poziomu hormonów.¹⁸⁵ W 2019 r. liczbę nowych przypadków złamań kości na świecie oszacowano na 178 milionów, co oznacza 33,4% wzrost od 1990 r.¹⁸⁶ Według szacunków Bone Health and Osteoporosis Foundation do 2025 r. co roku będzie przybywało około 3 milionów nowych, trudno gojących się złamań osteoporotycznych o koszcie leczenia wynoszącym 25,3 miliarda dolarów.¹⁸⁷ Wzrastająca liczba złamań kości oraz obserwowane tendencje w zakresie rosnących kosztów ich leczenia skłaniają badaczy do poszukiwania i charakteryzowania substancji stymulujących regenerację tkanki kostnej, o potencjalnym zastosowaniu w medycynie regeneracyjnej, osobno lub w połączeniu z biokompozytami.¹⁸⁷⁻¹⁸⁹

Jedną ze strategii przyjmowaną podczas kierunkowania badań w tym zakresie jest podejście stosowane m.in. przy opracowaniu szczepionek profilaktycznych, czyli zastosowanie czynnika szkodliwego w innej postaci lub podawanego na innej drodze w celu osiągnięcia efektu terapeutycznego. Jako substancja wspierająca regenerację tkanki kostnej, w oparciu o inicjowanie lub nasilenie procesów osteoindukcyjnych (pobudzenie osteogenego różnicowania mezenchymalnych komórek macierzystych w kierunku osteoblastów) i/lub osteokondukcyjnych (stymulacja adhezji, proliferacji i tworzenia macierzy kostnej przez osteoblasty)¹⁹⁰, rozważana jest bakteryjna PyoM, będąca bezpiecznym biomimetykiem złogów ochronotycznych powstających w przebiegu alkaptonurii (AKU). AKU jest rzadką chorobą metaboliczną, dziedziczną w sposób autosomalny recesywny, wynikającą z niedoboru oksydazy HGA w metabolizmie tyrozyny.¹⁹¹ W przebiegu AKU, HGA nie ulega przekształceniu do kwasu fumaryloacetoctowego, a z czasem polimeryzuje i gromadzi się w tkankach kolagenowych prowadząc do ochronozy. Proces powstawania osadów ochronotycznych nie jest w pełni poznany. Uważa się, że HGA polimeryzuje do benzochinonu, zanim przyjmie ostateczną postać polimeryczną związaną z kolagenem.^{191,192} Jednym z najbardziej typowych objawów AKU jest przewlekłe zwyrodnienie stawów, objawiające się zmianami strukturalnymi i nadmierną mineralizacją zachodzącą w tkance chrzęstnej.¹⁹³ Nagromadzenie polimerów HGA powoduje odkładanie się HA, minerału odpowiedzialnego za zwapnienie kości, co

dotychczas dodatkowo utwardza tkankę łączną.¹⁹⁴ Powyższe informacje skłaniają do podjęcia badań dla potwierdzenia możliwości kontrolowanego wykorzystania PyoM, będącej bakteryjnym biomimetykiem polimerycznych złogów ochronotycznych, jako stymulatora procesów regeneracji tkanki kostnej.

Założenia i cele pracy

Niniejsza praca doktorska poświęcona jest fizykochemicznej i biologicznej charakterystyce piomelaniny izolowanej z bakterii *P. aeruginosa* w kontekście interakcji tego polimeru z komórkami eukariotycznymi i bakteryjnymi, w celu weryfikacji ukierunkowanych właściwości tego bakteryjnego barwnika: przeciwbakteryjnych, cytoprotekcyjnych, przeciwapoptotycznych, immunomodulujących i stymulujących regenerację tkanek.

Zakażenie *H. pylori* niesie za sobą szereg negatywnych skutków wobec komórek gospodarza. Efekty te obejmują m.in. działanie cytotoksyczne związane z nadmiernym i przetrwałym stresem oksydacyjnym, który może powodować uszkodzenie materiału genetycznego komórek nabłonka żołądka, fibroblastów lub komórek odpornościowych i kierować je na drogę apoptozy. Zaburzona zostaje ciągłość bariery nabłonkowej żołądka, a pałeczki *H. pylori* unikają odpowiedzi odpornościowej gospodarza, m.in. poprzez zahamowanie procesu fagocytozy. Wzrost antybiotkooporności pałeczek *H. pylori*, w powiązaniu z wywoływanymi przez nie powikłaniami poinfekcyjnymi, ukierunkowuje badania na poszukiwanie nowych substancji biologicznie aktywnych, w tym pochodzenia bakteryjnego, hamujących wzrost tych bakterii oraz wykazujących właściwości cytoprotekcyjne, m.in. poprzez neutralizację ROS i nasilających procesy regeneracji komórek nabłonkowych żołądka.

Wzrastająca liczba trudno gojących się złamań kości, wymagających interwencji chirurgicznych, nasilenie osteoporozy wraz z wiekiem, a także rosnące koszty leczenia tych przypadków medycznych, skłaniają badaczy do poszukiwania nowych substancji stymulujących regenerację tkanki kostnej, które można by było stosować samodzielnie lub jako składnik biokompozytów. Podobieństwo strukturalne PyoM do ochronotycznych złogów powstających w AKU, które przyczyniają się do nadmiernej mineralizacji tkanki chrzęstnej, a także dostępne dane literaturowe, wskazujące na właściwości przeciwdrobnoustrojowe, przeciwutleniające i wspierające regenerację tkanek przez PyoM, stanowią istotną przesłankę do zbadania tego bakteryjnego barwnika jako stymulatora procesów osteoindukcyjnych i osteokondukcyjnych.

Biorąc pod uwagę powyższe, w części eksperymentalnej niniejszej pracy wyznaczono dwa nadrzędne cele dotyczące zbadania bakteryjnego polimeru jakim jest PyoM pod kątem jego właściwości prozdrowotnych i potencjalnego medycznego zastosowania:

- do niwelowania skutków działania cytotoksycznego wybranych komponentów *H. pylori* wobec komórek nabłonkowych żołądka, stymulacji procesów odnowy

komórek nabłonkowych żołądka oraz przywrócenia aktywności fagocytarnej komórek monocytarno-makrofagowych zahamowanej przez te komponenty na modelu *in vitro*,

- do ukierunkowanej stymulacji procesów regeneracji tkanki kostnej na modelu osteoblastów człowieka w hodowlach *in vitro*.

Wyznaczone cele szczegółowe obejmowały:

1. Opracowanie metody izolacji i oczyszczania PyoM rozpuszczalnej i nierozpuszczalnej w wodzie z hodowli *P. aeruginosa* na podłożu płynnym. Charakterystykę otrzymanych produktów w zakresie właściwości fizykochemicznych, termicznych i biologicznych związanych z bezpieczeństwem *in vitro* na modelu referencyjnych fibroblastów myszy lub monocytów człowieka oraz z bezpieczeństwem *in vivo* na modelu *Galleria mellonella* – [P.I.].
2. Charakterystykę właściwości przeciwbakteryjnych obu form PyoM przeciwko referencyjnym i klinicznym szczepom *H. pylori*, oraz weryfikację w badaniach *in vitro* właściwości cytoprotekcyjnych piomelanin, z uwzględnieniem ograniczenia wytwarzania ROS i apoptozy komórek nabłonka żołądka, fibroblastów oraz monocytów człowieka, jak również przydatności piomelaniny do wspomagania fagocytozy bakterii – [P.II.].
3. Charakterystykę właściwości osteoindukcyjnych i proregeneracyjnych otrzymanych wariantów PyoM w badaniach na modelu osteoblastów człowieka, a także właściwości przeciwbakteryjnych przeciwko klinicznym szczepom *Staphylococcus* sp. wyizolowanym z zakażonej tkanki kostnej – [P.III.].
4. Wskazanie potencjalnych stymulatorów regeneracji tkanki kostnej, z uwzględnieniem metabolitów bakteryjnych, jako przyszłych modyfikatorów biokompozytów, w celu zwiększenia efektywności odbudowy kości po ich implantacji – [P.IV.].

Materiały i metody

Materiały:**1. Linie komórkowe:**

- Fibroblasty myszy L929 (ATCC® CCL-1™, Manassas, Wirginia, USA), [P.I-II.]
- Monocyty człowieka THP-1 (ATCC® TIB-202™, Manassas, Wirginia, USA), [P.I-II.]
- Reporterowe monocyty człowieka THP1-Blue™ NF-κB (InvivoGen, San Diego, Kalifornia, USA), [P.I.]
- Komórki nabłonkowe gruczołakoraka żołądka człowieka AGS (ATCC® CRL-1739™, Manassas, Wirginia, USA), [P.II.]
- Osteoblasty człowieka hFOB 1.19 (ATCC® CRL-3602™, Manassas, Wirginia, USA). [P.III.]

2. Szczepy bakteryjne:

- Piomelanino-twórczy szczep *P. aeruginosa* Mel + (Katedra Immunologii i Biologii Infekcyjnej, Uniwersytet Łódzki, Łódź, Polska), [P.I-III.]
- Referencyjny szczep *H. pylori* CCUG 17874 (Culture Colection, University of Gothenburg, Gothenburg, Szwecja), [P.II.]
- Kliniczne szczepy *H. pylori* M91 i M102 (Katedra i Zakład Mikrobiologii, Uniwersytet Medyczny im. Piastów Śląskich we Wrocławiu, Wrocław, Polska, dzięki uprzejmości prof. dr hab. Grażyny Gościniak), [P.II.]
- Referencyjny szczep *S. aureus* 29213 (ATCC® 29213™, Manassas, Wirginia, USA), [P.III.]
- Kliniczne szczepy gronkowców wyizolowane z zakażonej tkanki kostnej: *S. aureus* MRSA i *S. felis* (Katedra Immunologii i Biologii Infekcyjnej, Uniwersytet Łódzki, Łódź, Polska). [P.III.]

3. Model *in vivo*:

- *Galleria mellonella* (Katedra Ekologii i Zoologii Kręgowców, Uniwersytet Łódzki, Łódź, Polska, dzięki uprzejmości dr hab. Mariusza Tszydla). [P.I.]

4. Stymulatory:

- Bakteryjna piomelanina rozpuszczalna w wodzie (PyoM_{sol}, Katedra Immunologii i Biologii Infekcyjnej, Uniwersytet Łódzki, Łódź, Polska), [P.I-III.]
- Bakteryjna piomelanina nierozpuszczalna w wodzie (PyoM_{insol}, Katedra Immunologii i Biologii Infekcyjnej, Uniwersytet Łódzki, Łódź, Polska), [P.I-III.]

- Syntetyczna piomelanina (sPyoM, Katedra Immunologii i Biologii Infekcyjnej, [P.I.]
Uniwersytet Łódzki, Łódź, Polska),
- LPS *H. pylori* CCUG 17874 (National University of Ireland, Galway, Irlandia, dzięki [P.II.]
uprzejmości prof. A.P. Morana),
- LPS *E. coli* O55:B5 (Sigma Aldrich, Darmstadt, Niemcy), [P.II.]
- Doksorubicyna (DOX, Sigma Aldrich, Darmstadt, Niemcy). [P.III.]

Metody:

1. Izolacja PyoM z hodowli *P. aeruginosa* Mel+, oczyszczenie oraz uzyskanie PyoM [P.I-III.]
w formie rozpuszczalnej lub nierozpuszczalnej w wodzie.
2. Synteza chemiczna PyoM z prekursora HGA w środowisku zasadowym. [P.I.]
3. Absorpcyjna spektroskopia w podczerwieni z transformacją Fouriera (FT-IR) [P.I.]
– technika zastosowana w celu scharakteryzowania struktury PyoM i obecności
grup funkcyjnych w badanych wariantach PyoM.
4. Termograwimetria (TGA) i skaningowa kalorymetria różnicowa (DSC) – techniki [P.I.]
użyte w celu określenia termostabilności PyoM.
5. Test redukcji MTT (*3-(4,5-dimethylthiazol-2-yl)-2,5-diphenyltetrazolium bromide*) [P.I-III.]
– test do oceny aktywności metabolicznej i żywotności fibroblastów L929,
monocytów THP-1, komórek nabłonkowych żołądka AGS i osteoblastów hFOB
1.19, traktowanych PyoM lub PyoM w kostymulacji z LPS *E. coli* lub LPS
H. pylori.
6. Test aktywacji szlaku NF-κB z wykorzystaniem reporterowych monocytów [P.I.]
stymulowanych PyoM.
7. Test redukcji resazuryny zastosowany do oceny żywotności bakterii *H. pylori* [P.II-III.]
lub *Staphylococcus* sp., traktowanych PyoM.
8. Test biokompatybilności i toksyczności układowej na modelu *Galleria mellonella* [P.I.]
z wyznaczeniem wskaźnika HISS (*Health Index Scoring System*) na podstawie
oceny żywotności, ruchliwości, melanizacji i formowania kokonu po traktowaniu
PyoM.

9. Sonda fluorescencyjna H₂DCFDA (*2,7-dichlorodihydrofluorescein diacetate*) [P.II.]
zastosowana do ilościowego oznaczania wewnątrzkomórkowych reaktywnych form tlenu w komórkach nabłonka żołądka AGS traktowanych PyoM lub PyoM w kostymulacji z LPS *E. coli* lub LPS *H. pylori*.
10. Test gojenia rany do oceny tempa migracji komórek nabłonka żołądka lub-osteoblastów w środowisku PyoM. [P.II-III.]
11. Test TUNEL (*terminal deoxynucleotidyl transferase dUTP nick end labelling*) do oznaczania nasilenia apoptozy w hodowlach komórek nabłonka żołądka AGS traktowanych PyoM lub PyoM i LPS *E. coli*, lub LPS *H. pylori*, a także w hodowlach osteoblastów hFOB 1.19 traktowanych PyoM lub PyoM i doksorubicyną. [P.II-III.]
12. Fluorymetryczny test pHrodo™ Green *E. coli* BioParticles™ lub znakowane fluorescencyjnie pałeczki *H. pylori* zastosowane do określenia aktywności fagocytarnej monocytów stymulowanych PyoM, lub kostymulowanych PyoM i LPS *E. coli*, lub LPS *H. pylori*. [P.II.]
13. Test CyQUANT™ do oceny nasilenia proliferacji osteoblastów hFOB 1.19 w hodowlach długoterminowych. [P.III.]
14. Test hydrolizy p-NPP (*paranitrophenylphosphate*) zastosowany do oceny aktywności ALP produkowanej przez osteoblasty hFOB 1.19 stymulowane PyoM. [P.III.]
15. Immunoenzymatyczny test fazy stałej (ELISA, *enzyme-linked immunosorbent assay*) do oceny stężenia cytokin (IL-6, IL-10 or TNF- α) wydzielanych przez osteoblasty hFOB 1.19 stymulowane PyoM w długoterminowych hodowlach. [P.III.]
16. Sekwencjonowanie kwasu rybonukleinowego (RNA, *ribonucleic acid*) i analiza transkryptomyczna osteoblastów hFOB 1.19 stymulowanych PyoM. [P.III.]

**Publikacje wchodzące
w skład rozprawy
doktorskiej**



Article

In Vitro and In Vivo Biocompatibility of Natural and Synthetic *Pseudomonas aeruginosa* Pyomelanin for Potential Biomedical Applications

Mateusz M. Urbaniak ^{1,2} , Małgorzata Gazińska ³ , Karolina Rudnicka ¹ , Przemysław Płociński ¹ ,
Monika Nowak ¹ and Magdalena Chmiela ^{1,*}

¹ Department of Immunology and Infectious Biology, Faculty of Biology and Environmental Protection, University of Łódź, 90-237 Łódź, Poland

² The Bio-Med-Chem Doctoral School, University of Lodz and Lodz Institutes of the Polish Academy of Sciences, 90-237 Łódź, Poland

³ Department of Engineering and Technology of Polymers, Faculty of Chemistry, Wrocław University of Science and Technology (WUST), 50-370 Wrocław, Poland

* Correspondence: magdalena.chmiela@biol.uni.lodz.pl

Abstract: Bacteria are the source of many bioactive compounds, including polymers with various physiological functions and the potential for medical applications. Pyomelanin from *Pseudomonas aeruginosa*, a nonfermenting Gram-negative bacterium, is a black–brown negatively charged extracellular polymer of homogentisic acid produced during L-tyrosine catabolism. Due to its chemical properties and the presence of active functional groups, pyomelanin is a candidate for the development of new antioxidant, antimicrobial and immunomodulatory formulations. This work aimed to obtain bacterial water-soluble (Pyo_{sol}), water-insoluble (Pyo_{insol}) and synthetic (sPyo) pyomelanin variants and characterize their chemical structure, thermosensitivity and biosafety in vitro and in vivo (*Galleria mellonella*). FTIR analysis showed that aromatic ring connections in the polymer chains were dominant in Pyo_{sol} and sPyo, whereas Pyo_{insol} had fewer C_{ar}-C_{ar} links between rings. The differences in chemical structure influence the solubility of various forms of pyomelanins, their thermal stability and biological activity. Pyo_{sol} and Pyo_{insol} showed higher biological safety than sPyo. The obtained results qualify Pyo_{sol} and Pyo_{insol} for evaluation of their antimicrobial, immunomodulatory and proregenerative activities.

Keywords: pyomelanin; *Pseudomonas aeruginosa*; chemical structure; biocompatibility



Citation: Urbaniak, M.M.; Gazińska, M.; Rudnicka, K.; Płociński, P.; Nowak, M.; Chmiela, M. In Vitro and In Vivo Biocompatibility of Natural and Synthetic *Pseudomonas aeruginosa* Pyomelanin for Potential Biomedical Applications. *Int. J. Mol. Sci.* **2023**, *24*, 7846. <https://doi.org/10.3390/ijms24097846>

Academic Editor: Marco Tatullo

Received: 27 January 2023

Revised: 17 April 2023

Accepted: 24 April 2023

Published: 25 April 2023



Copyright: © 2023 by the authors. Licensee MDPI, Basel, Switzerland. This article is an open access article distributed under the terms and conditions of the Creative Commons Attribution (CC BY) license (<https://creativecommons.org/licenses/by/4.0/>).

1. Introduction

Pseudomonas aeruginosa, a nonfermenting Gram-negative bacterium that is widespread in the environment and is an opportunistic pathogen, produces a variety of pigments, including pyocyanin, pyorubin, pyoverdine and pyomelanin. Pyomelanin is a negatively charged extracellular polymer of homogentisic acid (HGA) that is produced during L-tyrosine catabolism [1]. L-tyrosine is converted to 4-hydroxyphenylpyruvic acid (4-HPPA) by tyrosine aminotransferase, and then 4-HPPA is biotransformed to HGA by 4-hydroxyphenylpyruvate dioxygenase. Pyomelanin then forms spontaneously when secreted HGA autoxidizes to benzoquinone acetic acid, which then undergoes polymerization to form pyomelanin chains. Similar to chemically synthesized polymers of HGA, pyomelanin is a dark brown to black pigment [2,3]. The chemical structure of melanins, including pyomelanin, determines their oxidizing (quinone groups) and reducing (hydroxyquinone groups) properties that allow them to accept or donate electrons [4,5].

The primary function of microbial melanins is to protect cells from UV radiation [6]. In addition, pyomelanin increases the effectiveness of bacterial adhesion to surfaces, thus supporting the formation of biofilms and the extracellular transfer of electrons [7]. The

production of pyomelanin by bacteria in the marine bacterial genus *Pseudoalteromonas* is induced during biofilm formation and under heat stress, suggesting that this pigment is involved in the adaptation of these bacteria to grow in a hostile ecological niche [8]. Pyomelanin is produced by clinical *P. aeruginosa* isolates from patients with chronic lung infections. It remains unclear whether pyomelanin is relevant to the pathogenicity of these bacteria; its production is linked to a reduction in oxidative stress, which may be an important trait to improve bacterial survival within pulmonary macrophages [9,10]. Additionally, melanins of *Aspergillus fumigatus* protect the fungus from host reactive oxygen intermediates [11]. A study by Fonseca et al. revealed that metal binding and metal reduction by pyomelanin are necessary for iron acquisition [7]. Due to the antimicrobial and antioxidant activities of microbial melanins, including pyomelanin produced by *P. aeruginosa*, they can be used in the food industry to coat packaging to prolong food expiration dates [5]. Bacterial melanins can be exploited as dyes and colorants and used in cosmetics as sunscreen and oxidative stress-reducing substances, whereas in agriculture, they may help to retain metals and improve iron availability in the soil [12]. These compounds are promising candidates for the design of new drugs, including antitumor drugs, vaccine antigen carriers, adjuvants and optoacoustic imaging contrasts [13–15]. The treatment of infections with pyomelanin with an accompanying inflammatory reaction driven by oxidative stress has also been considered [16]. The increased sensitivity of several bacterial pathogens to antibiotics in the milieu of pyomelanin has also been demonstrated, as well as the antimicrobial activity of melanin itself and its iron ion complexes against *Helicobacter pylori*, *Candida albicans* and human immunodeficiency virus (HIV) [17,18].

Eukaryotic and bacterial melanins may exhibit immunomodulatory properties. Cuttlefish melanin is able to activate and polarize dendritic cells, while human neuromelanin activates the nuclear factor kappa B (NF- κ B) signaling pathway resulting with the secretion of pro-inflammatory cytokines: tumor necrosis factor alpha (TNF- α) and interleukin (IL)-6 [19]. The role of melanin in the regulation of innate immunity in humans is potentially due to the modulation of phagocytes and complement activity, reduction in the mRNA translation of proinflammatory cytokines and interaction with effector molecules [20]. Melanization is an important part of the cuticular wound healing process in arthropods and functions as part of the innate immune system in isopods by encapsulating parasites with melanin [21]. However, negatively charged melanin isolated from *Cryptococcus neoformans* diminished fungal cell susceptibility to cationic antimicrobial peptides of phagocytes, which was correlated with the downregulation of phagocytosis and diminished secretion of TNF- α , IL-1 β , IL-6 and IL-12 as well as modulation of complement activities [22]. The potential wide range of microbial melanin applications drives studies on natural, synthetic and recombinant melanins [23].

Hypothetically, natural bacterial or synthetic formulations of pyomelanin may vary in their biological activity. Before studying different applications of pyomelanin formulations, it seems valuable to verify whether there are differences in physicochemical properties, cytocompatibility, the ability to stimulate the activation of the NF- κ B pathway and in vivo toxicity between bacterial pyomelanin and its synthetic form.

Considering the potential application of pyomelanin in medicine, the aim of this study was to characterize the biochemical and physiological properties of natural water-soluble and water insoluble pyomelanin (Pyo_{sol} and Pyo_{insol}) isolated from a culture of *P. aeruginosa* and synthetic pyomelanin (sPyo), obtained by us under laboratory conditions, for further biomedical applications. We optimized *P. aeruginosa* growth conditions for the effective production of pyomelanin, developed an isolation procedure for natural water-soluble pyomelanin and a procedure for pyomelanin synthesis. The chemical structure of the bacterial and synthetic pyomelanin was investigated by Fourier transform infrared (FTIR) spectroscopy and the thermal properties were characterized by means of differential scanning calorimetry (DSC) and thermogravimetry (TGA). The cytocompatibility of pyomelanin from both sources was determined using an in vitro model on reference L-929 fibroblasts and THP-1 human monocytes. Noncytotoxic concentrations were established

in the reference MTT reduction assay. In our in vivo biosafety study, we used the *Galleria mellonella* insect model as an alternative to rodents. Larvae of *G. mellonella* are widely used in the toxicity assessment of new biopharmaceuticals, bioactive substances and newly synthesized chemicals [24]. Due to the ability to maintain larvae in a temperature range from 20 °C to 42 °C, this insect model mimics the physiological conditions of mammals during in vivo toxicity assessment [25]. In addition, *G. mellonella* larvae provide an inexpensive and convenient way, free from legal or ethical restrictions, to assess the safety of new biomolecules, and the results generated from this model show a strong correlation with those obtained from mammalian systems. The use of *G. mellonella* larvae provides a more accurate representation of the biocompound's interactions with the host organism than studies on cell lines, which allows for the precise selection of concentrations before animal testing [26]. Furthermore, the ability of pyomelanin to activate the nuclear factor kappa B (NF-κB) signaling pathway was determined using the human recombinant monocyte model THP1-Blue™ NF-κB.

2. Results

2.1. The Efficiency of the Pyomelanin Biosynthesis and Chemical Synthesis

To determine the application potential of different pyomelanin variants, we first analyzed the extraction and synthesis efficiencies. We extracted two variants of natural pyomelanin produced by *P. aeruginosa* during growth on pyomelanin minimal medium (PMM) dedicated to these bacteria: PMM I, PMM II and pyomelanin synthesized from HGA. The efficiency of the extraction of natural pyomelanin formulations vs. the efficiency of pyomelanin synthesis is shown in Table 1. Both variants of natural pyomelanin, Pyo_{insol} and Pyo_{sol}, were produced more efficiently by *P. aeruginosa* after 7 days of growth of this bacterium on PMM II than by PMM I medium (1.79 ± 0.18 g/L and 1.22 ± 0.10 , respectively, $p < 0.05$) (Table 1). Compared to the high-efficiency bacterial biosynthesis of pyomelanin, the yield of sPyo production from HGA was equal to 0.077 ± 0.01 g/1 g HGA.

Table 1. Efficiency of the Extraction of *P. aeruginosa* Pyomelanin from Minimal Growth Media and the Synthesis of Pyomelanin from HGA.

<i>P. aeruginosa</i> Growth Medium	Pyo _{sol} [g/L]	Pyo _{insol} [g/L]	sPyo [g/1 g of HGA]
PMM I	1.13 ± 0.12	0.71 ± 0.04	0.077 ± 0.01
PMM II	1.79 ± 0.18	1.22 ± 0.10	

2.2. Identification of the Functional Groups and Linkages in Pyomelanin Molecules

The structure of the pigments was investigated by FTIR spectroscopy, a technique in which a sample's absorbance of infrared light at various wavelengths is measured to determine the structure of molecules. The infrared spectrum includes absorbance bands corresponding with the various vibrations of the sample's atoms. Each chemical molecule will produce a unique infrared spectrum. It should be mentioned that structural characterization of melanin is elusive due to its complexity and metabolic residues, such as proteins, amino acids and carbohydrates, in cases of microbial origin. The FTIR spectra of microbial Pyo_{sol} and Pyo_{insol} and synthetic sPyo are presented in Figure 1. The FTIR spectra of bacterial Pyo_{sol} and Pyo_{insol} were similar at wavenumbers higher than 1600 cm^{-1} . Between 3700 and 3000 cm^{-1} , a large absorption band resulted from overlapping -OH groups and unsaturated carbon or aromatic rings.

At lower wavenumbers, the bands with three maxima assigned to the stretching vibrations of aliphatic C-H were at 2953 , 2925 , and 2855 cm^{-1} in Pyo_{insol} and 2960 , 2944 , and 2873 cm^{-1} in Pyo_{sol}. The band at 1700 cm^{-1} corresponding to carbonyl stretching (C=O) of the COOH groups was visible in Pyo_{insol}, whereas this band was absent in Pyo_{sol}. The bands at 1631 and 1613 cm^{-1} in Pyo_{insol} and at 1601 cm^{-1} in Pyo_{sol} were typical for C=C bonds conjugated with C=O groups (quinones). At wavelengths shorter than 1600 cm^{-1} ,

the differences between the spectra of Pyo_{sol} and $\text{Pyo}_{\text{insol}}$ were more considerable. The bands at 1515 cm^{-1} ascribed to aromatic $\text{C}_{\text{ar}}\text{-H}$ bonds, and at 1441 cm^{-1} from in-plane aromatic skeletal vibrations of $\text{C}=\text{C}$, were only visible in $\text{Pyo}_{\text{insol}}$. Similarly, the band of the phenolic-OH links at 1216 cm^{-1} appeared only in the $\text{Pyo}_{\text{insol}}$ FTIR spectrum. The band associated with the O-H bonds of hydroxyl groups attached to the ring was strong at 1402 cm^{-1} in Pyo_{sol} and weak at 1385 cm^{-1} in $\text{Pyo}_{\text{insol}}$. The strong band at 1082 cm^{-1} in Pyo_{sol} and the shoulder band at 1065 cm^{-1} in $\text{Pyo}_{\text{insol}}$ could be related to the stretching of a C-O band of a primary alcohol group (phenolic groups). The strong band at 857 cm^{-1} in Pyo_{sol} and weak band at 828 cm^{-1} in $\text{Pyo}_{\text{insol}}$ were related to out-of-plane deformation vibrations of aromatic $\text{C}_{\text{ar}}\text{-H}$ bonds.

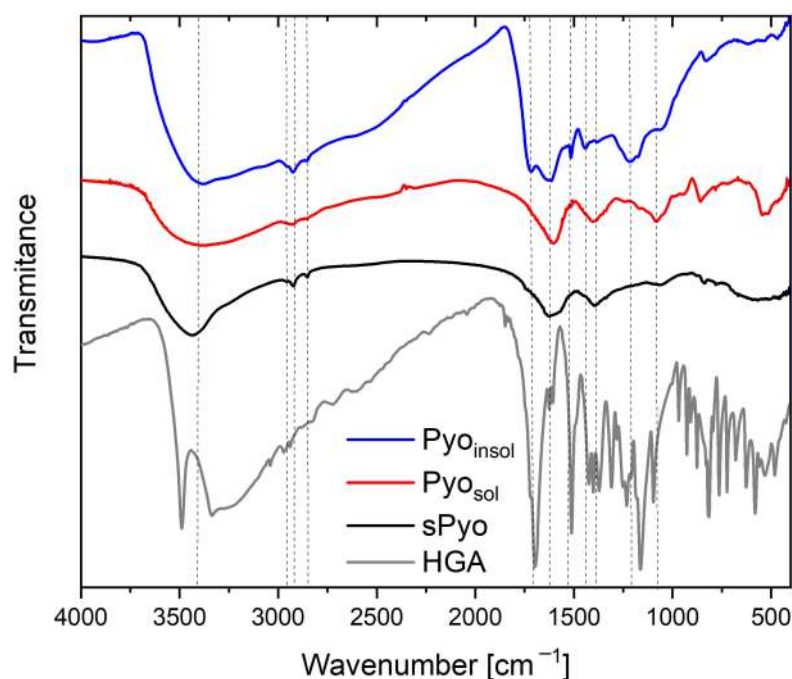


Figure 1. Fourier transform infrared (FTIR) spectra of the water-soluble pyomelanin (Pyo_{sol}), water-insoluble pyomelanin ($\text{Pyo}_{\text{insol}}$), synthetic pyomelanin (sPyo) and homogentisic acid (HGA).

The FTIR spectrum of sPyo in the range of $4000\text{--}1600\text{ cm}^{-1}$ was similar to the spectra of both types of bacterial pyomelanin, except that the band assigned to the O-H stretch had a narrower range of $3700\text{--}3300\text{ cm}^{-1}$. The bands corresponding to aliphatic C-H bonds were at 2957 , 2924 and 2852 cm^{-1} . The sPyo spectrum also presented a weak shoulder peak at 1738 cm^{-1} from COOH groups. The bands at 1515 and 1216 cm^{-1} visible for $\text{Pyo}_{\text{insol}}$ were absent, similar to that of Pyo_{sol} . There were bands at 1395 and 1062 cm^{-1} from O-H and $\text{C}_{\text{ar}}\text{-O}$ vibrations of hydroxyl groups attached to the ring, and bands from aromatic C-H bonds at 835 and 780 cm^{-1} . In the polymer chain of sPyo, there were more $\text{C}_{\text{ar}}\text{-C}_{\text{ar}}$ linkages between rings, as indicated by the absence of a band at 1515 cm^{-1} .

2.3. The Thermal Stability and Thermal Properties of Pyomelanins

To determine the thermal stability of the pigments, thermogravimetric measurements in an inert atmosphere were performed. Thermal stability is a key parameter determining the possibility of processing pyomelanin by thermal processing methods used for the fabrication of composites and blends with other thermoplastic biopolymers. The TGA curves and the first derivative of the mass with respect to time ($\text{dm}/\text{dt} = f(T)$) curves of the dyes are presented in Figure 2, and the estimated characteristic parameters of thermal degradation are collected in Table 2. Based on the shape of the TGA and first derivative curves, it can be concluded that the dyes differed in degradation mechanism. The common feature of the dyes was the presence of the first stage of mass loss occurring up to $125\text{ }^\circ\text{C}$.

The maximum rate of the first stage of mass loss, set as the maximum of the first peak on $dm/dt = f(T)$ curves, was located at a similar temperature denoted as the $T^{1st\ peak}$. This stage of mass loss could be assigned to the loss of volatile low molar mass species. The highest mass loss up to 125 °C was exhibited by Pyo_{sol} . Only at a temperature range of mass loss up to 125 °C did the endothermic effect occur for Pyo_{sol} , as indicated by the endothermic peak on the DSC curve of Pyo_{sol} (Figure 3). The temperature range of the endothermic effect, the corresponding highest mass loss in the case of Pyo_{sol} and the fact that Pyo_{sol} was isolated from the water phase, allows the assuming of the first stage of mass loss to water loss (Figure 2). The second stage of mass loss could be assigned to the beginning of pyrolysis of pyomelanin. The temperature of onset of the second mass loss can be taken as an upper limit of the thermal stability of pyomelanin (T_{deg}^{onset}). The highest T_{deg}^{onset} was observed for Pyo_{insol} (196.4 °C); for other pyomelanins, T_{deg}^{onset} was lower and was located at 173.0 °C and 158.0 °C for Pyo_{sol} and sPyo, respectively. Moreover, for sPyo, above 125 °C, continuous mass loss occurred up to the onset of the main degradation. Thus, Pyo_{insol} and Pyo_{sol} showed superior thermal stability to that of sPyo. Pyo_{sol} had a significantly greater residue at 800 °C (75%) than Pyo_{insol} and sPyo (ca. 40%), indicating a greater proportion of aromatic moieties or other conjugated unsaturated bonds in polymer chains.

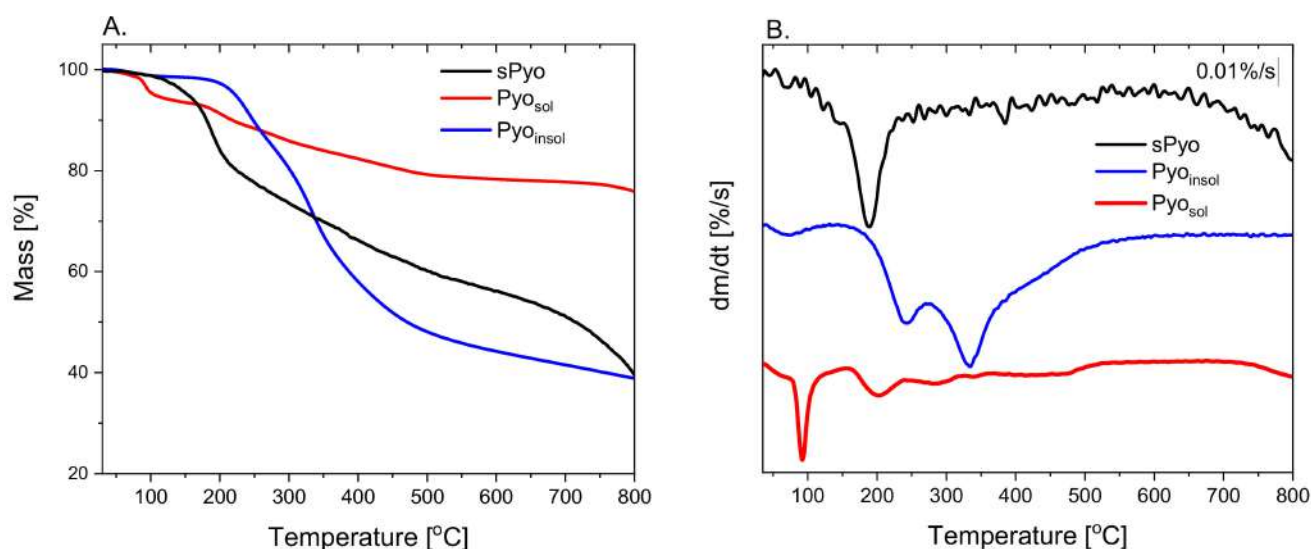


Figure 2. The thermogravimetry (TGA) (A) and the first derivative dm/dt (B) curves of the pyomelanins.

Table 2. Thermal Stability Parameters of the Polymers Estimated from Thermogravimetry and Thermal Properties from Differential Scanning Calorimetry.

Form of Pyomelanin	$T^{1st\ peak}$ [°C]	Mass Loss Up to 125 °C [%]	T_{deg}^{onset} [°C]	T_{deg}^{peak} [°C]	Residue at 800 °C [%]	T_1 [°C]	ΔH_1 [J/g]
sPyo	64.2	2.90	158.0	176.3	39.55	—	—
Pyo_{insol}	72.0	1.60	196.4	233.3	38.85	—	—
Pyo_{sol}	85.6	7.09	173.0	193.7	75.91	78.5	19.8

The TGA results confirmed that the procedures of isolation and purification of the pigments affect the thermal properties due to differences in the structure and composition of the final products, as indicated by FTIR analysis.

The first heating DSC curves of pyomelanin are presented in Figure 3, and the estimated thermal parameters are detailed in Table 2. On the DSC curves of the pigments, an endothermic peak corresponding to degradation was visible. The localization of the degradation peak maximum (T_{deg}^{peak}) was similar for sPyo and Pyo_{sol} , and that for Pyo_{insol}

started at a lower temperature. For Pyo_{sol} , a weak endothermic peak with a maximum at $78.5\text{ }^{\circ}\text{C}$ was visible. The assignment of the endothermic effect to water loss agreed with the TGA results. At this temperature range, mass loss occurred for Pyo_{sol} , with the highest rate at $85.6\text{ }^{\circ}\text{C}$, as estimated from the first derivative $dm/dt(T)$ curve. We also observed that Pyo_{sol} exhibited hygroscopic properties.

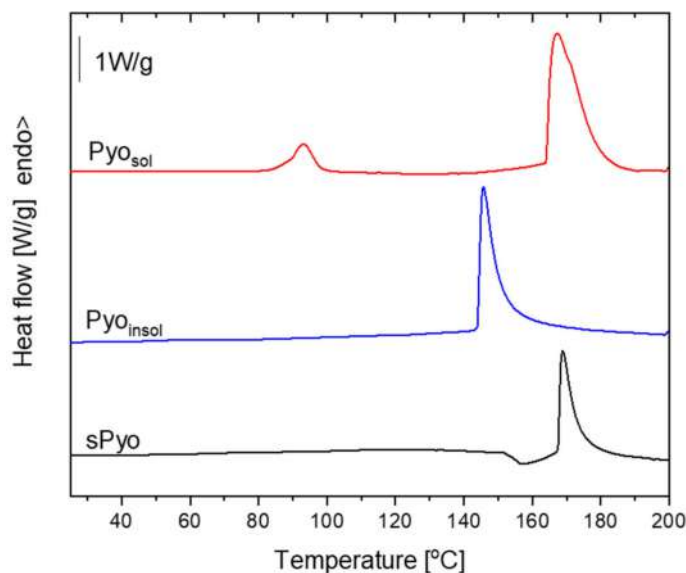


Figure 3. The first heating differential scanning calorimetry (DSC) curves of pyomelanin.

2.4. Biocompatibility

2.4.1. Bacterial Pyomelanins Show Higher Cytocompatibility Than the Synthetic Pyomelanin

Looking for new biomedical applications of bacterial polymers, including pyomelanin, requires characterizing their safety at the *in vitro* level and determining doses that do not show toxic effects. Moreover, differences in structure and thermal stability may translate into interactions of pyomelanin with cells through different ranges of safe concentrations. The influence of each form of pyomelanin on the viability of eukaryotic cells was assessed in the MTT reduction assay using the reference L-929 mouse fibroblasts and human THP-1 monocytes to exclude the cytotoxic effects toward immune cells. The ranges of safe concentrations of different pyomelanin formulations for eukaryotic cells are shown in Figure 4. Pyo_{sol} and $\text{Pyo}_{\text{insol}}$, in the full range of tested concentrations ($1\text{--}1024\text{ }\mu\text{g}/\text{mL}$), did not decrease the number of viable target cells, which were able to reduce MTT (both L-929 and THP-1-cell lines), below the 70% cell level, as required by the ISO norm. The unfavorable effect of reduced cell viability was observed only in the case of sPyo. Less than 70% of mouse fibroblasts or human monocytes were able to reduce MTT in the milieu of sPyo used in the concentration range $64\text{--}1024\text{ }\mu\text{g}/\text{mL}$ ($p < 0.05$) and $32\text{--}1024\text{ }\mu\text{g}/\text{mL}$ ($p < 0.05$), respectively (Figure 4).

2.4.2. Water-Soluble Pyomelanin Induces NF- κ B Pathway Activation

In this study, THP1-Blue™ NF- κ B human monocytes were used as biosensors of the NF- κ B-driven signaling pathway in innate immune cells. NF- κ B induction in these transformed cells results in the SEAP secretion. The amount of SEAP is proportional to cell activation. The levels of induction and activation of NF- κ B in THP1-Blue™ NF- κ B monocytes in response to the tested variants of pyomelanin are expressed as absorbance in Figure 5.

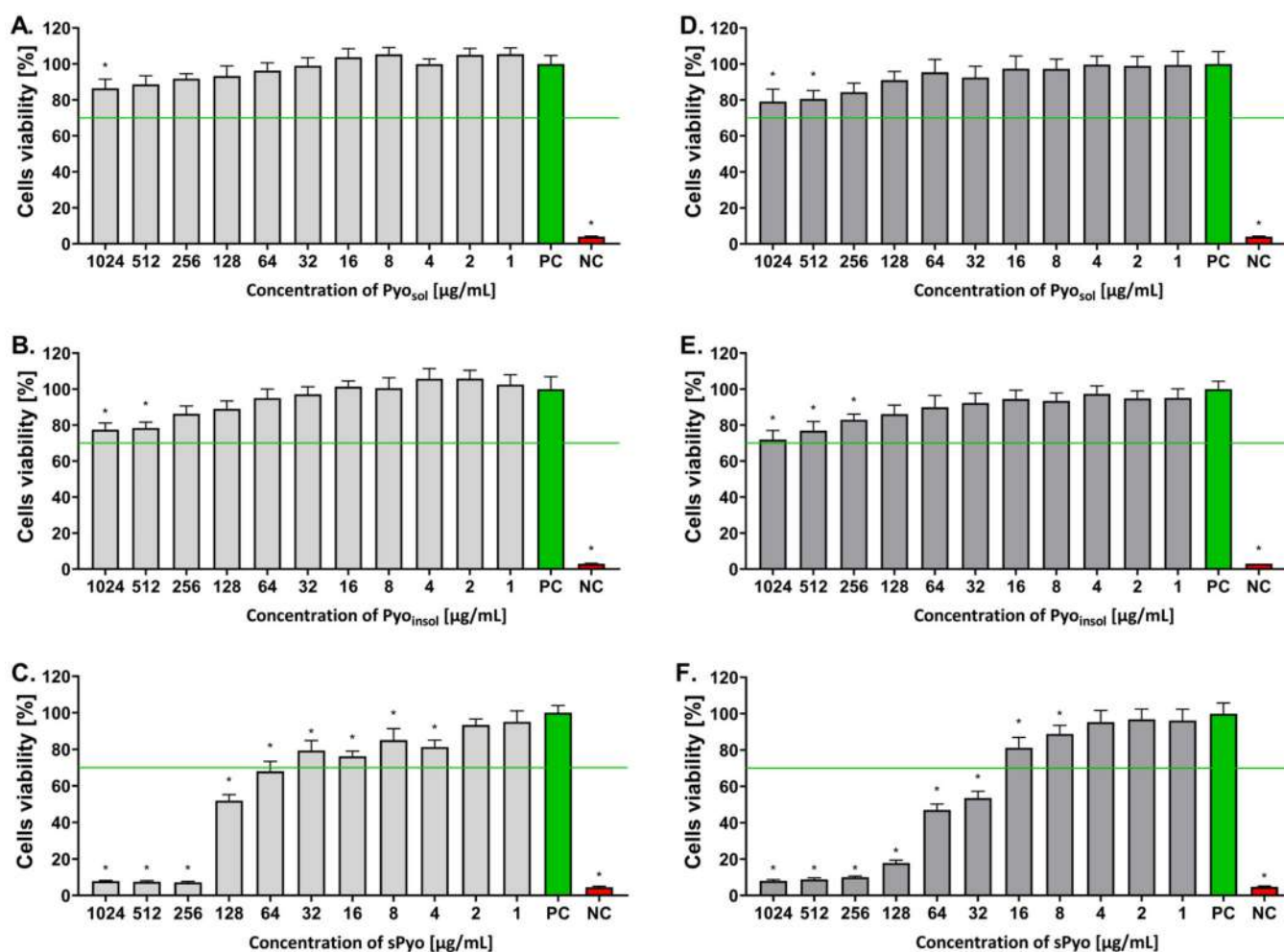


Figure 4. The percentage of viable cells after exposure to different concentrations of the tested pyomelanin variants. Viability of murine fibroblasts L-929 (A–C) and human monocytes (D–F) incubated for 24 h with water-soluble pyomelanin (Pyo_{sol}) (A,D), water-insoluble pyomelanin (Pyo_{insol}) (B,E) or synthetic pyomelanin (sPyo) (C,F), evaluated in the 3-(4,5-dimethylthiazol-2-yl)-2,5-diphenyltetrazolium bromide (MTT) reduction assay according to ISO-10993-5:2009. Cells incubated in the cell culture medium alone, without pyomelanin, served as a positive control (PC) of cell viability (100%). Cells treated with 3% H₂O₂ were a negative control (NC) (no viable cells). Data are presented as the mean \pm standard deviation (SD) of five separate experiments (six replicates for each experimental variant). The green line indicates the minimum level (70%) of viable cells, which are able to reduce MTT according to the ISO norm. Statistical significance was calculated using ANOVA analysis, followed by Dunnett's post hoc test. Significant difference *— $p < 0.05$): cells exposed to tested pyomelanins vs. cells in culture medium alone. Statistical significance between Pyo concentrations was calculated using ANOVA analysis, followed by Tukey's post hoc test. The cytotoxicity of all forms of Pyo was dose-dependent in the concentration range 1024–256 $\mu\text{g/mL}$ ($p < 0.05$).

Pyo_{sol} activated NF- κ B in the concentration range of 1–1024 $\mu\text{g/mL}$ (the absorbance ranged from 0.70 to 1.43, $p < 0.05$) (Figure 5A). In cell cultures treated with Pyo_{insol}, a significant induction of NF- κ B was observed in the concentration range of 64–1024 $\mu\text{g/mL}$ ($p < 0.05$) (Figure 5B). However, the level of activation was lower than that in cell cultures exposed to Pyo_{sol} (absorbance range: 0.30–0.53). Moreover, sPyo induced NF- κ B in the concentration range of 1–64 $\mu\text{g/mL}$; however, there were no differences between induction levels in response to different pyomelanin concentrations within this range (the absorbance

range 0.29–0.41) (Figure 5C). The level of NF- κ B activation in response to *E. coli* LPS shown as absorbance was equal to 2.07 ($p < 0.05$) (Figure 5A–C).

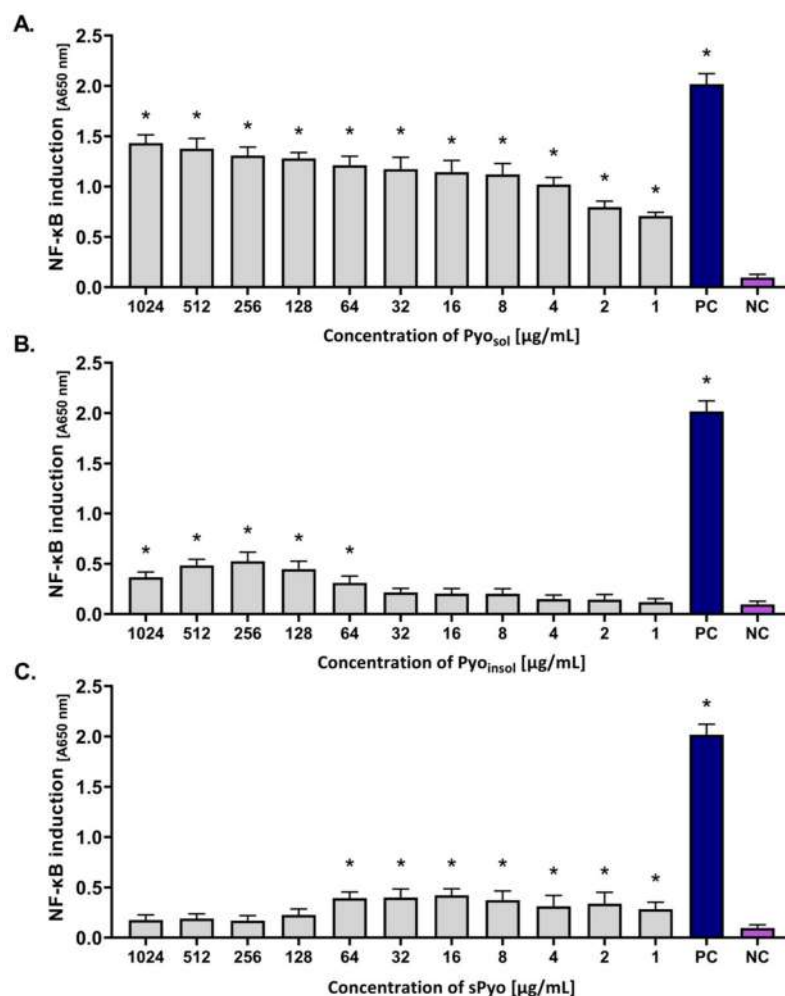


Figure 5. The level of activation of THP1-Blue™ NF- κ B monocytes in response to the tested variants of pyomelanin. Cells were incubated for 24 h with (A) water-soluble pyomelanin (Pyo_{sol}), (B) water-insoluble pyomelanin (Pyo_{insol}), (C) synthetic pyomelanin (sPyo), or lipopolysaccharide (LPS) of *Escherichia coli* as a positive control (PC). Cells in culture medium alone served as the negative control (NC). The secreted embryonic alkaline phosphatase, which was used as an indicator of nuclear factor kappa B (NF- κ B) activation, was quantified spectrophotometrically (OD = 650 nm) after enzymatic substrate conversion. Data are presented as the mean \pm standard deviation (SD) of five separate experiments (six replicates of each experimental variant). Statistical significance was calculated using ANOVA analysis, followed by Dunnett's post hoc test. Statistical significance between Pyo concentrations was calculated using ANOVA analysis, followed by Tukey's post hoc test. Significant difference *, $p < 0.05$. A (absorbance)—optical density 650 nm.

2.4.3. In Vivo Toxicity of Pyomelanin

In the current study, *G. mellonella* larvae were used as a nonmammalian insect model reflecting the biological complexity of live organisms, which is an ethically accepted alternative for the examination of new formulation safety in vivo. By assessing the four physiological functions of the wax moth larvae after injection with the tested variants of pyomelanin, the HISS of the insects was evaluated and presented as a heatmap (Figure 6). Larvae with a total score in the range of 8.5–10.0 points were regarded as healthy, and the substances tested were considered nontoxic in this in vivo larval model.

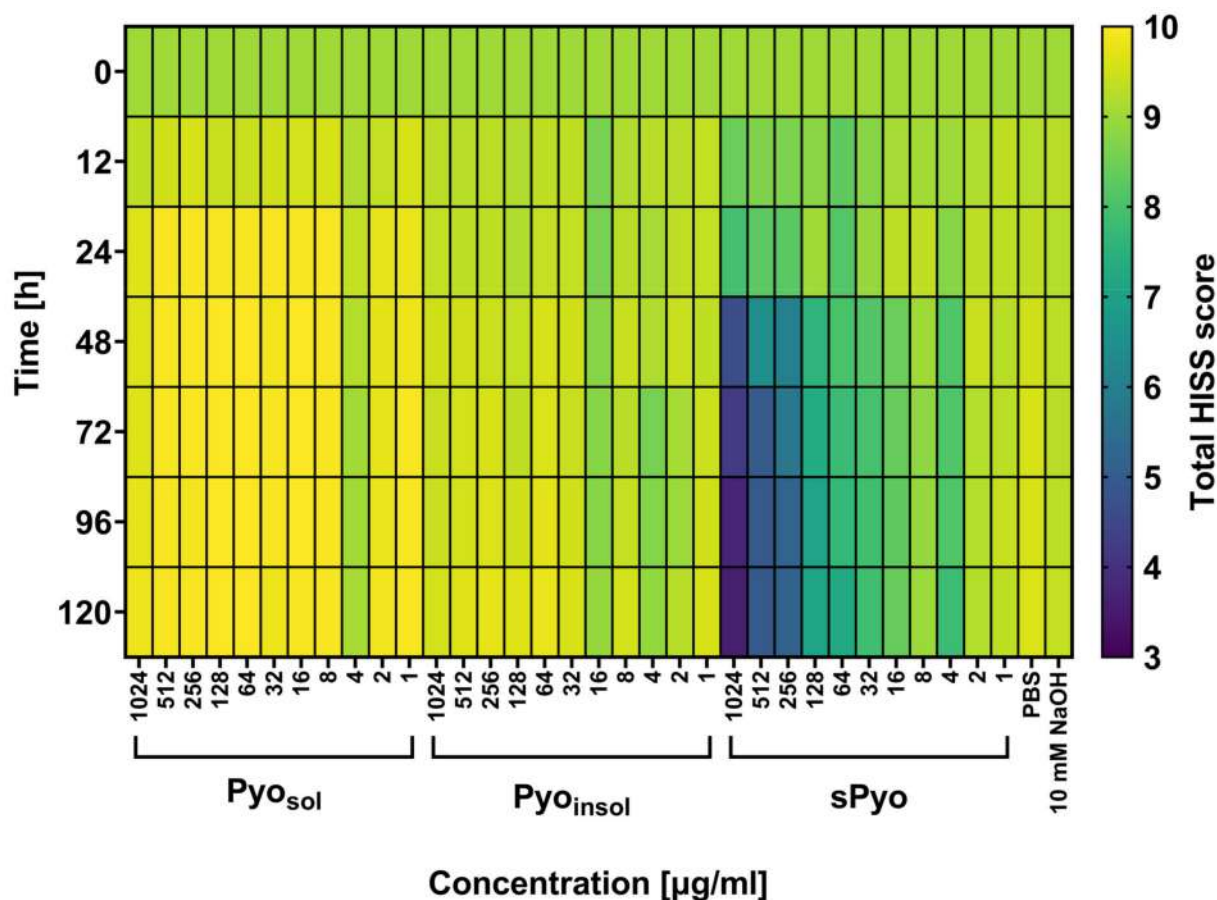


Figure 6. Total Health Index Scoring System (HISS) heatmap for *G. mellonella* larvae treated with tested pyomelanin variants. Larvae were injected with water-soluble (Pyo_{sol}), water-insoluble (Pyo_{insol}) or synthetic pyomelanin (sPyo) in the concentration range of 1–1024 $\mu\text{g}/\text{mL}$ or control solvent solutions: phosphate-buffered saline (PBS) or 50 mM NaOH. At 0, 12, 24, 48, 72, 96, and 120 h after the injection of pyomelanin, the health of the larvae was evaluated using HISS and expressed as the total HISS score. Statistical significance was calculated using ANOVA analysis, followed by Dunnett’s post hoc test. Statistical significance between Pyo concentrations was calculated using ANOVA analysis, followed by Tukey’s post hoc test. sPyo toxicity to *G. mellonella* was dose-dependent in concentration range 1024–64 $\mu\text{g}/\text{mL}$ ($p < 0.05$).

As shown in Figure 6, no deleterious effects of the two variants of bacterial pyomelanin (Pyo_{sol} and Pyo_{insol}) were seen in the *G. mellonella* in vivo model at 0, 12, 24, 48, 72, 96 and 120 h after injection of insect larvae with pyomelanin. The total HISS scores for larvae treated with *P. aeruginosa* pyomelanins were close to the baseline HISS score, which was equal to 9.0. The total HISS scores in larvae injected with sPyo in the range of 4–1024 $\mu\text{g}/\text{mL}$ were lower (7.79–3.58) than the total HISS scores in larvae inoculated with natural *P. aeruginosa* pyomelanin variants. Pyo_{sol} and Pyo_{insol} did not affect the viability of insect larvae, while sPyo used in the range of 64–1024 $\mu\text{g}/\text{mL}$ significantly decreased the number of live larvae (42–83%, $p < 0.05$) compared to control larvae not injected with pyomelanin (Supplementary Figure S2).

3. Discussion

In our study, we described for the first time the method of culturing *Pseudomonas aeruginosa* on the PMM II medium and the method of obtaining water-soluble pyomelanin (Pyo_{sol}). In addition, we compared the physicochemical and biological properties of bacterial Pyo_{sol} to its insoluble form (Pyo_{insol}) and synthetic pyomelanin (sPyo).

We compared our results with several reports on the efficiency of the production of microbial melanins, which depends on the metabolic abilities of bacteria and culture conditions. Madhusudhan et al. reported a production efficiency of extracellular water-soluble melanin of *Streptomyces lusitanus* at the levels of 0.264 g/L and 5.29 g/L [27]. Lagunas-Muñoz et al. showed that recombinant *E. coli* expressing the tyrosinase coding gene from *Rhizobium* produced 6.0 g/L melanin [28]. The yield of water-insoluble bacterial melanins showed a wide range for different species of bacteria cultured in bioreactors: 13.7 g/L for *Streptomyces kathirae*, 3.76 g/L for *Flavobacterium kingsejongi* and 0.125 g/L for *Streptomyces glaucens* [23,29,30]. Significant differences in melanin production efficiency were also observed within the *Pseudomonas* species, with 6.7 g/L water-insoluble melanin obtained from *Pseudomonas stutzeri* and 0.35 g/L obtained from *Pseudomonas putida* [31,32]. A high efficiency of bacterial pyomelanin production with limited secretion of undesirable substances is key to obtaining a bacterial pigment for further physicochemical and biological studies.

The FTIR spectra of microbial Pyo_{sol}, Pyo_{insol} and sPyo exhibit the characteristic bands of the pyomelanins described in the literature [33,34]. Based on the relatively high degree of similarity of the spectra of sPyo and Pyo_{sol}, it can be concluded that the structure of sPyo is more similar to that of Pyo_{sol} than that of Pyo_{insol}. The carbonyl stretching (C=O) of the COOH groups was only visible in Pyo_{insol}. The lack of this band can be similarly found in the literature for microbial melanin isolated in acid precipitation [4,35,36]. The FTIR spectrum of Pyo_{insol} was similar to the FTIR spectrum of melanin produced from a deep-sea sponge-associated *Pseudomonas* strain [35] and pyomelanin from a culture of *Halomonas titanicae* which was produced through the 4-hydroxyphenylacetic acid-1-hydroxylase route [6]. Lorquin et al. concluded that the presence of the band ascribed to aromatic C_{ar}-H has a significant meaning in terms of the type of ring linkages. This group suggested that a pyomelanin that does not have this band has fewer free C_{ar}-H locations and more Car-Car connections between rings in the chain structure [6]. It may suggest that Pyo_{sol} contained more Car-Car linkages than Pyo_{insol}. Moreover, the comparison of the FTIR spectra of sPyo and HGA showed that the sPyo did not contain HGA residue detectable by FTIR measurements. Differences in chemical structure may influence the solubility of various forms of pyomelanins, their thermal stability and biological activity; however, further studies are required.

The TGA and DSC results confirmed that the procedures of isolation and purification of the pigments affect the thermal properties due to differences in the structure and composition of the final products, as indicated by FTIR analysis. Pyo_{sol} showed a significantly greater residue at 800 °C than Pyo_{insol} and sPyo, indicating a greater proportion of aromatic moieties or other conjugated unsaturated bonds in polymer chains [37]. This result was in agreement with the FTIR results revealing a higher content of C_{ar}-C_{ar} linkages between rings in Pyo_{sol} than in the other pyomelanin samples. For Pyo_{sol}, we identified a weak endothermic peak with a maximum at 78.5 °C which is associated with water loss [38]. The presence of this peak only for Pyo_{sol} was a consequence of the isolation of pyomelanin from the aqueous phase. Similar to our DSC results for Pyo_{sol}, the showing of two endothermic peaks was reported for microbial melanin by Kiran et al. [35]. We also showed that Pyo_{sol} exhibited hygroscopic properties. Melanin is known for its hygroscopic character and strong association with water [39].

The use of bacterial-derived pyomelanin and synthetic pyomelanin as potential immunomodulators and bioactive substances for further targeted biomedical applications requires determining the range of cytocompatible concentrations to avoid negative effects on cell metabolism and viability. We have shown that bacterial pyomelanins are characterized by high in vitro safety for L-929 fibroblasts and THP-1 monocytes compared to the synthetic form of this pigment. The high level of Pyo_{sol} and Pyo_{insol} cytocompatibility resulted from the effective removal of lipopolysaccharide and other bacterial metabolites that are cytotoxic. The lower cytocompatibility of sPyo compared to Pyo_{sol} or Pyo_{insol} against L-929 fibroblasts and human monocytes, as shown in this study, might be due to polymerization and structural differences between sPyo and Pyo_{insol} or Pyo_{sol} (a lower

ability to create hydrogen bonds). Interestingly, no residual HGA was observed in the sPyo samples, which could adversely affect cell viability. However, further studies are needed to determine the components influencing the biological activity of the studied pyomelanins. Potentially, the biological activity depends on the complexity of interactions between various functional groups within each variant of pyomelanin.

Several studies have demonstrated the biosafety ranges of microbial melanins in vitro. Oh et al. reported that melanin from *Amorphotheca resinae* in the range of 200–4000 µg/mL did not affect the viability of human keratinocytes HaCaT after 24 h of exposure of cells [40]. Lorquin et al. showed that pyomelanin from *H. titanicae* and its synthetic form resulting from HGA polymerization in the milieu of Mn²⁺ were noncytotoxic to human epidermal keratinocytes [6]. Melanin from *Dietzia schimae*, which possesses photoprotective activity, was safe for human fibroblast hFB at concentrations below ≤500 µg/mL [41]. Pyomelanin produced by various *Pseudomonas* species may differ in cytotoxicity toward eukaryotic cells. In the study by Kurian and Bhat, the highest concentration of melanin from *Pseudomonas stuteri*, which was safe for L-929 fibroblasts, was 100 µg/mL [42]. The cytotoxicity of pyomelanin from *P. putida* against A-375, HeLa Kyoto, HEPG2 or Caco2 cell lines was examined by Ferraz et al. and expressed as the cytotoxicity index IC₅₀, with values of 1770 µg/mL, 2510 µg/mL, 890 µg/mL and 1080 µg/mL, respectively [43].

Monocytes play a key role in the development of inflammatory and immune responses, which determine the elimination of infectious agents, induction of antigen-specific adaptive immunity and tissue regeneration; thus, testing new components with medical potential in humans regarding the effectiveness of monocyte activation is needed [44]. The level of activation may vary depending on the cell type, the chemical structure of biocomponents and the cell milieu. In response to tissue damage, monocytes and macrophages deliver proinflammatory cytokines, including chemokines, which facilitate the recruitment of immunocompetent cells, and the removal of debris, which is a prerequisite for successful healing. In subsequent stages of healing, macrophages can reduce inflammation, through the secretion of anti-inflammatory cytokines, can control the differentiation of stem cells, and can regulate angiogenesis [45]. It has been revealed that acute inflammation or low doses of proinflammatory cytokines are necessary for the reconstruction of bone tissue; therefore, modulation of the NF-κB pathway by pyomelanin may influence bone remodeling [46].

In this study, we have shown that Pyo_{sol} is non-cytotoxic in the widest range of concentrations, which is compatible with NF-κB induction compared to the activity of sPyo or Pyo_{insol}. However, the poor activation of NF-κB by water-insoluble and synthetic forms of pyomelanin does not rule them out from further biological studies. Depending on the application context, the proinflammatory or anti-inflammatory activity of pyomelanin can be considered. Proinflammatory activity is desirable in fighting against infection and in the early stages of tissue regeneration, whereas to prevent chronic inflammation, anti-inflammatory properties of biocomponents are needed. Allam et al. reported that *Streptomyces longisporoflavus* melanin improves immune defense against *Escherichia coli* infection [47]. The severity of oxidative stress is the result of a strong inflammatory response due to the activation of monocytes. Langhfelder et al. reported on the ability of fungal melanins to neutralize such stress [11]. On the other hand, the initiation of regeneration processes requires the stimulation of monocytes to secrete proinflammatory cytokines, which was recently reported [19]. The Pyo_{sol} used in this study seems to meet the highest biological safety, combined with the activation of monocytes, and due to this may be further tested for immunomodulatory and pro-regenerative properties in different cell models.

The results from the in vivo model of *G. mellonella* obtained in this study correspond to the observations on the safety of various forms of pyomelanin in the in vitro model. These results are very useful in selecting potential pyomelanin applications. In particular, Pyo_{sol} and Pyo_{insol} seem to meet the requirements for further studies on potential medical applications. In contrast, sPyo can be further investigated for nonmedical applications.

4. Materials and Methods

4.1. Culture of *Pseudomonas aeruginosa*

To obtain pyomelanin with a limited content of undesirable substances (e.g., alginate, excess protein products), a new minimal liquid medium for *P. aeruginosa* cultivation was developed. Two versions of pyomelanin minimal medium (PMM) were prepared. The first PMM version (PMM I) contained 2.0 g of KH_2PO_4 , 5.0 g of NaCl, 0.1 g of MgSO_4 , 2.0 g of L-tyrosine and 2.0 g of glucose per 1000 mL of distilled water. The second version (PMM II) was additionally supplemented with 1.5 g of arabinose and 1.35 g of malic acid. All chemicals were purchased from PolAura, Dywity, Poland. After dissolving the substrates, the pH of both media was adjusted to 7.0 with 0.5 M NaOH. PMM I and PMM II were autoclaved at 121 °C, 2.5 Ba. Luria–Bertani (LB) broth medium was inoculated with the *P. aeruginosa* Mel⁺ strain deposited in the collection of the Department of Immunology and Infectious Biology UŁ, Poland, and cultured (37 °C, 18 h) to obtain an initial bacterial suspension. After incubation, 300 mL of PMM II was inoculated with 1.0 mL of a 1.0 McFarland bacterial suspension and grown for 5 days (37 °C, shaking at 120 rpm) when the culture medium changed to a deep black-brown color. To increase the production of pyomelanin, after cultivation, the bacterial cultures were exposed to sunlight for 2 days at room temperature.

4.2. Isolation of *Pyo_{insol}*

To isolate *Pyo_{insol}* from the cell-free supernatant, 300 mL of bacterial culture was centrifuged at 3300 × g for 15 min, and then the supernatant was acidified with 6.0 M HCl (PolAura, Dywity, Poland) to pH 2.0 and stored, protected from light, at room temperature for 5 days. Thereafter, the supernatant was boiled for 45 min to avoid the formation of melanoidins after cooling, and the supernatant was centrifuged at 3300 × g for 25 min. The pellet of *Pyo_{insol}* was washed three times with 25 mL of 0.1 M HCl and then three times with double distilled water. Afterward, 10 mL of ethanol (99.9%) (Chempur, Piekary Śląskie, Poland) was added to the pigment pellet and placed in a water bath (95 °C, 30 min). After storage in an incubator (50 °C, overnight), for complete evaporation of alcohol, the pyomelanin was washed twice with ethanol and air dried.

4.3. Isolation of *Pyo_{sol}*

To obtain *Pyo_{sol}*, the postculture bacterial cell-free supernatant was incubated with chloroform in a 1:1 ratio under shaking conditions for 24 h (room temperature, shaking at 120 rpm). The aqueous phase containing pyomelanin was then separated from the chloroform and protein phases using a separating funnel. To remove residual protein contaminants, the aqueous layer was centrifuged at 5300 × g for 30 min. *Pyo_{sol}* was concentrated and purified from low-molecular-weight soluble substances by centrifuging the supernatant on an ultrafiltration unit (3300 × g, 60 min., MWCO 30 kDa) (Sartorius, Göttingen, Germany). The bacterial pigment was dried at 50 °C overnight.

4.4. Synthesis of Pyomelanin

HGA (TCI, Eschborn, Germany), which is the main precursor for pyomelanin in *P. aeruginosa*, was used to prepare sPyo. HGA (1.0 g) was dissolved in 400 mL of distilled water (heated to 50 °C), and then a solution of 4.0 M NaOH was added to achieve pH 10.5. Autoxidation of HGA to sPyo was carried out for 10 days at 37 °C in the absence of light. The tube with the HGA solution was opened once a day to provide a new portion of oxygen. When a dark brown pigment was observed in the tube, sPyo was precipitated with 10.0 M HCl (to pH 6.0), left to sediment for 24 h and centrifuged (3300 × g, 25 min). The pyomelanin pellet was suspended in 2.2 M HCl and left for 2 days to stabilize the pigment. Then, sPyo was centrifuged (6600 × g, 10 min) and washed three times with 0.1 M HCl and double-distilled water.

4.5. Purification of Bacterial Pyomelanins

Lipopolysaccharides (LPSs) were removed from *P. aeruginosa* pyomelanin by affinity chromatography using Pierce™ High Capacity Endotoxin Removal Spin Columns (Thermo Scientific, Waltham, MA, USA). The resin and column were prepared and equilibrated according to the manufacturer's protocol. Samples of Pyo_{sol} and Pyo_{insol} (5 mg/mL) were applied to the columns, incubated for 3 h with gentle mixing, centrifuged at 500× g, collected into new tubes and dried at 50 °C overnight. The pyomelanin pellet was washed with chloroform, ethyl acetate, ethanol and water. For further experiments, the pyomelanin was stored in a dark and dry place at 4 °C. The methodology for the isolation and purification of bacterial pyomelanins is shown in Figure 7.

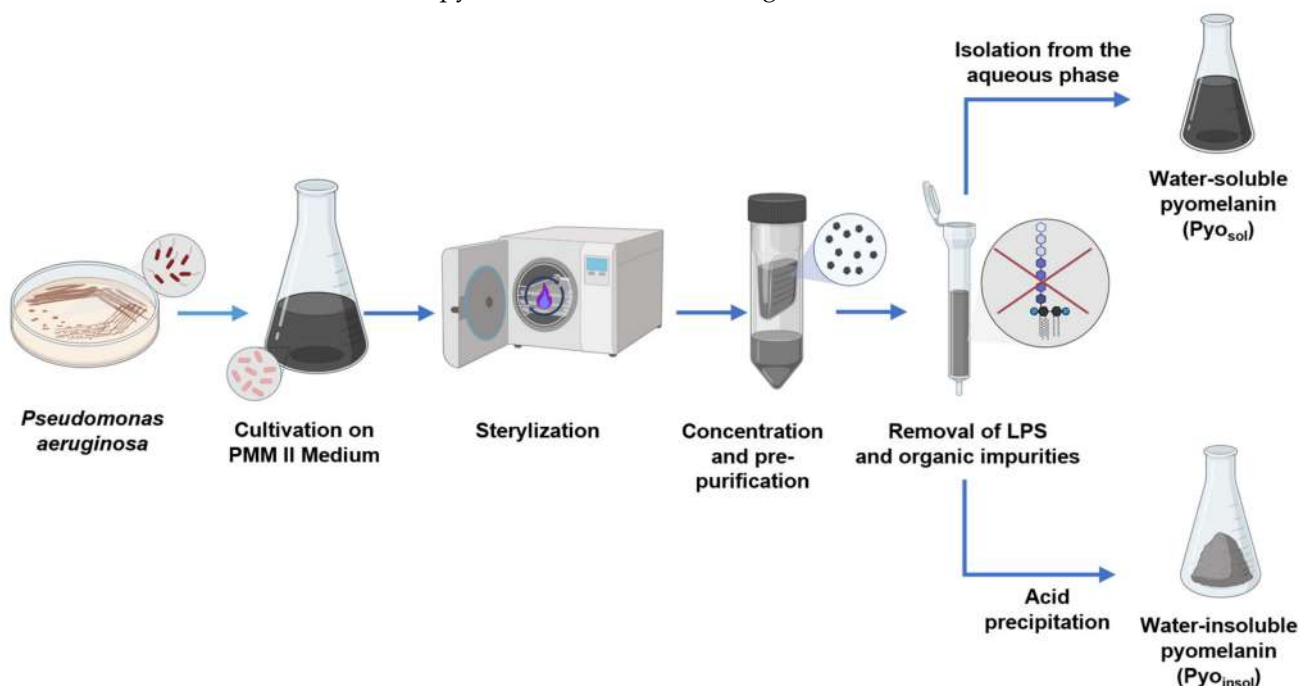


Figure 7. Schematic representation of isolation and purification of bacterial pyomelanins. Abbreviations: water-soluble pyomelanin (Pyo_{sol}), water-insoluble pyomelanin (Pyo_{insol}), synthetic pyomelanin (sPyo), lipopolysaccharide (LPS).

4.6. Fourier Transform infrared (FTIR) Spectroscopy

FTIR spectra in transmission mode were collected from 4000 to 400 cm⁻¹ using the KBr pellet technique on a Thermo Nicolet Nexus FTIR spectrometer (Thermo Fisher Scientific, Waltham, MA, USA) and analyzed with Thermo Scientific Omnic Software ver. 8.3.

4.7. Thermogravimetric Analysis (TGA)

TGA measurements were performed using a TGA/DSC1 Mettler Toledo system (Mettler Toledo, Greifensee, Switzerland) [48]. Samples were heated from 25 °C to 800 °C at a rate of 10 °C/min under 60 mL/min of nitrogen flow. The evaluation of the TGA curves was performed using STARe ver. 16.20c software (Mettler Toledo, Greifensee, Switzerland). The first derivative of mass over time was calculated with OriginPro ver. 2021 (OriginLab Corporation, Northampton, MA, USA) and plotted against temperature. The Savitzky-Golay smoothing algorithm was implemented. A 20 point window and a second-order polynomial was used.

4.8. Differential Scanning Calorimetry (DSC)

DSC measurements were performed using a Mettler Toledo DSC1 system (Mettler Toledo, Greifensee, Switzerland) coupled with a Huber TC 100 intracooler (Huber USA, Inc., Raleigh, USA) [49]. The instrument was calibrated using indium ($T_m = 156.6$ °C,

$\Delta H_m = 28.45 \text{ J/g}$) and zinc ($T_m = 419.7 \text{ }^\circ\text{C}$, $\Delta H_m = 107.00 \text{ J/g}$) standards. Samples (~3.5 mg) were measured in 40 μL aluminum pans under a constant nitrogen purge (60 mL/min) from 0 $^\circ\text{C}$ to 200 $^\circ\text{C}$. The heating and cooling rates were set to 10 $^\circ\text{C}/\text{min}$. The recorded DSC curves were normalized to the sample mass. The evaluation of the DSC curves was performed using STAR^e ver. 16.20c software (Mettler Toledo, Greifensee, Switzerland).

4.9. Assessment of Pyomelanin Biocompatibility

4.9.1. Cell Cultures

The biocompatibility of pyomelanin was assessed *in vitro* according to ISO 10993-5:2009 (Biological evaluation of medical devices—Part 5: Tests for *in vitro* cytotoxicity) using two cell lines: the reference L-929 (CCL-1TM) mouse fibroblasts and human monocytes THP-1 (TIB-202TM), which were obtained from the American Type Culture Collection (ATCC, Manassas, VA, USA). Prior to experiments, cells were cultured in Roswell Park Memorial Institute (RPMI)-1640 medium supplemented with 10% heat-inactivated fetal calf serum (FCS; HyClone Cytiva, Marlborough, MA, USA) and the antibiotics penicillin (100 U/mL) and streptomycin (100 $\mu\text{g}/\text{mL}$) (Sigma-Aldrich, Darmstadt, Germany). Mouse fibroblasts and human monocytes were incubated at 37 $^\circ\text{C}$ in a humidified atmosphere containing 5% CO_2 until the formation of the cell monolayer. Before being used in the experiments, the cell viability and cell density were assessed by trypan blue exclusion assay using a counting Bürker chamber (Blaubrand, Wertheim, Germany). The cells were used in the experiments only if cell viability was higher than 95%.

4.9.2. MTT Reduction Assay

The biocompatibility of pyomelanins was assessed *in vitro* in cell cultures using a 3-(4,5-dimethylthiazol-2-yl)-2,5-diphenyltetrazolium bromide (MTT, Sigma-Aldrich, Darmstadt, Germany) reduction assay as previously described [50] and as recommended by the Food and Drug Administration and ISO norm 109935 [ISO 10993-10995:2009. Biological evaluation of medical devices—Part 5: Tests for *in vitro* cytotoxicity]. L-929 fibroblasts or THP-1 monocytes adjusted to a density of 2×10^5 cells/mL were seeded (20,000 cells per well) in 96 well culture plates (Nunc Delta Surface, Nunc, Rochester, NY, USA) and incubated overnight prior to stimulation with pyomelanin. Cell morphology and confluency were controlled using an inverted contrast phase microscope (Motic AE2000, Xiamen, China). Stock solutions of $\text{Pyo}_{\text{insol}}$ or sPyo , 10 mg/mL in 50 mM NaOH (Polaura, Dywity, Poland) in complete RPMI-1640 (cRPMI-1640) were diluted with medium to concentrations of 1024, 512, 256, 128, 64, 32, 16, 8, 4, 2 and 1 $\mu\text{g}/\text{mL}$. An identical series of dilutions was prepared for Pyo_{sol} starting from a stock solution at a concentration of 2 mg/mL initially dissolved in cRPMI-1640. The pyomelanin solutions were sterilized by filtration using filters with a 0.22 μm pore diameter (Sartorius, Göttingen, Germany). Suspensions of pyomelanins were distributed to the wells of culture plates (6 replicates for each experimental variant) containing cell monolayers. After 24 h of incubation, the condition of the cell monolayers was verified under an inverted contrast phase microscope. The cell cultures in medium without pyomelanin were used as a positive control (PC) of cell metabolic activity, whereas the cell cultures in 3% H_2O_2 served as a negative control (NC). To quantify the metabolic activity of cells, 20 μL of MTT was added to each well, and incubation was carried out for the next 4 h. The plates were centrifuged at $450 \times g$ for 10 min, the supernatant was removed, and the formazan crystals were dissolved with 100 μL of dimethyl sulfoxide (Sigma Aldrich, Seelze, Germany). The absorbance was determined spectrophotometrically using a Multiskan EX reader (Thermo Scientific, Waltham, MA, USA) at 570 nm. The effectiveness of MTT reduction was calculated based on the following formula: MTT reduction relative to untreated cells (%) = (absorbance of treated cells/absorbance of untreated cells \times 100%) – 100%.

4.9.3. Activation of Monocytes

THP1-Blue™ NF-κB monocytes (InvivoGen, San Diego, CA, USA), derived from human THP-1 monocytes, were used to determine the activation of the NF-κB signal transduction pathway, as previously described [51], in response to exposure of cells to sPyo, Pyo_{insol} or Pyo_{sol}. THP1-Blue™ NF-κB cells are specific biosensors of the NF-κB pathway, which is typical for innate immune cells [52,53]. The induction of NF-κB results in secretion of embryonic alkaline phosphatase (SEAP) by these cells. Cell suspensions, 2×10^6 cells/mL in selective RPMI-1640 supplemented with heat-inactivated 10% FCS (HyClone, Cytiva, Marlborough, MA, USA), 25 mM 4-(2-hydroxyethyl)-1-piperazineethanesulfonic acid (HEPES), 100 U/mL penicillin, 100 µg/mL streptomycin, 2 mM glutamine and selective antibiotics (100 µg/mL normocin and 10 µg/mL blasticidin) (InvivoGen, San Diego, CA, USA), at a density below 2×10^6 cells/mL, were cultured for 5 days in a humidified 5% CO₂ atmosphere at 37 °C. Freshly prepared suspensions of monocytes in culture medium were distributed to the wells of culture plates (1×10^5 cells/well; 180 µL). Then, 20 µL of tenfold-concentrated pyomelanin solution was added to selected wells (in six replicates) to a final concentration of 1024, 512, 256, 128, 64, 32, 16, 8, 4, 2 and 1 µg/mL. Cells were incubated for 24 h in an incubator. Monocytes in selective RPMI-1640 alone served as a negative control (NC), whereas monocytes stimulated with 10 ng/mL LPS from *Escherichia coli* O55:B5 (Sigma-Aldrich, Darmstadt, Germany) were used as a positive control (PC) for NF-κB activation. The level of SEAP secretion was determined in the cell culture supernatants. Cell-free supernatant (20 µL) was mixed with 180 µL QUANTI-Blue™ (InvivoGen, San Diego, CA, USA) and incubated at 37 °C for 4 h. Absorbance was measured at 650 nm using a Multiskan EX reader (Thermo Scientific, Waltham, MA, USA). The results are expressed as the mean and standard deviation (SD) of five experiments performed in six replicates for each experimental variant.

4.9.4. In Vivo Toxicity Assay

Different formulations of pyomelanin were examined for their toxicity in vivo using the model of last instar *Galleria mellonella* larvae, which enables real-time cytotoxicity testing [53–55]. In the assessment of the last instar, the size of the larva, width and degree of sclerotization of the head capsule were analyzed, and the ecdysial line along the middle of the dorsal side was observed. Before the experiment, the last instar of larvae (purchased from a local vendor), confirmed by the specialist from the Department of Ecology and Vertebrate Zoology, Faculty of Biology and Environmental Protection, University of Łódź, Poland, were stored in the dark in a refrigerator at 15 °C to minimize transformation into adult form. Prior to conducting the assay, each larva was sterilized with a cotton swab dipped in 70% ethanol. The bioassay was performed in glass Petri dishes. Twelve larvae (200–300 mg weight) were injected with 10 µL of Pyo_{insol}, Pyo_{sol} or sPyo into the hemocoel via the intersegmental membrane near the last left proleg using a microsyringe (Sigma Aldrich, Darmstadt, Germany). Control larvae were injected with phosphate-buffered saline (PBS) or 10 mM NaOH (control solvent for Pyo_{sol} and sPyo). The physiological activities of insects or the number of dead insects were recorded at 0, 12, 24, 48, 72, 96 and 120 h after the injection. The larval health status was evaluated using the Health Index Scoring System (HISS), which is based on the following symptoms: larval mobility, cocoon formation, melanization of the body integuments and survival [55] (Table 3). In this system, the total melanization of the larvae (black larvae) and loss of larval motility correlate with the death of the larvae [56]. Representative pictures of morphological changes in larvae injected with Pyo_{sol}, Pyo_{insol} or sPyo are shown in Supplementary Figure S1.

Table 3. The Health Index Scoring System (HISS) for *G. mellonella* Larvae.

Category	Description	Score
Mobility	no movement	0
	minimal movement on stimulation	1
	movement when stimulated	2
	movement without stimulation	3
Cocoon formation	no cocoon	0
	partial cocoon	0.5
	full cocoon	1
Melanization	black larvae	0
	black spots on brown larvae	1
	≥3 spots on beige larvae	2
	<3 spots on beige larvae	3
	no melanization	4
Survival	dead	0
	alive	2

4.10. Statistical Analysis

The Kolmogorov–Smirnov test was used to test the normality of the data. Intergroup outcomes were compared for statistical significance using ANOVA (analysis of variance) followed by Dunnett’s post hoc test. Statistical significance between pyomelanin concentrations was calculated using ANOVA analysis, followed by Tukey’s post hoc test. In all cases, significance was accepted at $p < 0.05$. All analyses were performed using GraphPad Prism 9 software (GraphPad Software, San Diego, CA, USA).

5. Conclusions

Taking into account the need to search for biocomponents, including those of bacterial origin with multidirectional biological activity (antimicrobial, immunomodulatory and proregenerative), the aim of this study was to obtain natural bacterial pyomelanin from *Pseudomonas aeruginosa*, namely, Pyo_{sol} and Pyo_{insol}, and synthetic pyomelanin (sPyo). Furthermore, we characterized these three variants of pyomelanin in terms of chemical structure and biosafety for further targeted biomedical research. The culture medium increasing the production of pyomelanin was developed as well as the conditions for the isolation and synthesis of pyomelanin from HGA. FTIR analysis showed that the most important difference between variants of pyomelanin concerns the connections of aromatic rings in polymer chains. In the case of Pyo_{sol} and sPyo, the C_{ar}-C_{ar} connections between rings dominate the chain structure, whereas Pyo_{insol} showed fewer C_{ar}-C_{ar} links between rings. For Pyo_{sol}, the wide band at 3700–3000 cm⁻¹ indicated the presence of condensed double bonds as well as the presence of OH groups involved in hydrogen interactions, e.g., with water. We observed that Pyo_{sol} exhibited hygroscopic properties (atmospheric moisture caused clumping). TGA confirmed the highest water content in Pyo_{sol}. Further chemical research is required to fully define the structural differences in the molecules of different variants of pyomelanin. A high level of biological safety allows for the recommendation of Pyo_{sol} and Pyo_{insol} for further biomedical studies, including research on their antimicrobial, immunomodulatory, and proregenerative activities. Investigating the biosafety and modulation of the physiological activity of other cell lines will guide research on pyomelanin towards the development of pyomelanin bioactive preparations.

Supplementary Materials: The following supporting information can be downloaded at: <https://www.mdpi.com/article/10.3390/ijms24097846/s1>.

Author Contributions: Conceptualization, M.M.U. and M.C.; methodology, M.M.U., M.N. and M.G.; validation, M.M.U., M.N. and M.G.; formal analysis, M.M.U., K.R. and P.P.; investigation, M.M.U., M.N. and M.G.; resources, M.M.U., M.N. and M.G.; data curation, M.M.U., M.N. and M.G.; writing—original draft preparation, M.M.U., P.P. and M.C.; writing—review and editing, K.R., M.M.U., M.G.

and M.N.; supervision, M.C. and K.R.; project administration, K.R.; funding acquisition, K.R. All authors have read and agreed to the published version of the manuscript.

Funding: This research was funded by the Foundation for Polish Science through the European Union under the European Regional Development Fund, within the TEAM-NET program entitled “Multifunctional biologically active composite for application in bone regenerative medicine”. (POIR.04.04.00-00-16D7/18-00).

Institutional Review Board Statement: Not applicable.

Informed Consent Statement: Not applicable.

Data Availability Statement: The data generated during this study are available at University of Łódź, Faculty of Biology and Environmental Protection, Department of Immunology and Infectious Biology, Łódź, 90-237, Poland, and are available from the corresponding authors upon request.

Acknowledgments: The authors are thankful to Mariusz Tszedel, from the Department of Ecology and Vertebrate Zoology, Faculty of Biology and Environmental Protection, University of Łódź, for their expert evaluation and confirmation of the *Galleria mellonella* larval stage used in the in vivo toxicity assessment.

Conflicts of Interest: The authors declare no conflict of interest. The funders had no role in the design of the study; in the collection, analyses, or interpretation of data; in the writing of the manuscript; or in the decision to publish the results.

References

- Behzadi, P.; Baráth, Z.; Gajdács, M. It's Not Easy Being Green: A Narrative Review on the Microbiology, Virulence and Therapeutic Prospects of Multidrug-Resistant *Pseudomonas aeruginosa*. *Antibiotics* **2021**, *10*, 42. [[CrossRef](#)]
- Liebgoft, P.P.; Labat, M.; Amouric, A.; Tholozan, J.L.; Lorquin, J. Tyrosol Degradation Via the Homogentisic Acid Pathway in a Newly Isolated Halomonas Strain from Olive Processing Effluents. *J. Appl. Microbiol.* **2008**, *105*, 2084–2095. [[CrossRef](#)]
- Ketelboeter, L.M.; Potharla, V.Y.; Bardy, S.L. NTBC Treatment of the Pyomelanogenic *Pseudomonas aeruginosa* Clinical Isolate PA1111 Inhibits Pigment Production and Increases Sensitivity to Oxidative Stress. *Curr. Microbiol.* **2014**, *69*, 343–348. [[CrossRef](#)]
- David, C.; Daro, A.; Szalai, E.; Atarhouch, T.; Mergeay, M. Formation of Polymeric Pigments in the Presence of Bacteria and Comparison with Chemical Oxidative Coupling—II. Catabolism of Tyrosine and Hydroxyphenylacetic Acid by *Alcaligenes eutrophus* CH34 and Mutants. *Eur. Polym. J.* **1996**, *32*, 669–679. [[CrossRef](#)]
- Roy, S.; Rhim, J.W. New Insight into Melanin for Food Packaging and Biotechnology Applications. *Crit. Rev. Food Sci. Nutr.* **2021**, *62*, 4629–4655. [[CrossRef](#)]
- Lorquin, F.; Ziarelli, F.; Amouric, A.; Di Giorgio, C.; Robin, M.; Piccerelle, P.; Lorquin, J. Production and Properties of Non-Cytotoxic Pyomelanin by Laccase and Comparison to Bacterial and Synthetic Pigments. *Sci. Rep.* **2021**, *11*, 8538. [[CrossRef](#)] [[PubMed](#)]
- Fonseca, É.; Freitas, F.; Caldart, R.; Morgado, S.; Vicente, A.C. Pyomelanin Biosynthetic Pathway in Pigment-Producer Strains from the Pandemic *Acinetobacter baumannii* IC-5. *Mem. Inst. Oswaldo Cruz.* **2020**, *115*, e200371. [[CrossRef](#)] [[PubMed](#)]
- Zeng, Z.; Cai, X.; Wang, P.; Guo, Y.; Liu, X.; Li, B.; Wang, X. Biofilm Formation and Heat Stress Induce Pyomelanin Production in Deep-Sea *Pseudoalteromonas* sp. SM9913. *Front. Microbiol.* **2017**, *8*, 1822. [[CrossRef](#)] [[PubMed](#)]
- Rodríguez-Rojas, A.; Mena, A.; Martín, S.; Borrell, N.; Oliver, A.; Blázquez, J. Inactivation of the *hmgA* Gene of *Pseudomonas aeruginosa* Leads to Pyomelanin Hyperproduction, Stress Resistance and Increased Persistence in Chronic Lung Infection. *Microbiology* **2009**, *155*, 1050–1057. [[CrossRef](#)]
- Baishya, J.; Wakeman, C.A. Selective Pressures during Chronic Infection Drive Microbial Competition and Cooperation. *NPJ Biofilms Microbiomes* **2019**, *5*, 16. [[CrossRef](#)]
- Langfelder, K.; Streibel, M.; Jahn, B.; Haase, G.; Brakhage, A.A. Biosynthesis of Fungal Melanins and Their Importance for Human Pathogenic Fungi. *Fungal Genet. Biol.* **2003**, *38*, 143–158. [[CrossRef](#)] [[PubMed](#)]
- Zeng, Z.; Guo, X.P.; Cai, X.; Wang, P.; Li, B.; Yang, J.L.; Wang, X. Pyomelanin from *Pseudoalteromonas lipolytica* Reduces Biofouling. *Microb. Biotechnol.* **2017**, *10*, 1718–1731. [[CrossRef](#)] [[PubMed](#)]
- Weidenfeld, I.; Zakian, C.; Duester, P.; Chmyrov, A.; Klemm, U.; Aguirre, J.; Ntziachristos, V.; Stiel, A.C. Homogentisic Acid-Derived Pigment as a Biocompatible Label for Optoacoustic Imaging of Macrophages. *Nat. Commun.* **2019**, *10*, 5056. [[CrossRef](#)] [[PubMed](#)]
- Cheng, Z.; Valença, W.O.; Dias, G.G.; Scott, J.; Barth, N.D.; de Moliner, F.; Souza, G.B.P.; Mellanby, R.J.; Vendrell, M.; da Silva Júnior, E.N. Natural Product-inspired Profluorophores for Imaging NQO1 Activity in Tumour Tissues. *Bioorg. Med. Chem.* **2019**, *27*, 3938–3946. [[CrossRef](#)]
- Mavridi-Printezi, A.; Guernelli, M.; Menichetti, A.; Montalti, M. Bio-Applications of Multifunctional Melanin Nanoparticles: From Nanomedicine to Nanocosmetics. *Nanomaterials* **2020**, *10*, 2276. [[CrossRef](#)]

16. Li, H.; Zhou, X.; Huang, Y.; Liao, B.; Cheng, L.; Ren, B. Corrigendum: Reactive Oxygen Species in Pathogen Clearance: The Killing Mechanisms, the Adaption Response, and the Side Effects. *Front. Microbiol.* **2021**, *12*, 685133. [[CrossRef](#)]
17. Tapia, C.V.; Falconer, M.; Tempio, F.; Falcón, F.; López, M.; Fuentes, M.; Alburquenque, C.; Amaro, J.; Bucarey, S.A.; Di Nardo, A. Melanocytes and Melanin Represent a First Line of Innate Immunity against *Candida albicans*. *Med. Mycol.* **2014**, *52*, 445–454. [[CrossRef](#)]
18. Elobeid, A.S.; Kamal-Eldin, A.; Abdelhalim, M.A.K.; Haseeb, A.M. Pharmacological Properties of Melanin and its Function in Health. *Basic Clin. Pharmacol. Toxicol.* **2017**, *120*, 515–522. [[CrossRef](#)]
19. Cuzzubbo, S.; Carpentier, A.F. Applications of Melanin and Melanin-Like Nanoparticles in Cancer Therapy: A Review of Recent Advances. *Cancers* **2021**, *13*, 1463. [[CrossRef](#)] [[PubMed](#)]
20. Koike, S.; Yamasaki, K. Melanogenesis Connection with Innate Immunity and Toll-like Receptors. *Int. J. Mol. Sci.* **2020**, *21*, 9769. [[CrossRef](#)]
21. Bilandžija, H.; Laslo, M.; Porter, M.L. Melanization in Response to Wounding is Ancestral in Arthropods and Conserved in Albino Cave Species. *Sci. Rep.* **2017**, *7*, 17148. [[CrossRef](#)]
22. Liu, S.; Youngchim, S.; Zamith-Miranda, D.; Nosanchuk, J.D. Fungal Melanin and the Mammalian Immune System. *J. Fungi* **2021**, *7*, 264. [[CrossRef](#)]
23. Lee, H.S.; Choi, J.Y.; Kwon, S.J.; Park, E.S.; Oh, B.M.; Kim, J.H.; Lee, P.C. Melanin Biopolymer Synthesis Using a New Melanogenic Strain of *Flavobacterium kingsejongi* and a Recombinant Strain of *Escherichia coli* Expressing 4-Hydroxyphenylpyruvate Dioxygenase from *F. kingsejongi*. *Microb. Cell Fact.* **2022**, *21*, 75. [[CrossRef](#)] [[PubMed](#)]
24. Coates, C.J.; Lim, J.; Harman, K.; Rowley, A.F.; Griffiths, D.J.; Emery, H.; Layton, W. The Insect, *Galleria mellonella*, is a Compatible Model for Evaluating the Toxicology of Okadaic Acid. *Cell Biol. Toxicol.* **2019**, *3*, 219–232. [[CrossRef](#)] [[PubMed](#)]
25. Firacative, C.; Khan, A.; Duan, S.; Ferreira-Paim, K.; Leemon, D.; Meyer, W. Rearing and Maintenance of *Galleria mellonella* and its application to study fungal virulence. *J. Fungi* **2020**, *3*, 130. [[CrossRef](#)] [[PubMed](#)]
26. Piatek, M.; Sheehan, G.; Kavanagh, K. *Galleria mellonella*: The versatile host for drug discovery, In vivo toxicity testing and characterising host-pathogen interactions. *Antibiotics* **2021**, *12*, 1545. [[CrossRef](#)]
27. Madhusudhan, D.N.; Mazhari, B.B.Z.; Dastager, S.G.; Agsar, D. Production and Cytotoxicity of Extracellular Insoluble and Droplets of Soluble Melanin by *Streptomyces lusitanus* DMZ-3. *Biol. Med. Res. Int.* **2014**, *2014*, 306895.
28. Lagunas-Muñoz, V.H.; Cabrera-Valladares, N.; Bolívar, F.; Gosset, G.; Martínez, A. Optimum Melanin Production Using Recombinant *Escherichia coli*. *J. Appl. Microbiol.* **2006**, *101*, 1002–1008. [[CrossRef](#)]
29. Guo, J.; Rao, Z.; Yang, T.; Man, Z.; Xu, M.; Zhang, X. High-Level Production of Melanin by a Novel Isolate of *Streptomyces kathirae*. *FEMS Microbiol. Lett.* **2014**, *357*, 85–91. [[CrossRef](#)]
30. Ahn, S.Y.; Jang, S.; Sudheer, P.D.V.N.; Choi, K.Y. Microbial Production of Melanin Pigments from Caffeic Acid and L-Tyrosine Using *Streptomyces glaucescens* and FCS-ECH-Expressing *Escherichia coli*. *Int. J. Mol. Sci.* **2021**, *22*, 2413. [[CrossRef](#)]
31. Kumar, C.G.; Sahu, N.; Reddy, G.N.; Prasad, R.B.N.; Nagesh, N.; Kamal, A. Production of Melanin Pigment from *Pseudomonas stutzeri* Isolated from Red Seaweed *Hypnea musciformis*. *Let. Appl. Microbiol.* **2013**, *57*, 295–302. [[CrossRef](#)]
32. Martínez, L.M.; Martinez, A.; Gosset, G. Production of Melanins with Recombinant Microorganisms. *Front. Bioeng. Biotechnol.* **2019**, *7*, 285. [[CrossRef](#)] [[PubMed](#)]
33. Schmalder-Ripcke, J.; Sugareva, V.; Gebhardt, P.; Winkler, R.; Knemeyer, O.; Heinekamp, T.; Brakhage, A.A. Production of Pyomelanin, a Second Type of Melanin, Via the Tyrosine Degradation Pathway in *Aspergillus fumigatus*. *Appl. Environ. Microbiol.* **2009**, *75*, 493–503. [[CrossRef](#)]
34. Tahar, I.B.; Kus-Liśkiewicz, M.; Lara, Y.; Javaux, E.; Fickers, P. Characterization of a Nontoxic Pyomelanin Pigment Produced by the Yeast *Yarrowia lipolytica*. *Biotechnol. Prog.* **2020**, *36*, e2912. [[PubMed](#)]
35. Kiran, G.S.; Jackson, S.A.; Priyadharsini, S.; Dobson, A.D.W.; Selvin, J. Synthesis of Nm-PHB (Nanomelanin-Polyhydroxy Butyrate) Nanocomposite Film and Its Protective Effect against Biofilm-Forming Multi Drug Resistant *Staphylococcus aureus*. *Sci. Rep.* **2017**, *7*, 9167. [[CrossRef](#)]
36. Furtado, G.P.; Lourenzoni, M.R.; Fuzo, C.A.; Fonseca-Maldonado, R.; Guazzaroni, M.E.; Ribeiro, L.F.; Ward, R.J. Engineering the Affinity of a Family 11 Carbohydrate Binding Module to Improve Binding of Branched Over Unbranched Polysaccharides. *Int. J. Biol. Macromol.* **2018**, *120*, 2509–2516. [[CrossRef](#)]
37. Bair, H.E. *Thermal Characterization of Polymeric Materials*, 2nd ed.; Turi, E.A., Ed.; Academic Press: San Diego, CA, USA, 1997; pp. 2263–2420.
38. Lu, J. Characterization and Pseudopolymorphism of l-Phenylalanine Anhydrous and Monohydrate Forms. *Afr. J. Pharm. Pharmacol.* **2012**, *6*, 269–277. [[CrossRef](#)]
39. Cordero, R.J.; Casadevall, A. Functions of Fungal Melanin Beyond Virulence. *Fungal Biol. Rev.* **2017**, *31*, 99–112. [[CrossRef](#)] [[PubMed](#)]
40. Oh, J.J.; Kim, J.Y.; Son, S.H.; Jung, W.J.; Kim, D.H.; Seo, J.W.; Kim, G.H. Fungal Melanin as a Biocompatible Broad-Spectrum Sunscreen with High Antioxidant Activity. *RSC Adv.* **2021**, *11*, 19682–19689. [[CrossRef](#)]
41. Eskandari, S.; Etemadifar, Z. Biocompatibility and Radioprotection by Newly Characterized Melanin Pigment and its Production from *Dietzia schimae* NM3 in Optimized Whey Medium by Response Surface Methodology. *Ann. Microbiol.* **2021**, *71*, 17. [[CrossRef](#)]
42. Kurian, N.K.; Bhat, S.G. Data on the Characterization of Non-Cytotoxic Pyomelanin Produced by Marine *Pseudomonas stutzeri* BTCZ10 with Cosmetological Importance. *Data Brief* **2018**, *18*, 1889–1894. [[CrossRef](#)] [[PubMed](#)]

43. Ferraz, A.R.; Pacheco, R.; Vaz, P.D.; Pintado, C.S.; Ascensão, L.; Serralheiro, M.L. Melanin: Production from Cheese Bacteria, Chemical Characterization, and Biological Activities. *Int. J. Environ. Res. Public Health* **2021**, *18*, 10562. [[CrossRef](#)] [[PubMed](#)]
44. Ogle, M.E.; Segar, C.E.; Sridhar, S.; Botchwey, E.A. Monocytes and Macrophages in Tissue Repair: Implications for Immunoregenerative Biomaterial Design. *Exp. Biol. Med.* **2016**, *10*, 1084–1097. [[CrossRef](#)]
45. Oishi, Y.; Manabe, I. Macrophages in Inflammation, Repair and Regeneration. *Int. Immunol.* **2018**, *30*, 511–528. [[CrossRef](#)] [[PubMed](#)]
46. Lin, T.H.; Pajarinen, J.; Lu, L.; Nabeshima, A.; Cordova, L.A.; Yao, Z.; Goodman, S.B. NF- κ B as a Therapeutic Target in Inflammatory-Associated Bone Diseases. *Adv. Protein Chem. Struct. Biol.* **2017**, *107*, 117–154. [[PubMed](#)]
47. Prime, B.R.; Bair, H.E.; Vyazovkin, S.; Gallagher, P.K.; Riga, A. Thermogravimetric Analysis (TGA). In *Thermal Analysis of Polymers, Fundamentals and Applications*; Menczel, J.D., Prime, B.R., Eds.; John Wiley & Sons, Inc.: Hoboken, NJ, USA, 2009; pp. 241–317.
48. Menczel, J.D.; Judovits, L.; Prime, B.R.; Bair, H.E.; Reading, M.; Swier, S. Differential Scanning Calorimetry (DSC). In *Thermal Analysis of Polymers, Fundamentals and Applications*; Menczel, J.D., Prime, B.R., Eds.; John Wiley & Sons, Inc.: Hoboken, NJ, USA, 2009; pp. 7–239.
49. Allam, N.; El-Zaher, E.A.; Allam, A. Immunological Efficiency of Microbial Melanin on Bacterial Pathogenicity. *Int. J. Cancer Biomed. Res.* **2020**, *4*, 243–258. [[CrossRef](#)]
50. Mnich, E.; Kowalewicz-Kulbat, M.; Sicińska, P.; Hinc, K.; Obuchowski, M.; Gajewski, A.; Moran, A.P.; Chmiela, M. Impact of *Helicobacter pylori* on the Healing Process of the Gastric Barrier. *World J. Gastroenterol.* **2016**, *33*, 7536–7558. [[CrossRef](#)] [[PubMed](#)]
51. Biernat, M.; Szwed-Georgiou, A.; Rudnicka, K.; Płociński, P.; Pagacz, J.; Tymowicz-Grzyb, P.; Woźniak, A.; Włodarczyk, M.; Urbaniak, M.M.; Krupa, A.; et al. Dual Modification of Porous Ca-P/PLA Composites with APTES and Alendronate Improves their Mechanical Strength and Cytobiocompatibility towards Human Osteoblasts. *Int. J. Mol. Sci.* **2022**, *23*, 14315. [[CrossRef](#)]
52. Liu, T.; Zhang, L.; Joo, D.; Sun, S.C. NF- κ B Signaling in Inflammation. *Signal Transduct. Target. Ther.* **2017**, *2*, 17023. [[CrossRef](#)] [[PubMed](#)]
53. Zinatizadeh, M.R.; Schock, B.; Chalbatani, G.M.; Zarandi, P.K.; Jalali, S.A.; Miri, S.R. The Nuclear Factor Kappa B (NF- κ B) Signaling in Cancer Development and Immune Diseases. *Genes Dis.* **2021**, *8*, 287–297. [[CrossRef](#)] [[PubMed](#)]
54. Wu, G.; Yi, Y. Haemocoel Injection of PirA1B1 to *Galleria mellonella* Larvae Leads to Disruption of the Haemocyte Immune Functions. *Sci. Rep.* **2016**, *6*, 34996. [[CrossRef](#)] [[PubMed](#)]
55. Tsai, C.J.Y.; Loh, J.M.S.; Proft, T. *Galleria mellonella* Infection Models for the Study of Bacterial Diseases and for Antimicrobial Drug Testing. *Virulence* **2016**, *7*, 214–229. [[CrossRef](#)] [[PubMed](#)]
56. Allegra, E.; Titball, R.W.; Carter, J.; Champion, O.L. *Galleria mellonella* Larvae Allow the Discrimination of Toxic and Non-Toxic Chemicals. *Chemosphere* **2018**, *198*, 469–472. [[CrossRef](#)] [[PubMed](#)]

Disclaimer/Publisher's Note: The statements, opinions and data contained in all publications are solely those of the individual author(s) and contributor(s) and not of MDPI and/or the editor(s). MDPI and/or the editor(s) disclaim responsibility for any injury to people or property resulting from any ideas, methods, instructions or products referred to in the content.

In Vitro and In Vivo Biocompatibility of Natural and Synthetic *Pseudomonas aeruginosa* Pyomelanin for Potential Biomedical Applications

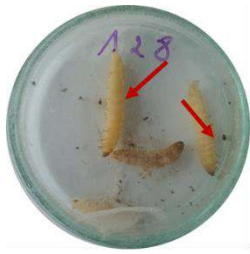
Mateusz M. Urbaniak ^{1,2}, Małgorzata Gazińska ³, Karolina Rudnicka ¹, Przemysław Płociński ¹, Monika Nowak ¹ and Magdalena Chmiela ^{1,*}

¹ Department of Immunology and Infectious Biology, Faculty of Biology and Environmental Protection, University of Łódź, 90-237 Łódź, Poland

² The Bio-Med-Chem Doctoral School, University of Lodz and Lodz Institutes of the Polish Academy of Sciences, 90-237 Łódź, Poland

³ Department of Engineering and Technology of Polymers, Faculty of Chemistry, Wrocław University of Science and Technology (WUST), 50-370 Wrocław, Poland

SUPPLEMENTARY MATERIAL



No melanization
4 point of HISS



Partial melanization
3-2 point of HISS



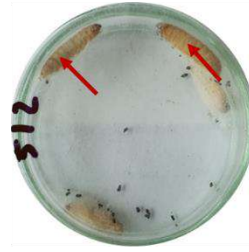
Majority melanization
1 point of HISS



Full melanization
0 point of HISS



No cocoon formation
0 point of HISS

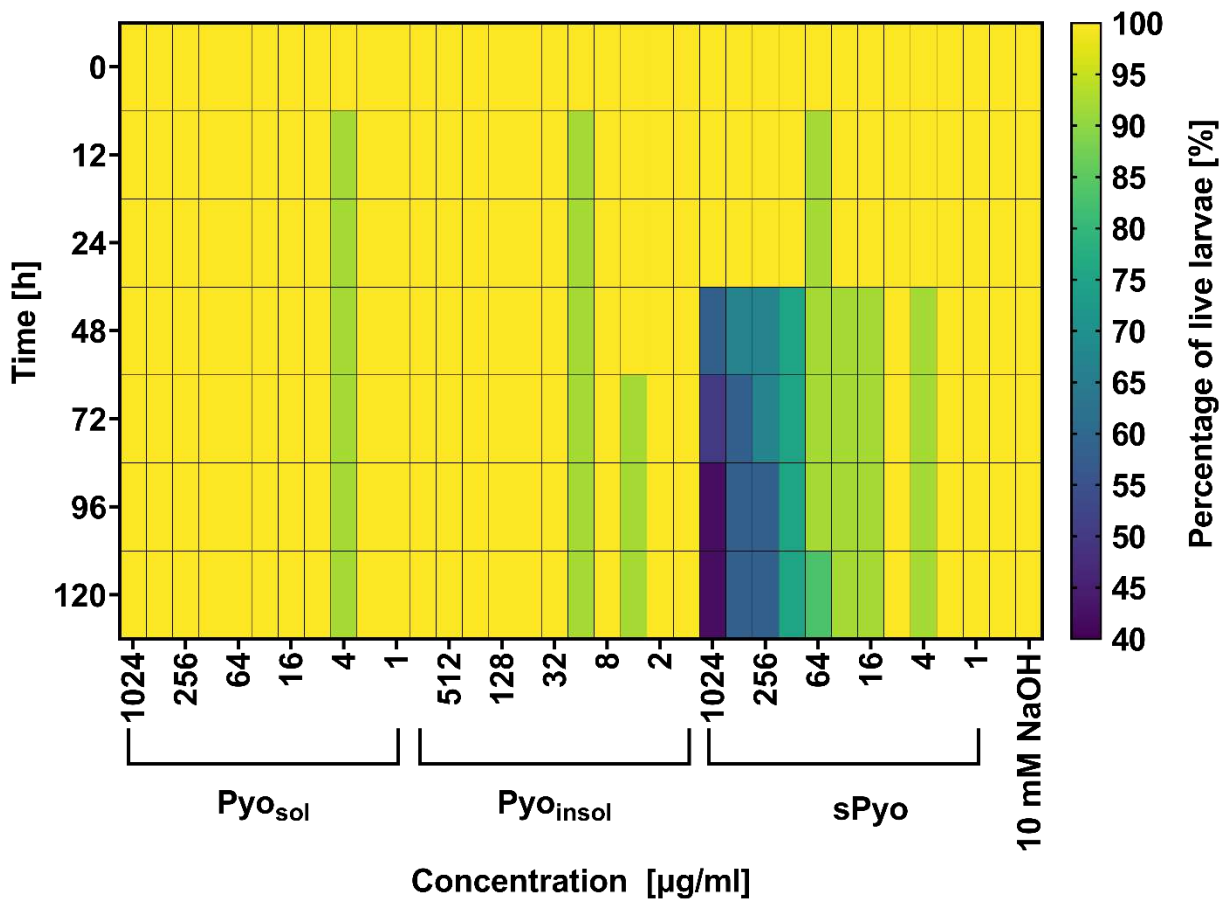


Partial cocoon formation
0.5 poin of HISS



Full cocoon formation
1 point of HISS

Supplementary Figure S1. Larval morphological changes observed in melanization and cocoon formation during Health Index Scoring System (HISS) assessment.



Supplementary Figure S2. Heatmap of toxicity for *G. mellonella* at 0, 12, 24, 48, 72, 96, and 120 hrs from the injection of water-soluble (Pyo_{sol}), water-insoluble (Pyo_{insol}), and synthetic (sPyo) pyomelanin in the concentration range 1-1024 µg/mL and control substances: phosphate buffer (PBS) and 50 mM NaOH.



Article

Can Pyomelanin Produced by *Pseudomonas aeruginosa* Promote the Regeneration of Gastric Epithelial Cells and Enhance *Helicobacter pylori* Phagocytosis?

Mateusz M. Urbaniak ^{1,2,*}, Karolina Rudnicka ¹, Grażyna Gościński ³ and Magdalena Chmiela ^{1,*}

¹ Department of Immunology and Infectious Biology, Faculty of Biology and Environmental Protection, University of Łódź, 90-237 Łódź, Poland; karolina.rudnicka@biol.uni.lodz.pl

² Bio-Med-Chem Doctoral School, University of Lodz and Lodz Institutes of the Polish Academy of Sciences, 90-237 Łódź, Poland

³ Department of Microbiology, Faculty of Medicine, Wrocław Medical University, 50-368 Wrocław, Poland; grazyna.gosciński@umed.wroc.pl

* Correspondence: mateusz.urbania@edu.uni.lodz.pl (M.M.U.); magdalena.chmiela@biol.uni.lodz.pl (M.C.)

Abstract: *Helicobacter pylori* (*H. pylori*) infection is the most common cause of chronic gastritis, peptic ulcers and gastric cancer. Successful colonization of the stomach by *H. pylori* is related to the complex interactions of these bacteria and its components with host cells. The growing antibiotic resistance of *H. pylori* and various mechanisms of evading the immune response have forced the search for new biologically active substances that exhibit antibacterial properties and limit the harmful effects of these bacteria on gastric epithelial cells and immune cells. In this study, the usefulness of pyomelanin (PyoM) produced by *Pseudomonas aeruginosa* for inhibiting the metabolic activity of *H. pylori* was evaluated using the resazurin reduction assay, as well as in vitro cell studies used to verify the cytoprotective, anti-apoptotic and pro-regenerative effects of PyoM in the *H. pylori* LPS environment. We have shown that both water-soluble (PyoM_{sol}) and water-insoluble (PyoM_{insol}) PyoM exhibit similar antibacterial properties against selected reference and clinical strains of *H. pylori*. This study showed that PyoM at a 1 µg/mL concentration reduced *H. pylori*-driven apoptosis and reactive oxygen species (ROS) production in fibroblasts, monocytes or gastric epithelial cells. In addition, PyoM enhanced the phagocytosis of *H. pylori*. PyoM_{sol} showed better pro-regenerative and immunomodulatory activities than PyoM_{insol}.

Keywords: pyomelanin; *Helicobacter pylori*; immunomodulation; apoptosis; phagocytosis



Citation: Urbaniak, M.M.; Rudnicka, K.; Gościński, G.; Chmiela, M. Can Pyomelanin Produced by *Pseudomonas aeruginosa* Promote the Regeneration of Gastric Epithelial Cells and Enhance *Helicobacter pylori* Phagocytosis? *Int. J. Mol. Sci.* **2023**, *24*, 13911. <https://doi.org/10.3390/ijms241813911>

Academic Editor: Giuseppe Zanotti

Received: 23 August 2023

Revised: 5 September 2023

Accepted: 8 September 2023

Published: 10 September 2023



Copyright: © 2023 by the authors. Licensee MDPI, Basel, Switzerland. This article is an open access article distributed under the terms and conditions of the Creative Commons Attribution (CC BY) license (<https://creativecommons.org/licenses/by/4.0/>).

1. Introduction

Helicobacter pylori (*H. pylori*) is a Gram-negative, helix-shaped, microaerophilic bacterium that colonizes the gastric mucosa of approximately half of the world's population [1]. *H. pylori* is one of the most successful gastric pathogens causing gastric and duodenal ulcers, gastric adenocarcinoma, mucosa-associated lymphoid tissue (MALT) lymphoma, and potentially other health dysfunctions leading to chronic inflammation, including coronary artery disease, iron deficiency anemia and autoimmune diseases [2–4]. The co-evolution of *H. pylori* within the human host has led to the development of efficient mechanisms for evading the innate immune response and the ability to colonize a gastric niche [5].

The primary adaptation mechanism of *H. pylori* is urease production, resulting in the alkalization of the acidic environment in the stomach and micro-niche formation ideal for *H. pylori* colonization followed by disruption of the intracellular tight junctions between epithelial cells and induction of an inflammatory response. Urease downregulates the production of arginase II and bactericidal nitric oxide (NO) in macrophages and promotes the survival of *H. pylori* within megasomes [6–9]. Other *H. pylori* virulence factors responsible for the disintegration of the gastric mucosa include vacuolating cytotoxin A (VacA)

and cytotoxin-associated gene A (CagA) protein [10]. VacA inhibits the lysosomal and autophagic killing of *H. pylori*, establishing an intracellular niche for bacterial survival in macrophages [11]. CagA is an oncoprotein that mediates a range of intra-cellular effects in gastric epithelial cells by affecting several signalling pathways to promote chronic inflammation and proliferation of gastric epithelial cells that change their polarity and morphology, contributing to an increased risk of gastritis or neoplasia [12,13].

H. pylori and components of these bacteria, including lipopolysaccharide (LPS), induce apoptosis of gastric epithelial cells and macrophages [14–16]. Furthermore, *H. pylori* LPS mimics the carbohydrate structures—Lewis antigens present in human gastric mucosa, erythrocytes, and endothelium, which may weaken the host's immune response towards these bacteria [17,18]. However, Lewis determinants of *H. pylori* LPS may drive the production of antibodies cross-reacting with the host components, resulting in the elevation of the complement-dependent inflammatory response [19]. Prolonged exposure of gastric epithelial cells to high levels of reactive oxygen species (ROS) generated during *H. pylori*-induced inflammation and subsequent redox imbalance lead to DNA damage, impairment of DNA repair mechanisms and cell apoptosis/necrosis [20].

The ability of *H. pylori* to avoid the response of innate immune mechanisms and the constant increase in antibiotic resistance are significant challenges in treating *H. pylori* infections [21]. A meta-analysis of 120 studies evaluating the effectiveness of first-line anti-*H. pylori* therapy showed that the eradication rate achieved in patients infected with resistant strains was only 67.4% [22]. The development of new drugs capable of eradicating *H. pylori* is highly recommended. One of the recent strategies concentrates on using bacterial metabolites, which may contribute to *H. pylori* eradication and modulation of the effector immune mechanisms impaired during infection. The potential candidate is pyomelanin (PyoM), a black-brown negatively charged extracellular polymer of homogentisic acid produced during L-tyrosine catabolism by *Pseudomonas aeruginosa* [23,24].

The presence of quinone structures in the PyoM molecule determines its oxidizing and reducing properties that allow for controlling the level of ROS [25]. The primary function of PyoM is protecting the bacterial cell from UV radiation [26] and the extracellular transfer of electrons [27]. The use of PyoM in the treatment of infections associated with excessive oxidative stress generated during inflammation is being considered [28]. Increased sensitivity of several bacterial pathogens to the antibiotics in the milieu of PyoM has been revealed, as well as the antibacterial activity of melanin against *H. pylori* has been demonstrated [29,30].

The study aimed to characterize the biological effects of water-soluble (PyoM_{sol}) and water-insoluble pyomelanin (PyoM_{insol}) regarding cytoprotective and pro-regenerative activity towards gastric epithelial cells. In addition, the antibacterial properties against *H. pylori* and the phagocytic efficiency of PyoM-stimulated monocytes, limited by the *H. pylori* component, were assessed.

2. Results

2.1. Antibacterial Activity of PyoM towards *H. pylori*

Both forms of PyoM, PyoM_{insol} and PyoM_{sol}, significantly reduced the viability of reference and clinical strains of *H. pylori* as examined by the resazurin reduction assay (Figure 1). The percentage of viable bacteria treated with PyoM formulations at a concentration of 16 µg/mL ($p < 0.001$) was significantly lower than the percentage of viable bacilli exposed to PyoM at a concentration of 1 µg/mL. Dose–response curves and MIC₅₀ as well as MIC₉₉ of PyoM against the reference *H. pylori* CCUG 17784 and two clinical isolates, *H. pylori* M91 and *H. pylori* M102 are shown in Figure 2. MIC₅₀ and MIC₉₉ were defined as the lowest concentration of the PyoM at which 50% and 99% of the *H. pylori* cells were killed, respectively. The PyoM_{sol} MIC₅₀ towards the reference *H. pylori* CCUG 17784 strain was 14.5 µg/mL and 19.5 µg/mL for *H. pylori* M91 or 18.6 µg/mL for *H. pylori* M102. The PyoM_{insol} MIC₅₀ against *H. pylori* CCUG 17784 was 7.2 µg/mL, while for *H. pylori* M91 was 18.4 µg/mL and 15.5 µg/mL towards *H. pylori* M102. The MIC₉₉ of PyoM_{sol} against the studied *H. pylori* strains was in the range 31.7–34.2 µg/mL, while MIC₉₉ of PyoM_{insol}

was in the range 19.3–29.0 $\mu\text{g}/\text{mL}$. For all *H. pylori* strains, the MIC₉₉ of clarithromycin or amoxicillin was significantly ($p < 0.001$) lower compared to the MIC of both forms of PyoM (Figure 2).

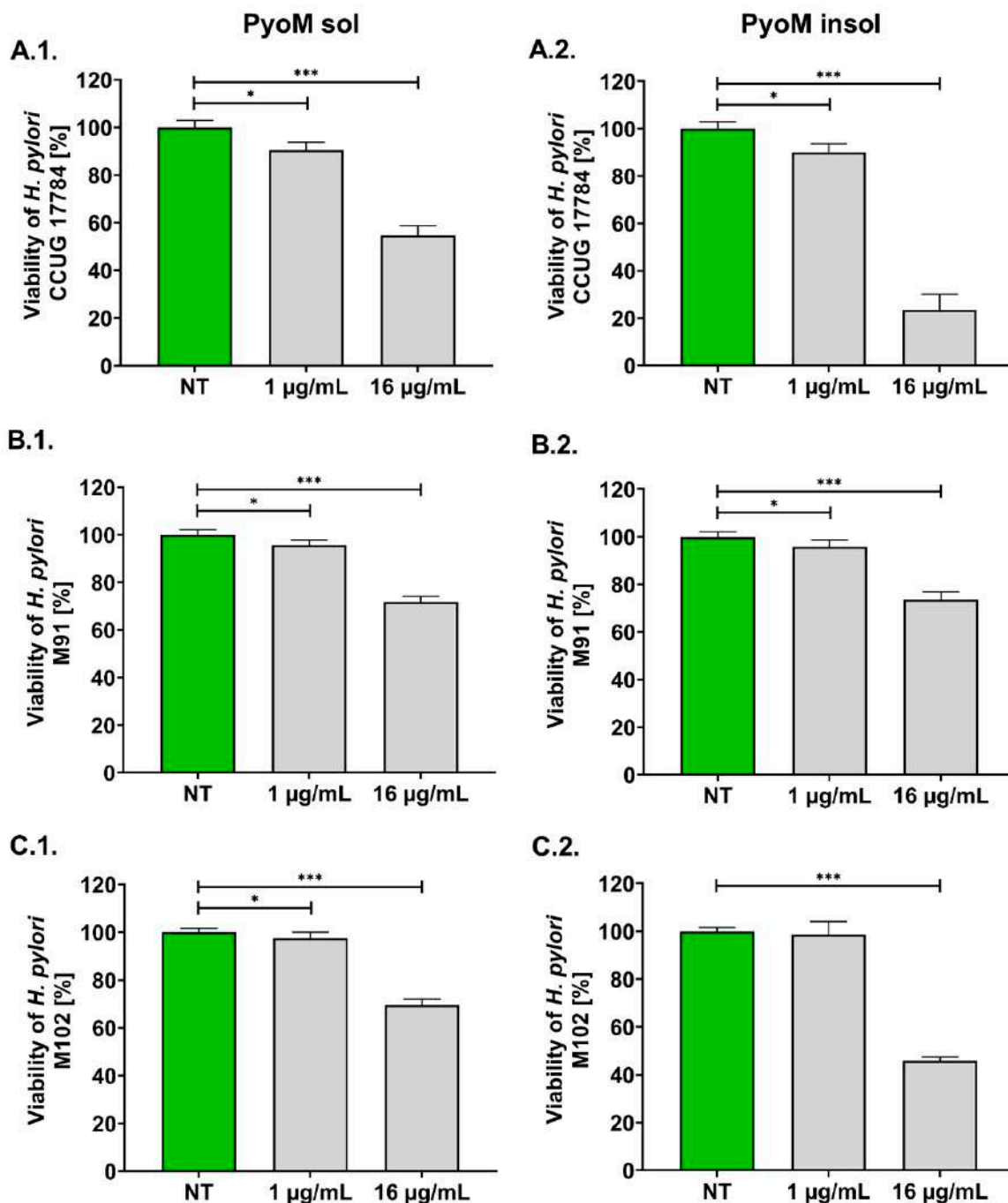
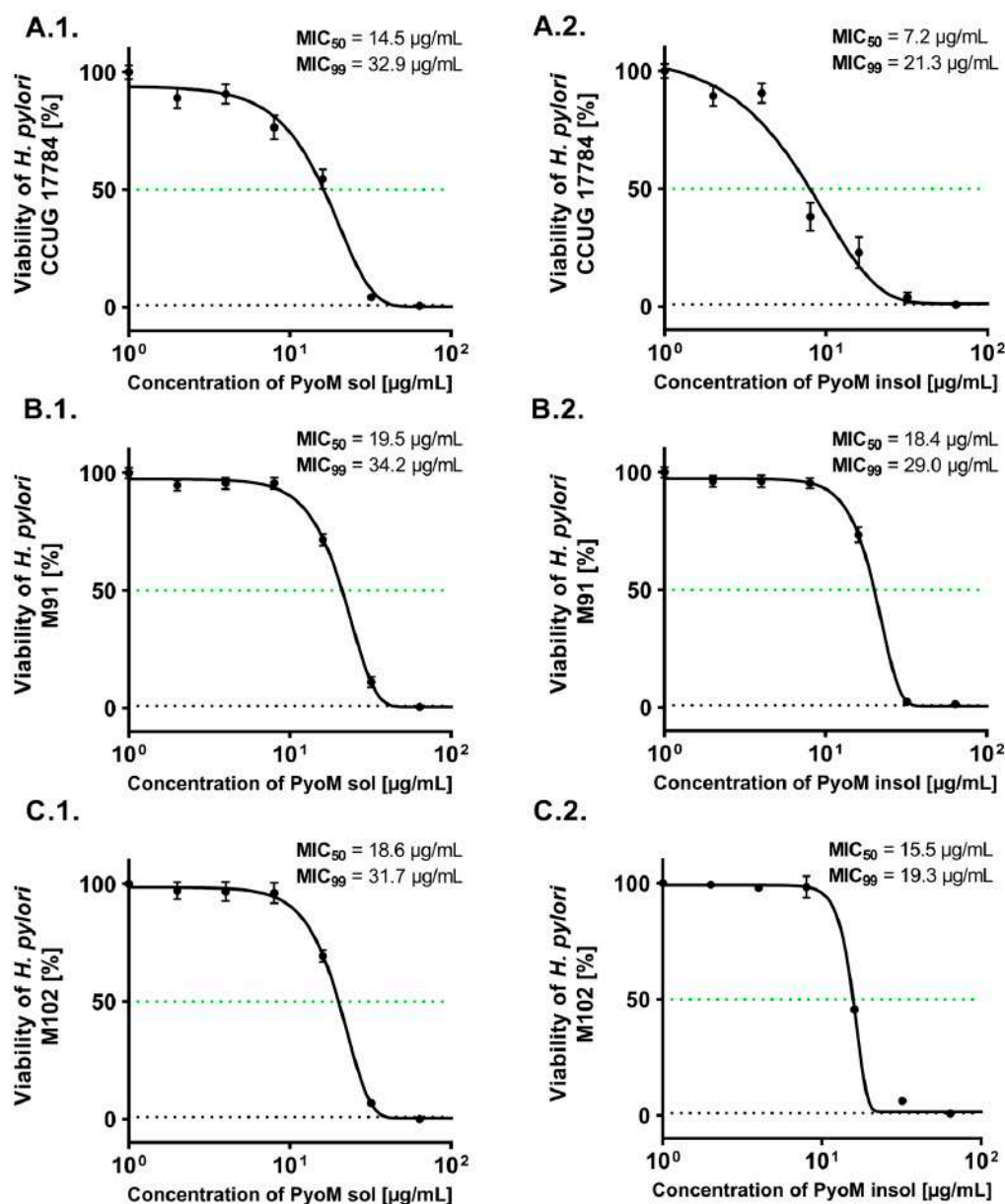


Figure 1. Antibacterial activity of pyomelanin against *Helicobacter pylori* strains. (1) Water-soluble pyomelanin (PyoM_{sol}) and (2) water-insoluble pyomelanin (PyoM_{insol}) were used at a concentration of 1 $\mu\text{g}/\text{mL}$ or 16 $\mu\text{g}/\text{mL}$. *H. pylori* strains: (A) CCUG 17784, (B) M91 and (C) M102. Results are shown as means with standard deviations (SD) of four independent experiments performed in four replicates for each experimental variant. Statistical significance for * $p < 0.05$; *** $p < 0.001$; NT—untreated bacterial cells.



<i>H. pylori</i> strain	MIC ₉₉ of clarithromycin [µg/mL]	MIC ₉₉ of amoxicillin [µg/mL]
CCUG 17784	0.13	0.02
M91	3.00	0.03
M102	0.02	0.02

Figure 2. Dose–response curves and minimum inhibitory concentration (MIC)₅₀ and MIC₉₉ of pyomelanin and reference antibiotics against *Helicobacter pylori* strains, clarithromycin or amoxicillin. (1) Water-soluble (PyoM_{sol}) and (2) water-insoluble pyomelanin (PyoM_{insol}). *H. pylori* strains: (A) CCUG 17784, (B) M91 and (C) M102. Results are shown as means with standard deviations (SD) of four independent experiments performed in four replicates for each experimental variant. The green line indicates the 50% level of *H. pylori* viability.

2.2. PyoM Neutralizes the Cytotoxic Effect of *H. pylori* LPS towards Gastric Epithelial Cells and Monocytes

We showed that PyoM_{sol} and PyoM_{insol} did not affect the metabolic activity and thus the viability of reference mouse fibroblasts L-929, human gastric epithelial cells AGS and human THP-1 monocytes at the concentration of 1 µg/mL or 16 µg/mL (Figure 3).

In cell cultures exposed for 24 h to *H. pylori* LPS alone, the percentage of viable cells significantly ($p < 0.001$) decreased to $75.1\% \pm 6.8\%$, $82.2\% \pm 4.3\%$ and $80.5\% \pm 6.8\%$, respectively. Similarly, the viability of studied cells in the presence of LPS *E. coli* significantly ($p < 0.001$) diminished. In cell cultures treated simultaneously with PyoM_{sol} or PyoM_{insol} at a concentration of 1 $\mu\text{g}/\text{mL}$ or 16 $\mu\text{g}/\text{mL}$ and *H. pylori* or *E. coli* LPS, the cell viability was similar to the viability of untreated cells, which suggests that PyoM neutralized the cytotoxic effect of LPS ($p < 0.001$).

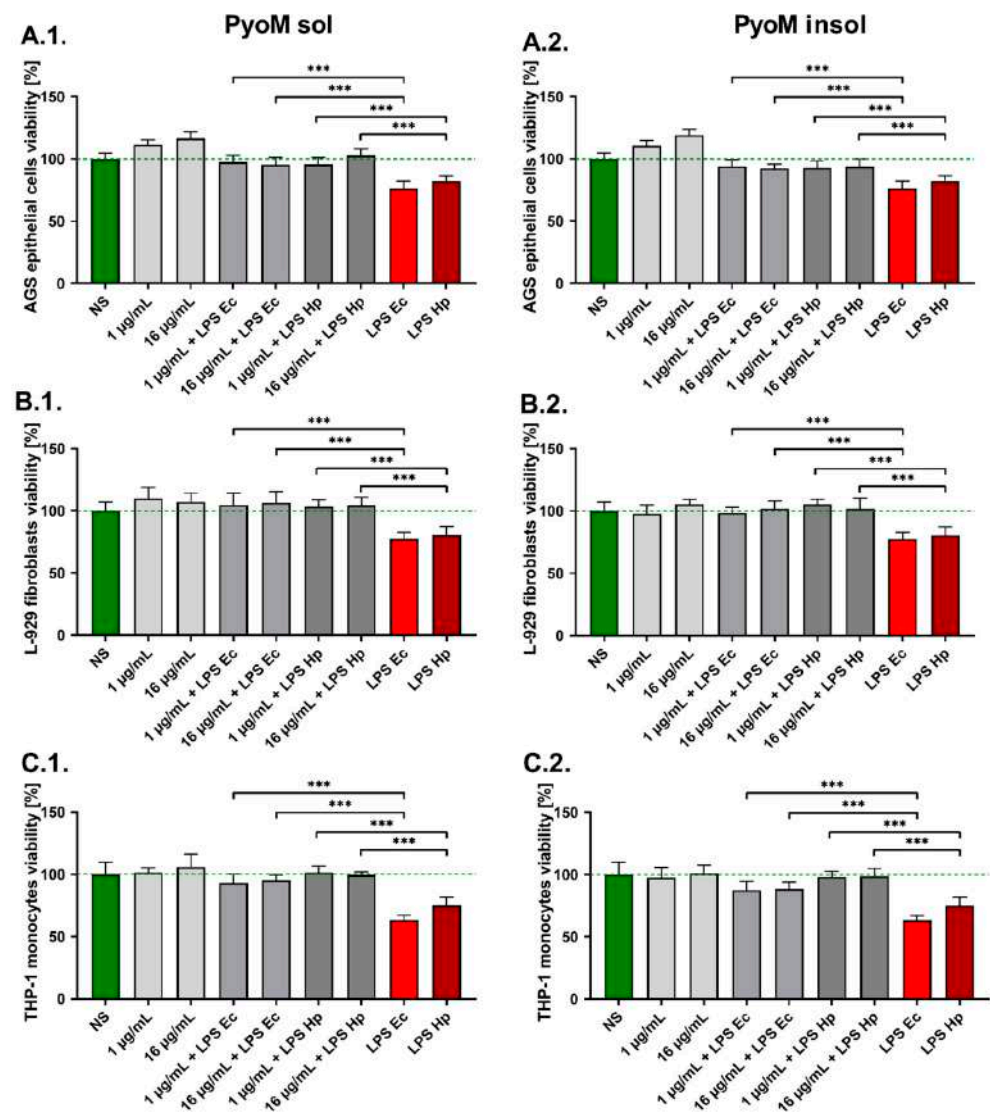


Figure 3. Reversion of the cytotoxic effect of *H. pylori* lipopolysaccharide (LPS) or *E. coli* LPS by pyomelanin. (1) Water-soluble (PyoM_{sol}) or (2) water-insoluble pyomelanin (PyoM_{insol}) at a concentration of 1 $\mu\text{g}/\text{mL}$ or 16 $\mu\text{g}/\text{mL}$. Cell cultures: (A) AGS gastric epithelial cells, (B) L-929 mouse fibroblasts and (C) THP-1 human monocytes. Cells were stimulated for 24 h with PyoM alone, lipopolysaccharide (LPS) *H. pylori* (LPS Hp) or LPS *E. coli* (LPS Ec) alone or both. Results are shown as means with standard deviations (SD) of six independent experiments performed in six replicates for each experimental variant. Statistical significance for *** $p < 0.001$. NS—unstimulated cells. The green line indicates the reference viability of unstimulated cells.

2.3. LPS-Induced Apoptosis Is Diminished in the Presence of PyoM_{sol}

The PyoM_{sol}-mediated neutralization of *H. pylori* LPS-induced cytotoxicity prompted us to examine whether the inhibition of cell apoptosis accompanies this phenomenon.

Neither PyoM_{sol} nor $\text{PyoM}_{\text{insol}}$ induced cell apoptosis manifested by the lack of an increase in the Apoptotic Index (AI) compared to untreated cells (Figure 4). The AI in AGS, L-929 and THP-1 cells increased significantly ($p < 0.001$) after cell exposure to *H. pylori* LPS compared to untreated cells (AI = 1.00), and was equal to 1.48 ± 0.09 , 1.17 ± 0.04 and 1.28 ± 0.08 , respectively. *E. coli* LPS, similar to *H. pylori* LPS, significantly ($p < 0.001$) increased the AI of gastric epithelial cells, fibroblasts and monocytes. In cell cultures carried out in the presence of PyoM_{sol} , the cell apoptosis induced by *H. pylori* LPS or *E. coli* LPS significantly diminished ($p < 0.01$) compared to the level of apoptosis after cell stimulation with *H. pylori* or *E. coli* LPS alone. However, $\text{PyoM}_{\text{insol}}$ only at a concentration of 1 $\mu\text{g}/\text{mL}$ ($p < 0.05$) decreased the AI of AGS and THP-1 cells co-stimulated with *H. pylori* LPS. By comparison, for $\text{PyoM}_{\text{insol}}$ (16 $\mu\text{g}/\text{mL}$), a reduction in the AI was demonstrated only for AGS cells co-stimulated with *E. coli* LPS.

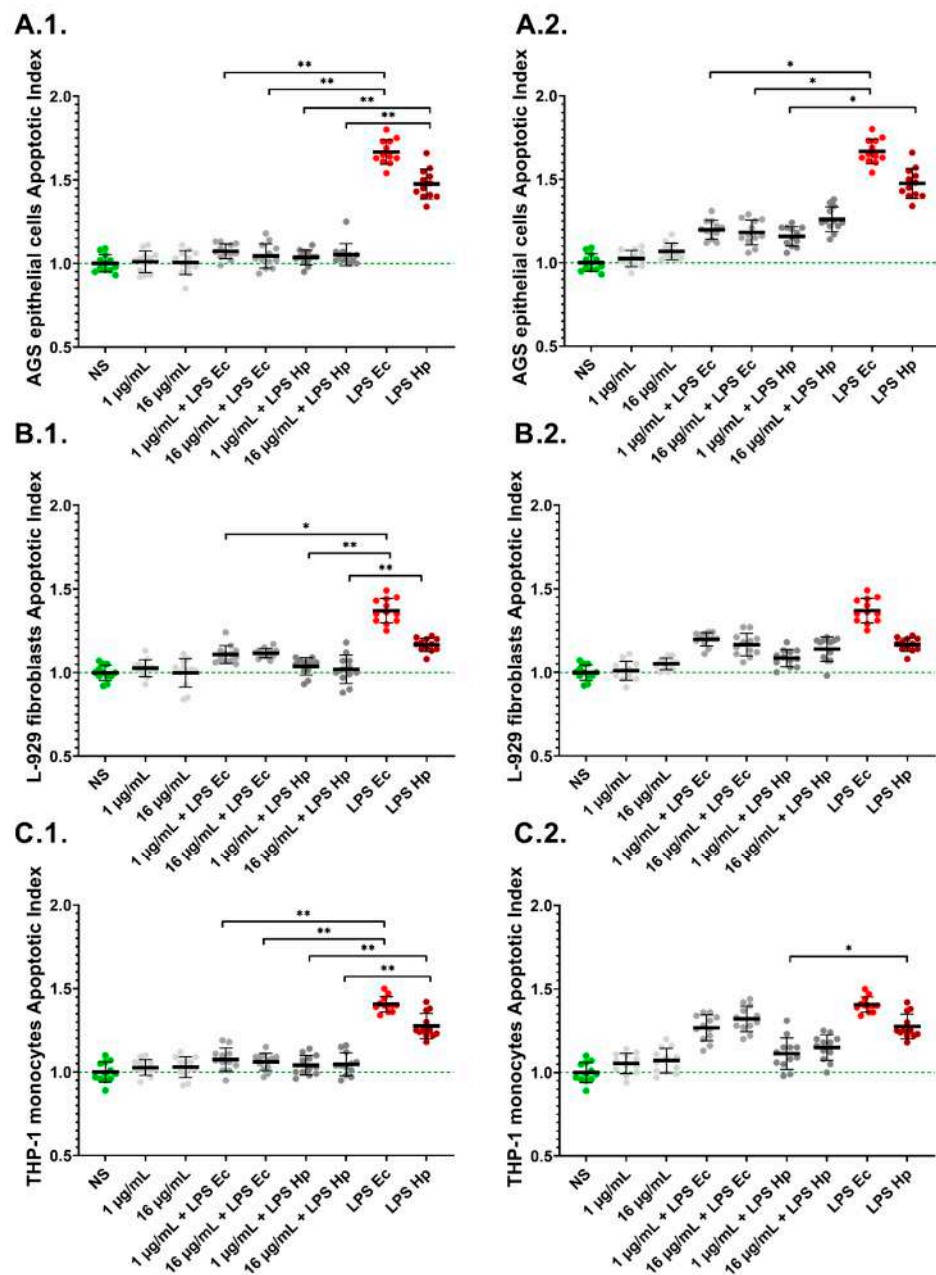


Figure 4. Diminishing cell apoptosis induced by *H. pylori* lipopolysaccharide (LPS) or *E. coli* LPS in the milieu of pyomelanin in cell cultures in vitro. (1) Water-soluble pyomelanin (PyoM_{sol}) or

(2) water-insoluble pyomelanin (PyoM_{insol}) were used at a concentration of 1 µg/mL or 16 µg/mL. (A) AGS gastric epithelial cells, (B) L-929 mouse fibroblasts and (C) THP-1 human monocytes were stimulated for 24 h with PyoM alone, lipopolysaccharide (LPS) *H. pylori* (LPS Hp) or LPS *E. coli* (LPS Ec) alone or both. The Apoptotic Index was calculated based on the relative fluorescence units (RFU) of stimulated cells vs. RFU of the control unstimulated cells. Results are shown as means with standard deviations (SD) of four independent experiments performed in triplicate for each experimental variant. Statistical significance for * $p < 0.05$; ** $p < 0.01$. NS—unstimulated cells. The green line indicates the reference Apoptotic Index of unstimulated cells.

2.4. PyoM Neutralizes Reactive Oxygen Species Produced by Cells Exposed to *H. pylori* LPS

The LPS of *H. pylori* and the reference *E. coli* LPS induced significantly higher ($p < 0.001$) ROS production in AGS cells after 30 min or 24 h as compared to the unstimulated cells (Figure 5). The AGS gastric epithelial cells after long-term (24 h) exposure to *H. pylori* LPS responded by ROS production more effectively than these cells after short-term (30 min) stimulation. Both forms of PyoM induced a significant ($p < 0.001$) reduction of ROS in cell cultures co-stimulated with PyoM and *H. pylori* LPS or *E. coli* LPS when compared to cells stimulated with LPS alone.

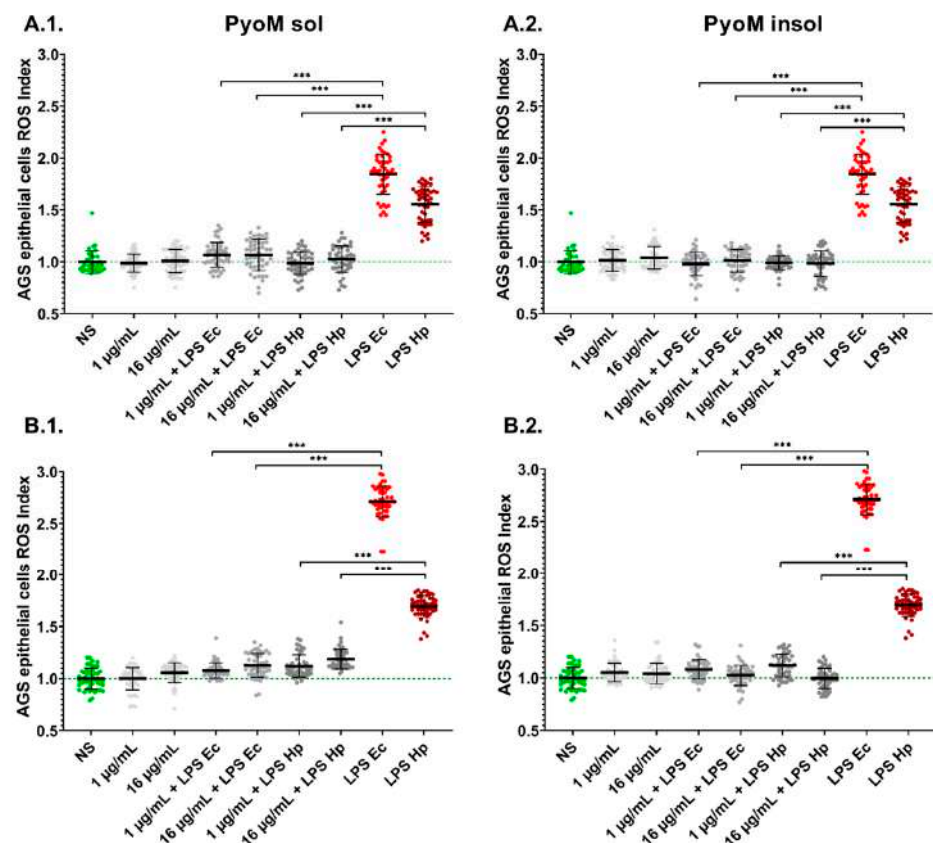


Figure 5. Neutralization by pyomelanin of reactive oxygen species (ROS) produced by AGS gastric epithelial cells. Cells were stimulated for 24 h with (1) water-soluble pyomelanin (PyoM_{sol}) or (2) water-insoluble pyomelanin (PyoM_{insol}) at a concentration of 1 µg/mL or 16 µg/mL alone or with lipopolysaccharide (LPS) of *H. pylori* (LPS Hp) or *E. coli* LPS (LPS Ec) in the milieu with or without pyomelanin (PyoM). ROS production index after (A) 30 min or (B) 24 h of cell stimulation with (1) PyoM_{sol} or (2) PyoM_{insol}. The ROS Index was calculated based on the relative fluorescence units (RFU) of stimulated cells vs. RFU of control unstimulated cells. Results are shown as means with standard deviations (SD) of six independent experiments performed in eight replicates for each experimental variant. Statistical significance for *** $p < 0.001$. NS—unstimulated cells. The green line marks the reference ROS Index of unstimulated cells.

2.5. *PyoM_{sol}* Promotes the Migration of Gastric Epithelial Cells Affected by *H. pylori* LPS

The migration of untreated AGS cells increased with time and the average percentages of cells in the wounded zone were: $28.9\% \pm 7.6\%$, $62.5\% \pm 4.5\%$ and 100% after 24, 48 and 72 h, respectively (Figure 6). *PyoM_{sol}* and *PyoM_{insol}* significantly stimulated the cell migration within the wound after 24 and 48 h, and the wound healing rate was $60.7\% \pm 4.8\%$ and $85.2\% \pm 1.8\%$ for *PyoM_{sol}* and $60.5 \pm 4.9\%$ and $79.3\% \pm 2.2\%$ for *PyoM_{insol}*, respectively. *E. coli* LPS significantly affected the cell migration by up to $9.7\% \pm 6.6\%$, $46.8\% \pm 6.0\%$, and $66.3\% \pm 4.3\%$ confluence in 24, 48 and 72 h cell cultures, respectively. *H. pylori* LPS at the same time points significantly reduced the rate of AGS cell migration to $12.2\% \pm 5.3\%$, $38.2\% \pm 7.8\%$ and $39.4\% \pm 6.3\%$, respectively. Co-stimulation of AGS cells with *PyoM_{sol}* and *H. pylori* LPS resulted in an increased wound closure to $29.7\% \pm 6.6\%$, $59.0\% \pm 3.1\%$ and $81.0\% \pm 2.4\%$ after 24, 48, and 72 h, respectively, when compared to the effect induced by LPS used separately. Compared to the effect of LPS used individually, co-stimulation of AGS cells with *PyoM_{insol}* and *E. coli* LPS increased the rate of wound closure by $27.2\% \pm 5.5\%$ and $64.2\% \pm 3.2\%$ after 24 and 48 h, respectively. We have shown that co-stimulation of AGS cells with *PyoM_{sol}* and *E. coli* LPS did not influence the rate of wound closure compared to the cells treated with LPS alone. Similar results were shown in AGS cell cultures exposed to *PyoM_{insol}* and *H. pylori* LPS.

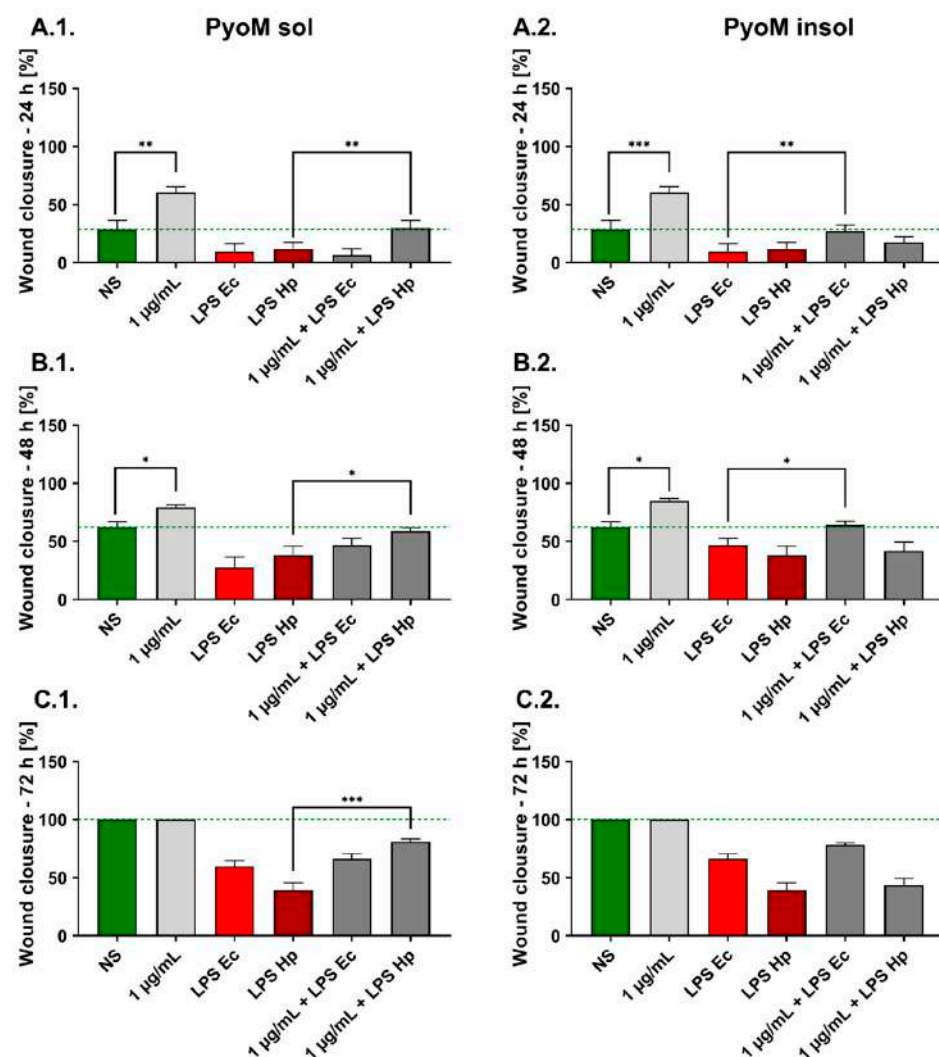


Figure 6. The effectiveness of AGS cell migration in wound healing assay. The cell cultures were exposed to (1) water-soluble pyomelanin (*PyoM_{sol}*) or (2) water-insoluble pyomelanin (*PyoM_{insol}*) alone,

lipopolysaccharide (LPS) of *H. pylori* (LPS Hp) or *E. coli* LPS (LPS Ec) alone or both to pyomelanin and LPS for (A) 24 h, (B) 48 h or (C) 72 h. Results are shown as means with standard deviations (SD) of four independent experiments performed in triplicate for each experimental variant. Statistical significance for * $p < 0.05$; ** $p < 0.01$; *** $p < 0.001$. NS—unstimulated cells. The green line indicates the reference wound closure of unstimulated cells.

2.6. *PyoM_{sol}* Enhances the Phagocytic Capacity of Monocytes towards Fluorescently Labelled *E. coli* or *H. pylori*

The fluorescently labelled reference *E. coli* (*E. coli* pHrodo™) or *H. pylori* were used in the phagocytosis assay performed with THP-1 monocytes exposed for 24 h to *H. pylori* LPS or *E. coli* LPS alone, *PyoM* alone or to LPS and *PyoM*. The results of the phagocytosis assay expressed as a Phagocytic Index (PI) are shown in Figure 7. The stimulation of monocytes with *PyoM_{sol}* or *PyoM_{insol}* resulted in a significant ($p < 0.001$) improvement in the phagocytosis of the reference *E. coli* pHrodo™. By comparison, *H. pylori* LPS significantly ($p < 0.001$) reduced the ability of monocytes to engulf *E. coli* pHrodo™ compared to untreated cells. However, co-stimulation of THP-1 monocytes with *PyoM_{sol}* (1 and 16 µg/mL) or *PyoM_{insol}* (1 µg/mL) and *H. pylori* LPS resulted in a reversion of the LPS-induced inhibition of phagocytosis. In addition, *PyoM_{sol}*, but not *PyoM_{insol}*, induced a significant ($p < 0.001$) increase in the phagocytic index of THP-1 monocytes co-stimulated with *E. coli* LPS, compared to those cells treated solely with LPS alone. In the case of live fluorescently labelled *H. pylori*, the *PyoM_{sol}* at a concentration of 1 µg/mL or 16 µg/mL significantly ($p < 0.001$) increased the PI of THP-1 monocytes compared to untreated cells. *PyoM_{insol}* showed a similar effect, however, only at a concentration of 1 µg/mL.

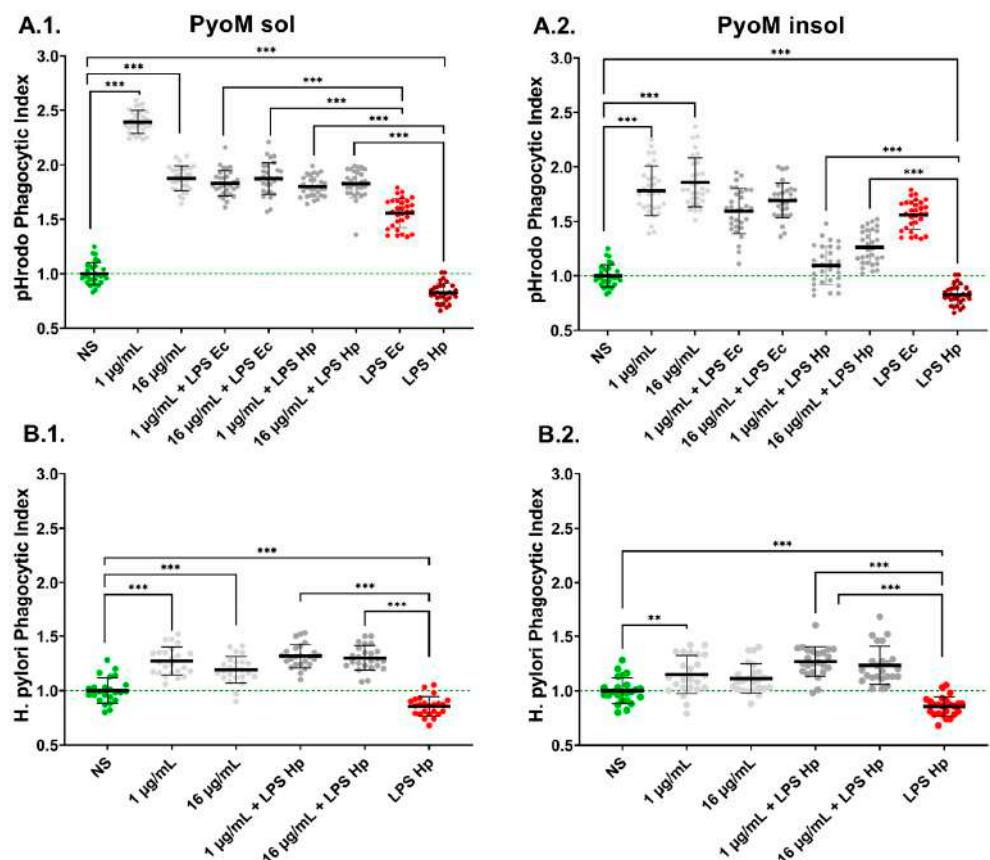


Figure 7. Upregulation of phagocytic activity of THP-1 human monocytes towards a fluorescently labelled *E. coli* or *H. pylori*, in vitro. THP-1 cells were stimulated with (1) water-soluble (*PyoM_{sol}*) or

(2) water-insoluble pyomelanin (PyoM_{insol}), lipopolysaccharide (LPS) of *H. pylori* (LPS Hp) or *E. coli* LPS (LPS Ec) alone or co-stimulated with the studied formulations of PyoM and *H. pylori* LPS or *E. coli* LPS. (A) Phagocytosis of reference *E. coli* pHrodo™ and (B) phagocytosis of *H. pylori* fluorescently labelled *H. pylori* with BacLight™. The Phagocytic Index was calculated based on relative fluorescence units (RFU) of stimulated cells vs. RFU of control unstimulated cells. Results are shown as means with standard deviations (SD) of four experiments performed in six replicates for each experimental variant. Statistical significance for ** $p < 0.01$; *** $p < 0.001$. NS—unstimulated cells. The green line indicates the reference Phagocytic Index of unstimulated cells.

3. Discussion

The discovery of *H. pylori* in 1982 by Warren and Marshall proved that the stomach, with its acidic pH, can be colonized by these bacteria [5]. Development of gastritis, gastric or duodenal ulcers, and even gastric cancer due to *H. pylori* infection depends on bacterial virulence factors, susceptibility of the host, efficiency of the immune mechanisms, and environmental conditions [31]. The increasing antibiotic resistance of this pathogen requires the search for new therapeutic agents with antibacterial activity [32,33]. Moreover, cytoprotective and immunomodulatory activity of therapeutic formulations should also be considered. This study demonstrated that PyoM_{sol} and PyoM_{insol} exhibit antibacterial activity against the reference and clinical *H. pylori* strains. The antibacterial activity of bacterial melanins was previously described by Vasanthabharathi et al., who showed that a pigment isolated from a marine strain of *Streptomyces* sp. inhibited the growth of *E. coli* and *Lactobacillus vulgaris* [34]. Zerrad et al. reported that melanin isolated from *Pseudomonas balearica* showed strong antimicrobial activity against *Staphylococcus aureus*, *E. coli* and *Candida albicans*, as well as the phytopathogenic *Erwinia chrysanthemi* and *E. carotovora* [35]. Xu et al. have suggested that the toxicity of fungal melanin towards *Vibrio parahaemolyticus* and *S. aureus* is related to the impairment in the bacterial cell membrane of these pathogens [36]. It was shown that melanin and glucan complexes diminish the viability of *C. albicans* and *H. pylori* [37].

Melanin compounds are known to bind redox active metal ions, including iron ions (Fe²⁺/Fe³⁺) [38]. The study of Waidner et al. showed that disturbances in the uptake of Fe ions by *H. pylori* result in reduced bacterial activity and the ability to colonize the stomach [39]. PyoM, by reduction of soluble Fe to insoluble Fe, provides homeostasis for Fe²⁺/Fe³⁺ ions, which is necessary for the survival of pyomelaninogenic bacteria [40]. Reducing the solubility of Fe in the *H. pylori* niche may result in disturbances in ion metabolism and limit the viability of these bacteria. Further studies are needed to confirm the iron-dependent mechanism of PyoM antibacterial activity against *H. pylori*.

We have shown that PyoM has a cytoprotective effect on fibroblasts, gastric epithelial cells and monocytes, which were primed with *H. pylori* LPS or the reference *E. coli* LPS in vitro. Potentially, in vivo PyoM may protect the gastric epithelium from *H. pylori*-driven damage and prevent the infiltration of *H. pylori* components through the epithelial barrier. These *H. pylori*-related effects have been demonstrated in earlier studies [16,41,42].

In this study, we determined the level of cell viability, apoptosis and ROS production to verify the cytoprotective mechanism of PyoM against *H. pylori* LPS-driven deleterious effects.

Apoptosis plays an essential role in gastric tissue physiology [43]. Especially, in *H. pylori*-induced chronic gastritis, where excessive apoptotic cell loss dominates over cell proliferation [44]. It has been shown that *H. pylori* and soluble components of these bacteria, including LPS, increase ROS generation in the gastric mucosa, which may contribute to apoptosis of gastric epithelial cells. In a model of primary gastric epithelial cells and fibroblasts of guinea pig, it was revealed that *H. pylori* LPS-mediated upregulation of ROS leads to an increased rate of apoptosis and reduced cell-to-cell integrity [16,45]. In this study, the percentage of cells undergoing apoptosis in the milieu of *H. pylori* LPS, in cell cultures of gastric epithelial cells, fibroblasts or monocytes in vitro, has been diminished in the presence of PyoM_{sol}. Further in vivo studies are needed to confirm this effect.

In *H. pylori*-infected patients, the increased ROS can be delivered by granulocytes and macrophages recruited to the gastric mucosa in response to chemotactic signals. Ding et al. showed that *H. pylori* may also generate ROS directly and contribute to the accumulation of ROS in gastric tissues [46]. *H. pylori* infection also contributes to the production of reactive nitrogen species (RNS), and this effect is related to nicotinamide adenine dinucleotide phosphate oxidase (Nox) and inducible nitric oxide synthase (iNOS) production [14]. Moreover, neutrophils and gastric epithelial cells also express iNOS, involved in the production of NO, which reacts with metal ions and ion superoxide, producing a strong oxidant—peroxynitrite [14,47]. Patients infected with *H. pylori* have elevated levels of ROS along with increased activity of NO-derived metabolites, indicating the activation of iNOS [48].

Lorguin et al., using a human keratinocyte model, showed that PyoM effectively suppresses ROS activity in cells exposed to UVA light [26]. Our studies have shown that both PyoM_{sol} and PyoM_{insol} neutralized the short-term and long-term activity of intracellular ROS induced by *H. pylori* LPS in a model of gastric epithelial cells, which was correlated with diminishing the number of cells undergoing apoptosis. These cytoprotective properties of PyoM are very promising since the leakage of the gastric epithelial barrier due to uncontrolled ROS production and excessive apoptosis may facilitate the systemic distribution of *H. pylori* components [41]. In the present study, we showed that PyoM_{sol} selectively improved the cell migration affected by *H. pylori* LPS, while PyoM_{insol} upregulated the cell migration inhibited in the presence of *E. coli* LPS. A different profile of cell migration in cell cultures exposed to *H. pylori* LPS or *E. coli* LPS and PyoM may result from some differences in the chemical structure of PyoM_{sol} and PyoM_{insol}, as well as their ability to bind individual bacterial LPS, *H. pylori* LPS or *E. coli* LPS.

Professional phagocytes remove pathogenic microorganisms and apoptotic cells and initiate an adaptive immune response by presenting antigens to lymphocytes [49]. It has been shown that in the presence of *H. pylori* LPS, the engulfment of these bacteria by phagocytes is diminished [50–52]. Also, surface haemagglutinins of *H. pylori* and urease may downregulate the ability of phagocytes to ingest these bacteria [6,53]. We have shown that PyoM_{sol} and PyoM_{insol} at a concentration of 1 µg/mL or 16 µg/mL effectively stimulated monocytes to increase phagocytosis of the reference *E. coli* pHrodo™. PyoM_{sol} in both concentrations enhanced the ingestion of fluorescently labelled *H. pylori*, while for PyoM_{insol}, only at 1 µg/mL. PyoM_{sol} also upregulated the engulfment of *E. coli* particles, which was diminished in the milieu of LPS *E. coli* or LPS *H. pylori*. In contrast, PyoM_{insol} only upregulated the phagocytic activity of monocytes diminished in the presence of *H. pylori* LPS; however, less effectively than PyoM_{sol}. Moreover, PyoM_{sol} upregulated the ingestion of *H. pylori*, which was inhibited by *H. pylori* LPS. These results indicate that PyoM_{sol} possesses better immunomodulatory potential towards monocyte phagocytic activity than PyoM_{insol}. Alviano et al. reported that soluble melanin isolated from *Fonsecaea pedrosoi* activated macrophages and neutrophils, resulting in increased phagocytosis and oxidative burst during incubation with *F. pedrosoi* and *C. albicans* [54].

H. pylori has developed a set of antioxidant proteins, including superoxide dismutase, catalase and arginase, which protect these bacteria from oxidative destruction during phagocytosis [55]. The question arises about the possible cellular mechanisms involved in upregulating *E. coli* or *H. pylori* engulfment by monocytes in the presence of PyoM, omitting antioxidative PyoM properties. PyoM possibly activates monocytes extracellularly through the cell surface receptors and induces metabolic reprogramming of phagocytes. A recent study by Chen et al. showed that fungal melanin of *Aspergillus fumigatus* may function as a pathogen-associated molecular pattern molecule. This fungal component induces in macrophages the activation of hypoxia-inducible factor 1 subunit alpha (HIF-1α) and phagosomal recruitment of mammalian target of rapamycin (mTOR)—Akt/mTOR/HIF1α axis resulting in a metabolic shift towards glycosylation, i.e., metabolic reprogramming of macrophages. As a result, the antimicrobial activity of macrophages was increased [56]. The study by Goncalves et al. revealed that by remodelling the calcium sequestration inside

the phagosome and impairing signalling via calmodulin, fungal melanin drives the above glycosylation pathway [57]. In the case of gastric mucosa, the antioxidative properties of PyoM may improve the protection of epithelial cells and immune cells from deleterious oxidative stress generated in the *H. pylori*-driven inflammatory milieu. Protective properties of PyoM against monocyte death in the milieu of *H. pylori* components (including LPS) may result in more effective eradication of this pathogen.

In conclusion, PyoM seems to be a promising candidate for diminishing the negative effects caused by *H. pylori* in the gastric mucosa. The in vitro gastro-protective activity of PyoM is related to its anti-oxidative properties in conjunction with the control of cell apoptosis. PyoM also possesses pro-regenerative activity since it stimulates the cell migration affected by *H. pylori* LPS. We showed that the ability of monocytes to engulf fluorescently labelled *E. coli* or *H. pylori* is significantly enhanced in the presence of PyoM. From two studied PyoM formulations, PyoM_{sol} better stimulated the migration of gastric epithelial cells and phagocytic activity of monocytes, which were affected by LPS *H. pylori* than PyoM_{insol}, and due to this, PyoM_{sol} is promising for further study in an in vivo model of *H. pylori* infection in *Caviae porcellus* (guinea pigs), which previously was characterized by us in terms of inflammatory and immune responses [52,58].

Despite the description of the antibacterial activity of PyoM, its bactericidal mechanism remains unknown, which is a limitation of this study. Further studies are required to determine the potential molecular targets for PyoM and the specificity of the antibacterial activity against Gram-negative and Gram-positive bacteria. Further research will be carried out to define the molecular basis underlying PyoM_{sol}/PyoM_{insol}-mediated cellular effects.

4. Materials and Methods

4.1. Growth Conditions of *Pseudomonas aeruginosa*

When starting a strain from a frozen stock, the *P. aeruginosa* Mel+ strain (Collection of Department of Immunology and Infectious Biology University of Łódź, Poland) was streaked out onto a Luria Broth (LB) agar plate, and a subsequent liquid culture started the next day. The LB broth was then inoculated with the single colony exhibiting Gram-negative rod-shaped morphology, positive oxidase test and a presence of pigmentation and incubated in aerobic conditions (37 °C, 18 h) to obtain an initial log-phase bacterial suspension. To isolate PyoM with the reduction of undesirable substances, the Pyomelanin Minimal Medium II (PMM II) (patent application number: PL438865) was used [24]. PMM II was inoculated with 1.0 mL of a 1.0 McFarland bacterial suspension and grown for five days in the microbiological incubator (37 °C, shaking at 120 rpm). When the colour of the medium changed from honey-like to black, the cultures were transferred to room temperature and exposed to sunlight, which stimulated the production of the pigment (48 h).

4.2. Isolation and Purification of PyoM_{insol} and PyoM_{sol}

The isolation and purification of two variants of pyomelanin were performed as previously described [24]. To isolate the water-insoluble pyomelanin (PyoM_{insol}), the bacterial culture was centrifuged (6600 × g), and supernatant was acidified to pH 2.0 with 6.0 M HCl (PolAura, Dywity, Poland). The PyoM_{insol} pellet was washed with HCl and double-washed with distilled water. Finally, the Pyo_{insol} pellet was suspended in pure ethanol (Chempur, Piekary Śląskie, Poland), and placed in a water bath (95 °C, 30 min.). PyoM_{insol} was washed twice with ethanol and air-dried. In order to obtain water-soluble pyomelanin (PyoM_{sol}), the bacterial cell-free supernatant was incubated with chloroform in a 1:1 ratio under shaking conditions for 24 h (room temperature, shaking at 120 rpm). The aqueous phase containing the PyoM_{sol} was separated from the chloroform and protein phase using a separating funnel. To remove residual protein contaminants, the aqueous layer was centrifuged (6600 × g), and then PyoM_{sol} was purified from low molecular weight soluble substances by ultrafiltration (MWCO 5 kDa) (Sartorius, Göttingen, Germany). The PyoM_{sol} was dried overnight at 50 °C. Endotoxin was removed via affinity chromatography using Pierce™

High Capacity Endotoxin Removal Spin Columns (Thermo Scientific, Waltham, MA, USA). The resin and column were prepared and equilibrated according to the manufacturer's protocol. The samples of PyoM_{sol} and PyoM_{insol} (5 mg/mL) were applied to the columns, incubated for 3 h with gentle mixing, centrifuged at 500× *g* and pellets were collected in the new tubes and dried at 50 °C overnight. PyoM_{insol} and PyoM_{sol} pellets were washed with chloroform, ethyl acetate, ethanol and water. For further experiments, the PyoM variants were stored in a dark and dry place at 4 °C.

4.3. Cell Cultures

The reference L-929 mouse fibroblasts, human AGS gastric adenocarcinoma epithelial cells and human THP-1 monocytes purchased from the American Type Culture Collection (ATCC, Rockville, MD, USA) were used and propagated as previously described [24,41]. Prior to experiments, L-929 and THP-1 cells were cultured in Roswell Park Memorial Institute (RPMI)-1640 medium supplemented with 10% heat-inactivated foetal calf serum (FCS; HyClone Cytiva, Marlborough, MA, USA), and the antibiotics penicillin (100 U/mL) and streptomycin (100 µg/mL) (Sigma-Aldrich, Darmstadt, Germany). AGS cells were grown in Dulbecco's Modified Eagle Medium/Nutrient Mixture F-12 (DMEM/F-12; Biowest, Nuaille, France), containing 10% heat inactivated FCS, and standard antibiotics. Cell cultures were incubated at 37 °C in a humidified atmosphere containing 5% CO₂. The cells were passaged with 0.25% trypsin in 0.02% ethylenediaminetetraacetic acid (EDTA) (Biowest, Nuaille, France). The cell viability and density were assessed using trypan blue (Blaubrand, Wertheim, Germany) exclusion assay. The cells were used in the experiments when cell's viability was higher than 95%.

4.4. Cell Stimulators

The reference *Helicobacter pylori* strain CCUG 17874 (purchased from Culture Collection, University of Gothenburg, Gothenburg, Sweden), positive for vacuolating toxin A (VacA) and cytotoxin associated gene A (CagA) protein, was grown under microaerophilic conditions (76 h, 37 °C). LPS from the reference *H. pylori* strain was prepared by hot phenol-water extraction, purified by proteinase K and RNA-se treatment and ultracentrifugation as previously described [59]. *Escherichia coli* (*E. coli*) LPS O55:B5 (Sigma-Aldrich, Darmstadt, Germany) was used as positive control. The stock solution of PyoM_{insol} was prepared in 50 mM NaOH and then diluted in phosphate-buffered saline (PBS), pH 7.4. The detrimental effect of the solvent, diluted in PBS, has been excluded in the preliminary study as previously described [24]. The concentration of PyoM was equal to 1 and 16 µg/mL for PyoM_{sol} and PyoM_{insol}, while the *H. pylori* LPS and *E. coli* LPS were used at a concentration of 25 ng/mL as described previously [16]. In cell-based assays, all components were dissolved in a cell culture medium dedicated to the appropriate cell line and sterilized by filtration using 0.22 µm pore size membrane filters (Sartorius, Göttingen, Germany).

4.5. Antibacterial Activity of PyoM_{insol} and PyoM_{sol}

The antibacterial activity of PyoM_{insol} and PyoM_{sol} against the reference *H. pylori* CCUG 17874 and two clinical isolates, *H. pylori* M91 (metronidazole-resistant strain) and *H. pylori* M102 (metronidazole and levofloxacin-resistant strain), was determined as the minimum inhibitory concentration (MIC) by the resazurin reduction assay [60]. The bacteria were cultured in Brucella Broth with 10% FCS to mid-log phase, and the inoculum was adjusted to 0.5 McFarland (1.5×10^8 CFU/mL) scale. Next, the bacterial suspension was diluted 100-fold in the medium. PyoM_{insol} and PyoM_{sol} were distributed into wells of a 96-well plate (Nunc, Rochester, NY, USA) containing 100 µL Brucella Broth with 10% FCS to form a series of 2-fold dilutions in the range of 1–1024 µg/mL. Then, the bacterial suspension (100 µL) was added to each well, and plates were incubated for 72 h at 37 °C. Control wells containing bacterial culture alone (positive control of bacterial growth), wells with bacterial medium alone (negative control) and wells with reference antibiotics (clarithromycin or amoxicillin) were included. To assess MIC, 20 µL of 0.02% resazurin

in sterile PBS was added to each well and left for 3 h. Fluorescence was measured at an excitation wavelength of 560 nm and emission wavelength of 590 nm using a SpectraMax[®] i3x Multi-Mode Microplate Reader (Molecular Devices, San Jose, CA, USA).

4.6. Cell's Viability Assay

The viability of cells treated with PyoM, LPS or co-stimulated with PyoM and bacterial LPS was assessed using a 3-(4,5-dimethylthiazol-2-yl)-2,5-diphenyltetrazolium bromide—MTT (Sigma Aldrich, Darmstadt, Germany) reduction assay as previously described [24]. L-929 fibroblasts, AGS gastric adenocarcinoma epithelial cells or THP-1 monocytes adjusted to a density of 2×10^5 cells/mL (100 μ L) were seeded in 96-well culture plates (Nunc, Rochester, NY, USA) and incubated overnight prior to stimulation. Cell morphology and confluency were controlled using an inverted contrast phase microscope (Motic AE2000, Xiamen, China). The solution of tested PyoM was distributed to the wells of cell culture plates (6 replicates for each experimental variant) containing cell monolayers. After 24 h of incubation, the condition of the cell monolayers was verified under an inverted contrast phase microscope. The cell cultures in the medium alone were used as a positive control (PC) of cell viability (100% viable cells). To quantify the cell viability, 20 μ L of MTT was added to each well, and incubation was carried out for the next 4 h. The plates were centrifuged ($450 \times g$, for 10 min), and the formazan crystals were dissolved with 100 μ L of dimethyl sulfoxide (Sigma Aldrich, Seelze, Germany). The absorbance was measured spectrophotometrically using a Multiskan EX reader (Thermo Scientific, Waltham, MA, USA) at 570 nm.

4.7. Reactive Oxygen Species

Intracellular ROS were determined in AGS cells after 30 min and 24 h incubation with PyoM or LPS alone or in a combination of both stimulators, using the 2',7'-dichlorodihydrofluorescein diacetate (H₂DCFDA) fluorescent probe (Thermo Scientific, Waltham, MA, USA) as recommended by the manufacturer. The AGS cell suspension in the culture medium (5×10^5 cells/mL) was distributed in 96-well black plates and left for 24 h (37 °C, 5% CO₂). Afterwards, cells were treated for 30 min or 24 h with PyoM_{insol} or PyoM_{sol}, in the presence or absence of *H. pylori* LPS or *E. coli* LPS, and then centrifuged ($200 \times g$, 5 min). After stimulation, the supernatants were replaced with 200 μ L 10 μ M H₂DCFDA, and incubated for 30 min (37 °C, 5% CO₂). Next, the cells were washed with Hanks' Balanced Salt Solution (HBSS) and suspended in 5 mM glucose solution in HBSS (200 μ L/well). Fluorescence was measured at 495 nm (excitation) and 525 nm (emission) using a SpectraMax[®] i3x Multi-Mode Microplate Reader (Molecular Devices, San Jose, CA, USA). The ROS Index was calculated based on relative fluorescence units (RFU) of stimulated cells versus RFU of control cells in the cell culture medium alone.

4.8. Apoptosis

The cell apoptosis was assessed using the commercial terminal deoxynucleotidyl transferase dUTP nick end labelling (TUNEL) assay (Cell Meter TUNEL Apoptosis Assay Kit, AAT Bioques, Sunnyvale, CA, USA), as recommended by the manufacturer. Cells (5×10^5 cells/mL) after stimulation for 24 h with PyoM_{insol} or PyoM_{sol} alone, with *H. pylori* LPS or *E. coli* LPS alone, were treated with fluorescent red dye that passively enters cells and selectively targets the nicks in DNA that form during apoptosis. The fluorescence of cells undergoing apoptosis was measured at 550 nm (excitation) and 590 nm (emission) using a SpectraMax[®] i3x Multi-Mode Microplate Reader (Molecular Devices, San Jose, CA, USA). The Apoptotic Index was calculated based on the relative fluorescence units (RFU) of treated cells versus the RFU of control cells in the cell culture medium alone.

4.9. Wound Healing Assay

AGS cells' migration ability was assessed in a "wound healing assay", as previously described [16]. Cells were seeded in six-well plates at the density of 5×10^5 cells per

well in DMEM/F-12 medium with 2% FCS, penicillin (100 U/mL) and streptomycin (100 µg/mL), and incubated in a humidified cell incubator (37 °C, 5% CO₂) until reaching optimal confluency. The cell monolayers were scratched with a sterile 200 µL pipette tip and designated as the start (time 0 h) of wound repair. Next, the culture medium was replaced with a solution of PyoM alone, bacterial LPS alone or both in a volume of 1 mL. Non-exposed cells in a culture medium alone were used as a control, exhibiting the spontaneous cell migration capacity. Wound images were taken at 0, 24, 48 and 72 h using a digital camera combined with an inverted contrast phase microscope (Motic AE2000, Xiamen, China), and the wound area was measured using the software Motic AE (version Motic Images Plus 2.0ML) (Xiamen, China). The wound healing in the milieu of tested formulations was expressed as the percentage of cells migrating to the wound zone compared to untreated cells.

4.10. Phagocytosis

The suspension of THP-1 monocytes in RPMI-1640 culture medium (5×10^6 cells/mL) was applied to the wells of a 96-well plate (100 µL/well), and cells were stimulated for 24 h with PyoM_{insol} or PyoM_{sol}, with or without *H. pylori* LPS or *E. coli* LPS. Before the experiment, live *H. pylori* rods were stained with the commercial LIVE/DEAD BacLight (ThermoFisher, Waltham, MA, USA) for 30 min at room temperature, then added into the wells containing the monocytes at a multiplicity of infection (MOI) of 50:1 and incubated for another 30 min. Next, the cells were washed five times with 5 mM glucose solution in HBSS, and the fluorescence (excitation wavelength of 485 nm and emission wavelength of 498 nm) was measured using a multifunctional reader SpectraMax i3 (Molecular Devices, San Jose, CA, USA). Phagocytic activity of THP-1 cells was also assessed using the reference fluorescently labelled bioparticles, pHrodo™ Green *E. coli* BioParticles™ Conjugate for Phagocytosis Kit (ThermoFisher Scientific, Waltham, MA, USA), as recommended by the manufacturer. Fluorescent *E. coli* were suspended in HBSS supplemented with glucose to a concentration of 1 mg/mL, sonicated for 10 min and transferred to plates (100 µL/well) containing monocytes. Following the 30 min incubation, the cells were washed three times with 5 mM glucose solution in HBSS, and the intensity of fluorescence was measured using a SpectraMax® i3x Multi-Mode Microplate Reader (Molecular Devices, San Jose, CA, USA) at 509 nm (excitation) and 533 nm (emission). The Phagocytic Index was calculated based on relative fluorescence units (RFU) of stimulated cells versus RFU of control cells in the cell culture medium alone.

4.11. Statistical Analysis

The Kolmogorov–Smirnov test was used to test the normality of the data. Intergroup outcomes were compared for statistical significance using ANOVA (analysis of variance) followed by Dunnett's post hoc test. In all cases, significance was accepted at $p < 0.05$. All analyses were performed using GraphPad Prism 9 software (GraphPad Software, San Diego, CA, USA).

5. Conclusions

Our findings suggest that PyoM isolated from *Pseudomonas aeruginosa* exhibits antibacterial properties against selected reference and clinical antibiotic-resistant strains of *H. pylori*. In this study, we showed that the cytotoxicity of *H. pylori* LPS towards the reference mouse fibroblasts, human monocytes and gastric epithelial cells was reduced in the presence of PyoM. This phenomenon was related to diminished oxidative stress and apoptosis. In addition, our study also demonstrated that PyoM upregulated the phagocytosis of *H. pylori*, however, PyoM_{sol} showed better properties than PyoM_{insol} in terms of enhancing the phagocytic activity of monocytes and increasing migration of gastric epithelial cells. PyoM may represent an interesting biomolecule in further studies of the immune response modulation during *H. pylori* infection.

Author Contributions: Conceptualization, M.M.U. and M.C.; methodology, M.M.U. and G.G.; validation, M.M.U.; formal analysis, M.M.U. and K.R.; investigation, M.M.U.; resources, M.M.U. and G.G.; data curation, M.M.U. and M.C.; writing—original draft preparation, M.M.U.; writing—review and editing, M.M.U., K.R. and M.C.; visualization, M.M.U.; supervision, M.C.; project administration, K.R.; and funding acquisition, K.R. All authors have read and agreed to the published version of the manuscript.

Funding: This research was funded by the Foundation for Polish Science through the European Union under the European Regional Development Fund, within the “TEAM-NET” program entitled “Multifunctional biologically active composite for application in bone regenerative medicine” [grant number POIR.04.04.00-00-16D7/18-00]. This study was supported by the Polish Ministry of Science and Higher Education through the European Union under the European Regional Development Fund, within the “Inkubator Innowacyjności+” program entitled “PioMelaCure—an pyomelanin preparation supporting the treatment of common *H. pylori* infections” [grant number MNiSW/2020/332/DIR].

Institutional Review Board Statement: Not applicable.

Informed Consent Statement: Not applicable.

Data Availability Statement: The data generated during this study are available from the University of Łódź, Faculty of Biology and Environmental Protection, Department of Immunology and Infectious Biology, Łódź, 90-237, Poland, and are available from the corresponding authors upon request.

Conflicts of Interest: The authors declare no conflict of interest. The funders had no role in the design of the study; in the collection, analyses, or interpretation of data; in the writing of the manuscript; or in the decision to publish the results.

References

1. Baj, J.; Forma, A.; Sitarz, M.; Piero, P.; Garrut, G.; Krasowska, D.; Maciejewski, R. *Helicobacter pylori* virulence factors—Mechanisms of bacterial pathogenicity in the gastric microenvironment. *Cells* **2021**, *10*, 27. [\[CrossRef\]](#)
2. Sukri, A.; Hanafiah, A.; Mohamad Zin, N.; Kosai, N.R. Epidemiology and role of *Helicobacter pylori* virulence factors in gastric cancer carcinogenesis. *Apmis* **2020**, *128*, 150–161. [\[CrossRef\]](#) [\[PubMed\]](#)
3. Tsay, F.W.; Hsu, P.I. *H. pylori* infection and extra-gastrointestinal diseases. *J. Biomed. Sci.* **2018**, *25*, 1–8. [\[CrossRef\]](#) [\[PubMed\]](#)
4. Nestegard, O.; Moayeri, B.; Halvorsen, F.A.; Tønnesen, T.; Sørbye, S.W.; Paulssen, E.; Johnsen, K.M.; Goll, R.; Florholmen, J.R.; Melby, K.K. *Helicobacter pylori* resistance to antibiotics before and after treatment: Incidence of eradication failure. *PLoS ONE* **2022**, *17*, e0265322. [\[CrossRef\]](#)
5. Malferteiner, P.; Camargo, M.C.; El-Omar, E.; Liou, J.M.; Peek, R.; Schulz, C.; Smith, S.I.; Suerbaum, S. *Helicobacter pylori* infection. *Nat. Rev. Dis. Prim.* **2023**, *9*, 19. [\[CrossRef\]](#)
6. Allen, L.A.H. Phagocytosis and persistence of *Helicobacter pylori*. *Cell Microbiol.* **2007**, *9*, 817–828. [\[CrossRef\]](#) [\[PubMed\]](#)
7. Schwartz, J.T.; Allen, L.A.H. Role of urease in megasome formation and *Helicobacter pylori* survival in macrophages. *J. Leukoc. Biol.* **2006**, *79*, 1214–1225. [\[CrossRef\]](#) [\[PubMed\]](#)
8. Kuwahara, H.; Miyamoto, Y.; Akaike, T.; Kubota, T.; Sawa, T.; Okamoto, S.; Maeda, H. *Helicobacter pylori* urease suppresses bactericidal activity of peroxynitrite via carbon dioxide production. *Infect. Immun.* **2000**, *68*, 4378–4383. [\[CrossRef\]](#)
9. Scott, D.R.; Marcus, E.A.; Wen, Y.; Singh, S.; Feng, J.; Sachs, G. Cytoplasmic histidine kinase (HP0244)-regulated assembly of urease with UreI, a channel for urea and its metabolites, CO₂, NH₃, and NH₄⁺, is necessary for acid survival of *Helicobacter pylori*. *J. Bacteriol.* **2010**, *192*, 94–103. [\[CrossRef\]](#)
10. Kao, C.Y.; Sheu, B.S.; Wu, J.J. *Helicobacter pylori* infection: An overview of bacterial virulence factors and pathogenesis. *Biomed. J.* **2016**, *39*, 14–23. [\[CrossRef\]](#)
11. Ansari, S.; Yamaoka, Y. *Helicobacter pylori* virulence factors exploiting gastric colonization and its pathogenicity. *Toxins* **2019**, *11*, 677. [\[CrossRef\]](#)
12. Ansari, S.; Yamaoka, Y. *Helicobacter pylori* virulence factor cytotoxin-associated gene A (CagA)-mediated gastric pathogenicity. *Int. J. Mol. Sci.* **2020**, *21*, 7430. [\[CrossRef\]](#)
13. Sundqvist, M.O.; Wärme, J.; Hofmann, R.; Pawelzik, S.C.; Bäck, M. *Helicobacter pylori* virulence factor cytotoxin-associated gene A (CagA) induces vascular calcification in coronary artery smooth muscle cells. *Int. J. Mol. Sci.* **2023**, *24*, 5392. [\[CrossRef\]](#)
14. Butcher, L.D.; den Hartog, G.; Ernst, P.B.; Crowe, S.E. Oxidative stress resulting from *Helicobacter pylori* infection contributes to gastric carcinogenesis. *Cell. Mol. Gastroenterol. Hepatol.* **2017**, *3*, 316–322. [\[CrossRef\]](#)
15. Cheok, Y.Y.; Tan, G.M.Y.; Lee, C.Y.Q.; Abdullah, S.; Looi, C.Y.; Wong, W.F. Innate immunity crosstalk with *Helicobacter pylori*: Pattern recognition receptors and cellular responses. *Int. J. Mol. Sci.* **2022**, *23*, 7561. [\[CrossRef\]](#)
16. Mnich, E.; Kowalewicz-Kulbat, M.; Sicińska, P.; Hinc, K.; Obuchowski, M.; Gajewski, A.; Moran, A.P.; Chmiela, M. Impact of *Helicobacter pylori* on the healing process of the gastric barrier. *World J. Gastroenterol.* **2016**, *22*, 7536–7558. [\[CrossRef\]](#)

17. Hug, I.; Couturier, M.R.; Rooper, M.M.; Taylor, D.E.; Stein, M.; Feldman, M.F. *Helicobacter pylori* lipopolysaccharide is synthesized via a novel pathway with an evolutionary connection to protein N-glycosylation. *PLoS Pathog.* **2010**, *6*, e1000819. [[CrossRef](#)] [[PubMed](#)]
18. Sijmons, D.; Guy, A.J.; Walduck, A.K.; Ramsland, P.A. *Helicobacter pylori* and the role of lipopolysaccharide variation in innate immune evasion. *Front. Immunol.* **2022**, *13*, 868225. [[CrossRef](#)]
19. Rudnicka, W.; Czkwianianc, E.; Płaneta-Małecka, I.; Jurkiewicz, M.; Wiśniewska, M.; Cieślowski, T.; Różalska, B.; Wadström, T.; Chmiela, M. A potential double role of anti-Lewis X antibodies in *Helicobacter pylori*-associated gastroduodenal diseases. *FEMS Microbiol. Immunol.* **2001**, *30*, 121–125. [[CrossRef](#)]
20. Jain, U.; Saxena, K.; Chauhan, N. *Helicobacter pylori* induced reactive oxygen species: A new and developing platform for detection. *Helicobacter* **2021**, *26*, e12796. [[CrossRef](#)]
21. Godavarthy, P.K.; Puli, C. From antibiotic resistance to antibiotic renaissance: A new era in *Helicobacter pylori* treatment. *Cureus* **2023**, *15*, e36041. [[CrossRef](#)] [[PubMed](#)]
22. Tshibangu-Kabamba, E.; Yamaoka, Y. *Helicobacter pylori* infection and antibiotic resistance—From biology to clinical implications. *Nat. Rev. Gastroenterol. Hepatol.* **2021**, *18*, 613–629. [[PubMed](#)]
23. Behzadi, P.; Baráth, Z.; Gajdács, M. It's not easy being green: A narrative review on the microbiology, virulence and therapeutic prospects of multidrug-resistant *Pseudomonas aeruginosa*. *Antibiotics* **2021**, *10*, 42. [[CrossRef](#)]
24. Urbaniak, M.M.; Gazińska, M.; Rudnicka, K.; Płociński, P.; Nowak, M.; Chmiela, M. In vitro and in vivo biocompatibility of natural and synthetic *Pseudomonas aeruginosa* pyomelanin for potential biomedical applications. *Int. J. Mol. Sci.* **2023**, *24*, 7846. [[CrossRef](#)]
25. Roy, S.; Rhim, J.W. New insight into melanin for food packaging and biotechnology applications. *Crit. Rev. Food Sci. Nutr.* **2021**, *62*, 4629–4655. [[CrossRef](#)] [[PubMed](#)]
26. Lorquin, F.; Ziarelli, F.; Amouric, A.; Di Giorgio, C.; Robin, M.; Piccerelle, P.; Lorquin, J. Production and properties of non-cytotoxic pyomelanin by laccase and comparison to bacterial and synthetic pigments. *Sci. Rep.* **2021**, *11*, 8538. [[CrossRef](#)]
27. Fonseca, É.; Freitas, F.; Caldart, R.; Morgado, S.; Vicente, A.C. Pyomelanin biosynthetic pathway in pigment-producer strains from the pandemic *Acinetobacter baumannii* IC-5. *Mem. Inst. Oswaldo Cruz.* **2020**, *115*, 1–6. [[CrossRef](#)]
28. Li, H.; Zhou, X.; Huang, Y.; Liao, B.; Cheng, L.; Ren, B. Reactive oxygen species in pathogen clearance: The killing mechanisms, the adaption response, and the side effects. *Front. Microbiol.* **2021**, *11*, 622534. [[CrossRef](#)] [[PubMed](#)]
29. Tapia, C.V.; Falconer, M.; Tempio, F.; Falcón, F.; López, M.; Fuentes, M.; Alburquenque, C.; Amaro, J.; Bucarey, S.A.; Di Nardo, A. Melanocytes and melanin represent a first line of innate immunity against *Candida albicans*. *Med. Mycol.* **2014**, *52*, 445–452. [[CrossRef](#)]
30. ElObeid, A.S.; Kamal-Eldin, A.; Abdelhalim, M.A.K.; Haseeb, A.M. Pharmacological properties of melanin and its function in health. *Basic. Clin. Pharmacol. Toxicol.* **2017**, *120*, 515–522.
31. Amieva, M.R.; El-Omar, E.M. Host-bacterial interactions in *Helicobacter pylori* infection. *Gastroenterology* **2008**, *134*, 306–323. [[CrossRef](#)] [[PubMed](#)]
32. Malfertheiner, P.; Link, A.; Selgrad, M. *Helicobacter pylori*: Perspectives and time trends. *Nat. Rev. Gastroenterol. Hepatol.* **2014**, *11*, 628–638. [[CrossRef](#)]
33. Savoldi, A.; Carrara, E.; Graham, D.Y.; Conti, M.; Tacconelli, E. Prevalence of antibiotic resistance in *Helicobacter pylori*: A systematic review and meta-analysis in World Health Organization regions. *Gastroenterology* **2018**, *155*, 1372–1382.e17. [[CrossRef](#)]
34. Vasanthabharathi, V.; Lakshminarayanan, R.; Jayalakshmi, S. Melanin production from marine *Streptomyces* Afr. *J. Biotechnol.* **2011**, *10*, 11224–11234.
35. Zerrad, A.; Anissi, J.; Ghanam, J.; Sendide, K. Antioxidant and antimicrobial activities of melanin produced by a *Pseudomonas balearica* strain. *J. Biotech. Lett.* **2014**, *5*, 87–94.
36. Xu, C.; Li, J.; Yang, L.; Shi, F.; Yang, L.; Ye, M. Antibacterial activity and a membrane damage mechanism of *Lachnum* YM30 melanin against *Vibrio parahaemolyticus* and *Staphylococcus aureus*. *Food Control* **2017**, *73*, 1445–1451. [[CrossRef](#)]
37. El-Naggar, N.E.A.; Saber, W.I.A. Natural melanin: Current trends, and future approaches, with especial reference to microbial source. *Polymers* **2022**, *14*, 1339. [[CrossRef](#)]
38. Żądło, A.; Sarna, T. Interaction of iron ions with melanin. *Acta Biochim. Pol.* **2019**, *66*, 459–462. [[CrossRef](#)] [[PubMed](#)]
39. Waidner, B.; Greiner, S.; Odenbreit, S.; Kavermann, H.; Velayudhan, J.; Stähler, F.; Guhl, J.; Bissé, E.; van Vliet, A.H.; Andrews, S.C.; et al. Essential role of ferritin Pfr in *Helicobacter pylori* iron metabolism and gastric colonization. *Infect. Immun.* **2002**, *70*, 3923–3929. [[CrossRef](#)]
40. Lorquin, F.; Piccerelle, P.; Orneto, C.; Robin, M.; Lorquin, J. New insights and advances on pyomelanin production: From microbial synthesis to applications. *J. Ind. Microbiol. Biotechnol.* **2022**, *49*, kuac013. [[CrossRef](#)]
41. Gajewski, A.Ł.; Gawrysiak, M.; Krupa, A.; Rechciński, T.; Chałubiński, M.; Gonciarz, W.; Chmiela, M. Accumulation of deleterious effects in gastric epithelial cells and vascular endothelial cells in vitro in the milieu of *Helicobacter pylori* components, 7-ketocholesterol and acetylsalicylic acid. *Int. J. Mol. Sci.* **2022**, *23*, 6355. [[CrossRef](#)]
42. Hill, B. Gastric mucosal barrier: Evidence for *Helicobacter pylori* ingesting gastric surfactant and deriving protection from it. *Gut* **1993**, *34*, 588–593. [[CrossRef](#)]
43. Von Herbay, A.; Rudi, J. Role of apoptosis in gastric epithelial turnover. *Microsc. Res. Tech.* **2000**, *48*, 303–311. [[CrossRef](#)]

44. Cover, T.L.; Krishna, U.S.; Israel, D.A.; Peek, R.M. Induction of gastric epithelial apoptosis by *Helicobacter pylori*. *Gut* **1996**, *38*, 498–501.
45. Gonciarz, W.; Krupa, A.; Hinc, K.; Obuchowski, M.; Moran, A.P.; Gajewski, A.; Chmiela, M. The effect of *Helicobacter pylori* infection and different *H. pylori* components on the proliferation and apoptosis of gastric epithelial cells and fibroblasts. *PLoS ONE* **2019**, *14*, e0220636. [[CrossRef](#)] [[PubMed](#)]
46. Ding, S.Z.; Minohara, Y.; Fan, X.J.; Wang, J.; Reyes, V.E.; Patel, J.; Dirden-Kramer, B.; Boldogh, I.; Ernst, P.B.; Crowe, S.E. *Helicobacter pylori* infection induces oxidative stress and programmed cell death in human gastric epithelial cells. *Infect. Immun.* **2007**, *75*, 4030–4039. [[CrossRef](#)] [[PubMed](#)]
47. Fu, S.; Ramanujam, K.S.; Wong, A.; Fantry, G.T.; Drachenberg, C.B.; James, S.P.; Meltzer, S.J.; Wilson, K.T. Increased expression and cellular localization of inducible nitric oxide synthase and cyclooxygenase 2 in *Helicobacter pylori* gastritis. *Gastroenterology* **1999**, *116*, 1319–1329. [[CrossRef](#)]
48. Ma, Y.; Zhang, L.; Rong, S.; Qu, H.; Zhang, Y.; Chang, D.; Pan, H.; Wang, W. Relation between gastric cancer and protein oxidation, DNA damage, and lipid peroxidation. *Oxid. Med. Cell. Longev.* **2013**, *2013*, 543760. [[CrossRef](#)]
49. Uribe-Querol, E.; Rosales, C. Phagocytosis: Our current understanding of a universal biological process. *Front. Immunol.* **2020**, *11*, 1066. [[CrossRef](#)]
50. Grębowska, A.; Moran, A.P.; Matusiak, A.; Bak-Romaniszyn, L.; Czkwianianc, E.; Rechciński, T.; Walencka, M.; Planeta-Małecka, I.; Rudnicka, W.; Chmiela, M. Anti-phagocytic activity of *Helicobacter pylori* lipopolysaccharide (LPS)-possible modulation of the innate immune response to these bacteria. *Pol. J. Microbiol.* **2008**, *3*, 185–192.
51. Fox, S.; Ryan, K.A.; Berger, A.H.; Petro, K.; Das, S.; Crowe, S.E.; Ernst, P.B. The role of C1q in recognition of apoptotic epithelial cells and inflammatory cytokine production by phagocytes during *Helicobacter pylori* infection. *J. Inflamm.* **2015**, *12*, 1–13. [[CrossRef](#)]
52. Gonciarz, W.; Chmiela, M.; Kost, B.; Piątczak, E.; Brzeziński, M. Stereocomplexed microparticles loaded with *Salvia cadmica* Boiss. extracts for enhancement of immune response towards *Helicobacter pylori*. *Sci. Rep.* **2023**, *13*, 7039. [[CrossRef](#)]
53. Chmiela, M.; Czkwianianc, E.; Wadstrom, T.; Rudnicka, W. Role of *Helicobacter pylori* surface structures in bacterial interaction with macrophages. *Gut* **1997**, *40*, 20–24. [[CrossRef](#)] [[PubMed](#)]
54. Alviano, D.S.; Franzen, A.J.; Travassos, L.R.; Holandino, C.; Rozental, S.; Ejzemberg, R.; Alviano, C.S.; Rodrigues, M.L. Melanin from *Fonsecaea pedrosoi* induces production of human antifungal antibodies and enhances the antimicrobial efficacy of phagocytes. *Infect. Immun.* **2004**, *72*, 229–237. [[CrossRef](#)]
55. Borlace, G.N.; Keep, S.J.; Prodoehl, M.J.; Jones, H.F.; Butler, R.N.; Brooks, D.A. A role for altered phagosome maturation in the long-term persistence of *Helicobacter pylori* infection. *Am. J. Physiol. Gastrointest. Liver Physiol.* **2012**, *303*, 169–179. [[CrossRef](#)] [[PubMed](#)]
56. Chen, Q.; Liu, F.; Wu, Y.; He, Y.; Kong, Q.; Sang, H. Fungal melanin-induced metabolic reprogramming in macrophages is crucial for inflammation. *J. Med. Mycol.* **2023**, *33*, 101359. [[CrossRef](#)]
57. Gonçalves, S.M.; Duarte-Oliveira, C.; Campos, C.F.; Aïmanianda, V.; Ter Horst, R.; Leite, L.; Mercier, T.; Pereira, P.; Fernández-García, M.; Antunes, D.; et al. Phagosomal removal of fungal melanin reprograms macrophage metabolism to promote antifungal immunity. *Nat. Commun.* **2020**, *11*, 2282. [[CrossRef](#)]
58. Walencka, M.; Gonciarz, W.; Mnich, E.; Gajewski, A.; Stawski, P.; Knapik-Dabrowicz, A.; Chmiela, M. The microbiological, histological, immunological and molecular determinants of *Helicobacter pylori* infection in guinea pigs as a convenient animal model to study pathogenicity of these bacteria and the infection dependent immune response of the host. *Acta Biochim. Pol.* **2015**, *62*, 697–706. [[CrossRef](#)] [[PubMed](#)]
59. Moran, A.P.; Helander, I.M.; Kosunen, T.U. Compositional analysis of *Helicobacter pylori* rough-form lipopolysaccharides. *J. Bacteriol.* **1992**, *174*, 1370–1377. [[CrossRef](#)]
60. Skindersoe, M.E.; Rasmussen, L.; Andersen, L.P.; Krogfelt, K.A. A novel assay for easy and rapid quantification of *Helicobacter pylori* adhesion. *Helicobacter* **2015**, *20*, 199–205. [[CrossRef](#)] [[PubMed](#)]

Disclaimer/Publisher’s Note: The statements, opinions and data contained in all publications are solely those of the individual author(s) and contributor(s) and not of MDPI and/or the editor(s). MDPI and/or the editor(s) disclaim responsibility for any injury to people or property resulting from any ideas, methods, instructions or products referred to in the content.

International Journal of Biological Macromolecules

Exploring the Osteoinductive Potential of Bacterial Pyomelanin Derived from *Pseudomonas aeruginosa* On Human Osteoblasts Model

--Manuscript Draft--

Manuscript Number:	IJBIMAC-D-24-01486
Article Type:	Research Paper
Section/Category:	CME article
Keywords:	pyomelanin; osteoinduction; osteoblast
Corresponding Author:	Mateusz M. Urbaniak University of Lodz POLAND
First Author:	Mateusz M. Urbaniak
Order of Authors:	Mateusz M. Urbaniak Karolina Rudnicka Przemysław Płociński Magdalena Chmiela
Abstract:	<p>Alkaptonuria (AKU) is a rare autosomal metabolic disorder resulting from a deficiency in tyrosine metabolism. In AKU, the deposition of homogentisic acid polymers contributes to the pathological ossification of cartilage tissue. The controlled use of biomimetics similar to deposits observed in cartilage may result in the development of an effective therapy that increases the mineralization and maturation of osteoblasts necessary for the regeneration of damaged bone tissue. One of the potential biomimetic candidates is pyomelanin (PyoM) - a polymeric biomacromolecule synthesized by <i>Pseudomonas aeruginosa</i>. This work presents comprehensive data on the osteoinductive, pro-regenerative and antibacterial properties, as well as the cytocompatibility of water-soluble (PyoMsol) or water-insoluble (PyoMinsol) PyoM. Both variants of PyoM support osteoinductive processes and maturation of osteoblasts due to the upregulation of OC, ALP, IL-6, IL-10 and TNF-α production. PyoM are cytocompatible polymers and limit doxorubicin-induced apoptosis towards osteoblasts. This cytoprotective PyoM activity is correlated with pro-regenerative properties expressed as osteoblasts migration. Moreover, PyoMsol and PyoMinsol exhibit antibacterial activity against staphylococci isolated from infected bones. The osteoinductive, pro-regenerative and antiapoptotic effects achieved through the PyoM stimulation of osteoblasts create new opportunities for designing biocomposites modified with this bacterial-derived biopolymer, offering novel prospects for various biological and medical applications.</p>
Suggested Reviewers:	<p>Michelle Kilcoyne michelle.kilcoyne@universityofgalway.ie</p> <p>Josef Jampilek josef.jampilek@uniba.sk</p> <p>Peter Lund p.a.lund@bham.ac.uk</p>
Opposed Reviewers:	

1 Exploring the Osteoinductive Potential of Bacterial
2
3
4 Pyomelanin Derived from *Pseudomonas*
5
6
7
8
9 *aeruginosa* On Human Osteoblasts Model
10
11
12
13
14
15
16

17 *Mateusz M. Urbaniak*^{1,2}, *Karolina Rudnicka*¹, *Przemysław Płociński*¹, *Magdalena Chmiela*¹
18
19
20

21 ¹University of Lodz, Faculty of Biology and Environmental Protection, Department of
22
23 Immunology and Infectious Biology Lodz, Poland
24

25
26 ²Bio-Med-Chem Doctoral School, University of Lodz and Lodz Institutes of the Polish
27
28 Academy of Sciences, Lodz, Poland
29
30

31
32
33
34
35
36
37
38
39
40
41
42
43
44
45
46
47
48
49
50
51
52
53 KEYWORDS: pyomelanin, osteoinduction, osteoblast, bone regeneration
54
55
56
57
58
59
60
61
62
63
64
65

ABSTRACT

1
2
3
4 Alkaptonuria (AKU) is a rare autosomal metabolic disorder resulting from a deficiency in
5
6 tyrosine metabolism. In AKU, the deposition of homogentisic acid polymers contributes to the
7
8 pathological ossification of cartilage tissue. The controlled use of biomimetics similar to
9
10 deposits observed in cartilage may result in the development of an effective therapy that
11
12 increases the mineralization and maturation of osteoblasts necessary for the regeneration of
13
14 damaged bone tissue. One of the potential biomimetic candidates is pyomelanin (PyoM) - a
15
16 polymeric biomacromolecule synthesized by *Pseudomonas aeruginosa*. This work presents
17
18 comprehensive data on the osteoinductive, pro-regenerative and antibacterial properties, as well
19
20 as the cytocompatibility of water-soluble (PyoM_{sol}) or water-insoluble (PyoM_{insol}) PyoM. Both
21
22 variants of PyoM support osteoinductive processes as well as the maturation of osteoblasts due
23
24 to the upregulation of osteocalcin (OC), alkaline phosphatase (ALP), interleukin (IL)-6, IL-10
25
26 and tumour necrosis factor (TNF)- α production. PyoM are cytocompatible in a wide
27
28 concentration range and limit doxorubicin-induced apoptosis towards osteoblasts. This
29
30 cytoprotective PyoM activity is correlated with pro-regenerative properties expressed as
31
32 osteoblasts migration. Moreover, PyoM_{sol} and PyoM_{insol} exhibit antibacterial activity against
33
34 staphylococci isolated from infected bones. The omnidirectional osteoinductive, pro-
35
36 regenerative and antiapoptotic effects achieved through the PyoM stimulation of osteoblasts
37
38 create new opportunities for designing biocomposites modified with this bacterial-origin
39
40 biopolymer with tailored properties, offering novel prospects for various biological and medical
41
42 applications.
43
44
45
46
47
48
49
50
51
52
53
54
55
56
57
58
59
60
61
62
63
64
65

1. INTRODUCTION

1
2
3 Regeneration of damaged bone is a multi-stage cascade of repair reactions that depend on the
4 activity of bone-forming cells (osteoblasts) and osteoclasts along with inflammatory,
5 endothelial and hematopoietic cells. Bone repair consists of three primary phases:
6 inflammation, bone production, and bone remodelling [1]. Osteoblasts derived from
7 mesenchymal stem cells constitute approximately 4–6% of the total bone cell population and
8 are largely responsible for forming, growing and remodelling bone tissue[2]. Mature osteoblasts
9 synthesize extracellular type I collagen (COL1) - and non-collagen proteins including
10 osteocalcin (OC), osteopontin (OPN), and alkaline phosphatase (ALP). The extracellular matrix
11 is first secreted as an unmineralized osteoid and then mineralized by the accumulation of
12 hydroxyapatite[3]. Bone remodelling consists of four sequential phases: the activation phase,
13 during which osteoclast progenitor cells are recruited to the damaged bone surface; the
14 resorption phase, in which mature osteoclasts resorb damaged bone; a reversal phase, in which
15 osteoclasts die, and osteoblast progenitor cells are recruited; and formation phase in which
16 mature osteoblasts produce new bone osteoid [4,5].

17
18 In the physiological microenvironment of bone tissue, there is a balance between bone
19 formation by osteoblasts and bone resorption by osteoclasts, ensuring the maintenance of
20 normal bone mass and mineral density [6]. Many proteins and cytokines secreted by osteoblasts,
21 osteoclasts and immune cells involved at various stages of bone turnover are responsible for
22 maintaining the balance between the process of bone formation and resorption [7]. The key
23 modifiers responsible for maintaining the balance in bone remodelling include OC, ALP,
24 osteoprotegerin (OPG), bone morphogenetic proteins, receptor activator of nuclear factor
25 kappa-light-chain-enhancer of activated B cells (RANK) ligand (RANKL), interleukin (IL)-1,
26 IL-6, IL-10, and tumour necrosis factor (TNF)- α [8–10]. Injuries, fractures, metabolic diseases,
27 osteoporosis or cancer can cause bone defects that are difficult to heal. This is a significant

1
2
3
4
5
6
7
8
9
10
11
12
13
14
15
16
17
18
19
20
21
22
23
24
25
26
27
28
29
30
31
32
33
34
35
36
37
38
39
40
41
42
43
44
45
46
47
48
49
50
51
52
53
54
55
56
57
58
59
60
61
62
63
64
65

problem in the case of large bones, where the missing tissue resulting from pathology is greater than the ability of spontaneous bone healing dependent on the osteoblast's activity [11]. The process of bone repair in connection with a fracture, osteoporosis or implantation procedure may be even more limited if a bacterial infection accompanies it. Therefore, searching for new compounds with multidirectional pro-regenerative, osteogenic and antibacterial activity is crucial [12–14].

Alkaptonuria (AKU) is a rare autosomal recessive metabolic disorder resulting from a deficiency of homogentisate 1,2-dioxygenase in tyrosine metabolism [15]. As a consequence, homogentisic acid (HGA) does not undergo metabolic transformations, and over time, it polymerizes and accumulates in collagen tissues, which leads to ochronosis. The process of ochronotic deposits formation is not fully understood. HGA is believed to polymerize into a benzoquinone intermediate before assuming its final polymeric form in collagen tissues [15,16]. One of the most typical symptoms of AKU is chronic joint degeneration, manifested by structural changes and mineralization occurring in cartilage tissue [17]. The accumulation of HGA polymers causes hydroxyapatite deposition, a mineral responsible for bone calcification, which further hardens the connective tissue [18].

In this study, by mimicking the pathological ossification induced in AKU, we are aiming to support osteoinductive processes and increase ossification, which is crucial during bone healing and tissue repair. By using pyomelanin (PyoM) produced by *Pseudomonas aeruginosa*, previously shown to be cytocompatible biomimetic of ochronotic deposits we recreate the mechanisms accompanying AKU, including the local accumulation of HGA polymers [19–21]. PyoM is a dark brown to black negatively charged extracellular polymeric pigment of HGA produced during L-tyrosine catabolism [22]. Two forms of this bacterial pigment are known: water-soluble (PyoM_{sol}) and water-insoluble (PyoM_{insol}) pyomelanin, which are obtained depending on the isolation procedure from the post-cultured supernatants [23]. The chemical

1 structure of PyoM determines their oxidizing (quinone groups) and reducing (hydroxyquinone
2 groups) properties, which are responsible for the elemental functions in the bacterial cell related
3
4 to protection against reactive oxygen species and UV light, electron transport and binding of
5
6 metal ions [24,25]. It has been shown that PyoM possesses antibacterial activity against various
7
8 bacterial species and supports the regeneration of gastric epithelial cells *in vitro* by
9
10 neutralization of reactive oxygen species [23,26,27]. PyoM also stimulates the activation of the
11
12 nuclear factor kappa-light-chain-enhancer of activated B cells (NF-κB), which is one of the
13
14 essential protein complex necessary to initiate the processes of tissue reconstruction and
15
16 regeneration [23,28].
17
18
19
20

21 The study aimed to determine the cytocompatibility of PyoM_{sol} and PyoM_{insol} towards human
22
23 osteoblasts and assessment of cell apoptosis. Furthermore, biological activities of PyoM
24
25 towards human osteoblasts have been tested regarding the role of PyoM as a biomimetic
26
27 polymer of ochronotic deposits in osteoinduction by assessment of the production of OC, ALP,
28
29 IL-6, IL-10 and TNF-α, and bone regeneration by evaluation of cell migration in wound healing
30
31 assay as well as cell proliferation. In addition, the antibacterial activity of PyoM against
32
33 staphylococci, the leading cause of bone infections accompanying medical interventions, was
34
35 assessed by resazurin reduction assay.
36
37
38
39
40

41 **2. MATERIALS AND METHODS**

42 **2.1. Growth Conditions of *Pseudomonas aeruginosa***

43
44
45 The growth conditions of *P. aeruginosa* have been established as previously described [23,26].
46
47 Briefly, *P. aeruginosa* Mel+ strain (Collection of Department of Immunology and Infectious
48
49 Biology University of Lodz, Poland) was inoculated after thawing onto a Luria Broth (LB) agar
50
51 plate and incubated for 24 h at a microbiological incubator (37°C). Next, the LB broth was
52
53 inoculated with the single colony exhibiting Gram-negative rod-shaped morphology, positive
54
55 oxidase test and a presence of pigmentation and incubated in aerobic conditions (37°C, 18 h)
56
57
58
59
60
61
62
63
64
65

1 to obtain an initial log-phase bacterial suspension. To isolate PyoM with the reduction of
2 undesirable substances, the Pyomelanin Minimal Medium II (PMM II) (patent application
3 number: PL438865) was used [23,26]. PMM II was inoculated with 1.0 mL of a 1.0 McFarland
4 bacterial suspension and grown for 5 days in the microbiological incubator (37°C, with shaking
5 at 120 rpm). When the color of the medium changed from honey-like to black, the cultures were
6 transferred to room temperature and exposed to sunlight, which stimulated the production of
7 the pigment.
8
9

10 **2.2. Isolation and purification of PyoM_{sol} and PyoM_{insol}**

11 The isolation and purification of water-soluble pyomelanin (PyoM_{sol}) and water-insoluble
12 pyomelanin (PyoM_{insol}) were performed as previously described [23,26]. Briefly, to isolate the
13 PyoM_{insol}, the bacterial culture was centrifuged, and the supernatant was acidified to pH 2.0
14 with 6.0 M HCl (PolAura, Dywity, Poland). The PyoM_{insol} pellet was washed with HCl and
15 double-washed with distilled water. Finally, the PyoM_{insol} pellet was suspended in pure ethanol
16 (Chempur, Piekary Śląskie, Poland) and placed in a water bath (95°C, 30 min.). PyoM_{insol} was
17 washed twice with ethanol and air-dried. To obtain PyoM_{sol}, the bacterial cell-free supernatant
18 was incubated with chloroform in a 1:1 ratio under shaking conditions for 24 h (room
19 temperature, shaking at 120 rpm). The aqueous phase containing the PyoM_{sol} was separated
20 from the chloroform and protein phase using a separating funnel. To remove residual protein
21 contaminants, the aqueous layer was centrifuged, and then PyoM_{sol} was purified from low
22 molecular weight soluble substances by ultrafiltration (MWCO: 30 kDa) (Sartorius, Göttingen,
23 Germany). The PyoM_{sol} was dried overnight at 50°C. Endotoxin was removed by affinity
24 chromatography using Pierce™ High Capacity Endotoxin Removal Spin Columns (Thermo
25 Scientific, Waltham, MA, USA). PyoM_{insol} and PyoM_{sol} pellets were washed with chloroform,
26 ethyl acetate, ethanol and water. For further experiments, the PyoM samples were stored in a
27 dark and dry place at 4°C.
28
29
30
31
32
33
34
35
36
37
38
39
40
41
42
43
44
45
46
47
48
49
50
51
52
53
54
55
56
57
58
59
60
61
62
63
64
65

2.3. Osteoblast Growth Conditions

1
2
3 The hFOB 1.19 osteoblasts were cultured in DMEM/Nutrient Mixture F-12 Ham (Gibco, Zug,
4
5 Switzerland), supplemented with inactivated bovine serum and geneticin (0.3 mg/mL; Gibco,
6
7 Zug, Switzerland), in cell incubator conditions (33°C, 5% CO₂), as previously described [29].
8
9
10 For the test, 1 mL of cell suspension (5×10⁵/mL) was transferred to a 6-well cell culture plate
11
12 (Thermo Fisher Scientific, Waltham, MA, USA) and incubated overnight in incubator
13
14 conditions to allow cells to adhere. Following the initial incubation, the medium was aspirated,
15
16 and 1.5 mL of osteogenic medium containing DMEM/Nutrient Mixture F-12 Ham
17
18 supplemented with 1% heat-inactivated fetal bovine serum, 0.3 mg/mL geneticin (Gibco, Zug,
19
20 Switzerland), 50 µg/mL ascorbate-2-phosphate (Sigma Aldrich, Darmstadt, Germany), 1 µM
21
22 dexamethasone (Sigma Aldrich, Darmstadt, Germany), and 10 mM β-glycerophosphate (Sigma
23
24 Aldrich, Darmstadt, Germany) was added to the control cell wells, and 1.5 mL of PyoM_{sol} or
25
26 PyoM_{insol} (1 µg/mL) dissolved in osteogenic medium was added to the test cells. Next, the
27
28 osteoblasts were cultured at 39°C, 5% CO₂, and the osteogenic medium with or without PyoM
29
30 variants was replaced every three days. The cell culture supernatants were collected after 4, 7,
31
32 11, 14, 18, 21, 24, and 28 days of incubation and stored at –80 °C for further evaluation of the
33
34 osteogenic differentiation markers. Cell lysates were collected on 7, 14, 21, and 28 days for
35
36 proliferation assessment and alkaline phosphatase (ALP) activity quantification, while cell
37
38 culture supernatants were collected to evaluate the level of selected cytokines.
39
40
41
42
43
44
45
46

2.4. Determination of PyoM_{sol} and PyoM_{insol} Cytocompatibility towards Osteoblasts

47
48 Studies on cytocompatibility of PyoM_{sol} or PyoM_{insol} were carried out using human fetal
49
50 osteoblasts hFOB 1.19 (ATCC, Rockville, MD, USA) according to ISO-10993-5-2009 norm
51
52 for testing components for potential biomedical application. The viability of control cells or
53
54 cells treated with PyoM variants was evaluated in 3-(4,5-dimethylthiazol-2-yl)-2,5-
55
56
57
58
59
60
61
62
63
64
65

1 diphenyltetrazolium bromide salt (MTT, Sigma Aldrich, Saint Louis, MO, USA) reduction
2 assay [23,29]. hFOB 1.19 osteoblasts were cultured in DMEM/Nutrient Mixture F-12 Ham
3 (Gibco, Zug, Switzerland) supplemented with inactivated bovine serum and geneticin (0.3
4 mg/mL; Gibco, Zug, Switzerland) in incubator conditions at 33°C, 5% CO₂, >90% humidity.
5
6 For the test, 100 µL of cell suspension (4×10⁵/mL) was transferred to a 96-well cell culture
7 plate and incubated overnight in incubator conditions to allow cells to adhere. The solutions of
8 tested PyoM_{sol} or PyoM_{insol} were distributed to the wells of cell culture plates (6 replicates for
9 each experimental variant) containing cell monolayers. After 24 h of incubation, the condition
10 of the cell monolayers was verified under an inverted contrast phase microscope. The cell
11 cultures in the medium alone were used as a positive control (PC) of cell viability (100% viable
12 cells). After the incubation, 20 mL of MTT (5 mg/mL) was added to each well and incubated
13 for 4 h. Following the incubation, plates were centrifuged (1200 rpm, 10 min), and supernatants
14 were replaced with 100 mL of DMSO per well to dissolve formazan crystals. After dissolving
15 formazan crystals, the absorbance was measured at 570 nm (Multiskan EX, ThermoFisher,
16 Waltham, MA, USA).
17
18
19
20
21
22
23
24
25
26
27
28
29
30
31
32
33
34
35
36

37 **2.5. Cell Apoptosis**

38
39
40 The cell apoptosis was assessed using the commercial terminal deoxynucleotidyl transferase
41 dUTP nick end labeling (TUNEL) assay (Cell Meter TUNEL Apoptosis Assay Kit, AAT
42 Bioques, Sunnyvale, CA, USA), as previously described [26]. The hFOB 1.19 osteoblasts
43 (4×10⁵ cells/mL), after 24 h exposed to PyoM_{sol} or PyoM_{insol} in the concentration of 1 µg/mL,
44 were treated with fluorescent red dye that passively crosses a cell membrane and selectively
45 targets the nicks in DNA that form during apoptosis. Doxorubicin (DOX, Sigma Aldrich,
46 Darmstadt, Germany) in the concentration of 50 µM was a positive control for the induction of
47 osteoblast apoptosis. The level of osteoblast apoptosis exposed simultaneously to PyoM
48 variants and DOX was also verified. The fluorescence of cells undergoing apoptosis was
49
50
51
52
53
54
55
56
57
58
59
60
61
62
63
64
65

1 measured at 550 nm (excitation) and 590 nm (emission) using a SpectraMax® i3x Multi-Mode
2 Microplate Reader (Molecular Devices, San Jose, CA, USA). The Apoptotic Index was
3
4 calculated based on the relative fluorescence units (RFU) of stimulated cells versus the RFU of
5
6 control cells in the cell culture medium alone.
7
8
9

10 **2.6. Wound Healing Assay**

11
12 The ability of hFOB 1.19 cells to migrate was assessed in a “wound healing assay”, as
13
14 previously described.[26,30] Cells were seeded in six-well plates at the density of 5×10^5 cells
15
16 per well in DMEM/Nutrient Mixture F-12 Ham (Gibco, Zug, Switzerland) supplemented with
17
18 inactivated bovine serum and geneticin (0.3 mg/mL; Gibco, Zug, Switzerland), and incubated
19
20 in humidified cell incubator (33°C, 5% CO₂) until reaching optimal confluency. The cell
21
22 monolayers were scratched with a sterile 200 µL pipette tip, which was designated as the start
23
24 (time 0 h) of wound repair. Next, the culture medium was replaced with solutions of PyoM_{sol}
25
26 or PyoM_{insol}. Non-exposed cells in a culture medium alone were used as a control, exhibiting
27
28 the spontaneous cell migration capacity. Wound images were taken at 0, 24, 48 and 72 h using
29
30 a digital camera combined with an inverted contrast phase microscope (Motic AE2000,
31
32 Xiamen, China), and the wound area was measured using the software Motic AE (version Motic
33
34 Images Plus 2.0ML, Xiamen, China). The wound healing in the milieu of tested PyoM was
35
36 expressed as the percentage of cells migrating to the wound zone compared to untreated cells.
37
38
39
40
41
42
43
44
45

46 **2.7. Osteoblast Proliferation**

47
48 The fluorescence CyQUANT Cell Proliferation Assay (Invivogen, San Diego, CA, USA) was
49
50 used to assess cell proliferation reflecting the cell regeneration capability as previously
51
52 described [29,31]. The proliferation of osteoblasts was evaluated after 7, 14, 21, and 28 days of
53
54 stimulation with PyoM. At the selected time points, cells were washed with phosphate buffered
55
56 saline (PBS) and frozen at -80 °C. After thawing at room temperature, cells were lysed in a
57
58
59
60
61
62
63
64
65

1
2
3
4
5
6
7
8
9
10
11
12
13
14
15
16
17
18
19
20
21
22
23
24
25
26
27
28
29
30
31
32
33
34
35
36
37
38
39
40
41
42
43
44
45
46
47
48
49
50
51
52
53
54
55
56
57
58
59
60
61
62
63
64
65

buffer containing CyQUANT-GR dye prepared according to the manufacturer's instructions. Fluorescence was measured at an emission wavelength of 480 nm and excitation wavelength of 520 nm using a SpectraMax i3x Multi-Mode Microplate Reader (Molecular Devices, San Jose, CA, USA). The standard curve was prepared for quantifying cell proliferation using known cell number reference suspensions.

2.8. Whole Cell Transcriptomic Analysis by RNA Sequencing

hFOB 1.19 cells grown at 33°C (proliferative conditions) or at 39°C (osteoinductive conditions) were subjected to lysis using one volume of RNase-free water mixed with three volumes of TRIzol LS Reagent (Thermo Fisher Scientific, Waltham, MA, USA), and the total RNA was isolated using Direct-zol™ RNA Miniprep Plus (Zymo Research, CA, USA) following the manufacturer's guidelines. To eliminate DNA contamination in the RNA samples, a TURBO DNA-free™ Kit (Thermo Fisher Scientific, Waltham, MA, USA) was utilized in accordance with the manufacturer's protocol. The integrity and quantity of RNA were assessed using Agilent RNA 6000 Nano Kit Agilent 2100 BioAnalyzer (Agilent Technologies, Santa Clara, CA, USA).

The preparation of total RNA sequencing libraries was performed following the protocol described in Kawka et al., 2023 [32]. RNA isolation, library generation, and RNA sequencing were performed independently in triplicate. In brief, 2 µg of RNA purified with AMPure XP (Becton Dickinson, Burlington, NC, USA) beads underwent rRNA depletion using a Ribo-off rRNA Depletion Kit (Human/Mouse/Rat, Vazyme, Nanjing, Jiangsu, China) to remove cytoplasmic and mitochondrial rRNAs, from human total RNA. The sequencing libraries were prepared according to the manufacturer's instructions for the KAPA Stranded RNA-Seq Kit (KAPA Biosystems, Roche, Basel, Switzerland). The quantity and quality of the libraries were assessed using an Agilent 2100 BioAnalyzer with a DNA 1000 chip. Subsequently, the cDNA libraries were sequenced using a NextSeq 550 System (Illumina) with a NextSeq 500/550 Mid

1 Output v.2 Sequencing Kit (150 cycles, 2×75bp) (Illumina, San Diego, CA, USA), ensuring a
2 yield of 5 to 10 million paired-end reads per sample libraries. For the analysis of RNA-Seq data,
3
4 Cutadapt version 2.8 was exploited to eliminate sequencing adapters, followed by quality
5
6 trimming using Sickle version 1.33, allowing for a minimum quality threshold of 30% and a
7
8 minimal read length of 20 base pairs. Reads that met the preset quality criteria were aligned to
9
10 human genome GRCh38 (retrieved from the gencode database, downloaded on December 1,
11
12 2018) with STAR RNA-seq aligner version 2.7 [33]. The sequencing counts were calculated by
13
14 the STAR script. In order to estimate transcriptional changes, we utilized the Degust RNA-Seq
15
16 analysis platform with default parameters (originally designed by D.R. Powell) [34]. In the
17
18 current study, transcripts exhibiting a log₂ fold change greater than or equal to an absolute value
19
20 of 1.585 (representing a change of threefold or more) and a false discovery rate (FDR) of less
21
22 than 0.05 were considered differentially expressed.
23
24
25
26
27
28

29 **2.9. Determination of Alkaline Phosphatase Activity**

30
31
32 The alkaline phosphatase (ALP) activity was measured in cell lysates based on para-
33
34 nitrophenylphosphate (p-NPP) hydrolysis assay as previously described [29,31]. The 100 μL of
35
36 p-NPP in the concentration of 4 μg/μL were added to 100 μL of cell lysates in a 96-well plate
37
38 and incubated at 37 °C for 30 min. Next, a 2 M NaOH solution was added to stop the enzymatic
39
40 reaction. The standard curve ranged from 0 to 10 IU/mL of ALP (Thermo Scientific, Waltham,
41
42 MA, USA), which was used to calculate the enzyme activity in the samples, shown as
43
44 international units (IU). The absorbance at 405 nm was measured using the Multiskan EX reader
45
46 (Thermo Scientific, Waltham, MA, USA).
47
48
49
50
51
52

53 **2.10. Cytokine Release Profile Characterization**

54
55 The concentration of interleukin IL-6, IL-10 or TNF-α in the osteogenic culture media of
56
57 osteoblasts incubated for 4, 7, 11, 14, 18, 21, 25 or 28 days with PyoM_{sol} or PyoM_{insol}, were
58
59
60
61
62
63
64
65

1 determined using specific enzyme-linked immunosorbent assay (ELISA) kits (R&D Systems,
2 Minneapolis, MN, USA), following with the manufacturer's instructions. The wells on a 96-
3 well half area plate (Greiner Bio-One GmbH, Kremsmünster, Austria) were coated overnight at
4 room temperature with cytokine-specific capture antibodies in PBS, then washed three times in
5 washing buffer (PBS/0.05% Tween 20), and blocked for 1.5 h with PBS containing 1% bovine
6 serum albumin (BSA). After washing the wells, tested cell culture supernatants or serial
7 dilutions of the reference recombinant human cytokines (50 µL), used for standard curve
8 establishing, were added and incubated overnight at 4°C. Then, wells were washed and
9 incubated for 2 h with a biotinylated monoclonal antibody diluted 1:60 in PBS/1% BSA.
10 Following washing, an enzyme streptavidin–horseradish peroxidase solution (diluted 1:40) was
11 added for 20 min. at room temperature. After washing, a mixture (1:1) of tetramethylbenzidine
12 (TMB) and hydrogen peroxide was applied. The colorimetric reaction was stopped with 1 M
13 H2SO4. Absorbance was measured at 450 nm using the Multiskan EX reader (Thermo
14 Scientific, Waltham, MA, USA).

34 **2.11. Antibacterial activity of PyoM_{sol} and PyoM_{insol}**

35 The antibacterial activity of PyoM_{sol} or PyoM_{insol} against the reference *Staphylococcus aureus*
36 ATCC 29213 and two clinical strains isolated from bone infection, *S. aureus* resistant to
37 methicillin (MRSA) and *S. felis*, was determined as the minimum inhibitory concentration
38 (MIC) by the resazurin reduction assay [35]. The bacteria were cultured in Mueller–Hinton
39 Broth (MHB) to mid-log phase, and the inoculum was standardized to 5×10⁵ CFU/mL as
40 recommended by European Committee on Antimicrobial Susceptibility Testing (EUCAST)
41 guidelines [36,37]. PyoM_{sol} or PyoM_{insol} were distributed into wells of a 96-well plate (Nunc,
42 Rochester, NY, USA) containing 100 µL MHB and the 2-fold PyoM dilutions were made in the
43 range of 1 – 1024 µg/mL. Then, the bacterial suspension (100 µL) was added to each well, and
44 plates were incubated for 24 h at 37 °C. Control wells contained bacterial culture alone (positive
45
46
47
48
49
50
51
52
53
54
55
56
57
58
59
60
61
62
63
64
65

1 control of bacterial growth), and wells with bacterial medium alone (negative control) were
2 included. To assess MIC, 20 μ L of 0.02% resazurin (Sigma Aldrich, Darmstadt, Germany) in
3 sterile PBS was added to each well and left for 3 h. Fluorescence was measured at an excitation
4 wavelength of 560 nm and emission wavelength of 590 nm using a SpectraMax® i3x Multi-
5 Mode Microplate Reader (Molecular Devices, San Jose, CA, USA).
6
7
8
9
10

11 **2.12. Statistical Analysis**

12
13 Statistical analyses and graphs were performed using GraphPad Prism version 9.1.0 for
14 Windows (GraphPad Software, San Diego, CA, USA). Data were compared using ANOVA with
15
16
17
18
19
20
21
22
23
24
25
26
27
28
29
30
31
32
33
34
35
36
37
38
39
40
41
42
43
44
45
46
47
48
49
50
51
52
53
54
55
56
57
58
59
60
61
62
63
64
65
Dunnett's post-hoc test.

3. RESULTS

3.1. Bacterial Pyomelanin is a Cytocompatible Biomacromolecule towards Human Osteoblasts and Diminishes DOX-induced Cell Apoptosis

In this study, we demonstrated that bacterial pyomelanin (PyoM_{sol} and PyoM_{insol} form) was cytocompatible towards hFOB 1.19 human osteoblast in a wide concentration range (Fig. 1A). PyoM_{sol} did not reduce the viability of the tested cells in the range of 1-1024 μ g/mL and met the requirements (>70.0% of viable cells) for cytocompatibility resulting from the ISO 10993-5-2009 norm. A similar effect was demonstrated for PyoM_{insol}, however, at a concentration of 1024 μ g/mL, this PyoM variant caused a significant ($p < 0.01$) decrease up to $54.7\% \pm 5.0\%$ in the human osteoblasts viability compared to the untreated cells (100% viable cells).

Neither PyoM_{sol} nor PyoM_{insol} alone induced cell apoptosis. There was no increase in the Apoptotic Index (AI) established for PyoM-treated cells vs untreated cells (Fig. 1B). The AI for hFOB 1.19 osteoblast increased significantly ($p < 0.001$) after cell exposure to proapoptotic DOX (positive control in apoptosis assay) compared to untreated cells (AI = 1.00), and was equal to 1.96 ± 0.17 . We have shown that both PyoM variants diminished the apoptotic effect

of DOX. After 24 h of co-stimulation of osteoblasts with DOX and PyoM_{sol} or PyoM_{insol}, the AI was significantly (<0.001) lower than in cells treated with DOX and amounted to 1.09 ± 0.08 and 1.37 ± 0.10 , respectively. Moreover, PyoM_{sol} abolished the proapoptotic activity of DOX more effectively ($p < 0.01$) than PyoM_{insol}.

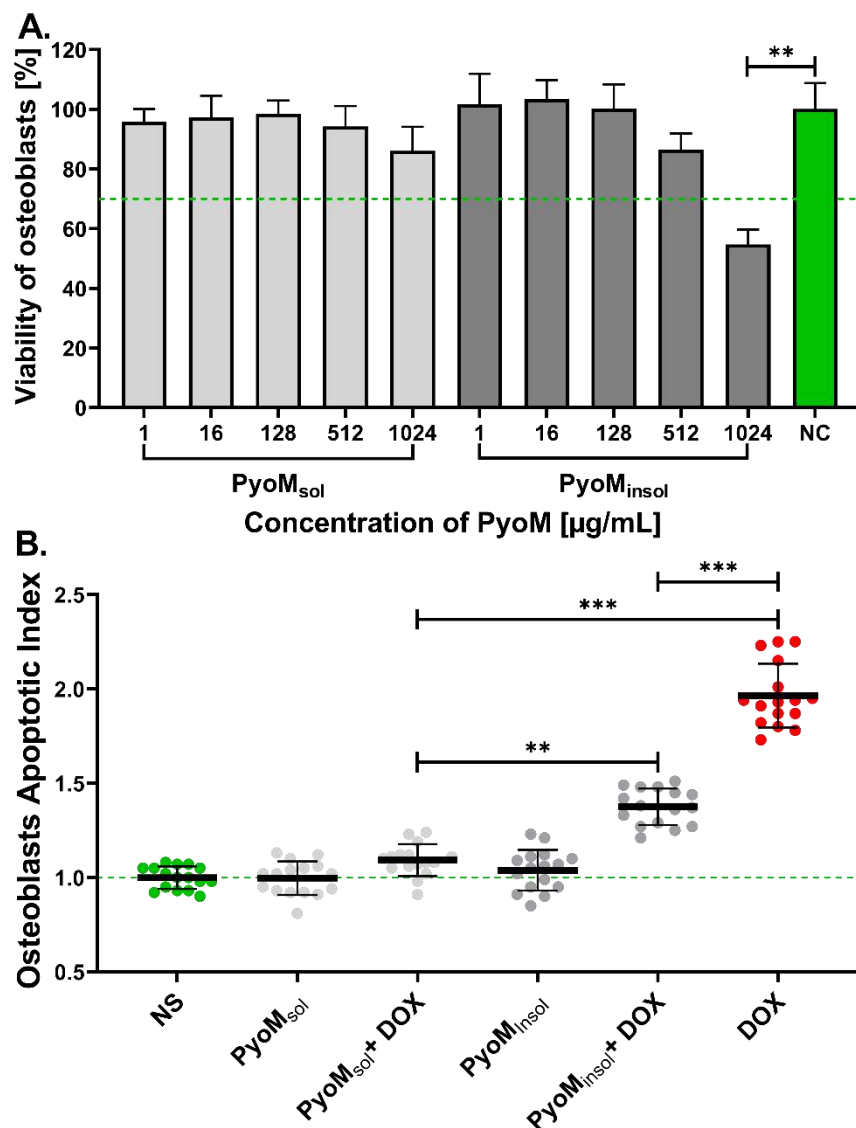


Fig. 1. A. The percentage of viable hFOB 1.19 osteoblasts after 24 h exposure to different concentrations of the water-soluble (PyoM_{sol}) or water-insoluble pyomelanin (PyoM_{insol}). Osteoblasts incubated in the culture medium alone (NC) served as a positive control of cell viability (100%). B. Diminishing cell apoptosis induced by doxorubicin (DOX) in the milieu

1 of PyoM_{sol} or PyoM_{insol} at the concentration of 1 µg/mL. The Apoptotic Index was calculated
2 based on the relative fluorescence units (RFU) of cells stimulated with PyoM vs RFU of the
3 control unstimulated cells (NS), in cell culture medium alone. Data are presented as the mean
4 ± standard deviation of four separate experiments (four replicates for each experimental
5 variant). Statistical significance for ** p < 0.01; *** p < 0.001.
6
7
8
9
10
11

12 **3.2. Pyomelanin Promotes the Migration of Damaged Osteoblasts**

13
14
15
16 PyoM_{sol} significantly stimulated the cell migration within the wound after 24, 48, and 72 h, and
17 the wound healing rate was 63.1% ± 9.2%, 72.2% ± 11.7% and 95.1% ± 7.6%, respectively
18 (Fig. 2A). Similar results were shown for osteoblasts exposed to PyoM_{insol}. PyoM_{insol} at the
19 same time points significantly promoted the cell migration by up to 44.7% ± 9.6%, 69.4% ±
20 6.4% and 93.2% ± 6.7% confluence, respectively. Only after 24 h cells exposed to PyoM_{sol}
21 showed a significantly (p < 0,05) higher percentage of wound closure compared to cells treated
22 with PyoM_{insol}. The migration of untreated hFOB 1.19 osteoblasts increased with time and the
23 average percentages of cells in the wounded zone were 32.7% ± 9.5%, 58.0% ± 10.6% and
24 82.8% ± 6.7% after 24, 48 and 72 h, respectively. Representative images of hFOB 1.19
25 osteoblast migration after 24, 48, and 72 h of PyoM stimulation are shown in Fig. 2B.
26
27
28
29
30
31
32
33
34
35
36
37
38
39
40
41
42
43
44
45
46
47
48
49
50
51
52
53
54
55
56
57
58
59
60
61
62
63
64
65

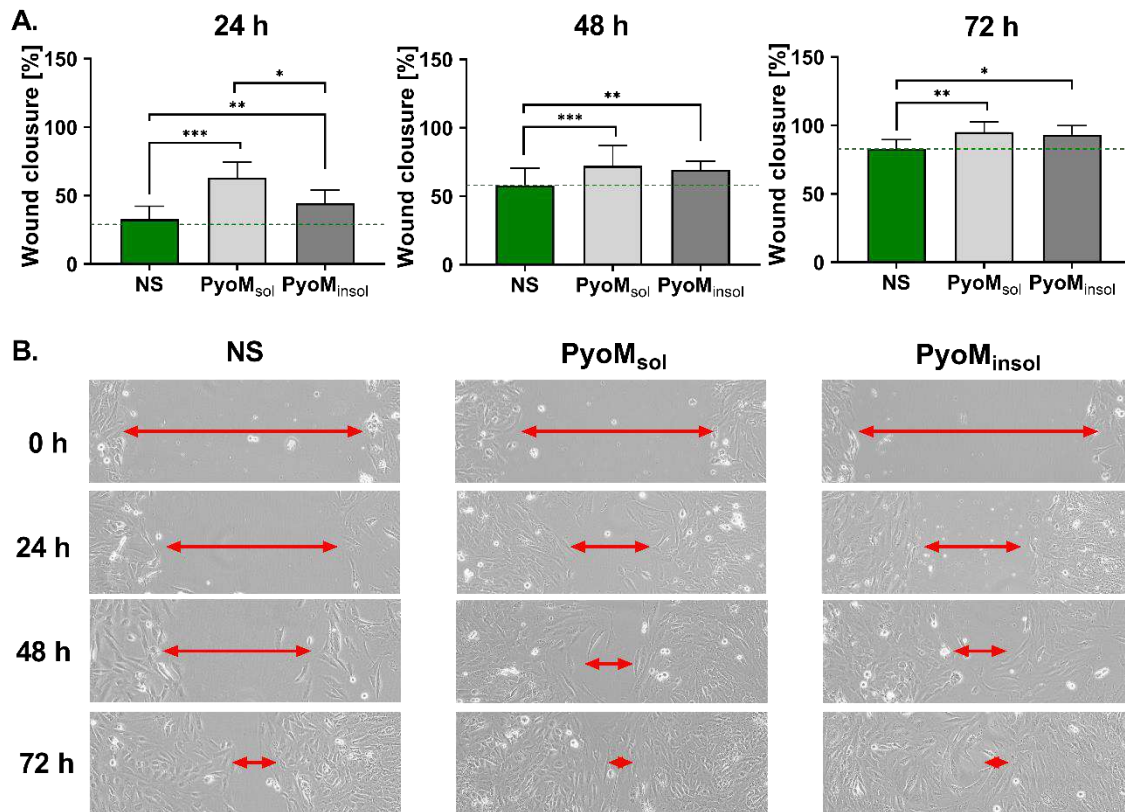


Fig. 2. A. The effectiveness of hFOB 1.19 osteoblasts migration in wound healing assay. The cell cultures were exposed to water-soluble (PyoM_{sol}) or water-insoluble pyomelanin (PyoM_{insol}) at the concentration of 1 $\mu\text{g}/\text{mL}$ for 24 h, 48 h or 72 h. Results are shown as mean \pm standard deviation of five independent experiments (four replicates for each experimental variant). Statistical significance for * $p < 0.05$; ** $p < 0.01$; *** $p < 0.001$. NS - cells not stimulated with PyoM. The green line indicates the reference wound closure of unstimulated cells in the cell culture medium alone. B. Representative images of hFOB 1.19 osteoblast migration after 24, 48, and 72 h of water-soluble (PyoM_{sol}) or water-insoluble pyomelanin (PyoM_{insol}) stimulation. In the microscopic images, the arrows indicate the width of the overgrown crack.

3.3. Pyomelanin Increases Differentiation and Maturation of Human Osteoblasts

Transcriptomic analyses revealed that PyoM_{sol}-treated osteoblasts differentiate more efficiently than the untreated cells when judging by the number of differentially expressed transcripts. Nontreated cells revealed 1307 transcriptional changes and PyoM_{sol}-treated cells exhibited

1
2
3
4
5
6
7
8
9
10
11
12
13
14
15
16
17
18
19
20
21
22
23
24
25
26
27
28
29
30
31
32
33
34
35
36
37
38
39
40
41
42
43
44
45
46
47
48
49
50
51
52
53
54
55
56
57
58
59
60
61
62
63
64
65

1431 significant changes (Supplementary Table 1). Relative changes in expression were also more pronounced in the case of pyomelanin-treated cells. A selection of transcripts relevant to osteoblasts differentiation is presented in the Fig. 3. Transcriptomic changes associated specifically with hFOB 1.19 differentiation upon PyoM_{sol} treatment include significant upregulation of bone morphogenic protein (BMP)-2 and tendency to increased expression of liver/bone/kidney – tissue nonspecific (TNSALP) form of alkaline phosphatase related to the bone maturation, in conjunction with upregulation of phosphatidylinositol 3-kinase – serine/threonine kinase (PI3K-Akt) and calcium dependent signaling pathways involved in cell proliferation and differentiation.

Despite cell migration in this study, the ability of cells to proliferate was determined since cell expansion is an essential step in the cell regeneration process. The assessment of cell proliferation was made based on DNA quantification using a fluorescence assay in which the fluorescence intensity of DNA corresponds to the number of cells. In cell cultures stimulated with PyoM_{sol} or PyoM_{insol}, the number of cells was higher within cultivation period ($p < 0.05$) compared to unstimulated cells (Fig. 4A). The mean number of cells after 28 days of stimulation with PyoM_{sol} ($3.67 \times 10^5 \pm 0.16 \times 10^5$) or PyoM_{insol} ($3.49 \times 10^5 \pm 0.15 \times 10^5$) was significantly higher ($p < 0.05$) than number of cells in untreated cultures ($2.85 \times 10^5 \pm 0.09 \times 10^5$). PyoM_{sol} promoted efficient osteoblast proliferation on the 7th day of osteogenic culture compared to the number of cells on the first day of the experiment.

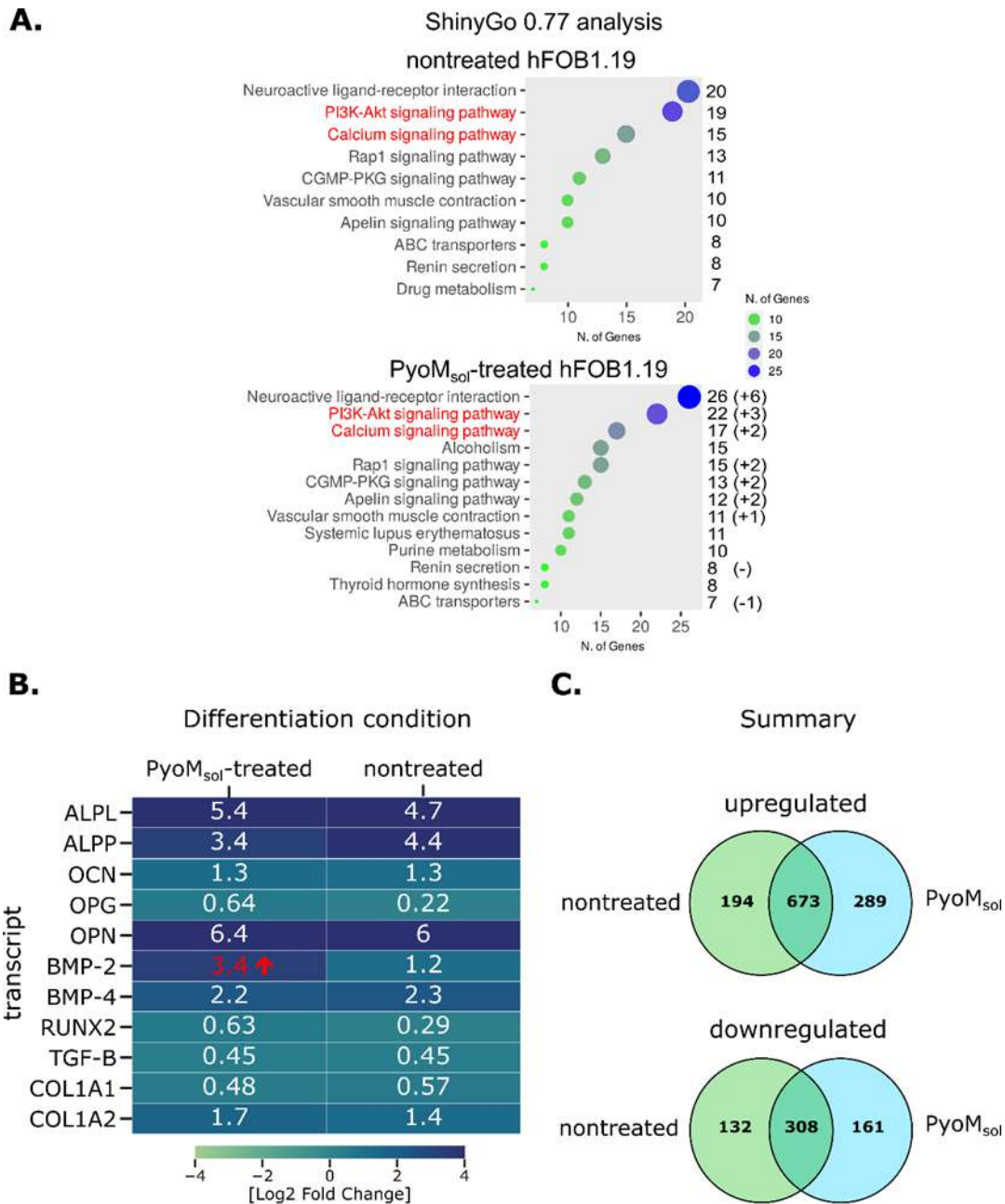
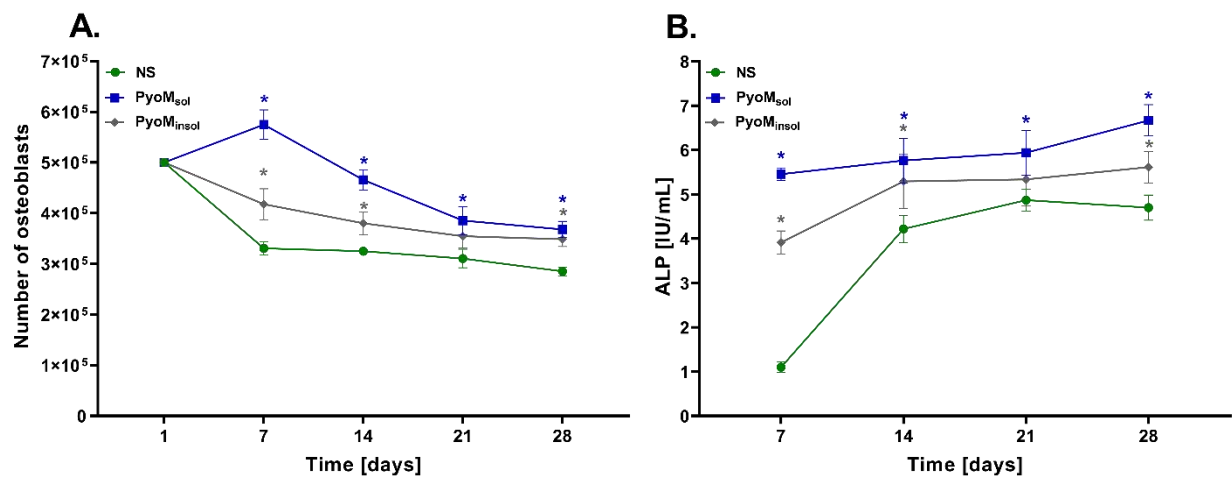


Fig. 3. Transcriptomic changes associated with hFOB 1.19 differentiation upon treatment with soluble pyomelanin (PyoM_{sol}) A. Ontology analysis of differentially expressed genes, overexpressed in hFOB1.19 osteoblasts during differentiation in osteoinductive media utilizing ShinyGo 0.77 online platform.[38] B. List of transcripts relevant to osteoblastic differentiation of hFOB cells in comparison between proliferative and differentiation conditions for PyoM_{sol} and nontreated cells. C. A summary of transcriptomic changes observed between hFOB 1.19 cells differentiating under standard conditions versus cells differentiating in media

1 supplemented with PyoM_{sol}. RNA was isolated from cells incubated in proliferative or
 2 differentiation conditions for 14 days. The change in BMP-2 expression between nontreated
 3 and treated cells (marked in red) exceeded the Log 2 FC of 2, preset as threshold for our
 4 analysis. ALPL, liver/bone/kidney or tissue nonspecific (TNSALP) ALP form, ALPP, placental
 5 ALP form; BMP, Bone Morphogenic Protein; CGMP-PKG (cyclic guanosine monophosphate
 6 protein kinase G), COL (collagen), OCN (osteocalcin), OPG (osteoprotegrin), RUNX (runt-
 7 related transcription factors), TGF-Beta (transforming growth factor beta), PI3-Akt (PI3-Akt,
 8 phosphatidylinositol 3-kinase – serine/threonine kinase (protein kinase B)), Rap1 (Ras –
 9 proximate -1 or Ras-related protein-1).

10
 11
 12
 13
 14
 15
 16
 17
 18
 19
 20
 21
 22 Moreover, stimulation of osteoblasts with PyoM_{sol} or PyoM_{insol} led to a significant increase in
 23 ALP expression compared to the activity of this osteoblastic marker detected in unstimulated
 24 cell cultures (Fig. 4B). On the 28th day of culture, ALP concentration reached 6.67 ± 0.35
 25 IU/mL, 5.61 ± 0.26 IU/mL, and 4.70 ± 0.29 IU/mL, respectively ($p < 0.05$).



26
 27
 28
 29
 30
 31
 32
 33
 34
 35
 36
 37
 38
 39
 40
 41
 42
 43
 44
 45
 46
 47
 48
 49
 50
 51
 52 Fig. 4. The influence of pyomelanin (PyoM) on cell growth and alkaline phosphatase
 53 production. A. Number of hFOB 1.19 osteoblasts after 1, 7, 14, 21, or 28 days of incubation
 54 with the water-soluble (PyoM_{sol}), water-insoluble pyomelanin (PyoM_{insol}) or culture medium
 55 alone – unstimulated cells (NS). B. The activity of alkaline phosphatase (ALP) produced by
 56
 57
 58
 59
 60
 61
 62
 63
 64
 65

1 hFOB 1.19 osteoblasts cultures exposed to PyoM_{sol}, PyoM_{insol} or culture medium alone (NS)
2 after 7, 14, 21 or 28 days showed in international units (IU). Results are shown as mean ±
3 standard deviation of four independent experiments in four replicates for each experimental
4 variant. Statistical significance for * p<0.05.
5
6
7
8
9

10 The secretion of osteocalcin (OC), the critical marker of osteoblast differentiation, was
11 increasing in culture supernatants of hFOB 1.19 osteoblasts exposed to PyoM_{sol} throughout the
12 entire culture period (Fig. 5A). The level of OC increased to a concentration of 901.0 ± 85.3
13 pg/mL and 668.1 ± 117.7 pg/mL on day 7th, and 2440.2 ± 128.3 pg/mL and 961.2 ± 97.7 pg/mL
14 on day 28th, respectively. Significant differences (p<0.05) in OC secretion were also shown for
15 cell cultures containing PyoM_{insol} vs unstimulated cell cultures, only for the 21st day of culture.
16
17
18
19
20
21
22
23
24

25 As shown in Fig. 5B, the production of interleukin IL-6 increased significantly (p<0.05)
26 throughout the entire course of the experiment in osteoblasts culture treated with PyoM_{sol}
27 reaching 291.5 ± 6.0 pg/mL on day 28, compared to unstimulated cultures (58.0 ± 10.4 pg/mL).
28
29
30
31
32 The increasing trend in IL-6 secretion was also demonstrated for cell cultures treated with
33 PyoM_{insol}; however, the difference was statistically significant from the 14th day of culture.
34
35
36
37

38 A similar secretion profile was found for IL-10. The maximum concentration of IL-10 in hFOB
39 1.19 osteoblast cultures exposed to PyoM_{sol} or PyoM_{insol} was demonstrated on the 14th day of
40 the experiment and were 849.1 ± 82.3 pg/mL and 471.2 ± 47.5 pg/mL, respectively (Fig. 5C).
41
42
43
44
45 Then, the concentration of IL-10 was decreasing over time in cell cultures exposed to PyoM_{insol},
46 while in cell cultures treated with PyoM_{sol} there was a second peak of IL-10 elevation from 25th
47 day to 28th day of culture. In the endpoint, on the 28th day, the concentration of IL-10 in the
48 osteoblast culture supernatant after stimulation of cells with PyoM_{sol} or PyoM_{insol} was
49 significantly higher (p<0.05) compared to the culture of osteoblasts propagated in culture
50 medium alone, 740.9 ± 79.8 pg/mL, 252.6 ± 37.7 pg/mL or 174.6 ± 20.5 pg/mL, respectively.
51
52
53
54
55
56
57
58
59
60
61
62
63
64
65

The level of TNF- α was significantly ($p < 0.05$) higher in cell culture supernatants after stimulation of cells with PyoM_{sol} or PyoM_{insol} on the 28th day, amounting to 391.2 ± 28.2 pg/mL and 517.0 ± 38.5 pg/mL, respectively, compared to unstimulated osteoblasts, 55.5 ± 14.7 pg/mL (Fig. 5D).

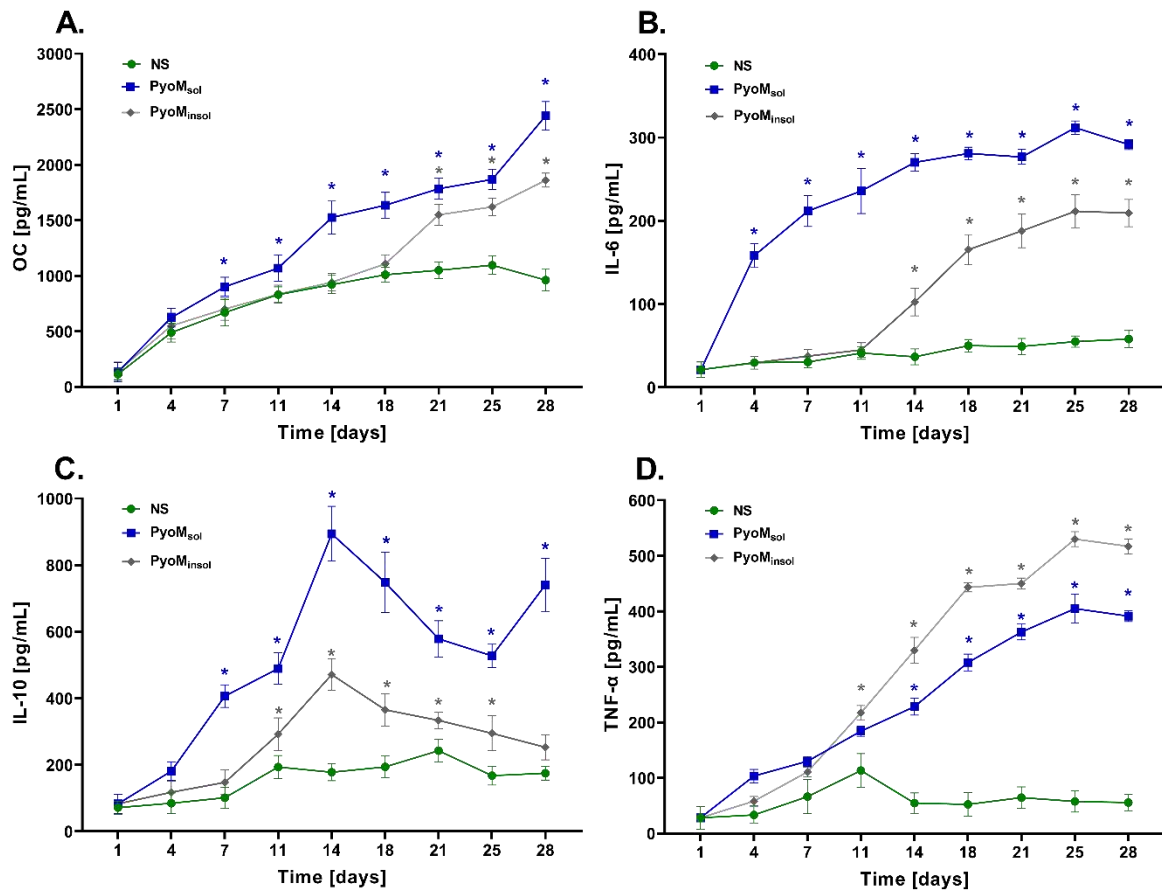


Fig. 5. Secretion of A. osteocalcin (OC), B. interleukin (IL)-6, C. IL-10, and D. tumor necrosis factor (TNF)- α in cell cultures of hFOB 1.19 exposed to water-soluble (PyoM_{sol}), water-insoluble pyomelanin (PyoM_{insol}) or culture medium alone – not stimulated cells (NS), after 1, 4, 7, 11, 14, 18, 21, 25, and 28 days. Results are shown as mean \pm standard deviation of four independent experiments in four replicates for each experimental variant. Statistical significance for * $p < 0.05$.

3.4. Antibacterial Activity of PyoM towards *Staphylococcus* spp.

1
2
3 Dose–response curves and MIC₅₀ of PyoM against the reference *S. aureus* ATCC 29213 and
4
5 two clinical isolates (*S. aureus* MRSA and *S. felis*) are shown in Fig. 6. MIC₅₀ was defined as
6
7 the lowest concentration of the bacterial PyoM at which 50% of the bacterial cells were killed.
8
9
10 Both forms of PyoM significantly (p<0.001) reduced the viability of reference and clinical
11
12 strains of *Staphylococcus* spp. as examined by the resazurin reduction assay. The lowest MIC₅₀
13
14 (57.6 µg/mL) for PyoM_{sol} was observed for the clinical *S. aureus* MRSA strain, while the
15
16 highest MIC₅₀ (153.1 µg/mL) was identified for the reference *S. aureus* ATCC 29213. Similar
17
18 inhibition of the metabolic activity was shown for PyoM_{insol}, where the lowest MIC₅₀ (93.3
19
20 µg/mL) was for *S. aureus* MRSA, and the highest MIC₅₀ (200.9 µg/mL) was demonstrated for
21
22 *S. aureus* ATCC 29213. PyoM_{sol} effectively limited the metabolism of the tested bacteria
23
24 compared to the PyoM_{insol}, which resulted in a significantly (p<0.001) lower MIC₅₀.
25
26
27
28
29
30
31
32
33
34
35
36
37
38
39
40
41
42
43
44
45
46
47
48
49
50
51
52
53
54
55
56
57
58
59
60
61
62
63
64
65

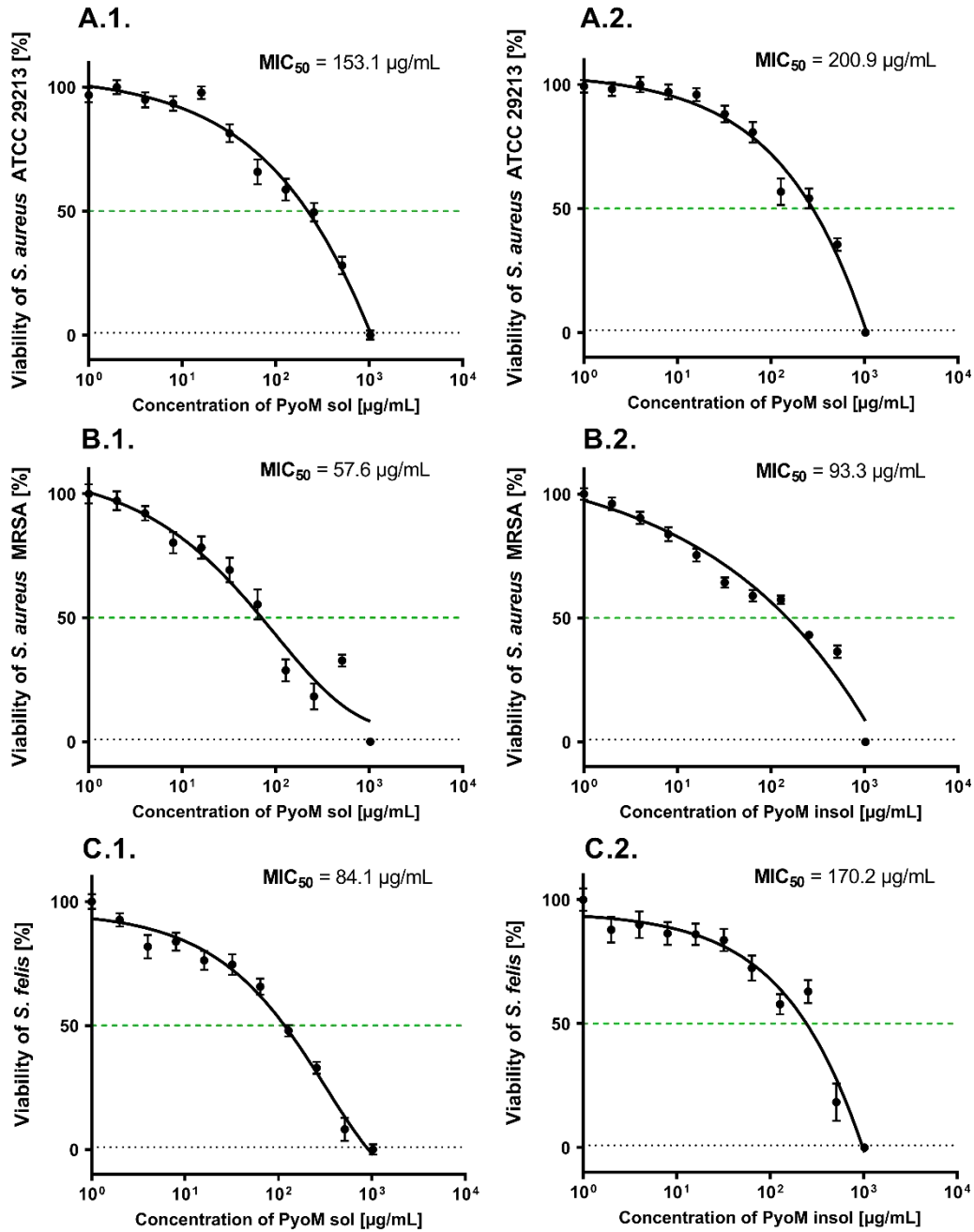


Fig. 6. Dose–response curves and minimum inhibitory concentration (MIC_{50}) of pyomelanin.

(1) Water-soluble ($PyoM_{sol}$) or (2) water-insoluble pyomelanin ($PyoM_{insol}$). *Staphylococcus*

strains: (A) reference *S. aureus* ATCC 29213, (B) clinical *S. aureus* MRSA and (C) *S. felis*.

Results are shown as mean \pm standard deviation of five independent experiments performed in four replicates for each experimental variant. The green line indicates the 50% level of bacterial viability.

4. DISCUSSION

1
2
3 Bone is a dynamic tissue that undergoes continuous remodelling due to precisely tailored bone
4 formation and bone resorption processes carried out by osteoblasts and osteoclasts. After an
5 injury, bone tissue can self-repair, restoring the damaged part to its original structure and
6 mechanical strength [39,40]. In 2019, the global number of new cases of bone fracture was
7 estimated to be 178 million, an increase of 33.4% since 1990 [41]. The increasing number of
8 bone fractures, including those related to osteoporosis, and the observed trends in the rising
9 costs of treating these diseases prompt researchers to look for new substances stimulating the
10 regeneration of bone tissue, which can be used individually or as part of biocomposites [42–
11 44]. One of such substances may be polymers of HGA responsible for the excessive ossification
12 in AKU, and pyomelanin, which is a biomimetic of ochronotic deposits produced by
13 *Pseudomonas aeruginosa* [19–21].
14
15
16
17
18
19
20
21
22
23
24
25
26
27
28
29

30 Pyomelanin derived from *P. aeruginosa* is a promising macromolecular metabolite that
31 upregulates osteoblast maturation with simultaneous antibacterial and migration-promoting
32 effects. This study demonstrated that PyoM_{sol} and PyoM_{insol} are cytocompatible biopolymers
33 for human hFOB 1.19 osteoblast cells in a wide range of concentrations. In previous studies,
34 we have shown that PyoM_{sol} and PyoM_{insol} do not reduce cell viability of reference L-929
35 fibroblasts, THP-1 monocytes, and AGS gastric epithelial cells [23,26]. Ferraz et. revealed that
36 PyoM isolated from the *Pseudomonas putida* bacteria is not toxic to the A-375 skin epithelial
37 cells, Hep G2 liver epithelial-like cells, and Caco-2 colorectal epithelial cells [45]. Moreover,
38 PyoM isolated from *Halomonas titanicae* and *Pseudomonas stutzeri* showed a high level of
39 cytocompatibility with human HaCeT keratinocytes and L-929 fibroblasts, respectively [24,46].
40 *In vitro* studies on the insect *Galleria mellonella* larvae model also confirmed the
41 biocompatibility of both forms of PyoM isolated from *P. aeruginosa* [23].
42
43
44
45
46
47
48
49
50
51
52
53
54
55
56
57
58
59
60
61
62
63
64
65

1 In this study, PyoM_{sol} and PyoM_{insol} did not induce apoptosis in human osteoblasts and partially
2 limited DOX-induced programmed cell death in bone-forming cells. Importantly, co-
3 stimulation of osteoblasts with PyoM_{sol} led to a complete abolition of DOX apoptotic activity.
4 These data are consistent with the results obtained using gastric epithelial cells AGS co-
5 stimulated with PyoM and lipopolysaccharide (LPS) of *Escherichia coli* or *Helicobacter pylori*,
6 where PyoM reversed the LPS-induced apoptosis [26]. The potential mechanism of PyoM-
7 related antiapoptotic effect may result from the anti-oxidative properties of this bacterial
8 polymer [24]. PyoM-mediated neutralization of reactive oxygen species (ROS), increasing the
9 frequency of DNA breaks, may prevent apoptotic cell death [26].
10
11
12
13
14
15
16
17
18
19
20
21

22 Osteoblasts, which are bone-forming cells, play indispensable roles in the formation and
23 remodelling of bone tissue. Osteoblast progenitor cells undergo proliferation and are
24 responsible for secretion and maturation of extracellular matrix and then matrix mineralization
25 [47]. Proliferation of progenitor cells in conjunction with the production of collagen,
26 fibronectin, OPN and transforming growth factor- β (TGF- β) receptor 1 are early steps in bone
27 development. Later on, cell proliferation is downregulated, and immature osteoblasts
28 differentiate into mature bone-forming cells that secrete COL1 and produce ALP to mature the
29 extracellular matrix. The final step in bone development is matrix mineralization, which occurs
30 through the expression of osteoblastogenic markers such as OPN, OC and bone sialoprotein,
31 with continued expression of ALP and COL1 [47]. Coordinated and precise secretion of
32 cytokines, including IL-6, IL-10, TNF- α or TGF- β , and activation of transcription factors of
33 osteoblasts and osteocytes ensure controlled regeneration and remodelling of bone tissue [9,47].
34
35
36
37
38
39
40
41
42
43
44
45
46
47
48
49
50
51

52 Cell migration is an essential marker of early cell pro-regenerative activity. In this study, we
53 showed that both PyoM variants promoted a migration of osteoblasts in wound healing assay.
54 The effectiveness of bone tissue development and its remodelling depend on progenitor cells'
55 replication effectiveness and mature osteoblasts' lifespan [48]. In this study, we showed that the
56
57
58
59
60
61
62
63
64
65

1 number of cells exposed for 28 days to PyoM_{sol} or PyoM_{insol} was higher than the number of
2 cells in cultures without PyoM. Interestingly, PyoM_{sol} on the 7th day of culture promoted
3 osteoblast proliferation. These result suggest that PyoM_{sol} potentially can play a role of
4 osteoblast growth-like factor, and both PyoM_{sol} and PyoM_{insol} are able to drive the cell
5 maturation. The transcriptomic studies may indicate the potential role of PyoM in the
6 maturation of bone cells due to upregulation of PI3-Akt and calcium channel related signaling
7 pathways and an increased production of some proteins involved in the bone cell maturation
8 [49–51].
9

10 This study revealed that PyoM_{sol} or PyoM_{insol} led to a significant increase in ALP expression in
11 osteoblasts compared to the activity of this osteoblastic marker detected in unstimulated cell
12 cultures. ALP is an extracellular, membrane-bound enzyme hydrolyzing the ester of
13 monophosphate at alkaline pH that is highly expressed in the cells of mineralized tissue [52].
14 In bones, ALP plays an essential role in mineralization, extracellular dephosphorylation, and
15 vitamin B6 metabolism and may be involved in regulating DNA synthesis and intracellular
16 protein production. ALP is also an early marker of osteoblastic activity and bone formation
17 [53].
18

19 One of the key protein hormone involved in bone formation is the non-collagenous protein OC
20 expressed and secreted only by osteoblasts [54]. We have shown that bacterial PyoM
21 significantly increased the secretion of OC by osteoblasts, which can be used as bacterial
22 metabolites for targeted reconstruction of bone tissue. It has been shown that OC, which is
23 secreted into the bone microenvironment, binds to calcium ions in hydroxyapatite and also
24 provides mechanical bone strength due to complexing with collagen via OPN [55].
25

26 The bone remodelling is facilitated by different cytokines produced by osteoblasts and
27 inflammatory cells, including neutrophils, macrophages and T lymphocytes [9]. It is known that
28 IL-6 promotes bone formation by increasing the differentiation of osteoblast precursors and
29
30
31

1 protecting osteoblasts from apoptosis [56,57]. IL-6-type cytokines can increase osteoblast
2 markers expression such as ALP, OC, and bone sialoprotein to enhance bone nodule formation
3 and extracellular matrix mineralization[58]. This cytokine may protect bone tissue against
4 resorption by downregulation of RANKL expression in osteoclasts and by stimulating the
5 production of the anti-osteoclastogenic cytokines IL-4 and IL-10 [59]. In this study, we
6 demonstrated that PyoM_{sol} and PyoM_{insol} significantly stimulated osteoblasts to secrete IL-6. It
7 seems noteworthy that treating osteoblast cultures with PyoM_{sol} resulted in higher
8 concentrations of this cytokine than the insoluble form. Moreover, the higher number of viable
9 osteoblasts during osteoinduction culture and more effective abolition of DOX-induced
10 apoptosis in the co-stimulation osteoblasts with PyoM_{sol} observed in this study may be
11 dependent on a higher level of IL-6 secretion than in the case of co-stimulation with PyoM_{insol}.

12 Our results indicate that stimulation of human osteoblasts with bacterial PyoM_{sol} or PyoM_{insol}
13 significantly upregulated the level of IL-10 secretion. It is known that IL-10 indirectly induces
14 bone formation through the p38 mitogen-activated protein kinase (MAPK) signaling pathway
15 [60]. Moreover, IL-10 inhibits the early phase of osteoclast progenitor cell differentiation into
16 osteoclast precursors and also downregulates osteoclast differentiation by increasing OPG to
17 suppress RANKL expression [61,62]. The bacterial PyoM may be beneficial in controlling
18 excessive osteoclastogenesis through IL-10-dependent inhibition of nuclear factor of activated
19 T-cells (NFATC1) expression and nuclear translocation by suppressing c-Fos and c-Jun activity.
20 However, future studies are needed confirm the role of IL-10 in driving this activation cascade
21 [63]. Animal experiments have proven that IL-10-deficient mice exhibit reduced bone mass,
22 increased mechanical fragility, and inhibition of bone formation [64,65].

23 TNF- α induces bone resorption and promotes osteoclast formation from bone marrow-derived
24 macrophages and osteoclast differentiation through numerous mechanisms, some of which are
25 autonomous of the RANKL/RANK axis [66]. TNF- α initiates and activates osteoclasts to resorb

1 bone, which may benefit bone repair during bone healing. However, the influence of TNF- α on
2 osteoblast function might be dose-dependent. It has been shown that this cytokine in low
3 concentrations stimulates mesenchymal precursor cells to differentiate into osteoblasts,
4 whereas, in high concentrations, TNF- α inhibits bone formation [67,68]. In this study, the
5 concentration of TNF- α in the cultures of osteoblasts exposed to tested PyoM variants was
6 higher than in control cell cultures. The level of TNF- α was higher in cell cultures of osteoblasts
7 exposed to PyoM_{insol} than PyoM_{sol}. This may result from different ligand – TNF- α receptor
8 interactions, however, the explanation of this suggestion needs further study. The observed
9 elevated TNF- α secretion in response to PyoM may suggest the role of this cytokine in
10 remodelling bone tissue. Considering the role of TNF- α in driving inflammatory response, the
11 lower activity of PyoM_{sol} than PyoM_{insol} in TNF- α induction may be beneficial for the bone
12 formation process. Further studies are necessary to deepen knowledge about the possible
13 mechanisms differentiating the PyoM variants as TNF- α stimulators.
14
15
16
17
18
19
20
21
22
23
24
25
26
27
28
29
30

31 The increasing number of antibiotic-resistant bacterial species has become a significant
32 problem worldwide in medical practice. This situation requires the development of new
33 substances with antibacterial potential that can be part of new therapies, including the usage of
34 biocomposite for bone regeneration, reducing the risk of infection [69]. In this study, PyoM_{sol}
35 and PyoM_{insol} exhibited antibacterial activity towards clinical *Staphylococcus* strains isolated
36 from bone infections. The bacterial killing was more effective after treatment of tested strains
37 with PyoM_{sol} than with PyoM_{insol}. Other researchers have also demonstrated the antibacterial
38 and antifungal properties of PyoM. Zerrad et al. reported that melanin isolated from
39 *Pseudomonas balearica* successfully reduced the viability of pathogenic *S. aureus*, *E. coli*, and
40 *Candida albicans* [70]. Xu et al., based on experiments with *Vibrio parahaemolyticus* and *S.*
41 *aureus*, suggested that PyoM damages bacterial cell membranes [71]. PyoM has also been
42 shown to inhibit the growth of *H. pylori* [26,72].
43
44
45
46
47
48
49
50
51
52
53
54
55
56
57
58
59
60
61
62
63
64
65

5. CONCLUSIONS

1
2
3 Many innovative biomolecules are being tested worldwide to develop advanced bone
4
5 regeneration strategies. The “perfect biomolecule” for the regeneration of bone defects would
6
7 support not only the growth and differentiation of osteoblasts, minimizing cell apoptosis, but
8
9 also reduce the risk of bacterial infections. A novel approach seems to be the controlled
10
11 imitation of pathological processes dependent on the deposition of HGA polymers occurring in
12
13 AKU to enhance the osteoinduction, mineralization and regeneration of bone tissue. The data
14
15 presented in this study indicate that the polymeric PyoM isolated from *P. aeruginosa* is
16
17 cytocompatible for osteoblasts, promotes cell survival and differentiation, as also limits the cell
18
19 apoptosis. The results presented in this study lead to considering PyoM as a stimulator of
20
21 osteoinductive processes and osteoblast maturation. The stimulation of osteoblasts with PyoM
22
23 provided appropriate conditions to promote *in vitro* bone regeneration by increasing the cell
24
25 migration and production of essential ossification markers, including ALP, OC, IL-6, IL-10,
26
27 and TNF- α . Although both PyoM variants display quite similar properties, PyoM_{sol} appears to
28
29 have greater osteoinductive and pro-regenerative potential due to the upregulation of cell
30
31 proliferation. PyoM_{sol} showed weaker ability to stimulate the production of pro-inflammatory
32
33 TNF- α by osteoblasts. This difference may also vote for PyoM_{sol} rather than PyoM_{insol} due to
34
35 diminishing the risk of deleterious inflammatory response as a result of medical intervention.
36
37 The comprehensive activity of PyoM in the processes of renewal, growth and maturation of
38
39 bone cells gives the opportunity to develop PyoM-modified biocomposites for therapeutic
40
41 applications in regenerative medicine. The antibacterial properties of PyoM reinforce this idea.
42
43 The omnidirectional osteoinductive effect achieved through the PyoM stimulation of
44
45 osteoblasts creates new opportunities for designing biocomposites modified with this bacterial-
46
47 origin biomacromolecule with tailored properties, offering novel prospects for various
48
49 biological and medical applications.
50
51
52
53
54
55
56
57
58
59
60
61
62
63
64
65

Acknowledgements

The authors would like to acknowledge Dr Marcin Słomka from the Biobank Facility at University of Lodz for performing the sequencing of RNA-Seq libraries. Biobank Lab, Department of Oncobiology and Epigenetics, Faculty of Biology and Environmental Protection, University of Lodz, Lodz, Poland.

Corresponding Author

*Mateusz M. Urbaniak; Department of Immunology and Infectious Biology, Faculty of Biology and Environmental Protection, University of Lodz, Lodz, Poland, e-mail: mateusz.urbaniak@edu.uni.lodz.pl, ORCID: 0000-0002-2800-2054,

*Magdalena Chmiela; Department of Immunology and Infectious Biology, Faculty of Biology and Environmental Protection, University of Lodz, Lodz, Poland, e-mail: magdalena.chmiela@biol.uni.lodz.pl, ORCID: 0000-0002-5447-2922.

Author Contributions

Mateusz M. Urbaniak: conceptualization, isolation and purification of pyomelanin, performing experiments, formal analysis, data analysis, writing of the manuscript; Karolina Rudnicka: funding, project management, writing of the manuscript; Przemysław Płociński: conceptualization, performing transcriptomic analysis, writing of the manuscript; Magdalena Chmiela: scientific supervision, data analysis, writing of the manuscript.

The manuscript was written through contribution of all authors. All authors have given approval to the final version of the manuscript and to publish the present version of the manuscript.

Funding Sources

This research was funded by the Foundation for Polish Science through the European Union under the European Regional Development Fund, within the “TEAM-NET” program entitled

1 “Multifunctional biologically active composite for application in bone regenerative medicine”
2 [grant number POIR.04.04.00-00-16D7/18-00].
3
4

5 REFERENCES 6

- 7
8 [1] M. Ansari, Bone tissue regeneration: Biology, strategies and interface studies, *Prog.*
9 *Biomater.* 8 (2019) 223–237. <https://doi.org/10.1007/s40204-019-00125-z>.
10
11
12
13 [2] R. Florencio-Silva, G.R.D.S. Sasso, E. Sasso-Cerri, M.J. Simões, P.S. Cerri, Biology of
14 bone tissue: Structure, function, and factors that influence bone cells, *Biomed. Res. Int.* (2015),
15 421746. <https://doi.org/10.1155/2015/421746>.
16
17
18
19 [3] H.C. Blair, Q.C. Larrouture, Y. Li, H. Lin, D. Beer-Stoltz, L. Liu, R.S. Tuan, L.J.
20 Robinson, P.H. Schlesinger, D.J. Nelson, Osteoblast differentiation and bone matrix formation
21 in vivo and in vitro, *Tissue. Eng. Part B Rev.* 23 (2017) 268–280.
22 <https://doi.org/10.1089/ten.teb.2016.0454>.
23
24
25
26 [4] J.C. Crockett, M.J. Rogers, F.P. Coxon, L.J. Hocking, M.H. Helfrich, Bone remodelling
27 at a glance, *J. Cell. Sci.* 124 (2011) 991–998. <https://doi.org/10.1242/jcs.063032>.
28
29
30
31 [5] B. Langdahl, S. Ferrari, D.W. Dempster, Bone modeling and remodeling: Potential as
32 therapeutic targets for the treatment of osteoporosis, *Ther. Adv. Musculoskelet. Dis.* 8 (2016)
33 225–235. <https://doi.org/10.1177/1759720X16670154>.
34
35
36
37 [6] J.Y. Noh, Y. Yang, H. Jung, Molecular mechanisms and emerging therapeutics for
38 osteoporosis, *Int. J. Mol. Sci.* 21 (2020) 1–22. <https://doi.org/10.3390/ijms21207623>.
39
40
41
42 [7] P. Szulc, Bone turnover: Biology and assessment tools, *Best Pract. Res. Clin.*
43 *Endocrinol. Metab.* 32 (2018) 725–738. <https://doi.org/10.1016/j.beem.2018.05.003>.
44
45
46
47
48
49
50
51
52
53
54
55
56
57
58
59
60
61
62
63
64
65

- 1
2
3
4
5
6
7
8
9
10
11
12
13
14
15
16
17
18
19
20
21
22
23
24
25
26
27
28
29
30
31
32
33
34
35
36
37
38
39
40
41
42
43
44
45
46
47
48
49
50
51
52
53
54
55
56
57
58
59
60
61
62
63
64
65
- [8] T. Ono, M. Hayashi, F. Sasaki, T. Nakashima, RANKL biology: Bone metabolism, the immune system, and beyond, *Inflamm. Regen.* 40 (2020), 32047573. <https://doi.org/10.1186/s41232-019-0111-3>.
- [9] J. Xu, L. Yu, F. Liu, L. Wan, Z. Deng, The effect of cytokines on osteoblasts and osteoclasts in bone remodeling in osteoporosis: A review, *Front. Immunol.* 14 (2023), 1222129. <https://doi.org/10.3389/fimmu.2023.1222129>.
- [10] T. Katagiri, T. Watabe, Bone morphogenetic proteins, *Cold Spring Harb. Perspect. Biol.* 8 (2016), 021899. <https://doi.org/10.1101/cshperspect.a021899>.
- [11] X. Lin, S. Patil, Y.G. Gao, A. Qian, The bone extracellular matrix in bone formation and regeneration, *Front. Pharmacol.* 11 (2020), 757. <https://doi.org/10.3389/fphar.2020.00757>.
- [12] W. Shuaishuai, Z. Tongtong, W. Dapeng, Z. Mingran, W. Xukai, Y. Yue, D. Hengliang, W. Guangzhi, Z. Minglei, Implantable biomedical materials for treatment of bone infection, *Front Bioeng Biotechnol* 11 (2023), 1081446. <https://doi.org/10.3389/fbioe.2023.1081446>.
- [13] J. Li, R.M.Y. Wong, Y.L. Chung, S.S.Y. Leung, K.-H. Chow, M. Ip, W.-H. Cheung, R. Man, Y. Wong, Fracture-related infection in osteoporotic bone causes more severe infection and further delays healing, *Bone Joint Res.* 11 (2022) 49–60. <https://doi.org/10.1302/2046-3758.112.BJR>.
- [14] M. Croes, B.C.H. van der Wal, H.C. Vogely, Impact of bacterial infections on osteogenesis: Evidence from in vivo studies, *J. Orthop. Res.* 37 (2019) 2067–2076. <https://doi.org/10.1002/jor.24422>.
- [15] A.M. Taylor, M.F. Hsueh, L.R. Ranganath, J.A. Gallagher, J.P. Dillon, J.L. Huebner, J.B. Catterall, V.B. Kraus, Cartilage biomarkers in the osteoarthropathy of alkaptonuria reveal low

turnover and accelerated ageing, *Rheumatology (Oxford)* 56 (2017) 156–164.
<https://doi.org/10.1093/rheumatology/kew355>.

[16] A.S. Davison, A.T. Hughes, A.M. Milan, N. Sireau, J.A. Gallagher, L.R. Ranganath, Alkaptonuria – Many questions answered, further challenges beckon, *Ann. Clin. Biochem.* 57 (2020) 106–120. <https://doi.org/10.1177/0004563219879957>.

[17] Y. Chow, B.P. Norman, N.B. Roberts, L.R. Ranganath, C. Teutloff, R. Bittl, M.J. Duer, J.A. Gallagher, H. Oschkinat, Pigmentation chemistry and radical-based collagen degradation in alkaptonuria and osteoarthritic cartilage, *Angew. Chem. Int. Ed. Engl.* 29 (2020) 11937–11942. <https://doi.org/10.1002/anie.202000618>.

[18] N.B. Roberts, S.A. Curtis, A.M. Milan, L.R. Ranganath, The pigment in alkaptonuria relationship to melanin and other coloured substances: A review of metabolism, composition and chemical analysis, *JIMD Rep* 24 (2015) 51–66. https://doi.org/10.1007/8904_2015_453.

[19] M.M. Nadzir, R.W. Nurhayati, F.N. Idris, M.H. Nguyen, Biomedical applications of bacterial exopolysaccharides: A review, *Polymers (Basel)* 13 (2021) 1–25. <https://doi.org/10.3390/polym13040530>.

[20] N. Farshidfar, S. Iravani, R.S. Varma, Alginate-based biomaterials in tissue engineering and regenerative medicine, *Mar. Drugs.* 21 (2023), 189. <https://doi.org/10.3390/md21030189>.

[21] F. Lorquin, P. Piccerelle, C. Orneto, M. Robin, J. Lorquin, New insights and advances on pyomelanin production: From microbial synthesis to applications, *J. Ind. Microbiol. Biotechnol.* 49 (2022), kuac013. <https://doi.org/10.1093/jimb/kuac013>.

[22] P. Behzadi, Z. Baráth, M. Gajdács, It's not easy being green: A narrative review on the microbiology, virulence and therapeutic prospects of multidrug-resistant *Pseudomonas aeruginosa*, *Antibiotics* 10 (2021), 42. <https://doi.org/10.3390/antibiotics>.

1
2
3
4
5
6
7
8
9
[23] M.M. Urbaniak, M. Gazińska, K. Rudnicka, P. Płociński, M. Nowak, M. Chmiela, In vitro and in vivo biocompatibility of natural and synthetic *Pseudomonas aeruginosa* pyomelanin for potential biomedical applications, *Int. J. Mol. Sci.* 24 (2023), 7846. <https://doi.org/10.3390/ijms24097846>.

10
11
12
13
14
15
16
17
18
19
20
[24] F. Lorquin, F. Ziarelli, A. Amouric, C. Di Giorgio, M. Robin, P. Piccerelle, J. Lorquin, Production and properties of non-cytotoxic pyomelanin by laccase and comparison to bacterial and synthetic pigments, *Sci. Rep.* 11 (2021), 8538. <https://doi.org/10.1038/s41598-021-87328-2>.

21
22
23
24
25
26
27
[25] S. Roy, J.W. Rhim, New insight into melanin for food packaging and biotechnology applications, *Crit. Rev. Food Sci. Nutr.* 62 (2022) 4629–4655. <https://doi.org/10.1080/10408398.2021.1878097>.

28
29
30
31
32
33
34
35
36
37
38
[26] M.M. Urbaniak, K. Rudnicka, G. Gościński, M. Chmiela, Can pyomelanin produced by *Pseudomonas aeruginosa* promote the regeneration of gastric epithelial cells and enhance *Helicobacter pylori* phagocytosis?, *Int. J. Mol. Sci.* 24 (2023), 13911. <https://doi.org/10.3390/ijms241813911>.

39
40
41
42
43
44
45
46
[27] A.S. ElObeid, A. Kamal-Eldin, M.A.K. Abdelhalim, A.M. Haseeb, Pharmacological properties of melanin and its function in health, *Basic Clin. Pharmacol. Toxicol.* 120 (2017) 515–522. <https://doi.org/10.1111/bcpt.12748>.

47
48
49
50
51
52
[28] D. Liu, Z. Zhong, M. Karin, NF- κ B: A double-edged sword controlling inflammation, *Biomedicines* 10 (2022), 1250. <https://doi.org/10.3390/biomedicines10061250>.

53
54
55
56
57
58
59
60
61
62
63
64
65
[29] A. Kurzyk, A. Szwed-Georgiou, J. Pagacz, A. Antosik, P. Tymowicz-Grzyb, A. Gerle, P. Szturner, M. Włodarczyk, P. Płociński, M.M. Urbaniak, K. Rudnicka, M. Biernat, Calcination and ion substitution improve physicochemical and biological properties of nanohydroxyapatite

for bone tissue engineering applications, *Sci. Rep.* 13 (2023), 15384.

<https://doi.org/10.1038/s41598-023-42271-2>.

[30] E. Mnich, M. Kowalewicz-Kulbat, P. Sicinska, K. Hinc, M. Obuchowski, A. Gajewski, A.P. Moran, M. Chmiela, Impact of *Helicobacter pylori* on the healing process of the gastric barrier, *World J. Gastroenterol.* 22 (2016) 7536–7558. <https://doi.org/10.3748/wjg.v22.i33.7536>.

[31] P. Piszko, M. Włodarczyk, S. Zielińska, M. Gazińska, P. Płociński, K. Rudnicka, A. Szwed, A. Krupa, M. Grzymajło, A. Sobczak-Kupiec, D. Słota, M. Kobielarz, M. Wojtków, K. Szustakiewicz, PGS/HAp microporous composite scaffold obtained in the TIPS-TCL-SL method: An innovation for bone tissue engineering, *Int. J. Mol. Sci.* 22 (2021), 8587. <https://doi.org/10.3390/ijms22168587>.

[32] M. Kawka, R. Płocińska, P. Płociński, J. Pawełczyk, M. Słomka, J. Gatkowska, K. Dzitko, B. Dziadek, J. Dziadek, The functional response of human monocyte-derived macrophages to serum amyloid A and *Mycobacterium tuberculosis* infection, *Front. Immunol.* 14 (2023), 1238132. <https://doi.org/10.3389/fimmu.2023.1238132>.

[33] A. Dobin, C.A. Davis, F. Schlesinger, J. Drenkow, C. Zaleski, S. Jha, P. Batut, M. Chaisson, T.R. Gingeras, STAR: ultrafast universal RNA-seq aligner. *Bioinformatics* (29) 2013, 15–21. <https://doi.org/10.1093/bioinformatics/bts635>.

[34] D. Powell, Degust: interactive RNA-seq analysis. Available at <http://degust.erc.monash.edu>.

[35] M.E. Sandberg, D. Schellmann, G. Brunhofer, T. Erker, I. Busygin, R. Leino, P.M. Vuorela, A. Fallarero, Pros and cons of using resazurin staining for quantification of viable *Staphylococcus aureus* biofilms in a screening assay, *J. Microbiol. Methods* 78 (2009) 104–106. <https://doi.org/10.1016/j.mimet.2009.04.014>.

1
2 [36] European Committee on Antimicrobial Susceptibility Testing. Breakpoint Tables for
3 Interpretation of MICs and Zone Diameters, European Committee on Antimicrobial
4 Susceptibility Testing, 2023, Växjö, Sweden.
5
6

7 [37] D. Słota, K. Piętak, W. Florkiewicz, J. Jampilek, A. Tomala, M.M. Urbaniak, A.
8 Tomaszewska, K. Rudnicka, A. Sobczak-Kupiec, Clindamycin-loaded nanosized calcium
9 phosphates powders as a carrier of active substances, *Nanomaterials* 13 (2023), 1469.
10 <https://doi.org/10.3390/nano13091469>.
11
12
13
14
15
16

17 [38] S. Xijin Ge, D. Jung, R. Yao, ShinyGO: a graphical enrichment tool for animals and
18 plants, *Bioinformatics* 8 (2020), 2628–2629. [https://doi.org/10.1093/bioinformatics/
19 btz931/5688742](https://doi.org/10.1093/bioinformatics/btz931/5688742).
20
21
22
23
24
25

26 [39] M.J.F. Blumer, Bone tissue and histological and molecular events during development
27 of the long bones. *Ann. Anat.* 235 (2021), 151704. <https://doi.org/10.1016/j.aanat.2021.151704>.
28
29
30

31 [40] A.D. Berendsen, B.R. Olsen, Bone development, *Bone* 80 (2015) 14–18.
32 <https://doi.org/10.1016/j.bone.2015.04.035>.
33
34
35
36

37 [41] A.M. Wu, C. Bisignano, S.L. James, G.G. Abady, A. Abedi, E. Abu-Gharbieh, R.K.
38 Alhassan, V. Alipour, J. Arabloo, M. Asaad, W.N. Asmare, A.F. Awedew, M. Banach, S.K.
39 Banerjee, A. Bijani, T.T.M. Birhanu, S.R. Bolla, L.A. Cámara, J.C. Chang, D.Y. Cho, M.T.
40 Chung, R.A.S. Couto, X. Dai, L. Dandona, R. Dandona, F. Farzadfar, I. Filip, F. Fischer, A.A.
41 Fomenkov, T.K. Gill, B. Gupta, J.A. Haagsma, A. Haj-Mirzaian, S. Hamidi, S.I. Hay, I.M. Ilic,
42 M.D. Ilic, R.Q. Ivers, M. Jürisson, R. Kalhor, T. Kanchan, T. Kavetsky, R. Khalilov, E.A.
43 Khan, M. Khan, C.J. Kneib, V. Krishnamoorthy, G.A. Kumar, N. Kumar, R. Laloo, S. Lasrado,
44 S.S. Lim, Z. Liu, A. Manafi, N. Manafi, R.G. Menezes, T.J. Meretoja, B. Miazgowski, T.R.
45 Miller, Y. Mohammad, A. Mohammadian-Hafshejani, A.H. Mokdad, C.J.L. Murray, M. Naderi,
46 M.D. Naimzada, V.C. Nayak, C.T. Nguyen, R. Nikbakhsh, A.T. Olagunju, N. Otstavnov, S.S.
47
48
49
50
51
52
53
54
55
56
57
58
59
60
61
62
63
64
65

1
2
3
4
5
6
7
8
9
10
11
12
13
14
15
16
17
18
19
20
21
22
23
24
25
26
27
28
29
30
31
32
33
34
35
36
37
38
39
40
41
42
43
44
45
46
47
48
49
50
51
52
53
54
55
56
57
58
59
60
61
62
63
64
65

Otstavnov, J.R. Padubidri, J. Pereira, H.Q. Pham, M. Pinheiro, S. Polinder, H. Pourchamani, N. Rabiee, A. Radfar, M.H.U. Rahman, D.L. Rawaf, S. Rawaf, M.R. Saeb, A.M. Samy, L. Sanchez Riera, D.C. Schwebel, S. Shahabi, M.A. Shaikh, A. Soheili, R. Tabarés-Seisdedos, M.R. Tovani-Palone, B.X. Tran, R.S. Travillian, P.R. Valdez, T.J. Vasankari, D.Z. Velazquez, N. Venketasubramanian, G.T. Vu, Z.J. Zhang, T. Vos, Global, regional, and national burden of bone fractures in 204 countries and territories, 1990–2019: A systematic analysis from the Global Burden of Disease Study 2019, *Lancet Healthy Longev.* 2 (2021) 580–e592. [https://doi.org/10.1016/S2666-7568\(21\)00172-0](https://doi.org/10.1016/S2666-7568(21)00172-0).

[42] A.R. Kemmak, A. Rezapour, R. Jahangiri, S. Nikjoo, H. Farabi, S. Soleimanpour, Economic burden of osteoporosis in the world: A systematic review, *Med. J. Islam. Repub. Iran.* 34 (2020) 1–8. <https://doi.org/10.34171/mjiri.34.154>.

[43] A. Szwed-Georgiou, P. Płociński, B. Kupikowska-Stobba, M.M. Urbaniak, P. Rusek-Wala, K. Szustakiewicz, P. Piszko, A. Krupa, M. Biernat, M. Gazińska, M. Kasprzak, K. Nawrotek, N.P. Mira, K. Rudnicka, Bioactive materials for bone regeneration: Biomolecules and delivery systems, *ACS Biomater. Sci. Eng.* 9 (2023) 5222–5254. <https://doi.org/10.1021/acsbiomaterials.3c00609>.

[44] D. Weycker, X. Li, R. Barron, R. Bornheimer, D. Chandler, Hospitalizations for osteoporosis-related fractures: Economic costs and clinical outcomes, *Bone. Rep.* 5 (2016) 186–191. <https://doi.org/10.1016/j.bonr.2016.07.005>.

[45] A.R. Ferraz, R. Pacheco, P.D. Vaz, C.S. Pintado, L. Ascensão, M.L. Serralheiro, Melanin: Production from cheese bacteria, chemical characterization, and biological activities, *Int. J. Environ. Res. Public Health* 18 (2021), 10562. <https://doi.org/10.3390/ijerph182010562>.

- 1
2
3
4
5
6
7
8
9
10
11
12
13
14
15
16
17
18
19
20
21
22
23
24
25
26
27
28
29
30
31
32
33
34
35
36
37
38
39
40
41
42
43
44
45
46
47
48
49
50
51
52
53
54
55
56
57
58
59
60
61
62
63
64
65
- [46] N.K. Kurian, S.G. Bhat, Data on the characterization of non-cytotoxic pyomelanin produced by marine *Pseudomonas stutzeri* BTCZ10 with cosmetological importance, *Data Brief* 18 (2018) 1889–1894. <https://doi.org/10.1016/j.dib.2018.04.123>.
- [47] D.S. Amarasekara, S. Kim, J. Rho, Regulation of osteoblast differentiation by cytokine networks, *Int. J. Mol. Sci.* 22 (2021) 1–16. <https://doi.org/10.3390/ijms22062851>.
- [48] R.L. Jilka, R.S. Weinstein, T. Bellido, P. Roberson, A.M. Parfitt, S.C. Manolagas, Increased bone formation by prevention of osteoblast apoptosis with parathyroid hormone. *J. Clin. Investig.* 104 (1999) 439–446. <https://doi.org/10.1172/JCI6610>.
- [49] R. Ren, J. Guo, Y. Chen, Y. Zhang, L. Chen, W. Xiong, The role of Ca²⁺/calcineurin/NFAT signalling pathway in osteoblastogenesis, *Cell. Prolif.* 54 (2021), 13122. <https://doi.org/10.1111/cpr.13122>.
- [50] M. Zayzafoon, Calcium/calmodulin signaling controls osteoblast growth and differentiation, *J. Cell Biochem.* 97 (2006) 56–70. <https://doi.org/10.1002/jcb.20675>.
- [51] S. Gao, B. Chen, Z. Zhu, C. Du, J. Zou, Y. Yang, W. Huang, J. Liao, PI3K-Akt signaling regulates BMP2-induced osteogenic differentiation of mesenchymal stem cells (MSCs): A transcriptomic landscape analysis, *Stem. Cell. Res.* 66 (2023), 103010. <https://doi.org/10.1016/j.scr.2022.103010>.
- [52] S. Vimalraj, Alkaline phosphatase: Structure, expression and its function in bone mineralization, *Gene* 754 (2020), 144855. <https://doi.org/10.1016/j.gene.2020.144855>.
- [53] B. Le-Vinh, Z.B. Akkuş-Dağdeviren, N.M.N. Le, I. Nazir, A. Bernkop-Schnürch, Alkaline phosphatase: A reliable endogenous partner for drug delivery and diagnostics, *Adv. Ther.* 5 (2022), 2100219. <https://doi.org/10.1002/adtp.202100219>.

- 1
2
3
4
5
6
7
8
9
10
11
12
13
14
15
16
17
18
19
20
21
22
23
24
25
26
27
28
29
30
31
32
33
34
35
36
37
38
39
40
41
42
43
44
45
46
47
48
49
50
51
52
53
54
55
56
57
58
59
60
61
62
63
64
65
- [54] S.C. Moser, B.C.J. van der Eerden, Osteocalcin — A versatile bone-derived hormone, *Front. Endocrinol.* 10 (2019), . <https://doi.org/10.3389/fendo.2018.00794>.
- [55] M.L. Zoch, T.L. Clemens, R.C. Riddle, New insights into the biology of osteocalcin, *Bone* 82 (2016) 42–49. <https://doi.org/10.1016/j.bone.2015.05.046>.
- [56] R.L. Jilka, R.S. Weinstein, T. Bellido, A.M. Parfitt, S.C. Manolagas, Osteoblast programmed cell death (apoptosis): Modulation by growth factors and cytokines, *J. Bone Miner. Res.* 13 (1998) 793-802. <https://doi.org/10.1359/jbmr.1998.13.5.793>.
- [57] F. Blanchard, L. Duplomb, M. Baud'huin, B. Brounais, The dual role of IL-6-type cytokines on bone remodeling and bone tumors, *Cytokine Growth Factor Rev.* 20 (2009) 19–28. <https://doi.org/10.1016/j.cytogfr.2008.11.004>.
- [58] S. Itoh, N. Udagawa, N. Takahashi, F. Yoshitake, H. Narita, S. Ebisu, K. Ishihara, A critical role for interleukin-6 family-mediated Stat3 activation in osteoblast differentiation and bone formation, *Bone* 39 (2006) 505–512. <https://doi.org/10.1016/j.bone.2006.02.074>.
- [59] F. Yoshitake, S. Itoh, H. Narita, K. Ishihara, S. Ebisu, Interleukin-6 directly inhibits osteoclast differentiation by suppressing receptor activator of NF-κB signaling pathways, *J. Biol. Chem.* 283 (2008) 11535–11540. <https://doi.org/10.1074/jbc.M607999200>.
- [60] E. Chen, G. Liu, X. Zhou, W. Zhang, C. Wang, D. Hu, D. Xue, Z. Pan, Concentration-dependent, dual roles of IL-10 in the osteogenesis of human BMSCs via P38/MAPK and NF-κB signaling pathways, *FASEB Journal* 32 (2018) 4917–4929. <https://doi.org/10.1096/fj.201701256RRR>.
- [61] D. Liu, S. Yao, G.E. Wise, Effect of Interleukin-10 on gene expression of osteoclastogenic regulatory molecules in the rat dental follicle. *Eur. J. Oral Sci* 114 (2006) 42–49. <https://doi.org/10.1111/j.1600-0722.2006.00283.x>.

- 1
2
3
4
5
6
7
8
9
10
11
12
13
14
15
16
17
18
19
20
21
22
23
24
25
26
27
28
29
30
31
32
33
34
35
36
37
38
39
40
41
42
43
44
45
46
47
48
49
50
51
52
53
54
55
56
57
58
59
60
61
62
63
64
65
- [62] L.X. Xin, T. Kukita, A. Kukita, T. Otsuka, Yosh. Niho, T. Iijima, .; Iijima, T. Interleukin-10 selectively inhibits osteoclastogenesis by inhibiting differentiation of osteoclast progenitors into preosteoclast-like cells in rat bone marrow culture system. *J. Cell. Physiol.* 165 (1995) 624–629, <https://doi.org/10.1002/jcp.1041650321>.
- [63] K. Lee, I. Seo, M.H. Choi, D. Jeong, Roles of mitogen-activated protein kinases in osteoclast biology, *Int. J. Mol. Sci.* 19 (2018), 3004. <https://doi.org/10.3390/ijms19103004>.
- [64] R. Dresner-Pollak, N. Gelb, D. Rachmilewitz, F. Karmeli, M. Weinreb, Interleukin 10-deficient mice develop osteopenia, decreased bone formation, and mechanical fragility of long bones, *Gastroenterology* 127 (2004) 792–801. <https://doi.org/10.1053/j.gastro.2004.06.013>.
- [65] M. Claudino, T.P. Garlet, C.R.B. Cardoso, G.F. De Assis, R. Taga, F.Q. Cunha, J.S. Silva, G.P. Garlet, Down-regulation of expression of osteoblast and osteocyte markers in periodontal tissues associated with the spontaneous alveolar bone loss of interleukin-10 knockout mice, *Eur. J. Oral Sci.* 118 (2010) 19-28. <https://doi.org/10.1111/j.1600-0722.2009.00706.x>.
- [66] K. Kobayashi, N. Takahashi, E. Jimi, N. Udagawa, M. Takami, S. Kotake, N. Nakagawa, M. Kinosaki, K. Yamaguchi, N. Shima, H. Yasuda, T. Morinaga, K. Higashio, T.J. Martin, T. Suda, tumor necrosis factor stimulates osteoclast differentiation by a mechanism independent of the ODF/RANKL-RANK interaction, *J. Exp. Med.* 191 (2000) 275-286. <https://doi.org/10.1084/jem.191.2.275>.
- [67] B. Osta, G. Benedetti, P. Miossec, Classical and paradoxical effects of TNF- α on bone homeostasis, *Front. Immunol.* 5 (2014). <https://doi.org/10.3389/fimmu.2014.00048>.
- [68] H. Kitaura, A. Marahleh, F. Ohori, T. Noguchi, Y. Nara, A. Pramusita, R. Kinjo, J. Ma, K. Kanou, I. Mizoguchi, Role of the interaction of tumor necrosis factor- α and tumor necrosis

1 factor receptors 1 and 2 in bone-related cells, *Int. J. Mol. Sci.* 23 (2022), 1481.
2 <https://doi.org/10.3390/ijms23031481>.
3
4

5 [69] E. Marcello, M. Maqbool, R. Nigmatullin, M. Cresswell, P.R. Jackson, P. Basnett, J.C.
6 Knowles, A.R. Boccaccini, I. Roy, Antibacterial composite materials based on the combination
7 of polyhydroxyalkanoates with selenium and strontium co-substituted hydroxyapatite for bone
8 regeneration, *Front. Bioeng. Biotechnol.* 9 (2021). <https://doi.org/10.3389/fbioe.2021.647007>.
9
10
11
12
13

14 [70] A. Zerrad, J. Anissi, J. Ghanam, K. Sendide, M. El Hassouni, Antioxidant and
15 antimicrobial activities of melanin produced by a *Pseudomonas balearica* strain, *Journal of*
16 *Biotechnology Letters* 5 (2014) 87-94.
17
18
19
20
21

22 [71] C. Xu, J. Li, L. Yang, F. Shi, L. Yang, M. Ye, Antibacterial activity and a membrane
23 damage mechanism of *Lachnum YM30* melanin against *Vibrio parahaemolyticus* and
24 *Staphylococcus aureus*, *Food Control* 73 (2017) 1445–1451.
25 <https://doi.org/10.1016/j.foodcont.2016.10.048>.
26
27
28
29
30
31

32 [72] N.E.A. El-Naggar, W.I.A. Saber, Natural melanin: Current trends, and future
33 approaches, with especial reference to microbial source, *Polymers* 14 (2022), 1339.
34 <https://doi.org/10.3390/polym14071339>.
35
36
37
38
39
40
41
42
43
44
45
46
47
48
49
50
51
52
53
54
55
56
57
58
59
60
61
62
63
64
65

Department of Immunology and Infectious Biology
Faculty of Biology and Environmental Protection
University of Lodz
Banacha 12/16, 90-237 Lodz
Poland

Editorial Board

International Journal of Biological Macromolecules

January 19, 2024

It is our pleasure to submit the manuscript entitled “Exploring the Osteoinductive Potential of Bacterial Pyomelanin Derived from *Pseudomonas aeruginosa* On Human Osteoblasts Model” by Mateusz M. Urbaniak, Karolina Rudnicka, Przemysław Płociński and Magdalena Chmiela with kind request for the review and evaluation of its suitability to the scope of the *International Journal of Biological Macromolecules*.

In this manuscript, we present novel approach to support osteoinductive processes and increasing ossification and osteoinduction (eg. during bone regeneration) by recreating the mechanisms accompanying alkaptonuria, including the local accumulation of homogentisic polymers, using pyomelanin – a bacterial biomimetic of ochronotic deposits previously characterized by our group. To our best knowledge, this is the first report demonstrating a comprehensive *in vitro* study on the osteoinductive, antiapoptotic and pro-regenerative activity of bacterial pyomelanin isolated from *Pseudomonas aeruginosa* toward human osteoblasts.

We believe that this manuscript fits the profile of *International Journal of Biological Macromolecules* as it presents a comprehensive biological evaluation of polymeric pyomelanin to promote osteoinduction of human osteoblasts, limit apoptosis, and reduce the risk of staphylococcal infections for future biomedical applications in bone tissue engineering and regenerative medicine.

We confirm that this manuscript has not been published elsewhere and is not under consideration by another journal. All authors have approved the manuscript and agree with its submission to *International Journal of Biological Macromolecules*. The authors have no conflicts of interest to declare.

Sincerely,

On behalf of the Authors,

Mateusz M. Urbaniak

Department of Immunology and Infectious Biology, Faculty of Biology and Environmental Protection,
University of Lodz, Lodz, Poland

Department of Immunology and Infectious Biology
Faculty of Biology and Environmental Protection
University of Lodz
Banacha 12/16, 90-237 Lodz
Poland

Exploring the Osteoinductive Potential of Bacterial Pyomelanin Derived from *Pseudomonas aeruginosa* On Human Osteoblasts Model

Mateusz M. Urbaniak, Karolina Rudnicka, Przemysław Płociński, Magdalena Chmiela

ABSTRACT

Alkaptonuria (AKU) is a rare autosomal metabolic disorder resulting from a deficiency in tyrosine metabolism. In AKU, the deposition of homogentisic acid polymers contributes to the pathological ossification of cartilage tissue. The controlled use of biomimetics similar to deposits observed in cartilage may result in the development of an effective therapy that increases the mineralization and maturation of osteoblasts necessary for the regeneration of damaged bone tissue. One of the potential biomimetic candidates is pyomelanin (PyoM) - a polymeric biomacromolecule synthesized by *Pseudomonas aeruginosa*. This work presents comprehensive data on the osteoinductive, pro-regenerative and antibacterial properties, as well as the cytocompatibility of water-soluble (PyoM_{sol}) or water-insoluble (PyoM_{insol}) PyoM. Both variants of PyoM support osteoinductive processes as well as the maturation of osteoblasts due to the upregulation of osteocalcin (OC), alkaline phosphatase (ALP), interleukin (IL)-6, IL-10 and tumour necrosis factor (TNF)- α production. PyoM are cytocompatible in a wide concentration range and limit doxorubicin-induced apoptosis towards osteoblasts. This cytoprotective PyoM activity is correlated with pro-regenerative properties expressed as osteoblasts migration. Moreover, PyoM_{sol} and PyoM_{insol} exhibit antibacterial activity against staphylococci isolated from infected bones. The omnidirectional osteoinductive, pro-regenerative and antiapoptotic effects achieved through the PyoM stimulation of osteoblasts create new opportunities for designing biocomposites modified with this bacterial-origin biopolymer with tailored properties, offering novel prospects for various biological and medical applications.

On behalf of the Authors,

Mateusz M. Urbaniak

Department of Immunology and Infectious Biology, Faculty of Biology and Environmental Protection,
University of Lodz, Lodz, Poland

Declaration of interests

The authors declare that they have no known competing financial interests or personal relationships that could have appeared to influence the work reported in this paper.

The authors declare the following financial interests/personal relationships which may be considered as potential competing interests:

Karolina Rudnicka reports financial support was provided by Foundation for Polish Science. If there are other authors, they declare that they have no known competing financial interests or personal relationships that could have appeared to influence the work reported in this paper.



Click here to access/download
Supplementary Material
Supplementary Table.xlsx

Bioactive Materials for Bone Regeneration: Biomolecules and Delivery Systems

Aleksandra Szwed-Georgiou, Przemysław Płociński, Barbara Kupikowska-Stobba, Mateusz M. Urbaniak, Paulina Rusek-Wala, Konrad Szustakiewicz, Paweł Piszko, Agnieszka Krupa, Monika Biernat, Małgorzata Gazińska, Mirosław Kasprzak, Katarzyna Nawrotek, Nuno Pereira Mira, and Karolina Rudnicka*



Cite This: <https://doi.org/10.1021/acsbomaterials.3c00609>



Read Online

ACCESS |

Metrics & More

Article Recommendations

ABSTRACT: Novel tissue regeneration strategies are constantly being developed worldwide. Research on bone regeneration is noteworthy, as many promising new approaches have been documented with novel strategies currently under investigation. Innovative biomaterials that allow the coordinated and well-controlled repair of bone fractures and bone loss are being designed to reduce the need for autologous or allogeneic bone grafts eventually. The current engineering technologies permit the construction of synthetic, complex, biomimetic biomaterials with properties nearly as good as those of natural bone with good biocompatibility. To ensure that all these requirements meet, bioactive molecules are coupled to structural scaffolding constituents to form a final product with the desired physical, chemical, and biological properties. Bioactive molecules that have been used to promote bone regeneration include protein growth factors, peptides, amino acids, hormones, lipids, and flavonoids. Various strategies have been adapted to investigate the coupling of bioactive molecules with scaffolding materials to sustain activity and allow controlled release. The current manuscript is a thorough survey of the strategies that have been exploited for the delivery of biomolecules for bone regeneration purposes, from choosing the bioactive molecule to selecting the optimal strategy to synthesize the scaffold and assessing the advantages and disadvantages of various delivery strategies.

KEYWORDS: bioactive materials, biomolecules, biomolecule delivery systems, bone healing, bone regeneration, biomaterials, composites, scaffolds



INTRODUCTION

Advanced strategies for the regeneration of various tissue defects continue to emerge in plastic and reconstructive medicine and in dentistry. Millions of individuals suffer from bone loss each year; and although bone tissue naturally possesses high regeneration potential, its capacity to repair itself can be limited by secondary factors such as the extent of bone loss, the age and sex of the individual, and comorbidities. Bone defects typically resulting from extensive trauma, tumors, infections, inflammation, or degenerative disorders can be healed with advanced treatments.

The need for hard tissue regeneration biomaterials has substantially increased as the world's population ages. Bone fractures, defects, and nonunions are a global healthcare problem. Moreover, fragility fractures, typically occurring in osteoporosis, located in wrists, hips, and vertebrae, can often be debilitating, put patients at an increased risk for a subsequent fracture, and can even be fatal among older

adults.¹ Worldwide, women over 50 years old have a 9.8–22.8% risk of fragility fractures.² The Bone Health and Osteoporosis Foundation estimates that 3 million fractures and \$25.3 billion in direct healthcare costs will arise annually by 2025. The total cost of care associated with osteoporotic fractures and nonunion fractions will reach \$95 billion in 2040.³

The gold standard—allografts—is impeded by potential infection, limited availability, and a high nonunion rate with host tissues. Biomaterials that mimic bone tissue are becoming

Received: May 8, 2023

Accepted: July 31, 2023

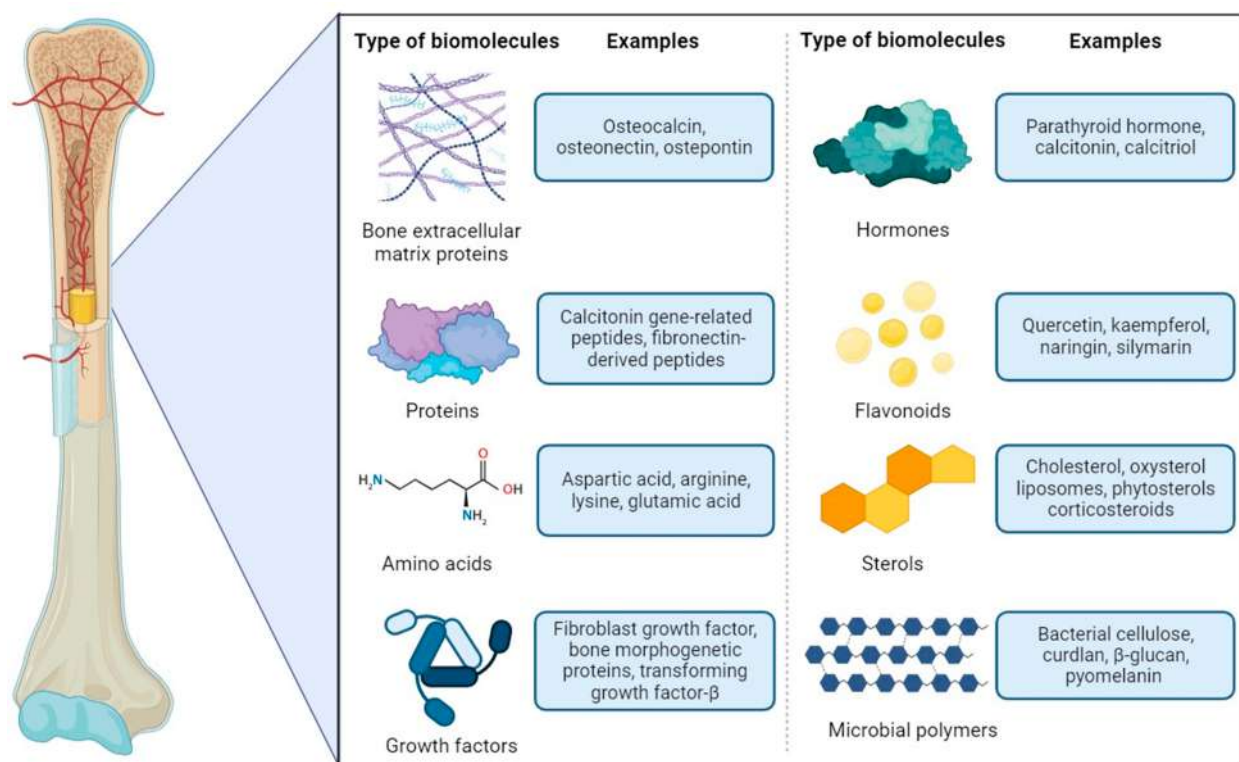


Figure 1. Types and examples of biomolecules used to support the regeneration of bone tissue.

critical components of reconstructive approaches for cases where autogenous bone grafts are not obtainable. There are currently a large variety of bone matrices that can be used to treat bone loss. Among them, there are materials delivering natural or synthetic materials that are compatible with regenerative medicine. New matrices are being developed each year, and these are commonly coupled with growth factors (GFs) and other bone growth stimulants and infused with antibiotics to lower the risk of infection. On the other hand, the World Health Organization identifies antibiotic resistance as one of the biggest threats to global health, and their overuse in prophylaxis for bone should be limited.⁴ The search for composites with optimal biocompatibility and osteointegrative, osteoconductive, and osteoinductive properties is ongoing. Expectedly, such new generation of biomaterials must also allow the efficient recruitment of mesenchymal stem cells (MSCs) that will colonize the scaffold and differentiate into bone tissue with the desired shape, form, and durability.

This paper reviews recent developments in using biomaterials and constructs for hard tissue repair and regeneration (Figure 1). The multidisciplinary group of chemists, material engineers, molecular biologists, biotechnologists, and microbiologists worked together to explore recent advances *in vitro* and *in vivo* research on the efficiency of bioactive molecules, their delivery platforms, and methods to produce polymeric materials. The first section of this review concentrates on bioactive components that support biocompatibility and bone regeneration using bone extracellular matrix (ECM), hormones, plant-derived flavonoids and sterols, peptides, amino acids, and microbial polymers. In the second section, we explore selected methods and pathways to produce materials and scaffolds, including polymers, inorganic fillers, and solvent-free techniques. Finally, we present the delivery methods that

ensure the activity of the biomolecules, e.g., obtained by surface functionalization, controlled and stimuli-driven delivery, and gene-delivery systems. The last sections discuss recent advances, highlighting challenges and possible solutions in the design and application of biomaterials in bone tissue engineering.

■ BIOMOLECULES USED FOR BONE REGENERATION

Bone Extracellular Matrix (ECM) Proteins. Bone tissue mainly comprises cells mounted in a biomineral matrix.⁵ The extracellular matrix (ECM) is a complex and constantly changing biological environment with specific mechanical and biochemical properties. The ECM plays a crucial role in regulating cell adhesion, proliferation, responses to growth factors, and differentiation, ultimately affecting the mature bone's functional characteristics. Osteoblast-lineage cells, including MSCs, osteoblasts, and osteocytes, can produce new bone when stimulated by the bone ECM, whereas osteoclasts can absorb bone.⁶ The structure of bone's biomineral scaffold consists of around 70% of inorganic calcium hydroxyapatite (HA) crystals— $\text{Ca}_{10}(\text{PO}_4)_6(\text{OH})_2$. The remaining 30% comprises organic elements, with collagens being the predominant proteinaceous components followed by noncollagenous proteins (NCPs), lipids, proteoglycan molecules, and other bone matrix proteins.⁷ Bone ECM proteins are vital factors in bone tissue's mechanical strength and adhesive characteristics of bone tissue.⁸ Moreover, ECM mineralization is an essential and critical step in bone repair and reconstruction. Matrix mineralization, and the synthesis and secretion of type I collagen and NCPs by osteoblasts, are hallmarks of bone formation. The scaffold frame formed by the deposition of collagen fibers constitutes the structural basis of bone mineralization, whereas NCPs are involved in HA

Table 1. *In Vitro* and *In Vivo* Studies That Have Reported the Osteogenic Effects of Bioactive Peptides in Bone Regeneration^{3,4}

Bioactive peptide [Reference(s)]	Composition [number of amino acids]	Binding site/potential pathway(s)	ECM-Derived Peptides	Genes or proteins up-/downregulated by peptide	Function
PepGen P-15 (P-15) [385–388]	15	Type I collagen binding sites	Upregulated: ALP, BMP-2, BMP-7; Runx2, COL1, OSTRX BSP, and integrin $\alpha 2$	Promoted: extracellular matrix production; proliferation and osteogenic differentiation; cell attachment, migration, and survival	
Arginine-glycine-aspartic acid (RGD) [389–392]	3	Integrin binding sites	Upregulated: ALP, RUNX2, osteocalcin, osteopontin, BSP, Sox9, Aggrecan, fibronectin, and collagen II	Promoted: Proliferation, mineralization, and osteogenic differentiation; cell attachment and survival	
Ser-Val-Tyr-Gly-Leu-Arg (SVVYGLR) [393–395]	7	RGD binding sites	Upregulated: integrin $\alpha v \beta 3$	Promoted: proliferation and neovascularization; angiogenesis and osteogenesis; adhesion, migration; tube formation of endothelial cells	
Glycine-phenylalanine-hydroxyproline-arginine (GEOGER) [396–399]	4	integrin $\alpha 2 \beta 1$ binding sites	Suppressed: NFAT, osteoclastogenesis-related mRNAs Upregulated: integrin $\alpha 2 \beta 1$ binding	Promoted: differentiation, bone regeneration, and osseointegration	
Collagen binding motif (CBM) [400, 401]	28	Collagen binding sites	Induced sustained activation of ERK; induced trans-activation of SRE, CRE, and AP-1; induced expression of type X collagen	Promoted: bone-related cell adhesion and growth; osteogenic differentiation	
Fibronectin-derived peptides (FN-derived peptides) [402–404]	7	–	–	Promoted: bone-related cell spreading; adhesion and mineralization	
BMP-Derived Peptides					
P17-BMP-2 [405]	17	–	–	Promoted: bone repair; osteoblast differentiation and bone regeneration	
P20-BMP-2 and P24-BMP-2 [406]	20 and 24, respectively	–	Upregulated: OCN, Runx2, and collagen I	Promoted: osteogenesis and differentiation of MSCs into osteoblasts	
BMP-7-derived peptide BFP-1 [407]	15	–	Upregulated: expression of CD44, CD47 and CD51	Enhanced: Ca ²⁺ content in cells; ALP activity; bone regeneration	
Other Peptides					
Calcitonin gene-related peptides (CGRPs) [61, 408–410]	37	Pathways: cAMP, Wnt, and AMPK-eNOS	Upregulated: expression of IGF-1, IGF-1 receptor and BMP-2 receptor; ALP, OC, and COLLA1	Promoted: cell proliferation, osteogenic differentiation, and angiogenesis Downregulated: apoptosis and inflammation	
Parathyroid hormone (1-34) (PTH 1-34) [411, 412]	34	Pathways: G(q)-signaling, b-arrestin recruitment, ERK 1/2 phosphorylation and phospholipase C	Upregulated: expression of Runx2 and COL2A1	Promoted: cell proliferation and chondrogenesis	
Osteogenic growth peptides (OGPs) [413–415]	14	Pathways: G1 protein-MAPK and RhoA/ROCK	Downregulated: expression of ALP and BMP-2 Upregulated: osteocalcin, collagen, BMP-2, ALP and mineralization TGF $\beta 1$, TGF $\beta 2$, TGF $\beta 3$, FGF-2, IGF-1	Promoted: cell proliferation and osteogenic differentiation; cartilage-to-bone transition	
Thrombin peptide 508 (TP508) [389, 416]	23	Pathways: JAK/STAT, NF- κ B, PDGF, PI3K/AKT, PTEN, and ERK/MAPK; cell cycle-G1/S checkpoint	Upregulated: expression of Runx2 and OPN	Downregulated: adipogenic differentiation Promoted: cell proliferation and osteogenic differentiation; chemotaxis, angiogenesis and revascularization	
NEMO-binding domain peptide (NBD) [417, 418]	6	Pathway: NF- κ B	Downregulated: TRAP activity, actin rings; RANKL-induced c- <i>Src</i> kinase activity	Downregulated: apoptosis, the effect of hypoxia Promoted: osteogenic differentiation of cells	
Cell-penetrating peptide (CPP) [419, 420]	30	–	–	Downregulated: bone resorption Transcription factor delivery of bone regeneration-related proteins or factors into cells	
AcN-RADARADARAD-ARADA-CONH ₂ (RADAI6-I 16) [421]	16	–	Upregulated: expression of Runx2 genes, ALP, and osteocalcin	Transcription factor delivery of bone-regeneration-related proteins or factors into cells	

deposition. The ECM also plays a critical role in regulating cell adhesion, movement, and migration.⁹

As said above, collagens are the main structural proteins present in the ECM of bone tissue, constituting over 20% of bone mass and up to 90% of bone's organic matrix.¹⁰ Type I collagen is the main collagen type implicated in bone mineralization; however, small quantities of type V collagen bound to HA crystals typically found in bone tissue. Collagen type III alongside with type V are thought to influence fibrillogenesis and fiber diameter of type I collagen. Collagen matrix organization is critical to maintain the optimal mechanical properties of the bone, and abnormalities in collagens hierarchical structures are associated with serious conditions, including osteogenesis imperfecta and Paget's disease.¹¹ Collagens, especially type I, are often used in bone replacement composites to improve their structural and functional properties.

Osteocalcin (OC) is among the most abundant NCPs in the bone matrix. OC is a relatively small matrix protein dependent on vitamins D and K. Each OC molecule contains three γ -carboxyglutamic acid molecules with a strong affinity for Ca^{2+} . The γ -carboxyglutamic acid moieties are responsible for the high affinity of OC for HA.^{12,13} Mature osteoblasts produce the 49 amino acids long OC protein, which is directly involved in the regulation of bone density. Moreover, OC promotes bone mineralization and formation and attracts osteoclast progenitors.^{14,15} OC is believed to influence the early stages of bone healing and regulate the activity of osteoblasts and hydroxyapatite binding.^{16–18} Previous studies demonstrated that OC could successfully enhance the adhesion of osteoblast-like cells on the surface of HA/collagen I containing materials *in vitro*.¹⁹ A study by Rammelt et al.²⁰ noted the significantly faster replacement of woven bone by lamellar bone when HA/collagen I implants were enriched with OC compared to unmodified implants. This result indicates that OC accelerates *de novo* bone formation rather than increasing the formation of new bone.²⁰

Another important NCP that can be used to tune the bone regeneration process is osteonectin, also known as secreted protein, acidic and rich in cysteine (SPARC) or BM-40.^{21,22} Osteonectin has a high affinity for collagen I and HA.²³ Like OC, osteonectin is involved in bone matrix mineralization.²⁴ It is also a modular protein that regulates cell behavior and can influence tissue remodeling, repair, development, and cell turnover.²⁵ A study by Zhu et al.²⁶ provided evidence that osteonectin regulates the mineralization process in osteoblasts and is a crucial component of the p38 signaling pathway. Osteonectin can also modulate bone density. Thus, it holds tremendous potential as a point for bone reconstruction and regeneration interventions.²⁶

Osteopontin (OPN) is another ECM NCP that can be used in the bone regeneration process. OPN is a member of the small integrin-binding ligand family N-glycosylated proteins, along with bone sialoprotein (BSP), dentin matrix protein 1, and matrix extracellular phosphoprotein. OPN mediates the attachment of bone cells to the mineral crystal structure and regulates bone resorption and calcification. Moreover, OPN is active in biological processes, such as wound healing, immunological reactions, tumorigenesis, atherosclerosis, and angiogenesis.²⁷ McKee, Pedraza, and Kaartinen²⁸ suggested that OPN may have an essential role in bone regeneration processes after surgical cutting when bone debris (powder) is cleared by macrophage phagocytosis after OPN opsonization

and a cement line (plane) is formed at the margins of the wound that integrates the newly repaired bone with the existing drilled bone.²⁸ Furthermore, other studies have shown that the so-called “glue” effect of some NCPs (OPN, OC, osteonectin) plays a significant role in promoting the integration of collagen fibrils and apatites.^{7,29}

Sun et al.³⁰ indicated that NCPs could be extracted from bone ECM and successfully coupled to the surfaces of nanofibrous (NF) gelatin scaffolds. *In vitro* studies revealed that NF-gelatin-NCP scaffolds promoted the osteoblasts' proliferation, differentiation, and mineralization. Importantly, *in vivo* calvarial bone defect experiments demonstrated that the scaffolds containing NCPs could recruit more host cells to the defect and regenerate more bone than the control scaffolds at 6 weeks postimplantation. Thus, integrating NCPs into scaffolds is a promising strategy for improving the bone regeneration process.³⁰

Other important protein components of ECM include positive (e.g., Periostin) and negative (matrix Gla protein, bone Gla protein) regulators of bone formation, mineralization, and remodeling (thrombospondins and R-spondins);⁶ however, their potential application in functionalization of bone replacement scaffolds has yet to be fully investigated.

Peptides. Bone tissue engineering (BTE) and research on peptides have expanded significantly in recent years. The outcomes of these extensive studies have shown that several peptides can support and stimulate the bone healing response.³¹ The practical advantage of using peptides over proteins is that they can be produced with precise control of their chemical structures. Moreover, compared to proteins, peptides are also more resistant to denaturation caused by temperature or pH variations than proteins and are easier to manipulate during grafting. Bioactive peptides that can promote the regeneration of local bone defects can be mainly divided into ECM-derived peptides, and bone morphogenetic protein (BMP)-derived peptides.³²

The most-studied ECM-derived peptides contain signaling domains, as they can connect to receptors on the surface of the cell membrane.³³ Selected examples of ECM-derived peptides that have been used in bone repair and regeneration studies are shown in Table 1.

Another group, the BMP-derived peptides (BMPs), are mostly GFs, which are responsible for inducing the formation of bone or cartilage.³⁴ BMPs that promote the bone healing response are mainly derived from BMP-2, BMP-7, and BMP-9. Studies have shown that BMP-derived peptides induce the osteogenic differentiation of hMSCs and bone regeneration. Moreover, BFP-1 enhanced the Ca 2p content in cells and induced their alkaline phosphatase (ALP) activity.³⁵ Selected examples of BMP-derived peptides that have been used for bone repair and regeneration studies are shown in Table 1.

In addition to ECM- and BMP-derived peptides, other peptides like calcitonin gene-related peptide (CGRP), parathyroid hormone, osteogenic growth peptides, or cell-penetrating peptides have also been studied concerning their potential to induce bone regeneration (Table 1).³⁴

Traditional bone graft can be substituted with injectable self-healing hydrogel loaded with peptides: osteogenic KP and angiogenic QK, which were designed from BMP2 and VEGF, respectively, to improve osteogenic differentiation and vascularization. Both peptides: KP and QK seemed to act synergistically by promoting bone formation in rat calvaria.³⁶

Although biomaterials support healing processes, their modification with peptide sequences can improve antimicrobial, proangiogenic, and immunomodulatory properties. New peptides with biofunctional activities are being discovered.³⁷ Thus, various scientific groups^{38–41} employed genomics to identify new short peptides, indicating their immunomodulatory properties toward keratinocytes, periodontal ligament cells, or endothelial cells in the context of regeneration, cytokine secretion, cell apoptosis, or viability. Also, peptides are frequently incorporated into biomaterials to improve the repairing of cardiovascular tissue.³⁷

Amino Acids. Amino acids are the building blocks of proteins. Polar and charged amino acids (AAs) are abundant in NCPs and involved in bone HA mineralization. The acidic domains of NCPs (e.g., OPN, bone sialoprotein, dentin matrix protein 1, and dentin phosphophoryn) are rich in negatively charged AAs, such as aspartic acid (Asp), glutamic acid (Glu), and phosphoserine (PSer). Such negatively charged AAs play a critical role in controlling HA nucleation and growth, and they also take part in bone and dentine HA mineralization. Positively charged AAs, such as arginine (Arg) and lysine (Lys), are involved in HA nucleation within ECM proteins such as collagen.^{42,43} Moreover, Arg and Lys may accelerate the process of bone fracture healing by improving collagen synthesis and local blood supply and supplementing GFs. In addition, Glu, Arg, and Lys boost bone mineral density (BMD) by stimulating growth hormone (GH) production.⁴⁴

Since amino acids containing amino groups can be used as aminolysis agents for biomaterials, three amino acids such as Ser, Gly, and Lys can be used to modify PLLA by surface modification to obtain nanofiber scaffolds. As shown by Zhang et al.,⁴⁵ a modification of PLLA nanofiber scaffolds with Ser, Gly, and Lys helped to improve the hydrophilic properties of such biomaterials, as well as to lower the pressure resistance of modified scaffolds.

GFs. The role of GFs has been widely recognized in the bone repair process. GFs are released by cells in the inflamed area. Those polypeptides regulate the events that occur during wound healing.^{46,47} The term growth factors refers to a class of polypeptide hormones that stimulate a wide range of cellular events, such as cell proliferation, chemotaxis differentiation, and ECM protein production. GFs can act locally and systematically to stimulate cell growth and function in several ways. Their activity is mainly regulated by binding to ECM receptors. Tissue repair animal model studies have provided evidence that GFs, such as epidermal growth factor (EGF), transforming growth factor (TGF)- α , TGF- β , platelet-derived growth factor, and fibroblast growth factor (FGF), are the key agents involved in the wound healing process. More importantly, studies have shown that a lack of any of these mediators at the injured site hampers the healing process. Thus, exogenous GFs are considered potent supplements in wound healing, serving as the foundation for upcoming regenerative therapies.⁴⁸

One of the families of growth factors that have been well-studied in bone regeneration is the family of BMPs. These proteins belong to the TGF- β superfamily and have been extensively studied in preclinical and clinical investigations of bone regeneration, including bone defects and spinal fusion. BMPs have been shown to be closely related to the processes of bone formation and regeneration.⁴⁹ In the human genome, 20 genes encode functional BMPs.⁵⁰ Bone regeneration is, in part, a recapitulation of embryonic development. Key steps

during bone morphogenesis are progenitors/stem cell chemotaxis and their proliferation and differentiation. The mechanism of action of BMPs involves signaling in all of these steps (chemotaxis, proliferation, and differentiation of osteoprogenitor cells) and, thus, the induction of bone formation by these cells. Thus, recombinant BMPs 2 and 7 have been approved by the Food and Drug Administration (FDA) for spine fusion, fracture healing, and oral surgery.^{34,49}

FGF2, or basic FGF (bFGF), is the most common FGF used in regenerative medicine, including bone regeneration,⁵¹ and its levels are increased in acute wounds. FGF2 plays a role in granulation tissue formation, re-epithelialization, and tissue remodeling. It may also regulate the synthesis and deposition of various ECM components, increase keratinocyte mobility during re-epithelialization, promote fibroblast migration, and stimulate collagenase production.⁵² In addition, FGF2 was shown to promote angiogenesis.⁵³

One of the most essential parts of the fracture healing/bone regeneration process is the state of the local vasculature. Thus, VEGF substantially stimulates local vascular regeneration in the fracture area. It has been shown that VEGF can increase MSC chemotaxis and stimulate osteoblast differentiation and proliferation. Therefore, VEGF plays a crucial role in new bone formation. *In vitro* studies have reported that VEGF stimulates the growth of vascular endothelial cells, which are the basic units of arteries, veins, and lymphatic systems. Notably, angiogenesis plays a critical role in endochondral ossification and, thus, the transformation of avascular cartilage tissue into vascular bone tissue. VEGF is released during this process by hypertrophic chondrocytes and causes the ingrowth of metaphyseal blood vessels through cartilage tissue and the formation of new bone.⁵⁴

Chen and Wu et al.⁵⁵ showed that applying stromal-derived factor-1 α (SDF-1 α) and TGF- β 1 to damaged cartilage can promote the migration and chondrogenic differentiation of MSCs. SDF-1 α is a chemokine and the ligand of C-X-C chemokine receptor type 4 (CXCR-4) that induces stem cell recruitment and migration. TGF- β 1 is a critical regulator of the chondrogenic differentiation of MSCs. Studies have reported that combining SDF-1 α and TGF- β 1 has a synergistic effect on enhancing *in vitro* chondrogenic potential and *in vivo* cartilage regeneration.⁵⁵

Hormones (Cofactors). The proper functioning of the endocrine system sustains skeleton development. Hormones are signaling molecules that act distal to their production site (the endocrine effect). They also regulate the synthesis and action of local factors, which directly affect cellular metabolism (autocrine and paracrine effects). Among the most critical hormones in bone formation-related processes are thyroid hormones, parathyroid hormone (PTH), calcitonin, calcitriol, androgens, estrogens, progesterone, insulin, glucocorticoids, and GH;¹³ and among these, the most important are GH and calcitropic hormones (PTH, calcitonin, and metabolites of vitamin D).

Thyroid hormones have opposite effects on bone. They stimulate the synthesis and mineralization of the osteoid matrix by osteoblasts and stimulate resorption by increasing the number and function of osteoclasts. The clinical outcome of the latter effect is bone loss in hyperthyroidism.⁵⁶

Calcium homeostasis is controlled by PTH through its direct actions on the bone and the kidneys and indirect actions on the intestine.⁵⁷ PTH is a signaling molecule shown to have the potential to enhance bone regeneration in significant bone

defects. The potential of PTH lies in its anabolic effect on bone. The FDA has approved a treatment for osteoporosis that encompasses daily injections of PTH, which increases BMD and bone volume. Therefore, PTH may promote bone regeneration and be an alternative to autografts and BMPs to treat large segmental defects and nonunions.⁵⁸ In a human case study documenting treatment with internal fixation, external fixation, and autograft combined with BMP-7 administration, the nonunion persisted unless the patient was supplemented with PTH 1-84.⁵⁹

Calcitonin is an inhibitor of bone resorption that reduces the number and activity of osteoclasts. Nonetheless, calcitonin appears to have only a transient effect, as osteoclasts seem to become nonresponsive to calcitonin within a few days.⁶⁰ *In vivo* studies have shown that CGRP also plays a role in bone development, metabolism, and repair. CGRP is a 37 residue peptide generated in specific neurons by alternative splicing of the calcitonin gene. *In vitro* studies have demonstrated that CGRP may stimulate osteoblast proliferation, differentiation, and maturation in osteoblast cell lines and bone marrow MSCs.⁶¹

Calcitriol is a steroid hormone that promotes bone mineralization. It increases the intestinal absorption of calcium and phosphate; thus, its activity is beneficial for the growth of the skeleton.^{60,62}

Sex hormones can also affect bone in numerous ways. Among others, androgens have an anabolic effect on bone by stimulating osteoblast receptors. Androgen deficiency has been associated with lower BMD, and testosterone administration to younger individuals was found to increase overall bone mass. Consistent with these findings, women with excess androgens also have higher bone densities than women with low/average levels of these hormones. Estrogens have a dual effect on bone metabolism. They favor bone formation by increasing the number and improving the function of osteoblasts; however, they also reduce resorption. Studies have shown that estrogens can increase the level of osteoprotegerin (OPG), which inhibits resorption. Thus, estrogens may play an essential role in the regulation of osteoclastogenesis. Moreover, progesterone has an anabolic effect on bone tissue. This effect may be direct, through the osteoblasts that possess hormone receptors, or indirect, through competition for the osteoblastic receptors of glucocorticoids.^{60,63} Scientific evidence has shown that high doses of glucocorticoids may have a catabolic effect on bone. This effect may be due to the inhibition of insulin-like growth factor (IGF-I) synthesis by osteoblasts and direct suppression of BMP-2 and Cbfa1, critical factors in osteoblastogenesis. In contrast, it has been demonstrated that glucocorticoids have an osteogenic capacity at physiological doses that promotes osteoblastic differentiation.⁶⁴

Another hormone that might be involved in the bone regeneration process is insulin. It has been proposed that insulin could stimulate osteoblast differentiation, which would enhance the production of OC, and subsequently, OC may be able to stimulate pancreatic β cell proliferation and skeletal muscle insulin sensitivity. It is still uncertain whether insulin stimulates bone directly or indirectly by increasing muscle work and, therefore, skeletal loading.^{65,66}

Flavonoids. New strategies are constantly being developed to promote the natural healing of bone lesions or regeneration. Medicinal plants are essential sources of compounds such as phytochemicals, vitamins, and other nutrients, and such compounds derived from plants may enhance bone healing.

Phytochemicals, especially flavonoids, may improve bone health due to their antioxidant and anti-inflammatory properties. Moreover, due to their inhibition of osteoclast cells and increased proliferation of osteoblasts, these compounds might help prevent bone loss and reduce inflammatory processes without producing the undesirable side effects of allopathic drugs.⁶⁷

Flavonoids can be divided into various classes based on their chemical structure.⁶⁸ Recent reports have shown that the flavonols quercetin and kaempferol can reduce bone resorption *in vitro* by directly targeting mature osteoclasts via the estrogen receptor (ER). Quercetin has anti-inflammatory properties and has been found to inhibit the proliferation of human adipose tissue-derived stromal cells and promote their differentiation into osteoblasts. Thus, quercetin can promote osteoblast differentiation and inhibit osteoclastogenesis, so it might be considered a potential drug for bone diseases and regeneration.⁶⁹

In traditional Chinese medicine, another flavonoid, naringin, is commonly used to treat osteoporosis and bone disorders. Studies have shown that naringin may promote the proliferation of bone marrow stromal cells (BMSCs), enhance the levels of BMPs, and increase the expression of bone markers (ALP, OCN, and OPN). It has also been demonstrated that naringin can abolish osteoclastogenesis and bone resorption by inhibiting RANKL-induced NF- κ B and ERK activation.^{70–74}

Hesperidin, whose effect on bone metabolism has been studied in rats, has been shown to improve femoral strength in adult rats and the total metaphyseal and diaphyseal BMD at the femur in young rats. However, poncirin (a flavanone glycoside) enhances the gene expression of the osteogenic transcription factor Runx2 and a transcriptional coactivator with a PDZ-binding motif (TAZ) and upregulates the expression of bone markers such as ALP and OCN in C3H10T1/2 cells. Hesperidin also promotes bone mineral deposition in BMSCs.⁶⁹

Silymarin (Smn) is another active polyphenolic flavonoid that has been used primarily due to its antioxidant and anti-inflammatory properties. By regulating the bone formation, Smn has been shown to be effective in treating bone fractures and osteoporosis. In *in vitro* and *in vivo* models, Smn directly affected cell adhesion, proliferation, and matrix secretion and the expression of osteogenic markers such as Col I, OCN, and Runx2. Notably, an enhanced regenerative process that provides more significant bone matrix deposition and tissue organization has been observed in *in vivo* models testing the activity of Smn.⁷³

Plant Sterols. It has been suggested that phytosterols may affect osteoblast proliferation and differentiation. *Cissus quadrangularis* (*Vitaceae* family, plant kingdom) is a plant species indigenous to southern Asia and Africa that has been widely studied in bone regeneration research.⁷⁴ *Cissus quadrangularis* extract (CQE) contains steroids that are considered positive stimulants of osteoblasts and bone growth and is used as a composite modification designed for bone healing. To date, alginate *O*-carboxymethyl chitosan (O-CMC) or poly(ϵ -caprolactone) PCL/HA composites have been modified with CQE to study their effect on osteoblasts. Composites with CQE cause a significant increase in peptide absorption; peptides are absorbed by the composite due to the electrostatic interactions between the protein and composite surface. Cellular research indicates that these biomaterials

enhance cell attachment to the composite surface and cell spreading throughout the composite. Cell proliferation increased significantly after only 72 h of stimulation, but it was suggested that CQE further enhances cell proliferation as the contact time increases. ALP, a marker of osteoblast differentiation, was significantly increased compared to that in the unmodified composite, and the effect grew over time. Moreover, the increase in ALP over time correlates with the significant increase in biomineralization by osteoblasts in the presence of a composite containing CQE compared to an unmodified composite (hydroxyapatite was detected by chemical analysis).^{75–77} However, the mechanism of CQE has yet to be determined, and more research is needed.

Seaweeds are marine plants that are widely present in Asian diets. Seaweeds have been studied for several years due to their bioactivity and potential use as pharmaceutical agents. One compound found in seaweed that has been studied is fucosterol, which is thought to affect bone regeneration.⁷⁸ Studies have investigated the use of fucosterol in osteoblast cell culture and ovariectomized female rats (an animal model of osteoporosis). Interestingly, the obtained results indicated that fucosterol increased ALP activity, mineralization, and bone density and significantly increased bone cell proliferation. On the other hand, it was suggested that fucosterol might decrease osteoclast differentiation and affect bone resorption, maintaining bone homeostasis, which is the balance between bone mineralization and resorption. Fucosterol can also enhance the production of OC and the reduction in CTx. Moreover, the effect of fucosterol was compared to that of estradiol, which has been presented as a postmenopausal osteoporosis therapy factor, and in many cases, fucosterol was superior.^{79,80}

Studies have shown that phytohormones may play a role in bone regeneration. β -Ecdysterone is a steroid hormone found in plants such as *Achyranthe bidentata*. β -Ecdysterone-mediated stimulation of osteoblasts results in significantly increased ALP levels and OPN activity. Moreover, β -ecdysterone may enhance mineralization and bone tissue formation *in vitro*. Gene sequencing analysis showed that genes involved in the BMP pathway were upregulated by β -ecdysterone. *In vivo* studies on the effect of β -ecdysterone on bone regeneration were performed using rat femurs. Four and eight weeks after bone defect initiation and β -ecdysterone injection, micro-CT imaging showed changes in the bone that were typical of healing; moreover, the bone density had significantly increased. Finally, a significant increase in the level of BMP-2 expression was detected, and this result was confirmed by an immunohistochemistry assay.⁸¹

Oxysterols. Oxysterols are small, cholesterol-derived molecules naturally occurring in human and animal tissues and blood circulation that have been reported to be osteoinductive factors.⁸²

20S-Hydroxycholesterol and 22S-hydroxycholesterol are compounds formed during the oxidation of cholesterol. Studies indicate that these compounds may affect the differentiation of osteogenic cells both *in vitro* and *in vivo*.⁸³ In the context of alveolar bone regeneration, oxysterols were shown *in vitro* and *in vivo* to significantly enhance ALP activity, mineralization, and calcium ion levels needed for proper regeneration. Oxysterols also promote increased osteogenic gene and protein (OCN or Runx2) expression. In addition, oxysterols stimulate an increase in Hedgehog pathway activation in which proteins such as Smo (a Hh receptor) or Gli1 (a transcription factor) are involved. *In vivo* studies performed on rats showed

progressive bone formation 10 and 15 days after extraction using micro-CT imaging and histological analysis; however, immunohistochemical analysis showed increased expression of ALP and OCN. In these studies, the promotion by oxysterols was at a level comparable to that of BMP-2.⁸⁴ The above-mentioned studies align with the *in vitro* research performed by Kwon, Lee, Hwang, and Heo.⁸⁵ Additionally, Aghaloo et al.⁸⁶ performed *in vivo* studies on rats with poly(lactic-co-glycolic acid) (PLGA) scaffolds coated with oxysterols, and Johnson et al.⁸⁷ performed studies on rats with collagen sponges containing various types of oxysterols (Oxy34 and Oxy49). All of the above-mentioned studies indicated that treatment prompted increased factors involved in bone regeneration.

Oxy49 is an oxysterol examined as a potential factor that can promote bone regeneration. *In vivo* studies performed using a rabbit cranial bone defect model and a collagen sponge containing Oxy49 showed increased expression of the osteogenesis markers COL1, OSX, OPN, and OCN. Additionally, the activity of ALP, the level of OC, and the mineralization process significantly increased. Finally, micro-CT analysis showed precise bone regeneration and density intensification after a collagen sponge containing Oxy49 was implanted into the cranium.⁸²

Oxysterols are still being examined as relatively new compounds in bone regeneration. In addition to 20S-hydroxycholesterol, 22S-hydroxycholesterol, Oxy34, and Oxy49, studies on oxysterols have also included Oxy4, Oxy18, and Oxy21, and all of these compounds may successfully promote osteogenesis. Notably, the potential of oxysterols is comparable to or even better than that of BMP-2.⁸⁸

Liposomes. Liposomes are lipid-based biocompatible vesicles widely used in therapies for bone healing to deliver drugs/bioactive particles and act as stimuli-responsive factors. Scaffolds containing liposomes have been proven to enhance bone regeneration. They help with the delivered molecule's solubilization, bioactive stabilization, or bioavailability. Liposomes combined with factors that promote bone healing enhance osteogenesis. Liposomes can deliver oxysterols, and the combination of these two factors enhances osteoregenerative processes both *in vitro* and *in vivo*.⁸⁹ Recently, novel liposomal nanocarriers, stereosomes, were developed and examined as agents to improve molecular stability. Lee et al.⁹⁰ produced and studied stereosomes containing 20S-hydroxycholesterol and purmorphamine coated on PLGA and polydiacetylene (PDA) layers that can activate bone regeneration by enhancing the Hedgehog signaling pathway, which is crucial for effective osteogenesis. Applying this stereosome resulted in a synergistic increase in ALP activity and level of mineralization in cells. Moreover, the studied biomolecules caused significant increases in the expression levels of genes involved in osteogenesis (ALP, Runx2, OCN, OPN, Col1, and Gli1). *In vivo* research performed on mice confirmed the cell study results, and micro-CT and histological analysis showed an increase in bone regeneration and mineralization in stereosome-treated animals compared to that in controls. Immunohistochemical analysis indicated enhanced expression of the osteogenic markers Runx2 and OCN. Research by Lee and colleagues⁹⁰ is in-line with that of Cui et al.⁸³ on stereosomes containing 20S-hydroxycholesterol and sterylamine.

Liposomes were formerly studied as effective agents to deliver the bone morphogenetic protein BMP-2 gene to the bone fracture site, which resulted in enhanced bone

regeneration.⁹¹ Currently, liposomes are successfully being used both as individual carriers of biomolecules and as additions to scaffolds.⁹²

Statins. Statins are well-known drugs used to lower LDL cholesterol levels and prevent the development of atherosclerosis. Almost 20 years ago, it was reported that hypercholesterolemic patients undergoing statin therapy had a reduced risk of bone fracture. Researchers have thus started investigating how BMD and turnover change after statin therapy and how statins may affect bone regeneration. Montagnani et al.⁹³ examined 30 women suffering from postmenopausal hypercholesterolemia. The studied group was treated with simvastatin daily for 1 year. During that time, the group did not receive any treatment that would affect bone metabolism (calcitonin, calcium, and vitamin D). Blood samples were collected every 3 months, and serum calcium, phosphate, and ALP levels were measured. Moreover, bone resorption and mineral density were assessed. The obtained results indicated that the treated patients had significant increases in total and bone ALP levels over time and BMD in the lumbar spine and femoral neck. In the same year, Ayukawa, Okamura, and Koyano⁹⁴ performed a study on rats in which titanium implants were installed in the tibiae, and a daily dose of simvastatin was given. The bone contact ratio and bone density measurements showed significant increases in the experimental group compared to that in the control group, which was not treated with simvastatin. Histological analysis showed newly formed bone and abundant bone trabeculae in the treated animals. Wong and Rabie⁹⁵ investigated whether adding statins accelerates osteogenesis in rabbits. After implantation of a collagen sponge combined with simvastatin into the calvarial fracture, the expression levels of VEGF, BMP-2, and Cbfa1 were enhanced and resulted in earlier osteoinduction and neovascularization. Wong and Rabie⁹⁶ also performed histological analysis to identify new bone formation that occurred 5 days after implantation of a simvastatin-modified collagen sponge.

Importantly, simvastatin is not the only statin compound studied in the context of bone regeneration. Moriyama et al.⁹⁷ investigated whether local fluvastatin application promotes osteogenesis after PLGA implantation into rat tibiae. Tibias were used for histological analysis 1, 2, and 4 weeks after implantation, indicating a significant amount of osteoid bone and increased mineralization. Masuzaki et al.⁹⁸ showed by histological analysis that, after fluvastatin-modified PLGA microsphere implantation into rat tibiae, bone formation was amplified, and the bone implant contact significantly increased. Additionally, the level of OCN, a bone metabolism marker, was significantly higher 2 and 4 weeks after implantation. Research by Rakhmatia, Ayukawa, Furuhashi, and Koyano⁹⁹ aligns with previous studies. Rats implanted with fluvastatin-modified carbonate apatite showed enhanced bone formation and bone volume by micro-CT analysis. Moreover, histological analysis confirmed these results and indicated significant intensification of bone mineralization.

In addition, *in vitro* research indicated that statins regulate the OPG/RANKL/RANK pathway. Statins can inhibit bone resorption, ROS generation, or osteoclastogenesis. Additionally, statins may affect osteogenesis promoters, such as BMP-2, TGF- β , or ALP. Statin-stimulated cells exhibited increased expression of the osteogenic genes Runx2 and OCN and the osteogenic proteins Runx2, OCN, and OPN.¹⁰⁰

Microbial Biopolymers. Bacteria and microscopic fungi produce natural polymers as part of their intrinsic physiology to create a mechanical protective layer that surrounds their cells. These polymers store molecules necessary for proper metabolism functions and create a biofilm that protects their cells from the harmful effects of the environment. Microorganisms can synthesize various types of biopolymers with different monomer compositions, molecular weights, 3D configurations, and cross-linking arrangements that can be tailored for specific applications in BTE.¹⁰¹ Microbial polymers are synthesized from enzymatic reactions that link monomers, such as sugars, amino acids, or hydroxy fatty acids, to create high molecular weight molecules. Microorganisms can produce various classes of biopolymers with potential biomedical applications, such as polysaccharides, polyamides, polyesters, and polyphosphates.¹⁰²

Bacterial cellulose (BC) is a linear homopolysaccharide biopolymer produced by many Gram-negative bacterial genera, such as *Komagataeibacter* (formerly *Gluconacetobacter*), *Agrobacterium*, *Acetobacter*, *Burkholderia*, *Erwinia*, *Pseudomonas*, and *Rhizobium*.^{103,104} BC is synthesized from glucose in the periplasmic space of bacterial cells by cellulose synthase, and its chemical structure is composed of β -D-glucopyranose units linked by β -1,4 glycosidic bonds. The biocompatibility, biodegradability, high crystallinity, porosity, and tensile strength with mechanical robustness make BC an interesting biopolymer that can be used in designing modern biomaterials for the targeted regeneration of bone tissue.¹⁰³

Bassi et al.¹⁰⁵ showed that intracranial implantation of a BC membrane led to bone neoformation and vascularization at the defect site and confirmed the activity of key ossification markers such as OC and OPN 60 days after biomaterial implantation.¹⁰⁵ BC is used by itself and in combination with other bioactive factors in designing biomaterials for bone regeneration. Hydrogels made from BC modified with gold nanoparticles significantly increased the activity of ALP, OC, and OPN in cell culture models and led to the formation of apatite deposits. In contrast, in a rabbit model, these hydrogels showed that new bone tissue with high mineral density had been formed.¹⁰⁶ Similar conclusions were drawn by Kheiry et al.,¹⁰⁷ who showed that modifying BC with fisetin contributes to the increase in ALP activity and the concentrations of OC and OPN in mesenchymal cells subjected to osteogenic differentiation.¹⁰⁷ Nanocomposites of BC modified with hydroxyapatite (HA), the main inorganic compound responsible for the mechanical properties of bones, promoted the proliferation and maturation of mesenchymal cells into osteocyte precursors and effectively contributed to the neoformation of bone tissue after implantation.¹⁰⁸ Unmodified BC does not have antibacterial properties; however, its porosity and good ability to biofunctionalize with molecules such as antibiotics, silver nanoparticles, lysozyme, or cationic surfactants can be used to design biomaterials that reduce the risk of postimplantation infections.^{109,110}

Another example of microbially produced polymers with potential for use in bone regeneration are β -glucans. β -Glucans are heterogeneous groups of polysaccharide polymers composed of D-glucose monomers linked by (1 \rightarrow 3), (1 \rightarrow 4), or (1 \rightarrow 6) glycosidic bonds. The cell walls of grains, bacteria, fungi, and yeast are a natural source of this biopolymer. The most well-known β -glucans synthesized by microbes are the linear (1 \rightarrow 3) and branched (1 \rightarrow 3; 1 \rightarrow 6) β -glucans found in *Saccharomyces cerevisiae*. The physiochem-

ical and biological properties of β -glucans strongly depend on the source, extraction method, polymer chain length, and extent of purification.^{111,112}

One of the fundamental problems in achieving an appropriate level of osseointegration with an implant is the excessive bone resorptive activity of osteoclasts. There is substantial scientific evidence to conclude that polycan, a β -glucan derived from *Aureobasidium pullulans*, reduces the number of active osteoclasts and inhibits the secretion of pro-osteolytic cytokines such as interleukin-1 β (IL-1 β) and tumor necrosis factor- α (TNF- α). β -Glucan, which is part of the *S. cerevisiae* cell wall, contributed to the downregulation of receptor activator for nuclear factor κ B ligand (RANKL) and the upregulation of OPG, which resulted in the inhibition of bone loss in a mouse model.¹¹³ The suppressive activity of β -glucan derived from baker's yeast against RANKL has also been demonstrated by Hara et al.¹¹⁴ Stimulation of mouse bone marrow cells with *S. cerevisiae* β -glucan inhibited differentiation from maturing osteoclasts by downregulating the nuclear factor of activated T cells 1 (NFATC1), which was caused by the suppression of NF- κ B signaling and *c-fos* expression.¹¹⁴ β -Glucan can not only inhibit osteoclast activity but also be used as a polymer when designing biocomposites modified with a ceramic phase. Biocomposites composed of (1 \rightarrow 3) β -glucan and HA meet important physicochemical requirements, such as the ability to undergo thermal sterilization without damaging the polymer structure, good porosity, flexibility, and self-adaption to the defect shape.¹¹⁵ Modifying such composites by adding HA-containing carbonate ions (CHA) increased the solubility and decreased the crystallinity of the ceramic phase, as well as intensified the attachment, proliferation, and differentiation of osteoblasts. In rabbit models, 6 months after implantation, the CHA/ β -glucan composite contributed to the increased formation of new cortical bone and intensified mineralization at the implantation site.¹¹⁶

An example of a linear bacterial (1 \rightarrow 3) β -glucan that has aroused interest in the design of new biocomposites for targeted bone tissue regeneration is Curdlan, which is produced by *Alcaligenes faecalis*.¹¹⁷ Curdlan limited osteoclast differentiation by suppressing NFATC1 activation via downregulation of the Syk kinase signaling pathway, which is responsible for osteoclast differentiation, maturation, and bone lytic activity.^{113,118} Curdlan can be modified to make highly elastic and biocompatible hydrogels or biocomposites. Curdlan/whey protein isolate/hydroxyapatite biomaterials showed a high cytocompatibility level and promoted OC production in an in vitro model of human osteoblasts.¹¹⁹ The addition of Curdlan to a chitosan/HA scaffold improved the porosity, water uptake capability, and biocompatibility of the composite and enhanced human osteoblast survival and proliferation on the scaffold, which are crucial to start the implant osseointegration process.¹²⁰ Toullec et al.¹²¹ reported that Curdlan–chitosan scaffolds were not cytotoxic and improved cell migration on the surface of the biocomposite; however, further studies are required to demonstrate the positive effect of this biomaterial on bone tissue regeneration.¹²¹

Bacterial exopolysaccharides (BEPSs), such as gellan and alginate, are classified as high molecular weight carbohydrate polymers and are secreted by cells into the external environment. BEPSs perform various physiological functions and can be adapted to the needs of regenerative medicine due

to their unusual physicochemical properties.¹²² Gellan isolated from *Sphingomonas paucimobilis* was incorporated into a composite in the form of a gum, and the addition of HA increased the adhesion of human adipose-derived stem cells to the surface.¹²³ Alginate secreted by *Pseudomonas aeruginosa* is being studied for use in bone tissue regenerative medicine as a carrier of GFs. The delivery of BMP-2 and BMP-7 using an alginate biomaterial enhanced the differentiation of bone marrow-derived stem cells to osteoblasts, and codelivering the BMP-2 and VEGF released from the alginate gels improved the reconstruction of bone defects.¹²⁴

Another interesting biopolymer produced by *P. aeruginosa* is pyomelanin, a black–brown pigment formed by the oxidative polymerization of homogentisic acid.¹²⁵ The use of melanin polymers, such as pyomelanin, seems to be an economical and affordable way to improve the physicochemical and osteoinductive properties of newly designed biocomposites.¹²⁶ Important premises indicating the need to investigate the role of pyomelanin as a modulator of bone tissue regeneration processes are the studies of Yoo et al.,¹²⁷ who showed that melanin isolated from *Gallus gallus domesticus* promoted the *in vitro* proliferation and differentiation of osteoblastic MG-63 cells through BMP-2 signaling and inhibited osteoclast formation.¹²⁷

■ METHODS TO PREPARE POLYMERIC MATERIALS AND SCAFFOLDS FOR BTE

The structure of human bone is complex and capable of bearing mechanical loads and resisting deformation.¹²⁸ Bone is also involved in multiple vital processes, including maintaining homeostasis and regulating blood pH.¹²⁹ Taking into consideration the complexity of bone structure, materials suitable for BTE should be capable of bearing mechanical loads, biocompatible, osteoconductive (allowing cells to move along the scaffold and slowly produce new bone),¹³⁰ osteogenic (stimulating bone growth),¹³⁰ and osteoinductive (stimulating stem cells to differentiate toward osteoblasts).¹³⁰ A novel biomimetic approach to designing a biodegradable scaffold that propagates osteoconductivity for bone and cartilage tissue applications includes replicating the ECM¹³¹ and providing suitable conditions for tissue regeneration.

There is a diverse range of materials that are applicable for BTE. These materials include polymeric materials, bioceramics, and preferably tailored composite materials that meet the requirements for the above-mentioned properties. Currently, several methods are known for producing polymer scaffolds, polymer–ceramic scaffolds, and multicomponent materials used in BTE. Methods of producing materials for BTE can be divided into two main groups: those obtained by solvent techniques and those obtained by techniques involving plasticization of the polymer material. This paper considers the most important and popular techniques for manufacturing three-dimensional scaffolds with potential applications in BTE, emphasizing polymer and composite scaffolds.

Polymers, Inorganic Fillers, and Composites. Polymeric materials are promising structural materials for scaffold preparation in BTE and usually act as a composite matrix and an active compound carrier (at least two ingredients). These macromolecules can be divided into those that are naturally derived and those that are synthetic. The former group includes polysaccharides, such as alginate,¹²⁹ chitosan,^{129,132} and hyaluronic acid,^{133,134} protein-based collagen,^{135,136} and

gelatin,^{132,137} which are capable of forming hydrogels as well as a variety of cellulose-based biofibers.¹³⁸

The application of natural polymers in bone regeneration systems minimizes the negative immunological response resulting from their high biocompatibility.¹³⁹ The main disadvantage of this group of materials is their low mechanical resistance, especially considering the load-bearing requirements in BTE, as concluded by Swetha et al.¹⁴⁰

Synthetic polymers are more amenable to chemical modification. For example, the presence of functional groups can allow the facile binding of cellular proadhesive ligands such as arginine–glycine–aspartic acid (RGD).¹⁴¹ On the other hand, natural collagen has an RGD sequence already incorporated into its structure. Synthetic polymers generally have higher mechanical resistance than natural polymers. Significant representatives of this group in BTE include poly(L-lactic acid) (PLLA),^{142,143} poly(ϵ -caprolactone) (PCL),^{144,145} poly(ethylene glycol) (PEG),¹⁴⁶ and the emerging polymer poly(glycerol sebacate) (PGS).¹⁴⁷

The role of inorganic ceramic materials has been significant in developing BTE since the 1990s.^{148,149} Among the most important compounds are crystalline hydroxyapatite (HA), β -tricalcium phosphate (β -TCP), and amorphous bioglasses. The modern approach to using ceramics in BTE involves their stimulation of osteogenesis by releasing active ions¹⁵⁰ (e.g., Ca^{2+} in the case of HA) and the ability to act as a mechanical support in the composite with a high compressive modulus.¹⁵¹ Such compounds should be resorbable over time.

HA and β -TCP are composed of calcium phosphate and therefore resemble the inorganic phase of human bone. Calcium phosphate-based substances play a vital role in biomineralization, which is essential to strengthen the osteogenic capability of the scaffold.^{152,153} Bioglasses constitute the other class of ceramics in BTE, which are materials composed of Si_2O , Ca_2O , and P_2O_5 and can enhance osteogenesis more rapidly than calcium phosphates.¹⁵⁴

Composite materials are based on at least two constituents and possess properties from each phase. Basic BTE composite materials are made of a polymeric matrix and an inorganic filler. Preparing composites aims to combine the desired features of both materials.

Pathways to Obtain BTE Composite Scaffolds. There is a broad array of techniques to manufacture and form BTE scaffolds. These techniques depend on the desired geometry, presence, and distribution of the filler, and most importantly, the chemical characteristics of the substrates. In terms of biodegradability, porosity is of vital importance. The degradation medium (e.g., water) can infiltrate scaffolds more freely if voids (pores) are present compared to water infiltration into the bulk material. Moreover, in thermosetting polymers such as PGS,¹⁵⁵ the degradation time can be adjusted by altering the curing time of the polymer bulk.¹⁵⁶ Porous scaffolds naturally promote osteoconductivity toward the inner layers of the scaffold. Therefore, the synthesis of porous materials is an important subject in BTE.

Electrospinning. The most facile method to manufacture highly porous nonwoven fibers in BTE is electrospinning.¹⁵⁷ This technique utilizes an electric current to deposit the polymer solution on the substrate to form a fiber. Electrospinning has attracted attention due to its ability to mimic the tissue ECM and the wide range of materials that are applicable for spinning. The components of electrospinning systems for BTE include a thermoplastic polymer solution, such as PLA or

PCL, with a combination of collagen, chitosan, silk, gelatin, hydroxyapatite, or β -TCP. The significance of such systems in terms of bone regenerative medicine is comprehensively described in a review paper by Jang, Castano, and Kim.¹⁵⁸

The electrospinning method can produce two-dimensional fiber networks. However, there are more effective methods for creating three-dimensional structures that can mimic the complexity of bone tissue. In bone tissue engineering, creating porous and hierarchical structures is important, which is difficult to achieve with electrospinning. Electrospinning requires optimizing many parameters, such as voltage, solution flow, and distance between the needle and collector.¹⁵⁹ The need to experiment and adjust these parameters can take time and lead to trial and error. In addition, electrospinning is a manufacturing process that is not highly repeatable. The electrospinning process uses organic solvents and/or chemicals that can be potentially toxic to cells and the body.¹⁶⁰ It is necessary to ensure adequate elimination of these substances to avoid negative effects on the biocompatibility and functionality of scaffolds. Fiber produced by electrospinning often has a very low density and mechanical strength compared to natural bone tissue. This can lead to poor structural stability of the scaffold and limit its use in stressed areas. Manufacturing homogeneous composite materials is also a challenge for electrospinning.

Thermally Induced Phase Separation (TIPS). TIPS is one of the most popular methods to obtain three-dimensional scaffolds for BTE. In this technique, the polymer needs to be homogeneously dissolved in a solvent with a high melting temperature (T_m) due to the subsequent freeze-drying process (1,4-dioxane is one of the most popular solvents in TIPS with $T_m = 11.8\text{ }^\circ\text{C}$ ¹⁶¹). Afterward, a ceramic filler such as bioglass or apatite can be introduced to the polymer solution¹⁶² and dispersed by stirring or ultrasonication.¹⁶³ After a suitable solution is obtained, a freeze-drying process is performed to remove the solvent from the composite matrix and generate pores. The main limitation of this method is the thermolability of the solvent used for scaffold preparation. On the one hand, the solvent should dissolve the polymer, and on the other hand, the solvent should be easily removed from the scaffold by lyophilization.

In the TIPS technique, an additional porogen, such as NaCl^{162,164} or a sugar,¹⁶⁵ can be introduced to increase pore size by more than $100\text{ }\mu\text{m}$. The porogen can subsequently be removed (washed away) from the matrix after lyophilization (e.g., TIPS followed by salt leaching (TIPS-SL)). This method gives the possibility of obtaining highly porous scaffolds (up to 98%)¹⁶² with an interconnected pore morphology.¹⁶⁶ The porosity and internal structure can be tuned by altering the polymer solution concentration, filler content, amount of porogen, and particle size.¹⁶⁷ There are a variety of polymer/filler compositions that have been fabricated by TIPS and reported for BTE applications. For example, PLLA/ β -TCP nanocomposite scaffolds¹⁴³ or PGS-based scaffolds¹⁶⁸ can be fabricated by TIPS-SL.

The TIPS (TIPS-SL) process requires the use of organic solvents, which can affect the scaffold's biocompatibility.¹⁶⁹ Some of these solvents can be toxic to cells, which can limit the use of scaffolds in the context of tissue engineering. The TIPS process can be time-consuming (at least a few days) and requires precise control of temperature, time, and other parameters. This can lead to longer production times and increased costs. Producing scaffolds with adequate porosity

Table 2. Applications of the Techniques by Which BTE Scaffolds Are Prepared^a

Formation technique	Composition	Remarks	Biological activity	References
Electrospinning	PLA/PGS	Mat for cardiovascular diseases	Cardiomyocyte morphology similar to that in the natural environment	422
	PLLA, PLLA/HA, PLLA/collagen/HA	Composites for bone tissue engineering	hFOB 1.19 cells had a higher proliferation rate and increased ALP activity in a PLLA/collagen/HA system	423
TIPS	PCL/PGS	The different solvents used for fiber preparation showed no cytotoxicity	Human cardiomyocytes, cytotoxicity	424
	PLLA/ β -TCP	Interconnected, hierarchical pore structures with a high porosity and compressive modulus in comparison to pristine PLLA scaffolds	Enhanced osteoblast (MG-63 cell) proliferation, penetration, and ECM deposition	143
FFF	PDLLA/45S5 bioglass	Anisotropic, bimodal pore architecture, >90% porosity	–	425
	PLGA/HA	Mechanical properties and water sorption enhanced by HA addition	Significantly higher rabbit MSC proliferation on the PLGA/HA scaffold in comparison to that on the pure PLGA scaffold	426
SLS	PDA-coated PLA scaffold	Facile route for BTE scaffold manufacturing: FDM printing + immersion coating; the PLA scaffold was more hydrophobic than the PDA-coated scaffold	PDA-coated PLA scaffolds allowed hADSC cells to adhere and grow better than the unmodified PLA scaffolds	176
	PCL	Indicates PCL is an important allogenic material in the field of reconstructive craniofacial surgery	Successful reconstruction of craniofacial defects regarding new bone formation	178
SLA	PLA	PLA maintained a semicrystalline structure even though the polymer chains were shortened and thermal degradation profile had changed	Printed PLA scaffolds were proven to be biocompatible and allowed bone cell colonization	427
	PCL/HA	Gradient architecture with interconnected porosity and the desired mechanical properties	Excellent biocompatibility; induction of osteochondral repair <i>in vivo</i>	428
SLA	CaP/PHBV and CHAp/PLLA	Sintered scaffolds with a biodegradable osteoconductive calcium phosphate matrix; gradual decrease in mechanical properties after immersion in PBS	In SaOS-2 cell culture, CaP facilitated ALP expression on both materials; no significant difference in proliferation or ALP activity between the CHA/PLLA nanoscaffold and PLLA scaffold	429
	PVA	Periodic, porous architecture; PVA is vulnerable to high laser power for SLS	Successful growth and adaptation of MG-63 cells	184
Melt mixing/extrusion	PCL/HA	Gradient architecture with interconnected porosity and the desired mechanical properties	Excellent biocompatibility; induction of osteochondral repair <i>in vivo</i>	428
	CaP/PHBV and CHA/PLLA	Sintered scaffolds with osteoconductive calcium phosphate and a biodegradable matrix; gradual decrease in mechanical properties after immersion in PBS	In SaOS-2 cell culture, CaP facilitated ALP expression on both materials; no significant difference in proliferation or ALP activity between the CHA/PLLA nanoscaffold and PLLA scaffold	429
Melt mixing/extrusion	PVA	Periodic, porous architecture; PVA is vulnerable to high laser power for SLS	Successful growth and adaptation of MG-63 cells	184
	PLLA/HA	Composites were extruded and patterned using a femtosecond laser	Human osteoblasts (ATCC CRL-11372 cells) were cultured on the laser-modified surface	430
Melt mixing/extrusion	PLLA/HA	Composites extruded using co-rotating twin-screw extruder and irradiated using a CO ₂ laser	Not tested	431
	PLLA	PLLA foil extruded using a conical single screw extruder and irradiated using a UV laser	Not tested	432
Melt mixing/extrusion	PLLA/HA	Composites extruded using a co-rotating twin-screw extruder	Human adipose-derived stromal cells (hASCs)	433
	PLLA/HA	Composites extruded using a co-rotating twin-screw extruder	Human adipose-derived stromal cells (hASCs)	433

^aAbbreviations: poly(D,L-lactide), PDLLA; poly(lactic-co-glycolic acid), PLGA; calcium phosphate, CaP; carbonated hydroxyapatite, CHA; poly(hydroxybutyrate-co-hydroxyvalerate), PHBV; phosphate-buffered saline, PBS; alkaline phosphatase, ALP; poly(vinyl alcohol), PVA.

and interconnected pores is crucial for bone tissue regeneration.¹⁷⁰ However, the TIPS process can be difficult to control in terms of the porosity. It can be difficult to achieve uniform pore sizes and shapes, which can affect the scaffold's effectiveness in regenerating bone tissue. The use of the TIPS-SL technique only partially solves the problem, as the pore size is increased, but at the same time, a material with lower strength parameters is obtained.¹⁷¹

Solvent-Free Techniques. 3D Printing (3DP). 3DP techniques consist of slicing a computer-aided design (CAD) model into layers and its subsequent manufacture. This paper will cover only the method by which BTE scaffolds can be obtained, including techniques such as selective laser sintering (SLS),¹⁷² fused deposition modeling (FDM)/fused filament fabrication (FFF),¹⁷³ and stereolithography (SLA),¹⁷⁴ which are based on different operation principles. However, these methods are additive manufacturing techniques, which are, among other techniques, used to prepare scaffolds or implants for bone regeneration. There are a variety of biodegradable polymer/ceramic systems for BTE that have been manufactured by means of 3DP (Table 2). The major advantage of 3DP when manufacturing scaffolds for biomedical applications is the possibility to obtain a reproducible and well-defined architecture that meets the needs of patients.

3D printing processes are most often conducted at high temperatures (SLS, FFF/FDM) due to thermoplastic materials being processed at temperatures as high as 160–200 °C.¹⁷⁵ For this reason, the introduction of bioactive particles, which are often sensitive to temperature, is difficult. The use of UV irradiation for cross-linking during the 3D printing (SLA) process degrades the polymer from which the scaffold is made.¹⁷⁶

FDM/FFF. An operating principle of FDM/FFF is extrusion on a thermoplastic filament (usually 1.75, 2.85, or 3.0 mm in diameter) through a nozzle, followed by deposition on the printing bed. After a layer is delivered, the extruder moves upward, and the next layer is laid. The resolution of the printout is mainly affected by the extrusion rate, motor speed, and nozzle diameter. The main advantages of FDM are the simplicity of the process and high printing efficiency. On the other hand, the main limitation involves the thermoplastic characteristics of the material with the existence of a molten phase. Additionally, the process is relatively slow and has low accuracy. Moreover, complex geometries require auxiliary supports, which are removed during postprocessing. The filament for FFF is produced by means of melt extrusion.

Polymers for BTE applications include thermoplastic materials such as PCL, poly(vinyl alcohol) (PVA), and polylactides. This technique provides the possibility of introducing a ceramic phase into the blend¹⁷⁷ for superior osteoconductivity. Furthermore, the infill architecture of the FDM printout affects the *in vivo* behavior of the scaffold, as the honeycomb internal structure of the FDM scaffold has been indicated to increase bone ingrowth.¹⁷⁸

SLS. The SLS operation principle is based on layer-by-layer fusing/sintering of particles on a powder bed by heat generated from a laser beam.¹⁷⁹ By means of rollers, the printing bed is coated with a preset layer of powder, which is sintered according to the CAD model. The printing bed moves downward incrementally, and the process repeats until the final printout is completed.¹⁷⁹

The SLS technique is limited by the ability of the particles to absorb the wavelength of laser light as well as the laser energy

density. System optics and resolution also affect the final structure and porosity of the material. Particle size, sphericity, and chemical characteristics are of vital importance for materials submitted for SLS. Usually, microspheres with a defined size (20–80 μm) for use in the SLS process are produced by emulsion solvent evaporation.^{180,181} However, one can purchase presynthesized SLS powders, such as PCL (CAPA 6501, Solvay Caprolactones, Warrington, Cheshire, UK), poly(hydroxybutyrate-cohydroxyvalerate) (PHBV) (ICI, UK), or PVA (Nippon Synthetic Chemical Industry Co. Ltd., Japan). Among the wide array of biodegradable materials for SLS, PVA is of particular interest due to its flexibility and semipermeability, which can allow oxygen and nutrient exchange, which is necessary for the cellular culture on the scaffold to thrive.¹⁸²

The SLS process requires the material to have a low melting point and be able to form intermolecular bonds after exposure to a laser.¹⁸³ The main advantage of using SLS scaffolds for BTE is the possibility of obtaining a porous structure that mimics the bone ECM. The overall porosity of the SLS printout can be higher than anticipated due to the formation of micropores in the scaffold.¹⁸⁴ On the other hand, this technology is expensive and requires a complex modeling procedure.

SLA. The SLA approach in additive manufacturing utilizes ultraviolet (UV) light to trigger selective photopolymerization. The printing procedure involves submerging the printing bed in the photopolymer reservoir with subsequent layer-by-layer exposure to UV radiation in accordance with the CAD model. The SLA method is comparable to SLS; however, SLA uses a liquid prepolymer. After the layer is photocured, the printing bed slides down, and the process is repeated until the last layer is irradiated.¹⁸⁵ SLA material diversity is limited by the requirements of biodegradability and lack of cytotoxicity. Materials for SLA scaffold-based tissue engineering include derivatives of PEG acrylate, PEG methacrylate, PVA, and modified polysaccharides, such as hyaluronic acid and dextran methacrylate, in addition to poly(propylene fumarate) (PPF) and PCL-based resins.¹⁸⁶

For biomedical applications, the properties of SLA resins can be adjusted; for example, reducing the percentage of DEF in the PPF resin increases the viscosity of the solution and promotes cross-linking, which results in a final product with superior mechanical properties.¹⁸⁷ However, a higher degree of polymer cross-linking affects the degradation rate. Lower cross-linking degree facilitates degradation. It is a vital parameter considering the resorption of biomaterial *in vivo*.

Melt Mixing. Melt mixing is the most important continuous method by which polymer/filler composites are obtained. One type of melt mixing is the twin-screw co-rotating extrusion (TSCE). TSCE is the most effective means to distribute filler in the polymer matrix and enables even filler distribution, even on the nanoscale.¹⁸⁸ TSCE utilizes an instrument that consists of a motor, heated cylinder, screws, hopper, die, and control equipment (thermocouple, pressure sensor). Two screws are installed inside the cylinder on a shaft and rotate in the same direction. These screws are made of configurable sections (mixing and conveying sections) that can be arranged in various configurations.¹⁸⁹ A preprepared material in the form of a granule or powder is dosed into the first zone of the extruder (feeding zone). Screws, rotating with speeds usually ranging from several dozen to a few hundred, plasticize, transport, and homogenize the material to the extruder head.

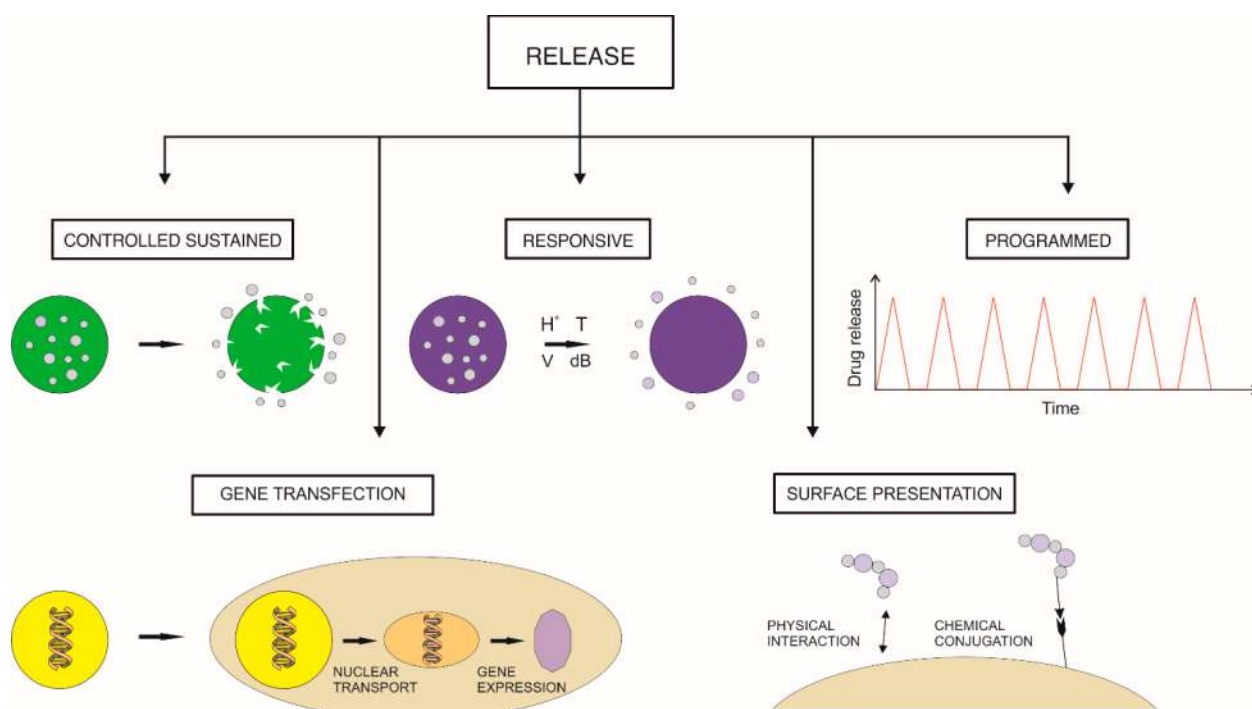


Figure 2. Strategies for the delivery of bioactive agents in bone regeneration.

After this process, the material in the form of a filament is allowed to cool down (using a water bath or in air) and pelletized. The advantages of this method are the fast homogenization and good dispersion of the filler. Disadvantages of this method include thermal degradation of the polymer during the process, the need for a relatively high amount of the polymer for extrusion, and large losses during processing. Extrusion is not actually a scaffolding manufacturing method, but is a preliminary method used to homogenize composite components. The material is obtained in the form of pellets or filaments and in this form is used for 3D printing.

METHODS TO DELIVER BIOACTIVE MOLECULES

Bone Regeneration Biomolecule Delivery Platforms and Release Strategies. Bone regeneration involves multiple stages, including the inflammatory phase, callus formation phase, callus removal/bone deposition phase, and bone remodeling.⁸ Each phase is driven by different biochemical signals, which have to be delivered at a specific time in a coordinated and sequential manner.¹⁹⁰ To achieve the best therapeutic outcome, orthopedic implants loaded with bioactive factors should release these factors at a dose and time that reflects this physiological pattern. Biomolecule dosing should also be tailored to the patient's clinical status, i.e., cause, location, and severity of bone defect, age, and presence of coexisting conditions. A number of biomolecule delivery platforms and release strategies have been proposed to provide treatment options customized to different types of biofactors and for different types of bone defects. The platforms developed to date provide a wide range of dosing profiles that depend on the implant material, structure and size, biomolecule immobilization technique, and amount and spatial distribution of the biomolecules. Biomolecule delivery platforms can be categorized into five main types: surface-functionalized, controlled/sustained release, preprogrammed

release, stimuli-responsive, and those for gene delivery, as depicted in Figure 2.

Surface-Functionalized Delivery Platforms. Surface-functionalized implants are being intensively explored in bone regenerative medicine^{191–193} as delivery platforms for BMPs,^{194–196} platelet-derived growth factor (PDGF),¹⁹⁷ TGF- β ,¹⁹⁸ and vitamins D and K.¹⁹⁹ During the fabrication of surface-functionalized implants, biomolecules are introduced onto the implant surface by physical adsorption,^{200,201} chemical conjugation,^{191,192} or ligand–receptor binding.

Physical adsorption (Figure 3A) occurs when biomolecules attach to the scaffold material via electrostatic, hydrophobic,

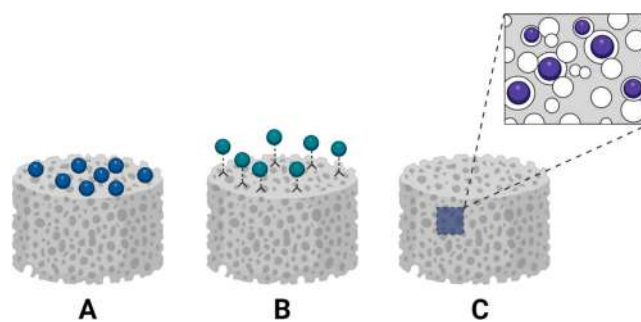


Figure 3. Physical and chemical strategies to immobilize bioactive compounds on biomaterials: (A) physical adsorption, (B) covalent binding, and (C) entrapment in a polymer matrix.

van der Waals interactions, or hydrogen bonding.²⁰⁰ The release kinetics of biomolecules immobilized by physical adsorption depends on their affinity for the implant material and can be controlled by environmental conditions such as temperature and pH. To enhance biomolecule adsorption to biomaterials, their surface can be pretreated with charged molecules such as amino acids (e.g., serine, asparagine) or acids (e.g., pyrophosphoric acid,^{202,203} mercaptosuccinic

acid²⁰⁴). Charged biomaterial surfaces can selectively attract molecules of interest (e.g., lysozyme,²⁰⁵ BMP-2²⁰⁶), while oppositely charged molecules are repulsed. Physisorption has been widely used to immobilize osteoinductive biomolecules (e.g., BMP-2,^{194,195} PDGF,¹⁹⁷ TGF- β 198]) in a variety of scaffolds, including collagen and gelatin sponges,²⁰⁷ poly-(glycolic acid) meshes, poly(D,L-lactide) scaffolds,²⁰⁸ hydroxyapatite,^{206,209} tricalcium phosphate ceramics, and others. This technique has also been used to fabricate INFUSE Bone Graft from Medtronic (an absorbable collagen sponge soaked with BMP-2) for recombinant BMP-2 delivery, which is currently the only FDA-approved BMP-2 product that is commercially available. However, the major limitations of materials functionalized via physisorption include poor drug retention and limited control over the biomolecule release rate due to weak biomolecule bonding. This type of materials typically suffer from burst release,²¹⁰ which is defined as a sudden initial release of a drug bolus resulting from its rapid desorption from the material surface. The main risk of burst release is the overdose of a therapeutic molecule in the immediate postimplantation period, which is usually associated with reduced drug absorption and rapid drug depletion. Supraphysiological doses of BMP-2 have also been shown to cause serious side effects such as spine swelling, neck edema, tumor formation, osteolysis, and ectopic bone formation,²¹¹ which remain among the biggest challenges of the current clinical approaches to bone healing based on BMPs.²¹¹

More stable attachment of biofactors to the scaffold surface can be achieved by chemical conjugation.^{212–214} Chemical conjugation methods are based on the formation of covalent bonds between biomolecules and biomaterials (Figure 3B) through the course of chemical reactions such as carbodiimide-mediated amidation, esterification, or click reactions.^{215–217} Since the majority of osteoinductive biomolecules are proteins, the most commonly used covalent coupling methods are based on carbodiimide-mediated reactions between the protein amine groups and carboxyl groups of the biomaterial.¹⁹³ Due to the inert nature of many materials used in regenerative bone therapies (e.g., polyesters), these materials require surface functionalization prior to biomolecule attachment. Material surface functionalization aims to add or expose reactive functional groups (e.g., amines, carboxyls, hydroxyls) that can form covalent bonds with the functional moieties of the biomolecules. Functionalization can be attained by plasma treatment,²¹⁸ chemical etching,²¹⁴ and oxidation.²¹² Biomolecules can be grafted either directly onto functionalized material surfaces²¹⁹ or via linker molecules (spacers), such as silane²²⁰ or PEG molecules.²²¹ The role of spacer molecules is to increase the distance between the biomolecule and the biomaterial surface, which preserves the proper conformation and spatial orientation of the biomolecule and prevents its denaturation, which can be caused by direct contact with a solid surface.²²² Spacer molecules may also provide a wide range of properties that facilitate bone regeneration or implant integration. For example, heparin,^{213,223} a key protein involved in tissue repair, is often introduced onto a material surface to act as both a spacer and anticoagulation and anti-inflammatory factor.²²⁴ Similarly, PEG,²²¹ known for its ability to reduce nonspecific protein binding, can be used as a spacer molecule, providing an antifouling effect *in vivo*. Chemical conjugation methods have been broadly employed for bone implant surface functionalization with biomolecules such as BMP-2,²¹³ VEGF,²²⁵ the adhesion peptide RGD,²²⁶ and TGF- β .²¹⁴ This

immobilization strategy allows prolonged biomolecule presentation compared to physical adsorption.²²⁷ The main disadvantage of biomolecule chemical conjugation lies in the harsh conditions required for many coupling reactions (e.g., the use of toxic or denaturing reagents such as organic solvents) that may lead to reduced biomolecule activity.²²⁸ To minimize the loss in activity, an array of bioconjugation reactions that can be performed in aqueous solutions under mild conditions have been developed (e.g., conjugation via a hydrazone and oxime formation reactions²²⁹ or alkyne–azide coupling²³⁰).

The bonding of biomolecules to the biomaterial surface can also be achieved by biomimetic ligand–receptor pairing. The most popular conjugation method relies on the interaction between biotin and avidin, which is the strongest known noncovalent bond.¹⁹² This bond remains stable even under harsh conditions, including extreme temperatures and pH values, organic solvents, and other denaturing reagents. Due to the wide variety of commercially available biotinylated biomolecules, this approach has gained much attention in bone implant functionalization.²³¹ It has been successfully applied to immobilize biomolecules such as BMP-2,^{232,233} fibroblast growth factor-2 (FGF-2),²³³ and fibronectin²³⁴ on the surface of biomaterials including gelatin/hydroxyapatite composites,²³² hydroxyapatite-coated nanofibers,²³³ and titanium implants.²³⁴

The key benefit of biomolecule surface presentation is the direct exposure of immobilized factors to the host body fluids and cells infiltrating the biomaterial/tissue interface. This implant design may significantly accelerate the recruitment of immune cells and mesenchymal progenitor cells involved in the early stages of bone repair (inflammation and revascularization), which are considered the most critical for successful healing.

Controlled/Sustained Release Delivery Platforms.

Biomolecules used in bone regeneration often suffer from low stability and a short half-life *in vivo*.²³⁵ These issues are particularly prevalent in the case of protein biomolecules (e.g., BMPs, OPN, OC), the bioactivity of which depends on their 3D structure, and can be easily lost *in vivo* due to hydrolysis, proteolysis, and endocytosis.²³⁶ Disrupted protein structure not only leads to the loss of biological activity but also increases immunogenicity and the risk of implant rejection by the host.²³⁵ One approach to prolong the biological activity of biomolecules *in vivo* is to immobilize them in controlled/sustained release delivery systems. The most straightforward strategy to attain the sustained release of biomolecules is to physically encapsulate them within a matrix material (Figure 3C),²³⁷ e.g., a PEG hydrogel,²³⁸ gelatin,²³⁸ or collagen–hydroxyapatite matrix.²³⁹ In this approach, the biomolecule is added to the polymer solution prior to scaffold fabrication, which may be followed by the covalent cross-linking of biomolecules to the polymer matrix.²⁴⁰ The simplicity of this method has contributed to its widespread use in BTE to entrap biomolecules such as BMPs,²³⁹ PDGF, and VEGF.²³⁸ Biomolecules immobilized directly in the matrix are released by diffusion and polymer degradation. The biomolecule release rate depends fundamentally on the matrix porosity and degradation rate, as well as the affinity of the released molecules for the polymer molecules (e.g., chemical affinity, or affinity based on electrostatic interactions). Release kinetics can be controlled by properly selecting the matrix material (with the desired degradation rate and charge) and scaffold

fabrication technique. However, this immobilization strategy offers relatively poor control over the biofactor delivery rate. Another drawback lies in the fact that biomolecules typically need to be added to the polymer solution prior to scaffold fabrication. Since scaffold manufacturing procedures often involve the use of toxic reagents (cross-linking agents, organic solvents) and nonphysiological conditions such as elevated temperature or UV irradiation, they can significantly diminish biomolecule activity.²²⁷

These limitations have driven research toward the development of protective micro- and nanocarriers that shield the immobilized biomolecules from unfavorable external conditions. Due to the simplicity of the fabrication, the most popular biomolecule delivery vehicles are spherical polymeric carriers such as microspheres,²⁴¹ microcapsules, and nanospheres.^{242–244} Among spherical carriers, micro- and nanospheres made of biodegradable polymers such as poly(lactic acid) (PLA), PLGA,²³⁹ and alginate have found the broadest use in bone reconstruction.^{243–247} The kinetics of protein release from these carriers can be adjusted to a specific application by tailoring the particle size, porosity, and degradation rate, which can be attained by proper selection of the carrier material and fabrication method.²⁴⁸ An important disadvantage of biodegradable nano- and microspheres is the limited control over the biomolecule delivery rate and initial burst release.²⁴⁹ These issues can be resolved by coating the nano- or microspheres with a semipermeable membrane, which creates a significant barrier to biomolecule transport. Biomolecule release from core–shell microcapsules relies on molecular diffusion through membrane pores. The rate of diffusion is dictated by the size and distribution of the pores and membrane thickness.²⁵⁰ These properties can be modulated by altering the microcapsule manufacturing method,²⁵¹ composition of the membrane-forming solution,²⁵² and process parameters.²⁵¹

Another type of biomolecule carrier used for controlled/sustained delivery of biomolecules facilitating bone regeneration is liposomes.^{253,254} Liposomes exhibit a high affinity for cell membranes, which ensures their easy uptake by cells.²⁵⁵ However, liposomes are highly susceptible to changes in pH and temperature, enzymatic degradation, oxidation, and hydrolysis,²⁵⁶ contributing to their relatively low stability in physiological environments. Another major drawback of liposomes is their tendency to aggregate, fuse, and leak the encapsulated molecules. Due to these limitations, the use of liposomes in bone regeneration is much less widespread than the use of polymer carriers.

Spherical biomolecule carriers can be introduced directly into bone defects^{257–259} or embedded in a polymer matrix, e.g., an injectable hydrogel^{26,298} or a solid scaffold,^{260,261} prior to implantation. Solid implants can be fabricated by suspending biomolecule carriers in a polymer solution that is subsequently molded¹⁹⁸ or 3D-printed²⁶² into the desired shape, followed by matrix solidification. Alternatively, the particles may be installed onto the implant surface; for example, via a solvent annealing technique based on seeding a carrier suspension in a volatile solvent onto the scaffold surface and solvent evaporation.²⁴⁸ Numerous studies have shown that incorporating biomolecule-loaded carriers into polymer matrices significantly prolongs the biomolecule release duration.²⁴² As a result, bioactive agents can be released over extended periods ranging from weeks^{257,258} to months,²⁴⁸ greatly improving their capability to induce bone forma-

tion.^{257–259} Scaffolds containing spherical particles also exhibit considerably higher mechanical resistance than implants composed solely of a polymer matrix.^{260–263}

Scaffolds incorporating polymer carriers loaded with biomolecules hold great promise for the development of biomimetic tissue constructs. To create a tissue construct, biomolecule carriers can be incorporated into a scaffold seeded with cells (e.g., progenitor cells). Biomolecules released from the carriers modulate cell behaviors, including their migration, adhesion, differentiation, and proliferation. For example, microspheres loaded with BMP-2 or IGF-1 incorporated into hydrogel scaffolds induce osteogenic differentiation of MSCs entrapped in a gel.²⁶⁴ Microspheres loaded with proangiogenic factors (e.g., VEGF and FGF) have been utilized to promote scaffold vascularization in the fabrication of prevascularized bone implants.^{265,266}

Significant progress in biomimetic bone construct engineering has been made since the introduction of 3D printing. 3D printers can precisely control the spatial distribution of the biomolecule-loaded carriers within the scaffold and recreate the tissue-specific 3D organization of biochemical cues.²⁶² In addition, multiple types of carriers (made of materials that degrade at different rates or carry different biomolecules, such as those that can act synergistically) can be combined into a single construct.²⁶⁷ This type of design can provide the sequential release of various biochemical signals in a spatially and temporally controlled manner that mimics the physiological release of biofactors during osteogenesis.

Preprogrammed Release Delivery Platforms. Recreating the precise timing of biomolecule release during physiological bone healing remains one of the biggest challenges in bone regenerative medicine. To address this issue, preprogrammed release delivery platforms have been introduced. This type of platform is designed to deliver biomolecules at specific time points corresponding to their physiological release pattern. Among preprogrammed release delivery platforms, the pulsatile delivery systems^{268–270} have emerged as a promising approach to achieving precise temporal control over biomolecule release. These systems deliver therapeutic agents in pulses at predetermined intervals over an extended period (usually several months).^{270,271} Pulsatile release platforms may be based on multilayer or multicompartment constructs, where each compartment contains and releases the biomolecule at its own unique rate. Particular compartments can be made of different matrix materials (e.g., biodegradable polymers such as PLGA,²⁷² gelatin,²⁷¹ poly(4-vinylpyridine), alginate,^{272,273} PLLA²⁷⁴) with different degradation rates. The degradation of each compartment leads to a burst (pulse) of bioactive agents. The lag time between pulses can be precisely tuned by varying the molecular weights of the polymers, combining materials with different degradation rates in various proportions (e.g., glycolic and lactic acid in a PLGA copolymer),²⁷¹ or adjusting the size/thickness of particular compartments. Another approach to pulsatile release is based on implantable microchip devices made of several reservoirs containing discrete doses of bioactive agent(s). The sequential release from each reservoir may be attained by sealing the reservoir with biodegradable PLGA membranes with various compositions²⁷⁰ or preprogramming the chip to open particular reservoirs at predetermined time points. Reservoir openings can also be triggered remotely using wireless communication.²⁷⁵

Preprogrammed delivery devices can be employed to provide accurate doses of single or multiple bioactive molecules. Single biomolecule dosing is particularly useful in the case of biofactors, the effect of which depends strongly on administration frequency. An example of such a biomolecule is PTH, which is used to stimulate bone formation in the treatment of osteoporosis. PTH can act anabolically (promoting bone formation) when administered intermittently²⁷⁶ and catabolically (leading to bone degradation) when administered continuously.²⁷⁷ For pulsatile PTH delivery, devices composed of multiple layers of biodegradable polymers have been proposed.^{268,269,274} For example, Dang et al. developed a pulsatile PTH delivery device consisting of alternating alginate layers loaded with the drug (PTH) and poly(anhydride) (PA) isolation layers that did not contain the drug.²⁶⁹ Such a device can release daily PTH pulses, upon the gradual degradation of its subsequent layers, for up to several weeks, after which the body completely resorbs the device without the need for implant removal. This system has been demonstrated to have a superior ability to induce new bone formation and much fewer side effects than conventional therapy that relies on daily systemic PTH injections. Another platform for PTH delivery, an implantable silicon microchip that releases drugs by wireless control, has successfully passed safety and efficacy evaluations in clinical studies.²⁷⁵ This type of device may provide a valuable alternative to the current FDA-approved PTH therapies in the near future.

The second goal of preprogrammed delivery systems is to allow the sequential release of multiple biomolecules involved in natural bone regeneration, including osteogenic, immunomodulatory, and proangiogenic factors such as BMPs,^{272,278} IGF-1,²⁷⁹ VEGF,^{272,280,281} PDGF, TGF- β 1,²⁸⁰ interferon- γ , and interleukin-4 (IL-4).^{282–284} Sequential delivery of biomolecules has been shown to improve osteogenic outcomes in a number of *in vitro* and *in vivo* studies.^{272,278,269,285} Based on the accumulating evidence that the current clinical approaches based on high biomolecule concentrations cause numerous side effects,²⁸⁶ the preprogrammed devices that are currently under development have been designed to release bioactive agents at much lower doses (e.g., 6.5 μ g of BMP-2 vs 6–12 mg in INFUSE Bone Graft).²²⁷ Low-dose devices, therefore, can potentially resolve the safety concerns of the regenerative bone therapies currently employed in clinical practice.

Stimuli-Responsive Delivery Platforms. Another group of biomolecule delivery platforms is stimuli-responsive systems.^{196,287} These systems are able to deliver biomolecules on demand in response to specific stimuli, which can be categorized as physiological signals coming from the patient's body (e.g., temperature, pH, body fluid composition, oxygen concentration, etc.^{288,289}) and external stimuli such as exposure to ultrasound,^{290,291} near-infrared light,²⁹² or electric²⁹³ or magnetic fields.²⁹⁴ The main aim of stimuli-responsive release is to achieve time- and site-specific drug delivery, which can effectively eliminate the systemic side effects of therapy.

Delivery platforms triggered by physiological stimuli do not require exposing the patient to external factors and are therefore considered safer and more convenient. For this reason, physiological stimuli-responsive platforms have been more extensively explored in bone regeneration than external stimuli-responsive platforms.²⁹⁵ An example of a system triggered by a physiological stimulus is polyelectrolyte microbeads (dextran methacrylate-AMPS microbeads) that

release PTH in response to an increase in the Ca²⁺ concentration, which occurs in patients with osteoporosis due to bone loss.²⁹⁶ A different strategy for physiological stimuli-mediated release is based on the cleavage of the material encapsulating the biomolecule by enzymes naturally occurring in the bone ECM, such as metalloproteinases (MMPs) or collagenases.^{297,298} Since most synthetic biomaterials are not susceptible to enzymatic degradation, to create enzyme-sensitive delivery systems, the matrix material needs to be functionalized with enzyme cleavage sites. This can be achieved by chemically modifying the matrix with molecules containing specific amino acid sequences that can be recognized by enzymes, such as cleavable oligopeptides^{299,300} or cross-linkers (e.g., bis-cysteine peptides).²⁹⁷ In the presence of proteases secreted by host cells at the implantation site, the cross-linker is cleaved, which results in cell-mediated degradation of the polymer matrix and release of the entrapped biomolecules. Enzyme-sensitive systems used in BTE mainly employ PEG derivative hydrogels³⁰¹ and hyaluronic acid hydrogels.³⁰² These systems have been utilized for the local delivery of GFs (e.g., BMP-2,²⁸⁸ VEGF²⁹⁸) and chemokines e.g., stromal cell derived factor-1 α (SDF-1 α).³⁰²

The next group of stimuli-responsive systems is temperature-sensitive delivery platforms. These platforms typically employ thermoresponsive polymers^{303–309} that undergo gel–sol or sol–gel transitions at body temperature. Gel–sol transition leads to the release of biomolecules immobilized in hydrogel implants or microspheres³⁰⁹ upon implantation. Materials that transition from a sol to a gel at 37 °C are being used as *in situ* forming injectable hydrogels that remain liquid at room temperature but rapidly solidify into a gel upon injection, allowing long-term drug release. The most widely used thermogelling polymers are based on poly(*N*-isopropylacrylamide)³¹⁰ and polyester block copolymers.^{311–314} Due to their injectability and gelation under physiological conditions, these polymers have been broadly applied to deliver biomolecules such as VEGF³¹⁰ and BMP-2.³¹²

Among the platforms that are sensitive to physiological stimuli, pH-sensitive systems have elicited much interest in bone regeneration. These platforms are based on materials that undergo a sol–gel transition, degradation, or volume change (swelling/shrinking) in response to changes in pH. For instance, at the desired pH, polymers may transition from a tightly packed to an expanded state,³¹⁵ which leads to polymer swelling, liquefaction, and drug release. The pH range that triggers phase transition can be tailored to a specific target site by incorporating ionizable groups with specific pK values, that match the desired pH, into the polymer molecules.³¹⁵ pH-sensitive materials employed in BTE include, among others, poly(NIPAAm-co-AAc) hydrogels,³¹⁶ alginate/chitosan polyelectrolyte complexes,³¹⁷ and chitosan^{318,319} and transition either at physiological pH (~7.4) or under the acidic conditions (pH 5–6) found in healing tissues.³²⁰ Numerous pH-responsive platforms have been developed for the on-demand delivery of biomolecules such as BMP-2,³¹⁷ VEGF, EGF,²⁹² and dexamethasone.³¹⁸ For greater control over biomolecule delivery, temperature- and pH-sensitive polymers can be combined into dual stimuli-responsive platforms that are sensitive to both pH and temperature.³²⁰ pH- and thermosensitive hydrogels can be fabricated by adding pH-responsive end groups to thermosensitive block copolymers. Such an approach has been employed to generate dual-responsive poly(ϵ -caprolactone-co-lactic acid) (PCLA)/PEG

hydrogels for BMP-2 delivery.³²¹ Combining two mechanisms to control drug release ensures highly specific dosing within a narrow range of physiological conditions.

Gene Delivery Platforms. With advancements in genetic engineering, gene delivery platforms have been proposed as a new approach to release biomolecules accelerating bone regeneration.^{322,323} Gene delivery aims to upregulate the synthesis of biofactors involved in bone regeneration or silence signaling pathways that inhibit osteogenesis^{324,325} locally in the bone defect. The most common strategy for gene delivery is transfection of the target cells, which can be either host cells infiltrating an osseous defect or foreign cells transplanted into the lesion. Introducing genes encoding osteoinductive factors into cells allows their continuous expression and sustained release for extended periods, which may resolve the issue of the short half-life of biomolecules. Moreover, biofactors synthesized directly at the regeneration site in their native form display higher activity than exogenous recombinant proteins. Gene transfection is performed using vectors (viral or nonviral) that carry the foreign gene into the cell. The key advantage of viral vectors is their high transfection efficiency. Viral vectors (mostly adenoviral and retroviral vectors) have been broadly used for the local delivery of genes encoding osteoinductive agents such as BMPs,^{326,327} VEGF,^{328,329} LIM mineralization protein-1 (LMP-1),³³⁰ and cyclooxygenase-2.³³¹ Viral vectors can be introduced into the bone defect directly by injection of a viral particle suspension³²⁶ or by implantation of a polymer matrix incorporating the vector.^{332,333} It has been shown that gene delivery using viral vectors leads to high gene expression levels in bone defects over a period of several weeks (typically 4–6 weeks),³³⁴ which accelerates bone healing considerably.^{326,335,336} However, viral vectors raise serious safety concerns regarding the activation of the host immune response as well as tumor formation due to the risk of random insertion of the transferred gene into the host genome.³³⁷

To overcome these issues, nonviral vectors have been proposed as safer alternatives to viral vectors. Nonviral vectors may take the form of plasmids,³³⁸ which are small circular pieces of free DNA carrying the transgene or other forms of nucleic acids such as cDNA,⁹¹ siRNA³²⁴ or microRNAs,³⁴⁴ (miRNA), which are small noncoding RNAs able to post-transcriptionally regulate pathophysiological signaling pathways via degradation of mRNA or inhibition of translation.³³⁹ Plasmids have been demonstrated to effectively deliver the PTH,³⁴⁰ VEGF,³⁴¹ and BMP-4³⁴² genes into host cells and successfully induce new bone formation. However, since naked DNA is easily degraded by nucleases, high doses are typically required to exert relevant therapeutic effects. To preserve the integrity of the transferred genes, plasmids,³⁴³ or other forms of nucleic acids such as cDNA,⁹¹ miRNA,³⁴⁴ and siRNA³²⁴ can be incorporated into protective polymer matrices called gene-activated matrices (GAMs, e.g., collagen sponges,^{342,345} collagen/calcium phosphate scaffolds,³⁴⁰ and triacrylate/amine-gelatin constructs³⁴⁶) or gene delivery vehicles such as liposomes^{347,348} or polycation-based nanoparticles. Liposomes used for gene delivery are usually based on cationic lipids, which spontaneously form complexes with nucleic acids due to the electrostatic interactions between the positively charged lipids and negatively charged nucleic acid molecules. The resulting lipoplexes protect DNA from degradation and are easily taken up by cells via endocytosis.³⁴⁹ Liposomal vectors have been demonstrated to effectively deliver biomolecule genes (e.g., VEGF and BMP-2) into bone defects.^{91,350} *In vivo*

studies have shown that the host cells surrounding an osseous lesion take up liposomes carrying BMP-2 cDNA and effectively express the transgene for up to 4 weeks, leading to enhanced bone formation. Nonetheless, the significant drawbacks of liposomes are the poor stability of lipoplexes in physiological fluids, their rapid clearance from the target site, and their tendency to aggregate.³⁵¹ A variety of strategies have been developed to improve the performance of liposomes as gene carriers. Modifications of the liposome physicochemical properties, including size, charge, lipid composition, lipid-to-DNA ratio, and chain length, have been shown to increase liposome stability and cellular uptake.²⁵³ To allow tissue-specific gene delivery, liposomes have been modified with functional groups with a high affinity for bone (e.g., pyrophosphate³⁵² or bisphosphonate groups²⁵⁴) or ligands that bind to specific receptors on the surface of the target cells (e.g., peptides, antibodies, or aptamers^{351,353}). To prolong the retention of liposomes at the implantation site, liposomes have also been encapsulated in hydrogels,³⁵⁴ core-shell nanofibers,³⁵⁵ and microspheres.³⁴⁴

Another type of nonviral vector is polycation-based nanoparticles. Polycations such as polyethylenimine (PEI), poly-L-lysine (PLL), and chitosan^{356,357} have the ability to form complexes with nucleic acids due to their positive charge. During complex formation, the genetic material is condensed into nanostructures called polyplexes. The cationic regions of the polyplexes easily bind to negatively charged cell membranes, which promotes their uptake and contributes to the increased transfection efficiency compared to naked plasmids.³⁵⁸ However, the polycationic regions of polyplexes can disrupt the integrity of cell membranes, resulting in cytotoxicity toward host cells.³⁵⁹ To reduce this effect, the surface properties of polyplexes may be altered by chemical modifications, such as acetylation³⁶⁰ or carboxyalkylation.³⁶¹

Each biomolecule delivery platform described above has its advantages and disadvantages. Current research has focused on combining the advantages of the systems developed to date into a single platform. The field of tissue engineering is currently progressing toward multicomponent systems comprising multiple types of biomolecule delivery vehicles.³⁶² An interesting example of such a platform is a two-stage delivery system for the local delivery of miRNA (microRNA) that activates the osteoblastic activity of endogenous stem cells.³⁴⁴ This platform is composed of nanosized core-shell miRNA/polyplexes encapsulated in biodegradable polymer microspheres attached to an NF polymer scaffold. Such a design ensures high transfection efficiency due to the use of polyplexes. Encapsulating polyplexes within microspheres allows their release to occur in a controlled and sustained manner, while the attachment of microbeads to the NF scaffold enables their proper spatial distribution and effective fixation at the implantation site. This combination translated to greatly improved therapeutic effects in osteoporotic mice. The volume of the new bone formed upon implantation of this scaffold was six times higher than that in the group treated with naked miRNA.³⁴⁴ To allow further advancements in the field, the most recent studies aim to combine multicomponent scaffolds with different classes of signaling molecules and cells (particularly stem cells) that perform diverse biological functions during osteogenesis into a single biomimetic bone construct.²⁶⁸ To drive the progress of bioactive bone implants toward clinical translation, future research will need to resolve

the issue of recreating the bone-specific spatial organization of biomolecules and cells within such constructs.

■ CHALLENGES AND SOLUTIONS IN THE DEVELOPMENT OF BIOACTIVE MATERIALS FOR BONE REGENERATION

Bioactive materials designed to deliver biomolecules to bone defects have contributed to significant progress in the field of bone regeneration and reconstruction. Multiple studies have confirmed that these materials can effectively accelerate new bone formation and, more importantly, engage in a complex biochemical dialogue with the host cells. Over the last several decades, the materials applied in bone regeneration have evolved from simple bioinert bone substitutes to highly advanced bioartificial systems able to both provide the mechanical support and respond to signaling factors secreted by the surrounding tissues. Currently researched bioactive implant materials have the potential to address key safety concerns of the current FDA-approved clinical approaches to bone healing based on BMP-2, i.e. the adverse side effects caused by supraphysiological BMP-2 concentrations.²¹¹

The limitations of current strategies for the treatment of bone defects have driven research toward the development of the biomolecule delivery platforms that would contain lower doses of biomolecules¹⁹⁶ and provide a more precise control over their release. Despite promising results from research studies, so far only a few systems have reached the clinical setting. INFUSE Bone Graft from Medtronic, which is a collagen sponge soaked with recombinant BMP-2, is currently the only FDA-approved BMP-based product used in clinical practice. The vast majority of bioactive materials for bone regeneration applications remain at *in vitro* or animal testing stage, as they suffer still from relatively limited control over the biomolecule release rate. One of the approaches to resolving the issue of rapid biomolecule release (e.g., burst release) relies on multicomponent composite materials incorporating biomolecule-loaded carriers such as microspheres,²⁴¹ core-shell microcapsules,³⁶³ or nanospheres.^{242–244} Biomolecule carriers provide much more precise control over the release kinetics of the therapeutic agent and can greatly prolong the duration of biomolecule release.²⁴² As a result, multicomponent materials can deliver biomolecules gradually over extended periods ranging from weeks^{257,258} to even months,²⁴⁰ which considerably improves their capability to induce bone formation.^{257–259}

Another key challenge in the field of bioactive bone implant materials is tailoring the timing and order of biomolecule release to release patterns occurring in the physiological bone healing. This challenge can be addressed by the stimuli-responsive delivery platforms,¹⁹⁶ which release the biomolecules on-demand in response to specific stimuli (e.g., host cell-driven degradation of the polymer matrix) or preprogrammed delivery platforms secreting biomolecules at specified time intervals (e.g., implants releasing therapeutic agents by wireless control²⁷⁴).

An important factor hindering further advancements in bioactive materials for bone regeneration is low stability and the short half-life of biomolecules *in vivo*. The direction of research that seems the most promising in overcoming this problem is developing gene delivery platforms that allow *in situ* expression of factors promoting bone healing.^{323,339} These systems can effectively eliminate the problem of rapid loss of biomolecule activity at the target site by providing its

continuous expression and sustained release locally in the bone defect.^{326–330}

More studies are also necessary to improve control over the spatial distribution of the biomolecules or/and immobilized cells within the bioactive materials. The technology that can contribute to significant progress in this area is 3D bioprinting.³⁶⁴ This technology may enable manufacturing of personalized bone grafts combining multiple types of cells and materials loaded with different bioactive factors into a single platform. It is expected to allow us to recreate tissue-specific 3D organization of biochemical cues and cells within biomimetic bone tissue constructs in the near future. The development of cell-loaded bioactive materials able to sequentially deliver multiple biomolecules in a spatially and temporally controlled manner would represent a significant milestone in our progress toward smart biomaterials for bone regeneration applications.

As mentioned above, bone is a very complex multifunctional connective tissue whose properties allow it to perform several highly specialized functions in the human body. To serve its structural purposes and protect the vital organs (e.g., rib cage or braincase), bone has to be resilient. On the other hand, bones need to be stiff to provide the proper reaction to muscle contractions and withstand the applied forces (load). Moreover, bone remains a reservoir of minerals, particularly calcium and phosphate, and it provides niches for many cell types, including crucial progenitor and multipotent cells. To effectively carry out all of these tasks, the skeleton exists in a dynamic equilibrium characterized by continuous osteoclast-mediated bone resorption and osteoblast-mediated bone deposition. These highly orchestrated and simultaneous processes result in an imperceptible change in a bone mass called bone remodeling.³⁶⁵

Recently, the majority of studies on bone remodeling at the cellular level have focused on the roles of mature osteoblasts and osteoclasts and their respective precursor cells. It is worth noting that when mediating bone remodeling, there is growing recognition of the roles of two other types of cells found in bone, namely, osteocytes and bone lining cells. Osteocytes are mechanoreceptors derived from osteoblasts that remain trapped in the matrix.³⁶⁶ It has been proposed that osteocyte programmed cell death initiates the bone remodeling.³⁶⁷ The role of bone lining cells remains quite unclear and requires future investigation. However, it has been postulated that these cells play a role in the coupling of bone resorption to bone formation.³⁶⁸ It has also been confirmed that immune cells are capable of producing factors that both aid and suppress osteoclastogenesis. An altered balance between the expression of stimulating or suppressing factors will have an impact on bone homeostasis.³⁶⁷

Despite the unique capacities of self-regeneration and self-remodeling, several musculoskeletal diseases, such as osteogenesis imperfecta, osteoarthritis, osteomyelitis, and osteoporosis, can affect the physiological functions of bone tissue, which may have consequences on the quality of life of a patient. Furthermore, such diseases, combined with traumatic injuries, orthopedic surgeries, or primary tumor resection, may result in the damage and degeneration of tissues.³⁶⁹

One condition that comes with an increased risk of fracture in response to minimal or low velocity force and impaired bone regeneration is osteoporosis. Osteoporosis is defined by a decrease in bone strength due to lower bone density. In general, the areas most prone to fractures are the nonvertebral

areas. These sites are characterized by bone that is composed of mainly compact or cortical tissue that accounts for 80% of the total bone mass in an adult skeleton, while trabecular tissue makes up the remaining 20%.³⁷⁰ Peak bone mass is reached at the end of the third decade of human life. After this point, the balance between bone formation and bone resorption is impaired, with a relative increase in bone resorption that leads to net bone loss. According to recent research, after the age of 65, the majority of bone loss is cortical bone loss. Nonetheless, the postmenopause bone loss observed in women is mainly trabecular bone loss. The consequence of the imbalance between bone formation and resorption and the subsequent deterioration of the skeletal microarchitecture will result in the loss of bone tissue and bone strength.³⁷¹

The basic diagnostic techniques that determine bone strength and lead to targeted intervention strategies in osteoporosis treatment include BMD measurements, bone geometry determinations, evaluations of bone microstructure, extent of bone mineralization, and examinations of the properties of the bone matrix or the presence of a fragility fracture.³⁷² Osteoporotic fractures are associated with serious consequences, such as a diminished quality of life, decreased functional independence, and increased morbidity and mortality. Therefore, there is a great need to improve diagnostic strategies and optimize the prevention and treatment of osteoporosis.³⁶⁷

Taking these factors into consideration, an improved understanding of the pathophysiology of osteoporosis will result in better therapeutic and diagnostic procedures for this disease. It is worth noting, in light of the growing prevalence of osteoporosis and its association with the danger of trauma, discovering factors that can modulate the risk of osteoporotic trauma would significantly increase the number of people that qualify for treatment.³⁶⁷

Recently, the role of the immune system in the pathogenesis of osteoporosis has increasingly been recognized, prompting the emergence of the field of osteoimmunology. The immune system has been postulated to play an essential role in the etiology of bone disease by unbalancing the actions of bone-resorbing osteoclasts and bone-forming osteoblasts.^{372,373}

Clinical examinations of autoimmune disease samples have demonstrated that autoantibodies can induce the differentiation and activation of osteoclasts and alter bone mineral content. The immunological causes of bone destruction appear to stem from inflammation and autoimmunity. For instance, independent risk factors for the development of bone erosions and osteoporosis in rheumatoid arthritis (RA) are autoantibodies such as rheumatoid factor (RF) and anticitrullinated protein (ACPA).^{340,374,375}

RA is a chronic autoimmune inflammatory disease that is characterized by local bone erosion, joint space narrowing, and extra-articular manifestations caused by the production of two main autoantibodies, RF and ACPA, against common autoantigens that are widely expressed outside the joints. Severe cases of RA may result in periarticular osteopenia, systemic osteoporosis, and systemic bone erosion. Elevated inflammatory cytokines (such as TNF- α , IL-1, IL-6, IL-7, and IL-17) in RA are involved in bone destruction through the recruitment of osteoclast precursors to the bone environment, where they differentiate into mature cells. These inflammatory cytokines induce the overexpression of RANKL and decrease the levels of OPG (an alternate receptor of RANK), and this perturbation leads to increased osteoclastogenesis. Never-

theless, significant amounts of anti-inflammatory cytokines have also been reported to be present in RA joints. Cytokines, such as IL-10, IL-13, and TGF- β , negatively affect joint destruction and the inflammation associated with RA. In summary, chronic inflammation of the synovium and thus bone destruction in RA is caused by a complex network of inflammatory cytokines. Thus, therapies aimed at inflammatory cytokines and/or lymphocyte activation may modify RA treatment by blocking local and systemic inflammatory cascades and supporting the beneficial effects against bone and joint destruction.^{376–378}

RA along with other inflammatory autoimmune diseases (systemic lupus erythematosus (SLE), ankylosing spondylitis (AS), and inflammatory bowel disease (IBD)) continue to be increasing public health problems worldwide. A better understanding of the mechanisms by which the inflammatory cytokine network induces chronic inflammation in autoimmunity will provide new therapeutic approaches to reduce bone destruction in inflammatory autoimmune diseases.³⁷⁶ Even though primary bone cancers are rare, bone often becomes a plausible niche for the metastatic spread of various cancers. Surgical, irradiation, or chemotherapy-based cancer removal does not generally guarantee complete clearance of all cancer cells. On the other hand, several cancer treatment options may induce bone loss, causing or enhancing osteoporosis in these patients. Remnant tumor tissue promotes the release of inflammatory cytokines and osteoclast activation, which in turn, drive the excessive degradation of transplanted bone tissue or bone-mimicking implants. Traditional resection and reconstruction cannot provide adequate bone healing and regeneration in such cases.³⁷⁹ Recently, magnetic field-responsive nanoparticles containing Fe₃O₄ were developed to kill cancer cells in response to external magnetic field sources by elevating the temperature of the tissues in contact with nanoparticles. The magnetic field application is safe for the end user and leaves the normal surrounding tissue untouched. Intriguingly, the application of Fe₃O₄ nanoparticles and application of magnetic hyperthermia enhanced bone regeneration by an unclear mechanism.^{380,381} Other types of intelligent, tumor-killing materials were developed based on the controlled release of cytotoxic butyrate or Fe-CaSiO₃, which can be further enhanced by photothermal therapy.^{382,383} Such therapies are characterized by noninvasiveness and high controllability, showing great promise in bone tissue regeneration applications.

Before planning a therapeutic strategy aimed at treating specific diseases, it is important to recognize that bone regeneration is highly dependent on the formation of a new blood vessel network. The efficiency of the formation of new bone broadly depends on the growth rate and the extent of the blood vessels. Thus, when reconstructing large bone defects using cell-based tissue engineering, it is important to improve the strategies employed for bone vascularization. This is of particular importance when seeding cells in the central region of the scaffolds, as cells may die due to insufficient access to nutrients and oxygen. Traditional methods employed for engineering vascularized bone directly target the defect site, thus optimizing the healing process. Among them, we can include culturing BMSCs, endothelial progenitor cells, endothelial growth factors, and FGFs, along with endothelial cell monoculture and the coculture of endothelial cells and bone-forming cells. Despite its potential, the clinical applications of tissue-engineered vascularized bone are still

very limited. To determine the appropriate release kinetics of GFs and establish new tissue engineering scaffolds for inducing angiogenesis and bone morphogenesis, further research is needed. Finally, the newly designed scaffolds should also support the differentiation of stem cells into vascular precursors for osteogenesis.³⁸⁴

CONCLUSIONS

Globally, an estimated 175 million people suffer from bone fractures yearly, and many require implantation surgeries to fill in bone defects. Stimulation of the regeneration process of extensive bone tissue defects is challenging, and autologous graft is often excluded as an option to treat affected individuals. Significant defects can be the cause of the development of disabilities.

The growing field of bone replacement material engineering aids the healthcare systems in treating complex and extensive cases of bone loss. Currently, many innovative biomedical approaches are being tested worldwide to develop advanced bone regeneration strategies. The most advanced scaffolds are the fruits of the work of multidisciplinary research groups involving material chemists, material engineers, biologists, and medical professionals. Since the legislation process is demanding regarding product biosafety and biocompatibility, most advanced bone-replacement scaffolds are at various stages of design, preclinical, or clinical studies. A separate group of recipients are people whose bone loss is associated with degenerative diseases and cancer. Even more sophisticated and personally dedicated advanced solutions are needed in such cases, remaining the major challenge in the field of bone regeneration.

The “perfect scaffold” for treating bone defects would be made of biomaterials that mimic the properties of the natural bone, ideally containing living and dividing progenitor cells in its structure. Such an environment would support not only the growth and differentiation of bone tissue but also its vascularization and even innervation, which requires the presence of numerous signaling molecules, growth factors, and metabolites found in natural bone. The complexity of such a system causes problems in the fabrication of the perfect scaffold and in ensuring its stability and viability. The methodological advances presented in our review show that the scientific world is getting closer to formulating a recipe for producing a near-perfect implant. Functionalization of modern implants with osteoconductive fractions of hydroxyapatites, collagens, growth factors, bioactive peptides, and metabolites is entirely feasible thanks to overcoming technological gaps in material fabrication approaches.

Looking at the popularity of this research topic and the extensiveness and complexity of scientific approaches, we are convinced that, in the next few years, perfect implants will enter the healthcare market. These solutions will present ideal mechanical properties, be bioresorbable, and be fully replaced with the patients healthy and adequately vascularized bone tissue.

AUTHOR INFORMATION

Corresponding Author

Karolina Rudnicka – Department of Immunology and Infectious Biology, Faculty of Biology and Environmental Protection, University of Lodz, Lodz 90-136, Poland;
Email: karolina.rudnicka@biol.uni.lodz.pl

Authors

Aleksandra Szwed-Georgiou – Department of Immunology and Infectious Biology, Faculty of Biology and Environmental Protection, University of Lodz, Lodz 90-136, Poland

Przemysław Płociński – Department of Immunology and Infectious Biology, Faculty of Biology and Environmental Protection, University of Lodz, Lodz 90-136, Poland

Barbara Kupikowska-Stobba – Biomaterials Research Group, Lukasiewicz Research Network - Institute of Ceramics and Building Materials, Krakow 31-983, Poland

Mateusz M. Urbaniak – Department of Immunology and Infectious Biology, Faculty of Biology and Environmental Protection, University of Lodz, Lodz 90-136, Poland; The Bio-Med-Chem Doctoral School, University of Lodz and Lodz Institutes of the Polish Academy of Sciences, University of Lodz, Lodz 90-237, Poland; orcid.org/0000-0002-2800-2054

Paulina Rusek-Wala – Department of Immunology and Infectious Biology, Faculty of Biology and Environmental Protection, University of Lodz, Lodz 90-136, Poland; The Bio-Med-Chem Doctoral School, University of Lodz and Lodz Institutes of the Polish Academy of Sciences, University of Lodz, Lodz 90-237, Poland; orcid.org/0000-0001-7698-4710

Konrad Szustakiewicz – Department of Polymer Engineering and Technology, Faculty of Chemistry, Wrocław University of Technology, Wrocław 50-370, Poland

Paweł Piszko – Department of Polymer Engineering and Technology, Faculty of Chemistry, Wrocław University of Technology, Wrocław 50-370, Poland; orcid.org/0000-0002-7577-8509

Agnieszka Krupa – Department of Immunology and Infectious Biology, Faculty of Biology and Environmental Protection, University of Lodz, Lodz 90-136, Poland

Monika Biernat – Biomaterials Research Group, Lukasiewicz Research Network - Institute of Ceramics and Building Materials, Krakow 31-983, Poland

Malgorzata Gazińska – Department of Polymer Engineering and Technology, Faculty of Chemistry, Wrocław University of Technology, Wrocław 50-370, Poland; orcid.org/0000-0002-2972-7620

Mirosław Kasprzak – Biomaterials Research Group, Lukasiewicz Research Network - Institute of Ceramics and Building Materials, Krakow 31-983, Poland

Katarzyna Nawrotek – Faculty of Process and Environmental Engineering, Lodz University of Technology, Lodz 90-924, Poland; orcid.org/0000-0001-6371-2257

Nuno Pereira Mira – iBB-Institute for Bioengineering and Biosciences, Department of Bioengineering, Instituto Superior Técnico, Universidade de Lisboa, Lisboa 1049-001, Portugal; Associate Laboratory i4HB-Institute for Health and Bioeconomy at Instituto Superior Técnico, Universidade de Lisboa, Lisboa 1049-001, Portugal; Instituto Superior Técnico, Universidade de Lisboa, Lisboa 1049-001, Portugal; orcid.org/0000-0001-7556-0385

Complete contact information is available at:

<https://pubs.acs.org/10.1021/acsbiomaterials.3c00609>

Author Contributions

A.S.-G. (conceptualization, writing-original draft preparation, literature search, and editing), P.P. (conceptualization, writing-original draft preparation), B.K.-S. (conceptualization, writing-original draft, figure preparation, writing - review & editing),

M.M.U. (writing and editing, figure preparation), P.R.-W. (writing and editing, figure preparation), K.S. (writing-sections), P.P. (writing-sections), A.K. (review-biological aspects), M.B. (review-chemical aspects), M.G. (review-biomaterial/composites sections), M.K. (writing), K.N. (writing), N.P.M. (review-chemical engineering), and K.R. (supervision, funding acquisition, coordination of the writing process).

Notes

The authors declare no competing financial interest.

ACKNOWLEDGMENTS

This research was funded by the Foundation for Polish Science through the European Union under the European Regional Development Fund, within the TEAM-NET program entitled “Multifunctional biologically active composite for application in bone regenerative medicine” (POIR.04.04.00-00-16D7/18-00). The work of Karolina Rudnicka (Poland) and Nuno Pereira Mira (Portugal) was done within the cooperation in framework of EuroMicroH-COST Action CA18113.

REFERENCES

- (1) Willers, C.; Norton, N.; Harvey, N. C.; Jacobson, T.; Johansson, H.; Lorentzon, M.; McCloskey, E. V.; Borgström, F.; Kanis, J. A. Osteoporosis in Europe: A compendium of country-specific reports. *Arch. Osteoporosis* **2022**, *17* (1), No. 23.
- (2) Kanis, J. A.; Norton, N.; Harvey, N. C.; Jacobson, T.; Johansson, H.; Lorentzon, M.; McCloskey, E. V.; Willers, C.; Borgström, F. SCOPE 2021: A new scorecard for osteoporosis in Europe. *Arch. Osteoporosis* **2021**, *16* (1), No. 82.
- (3) What is osteoporosis and what causes it?. *Bone Health & Osteoporosis Foundation (BHOFF)*. 2023. <https://www.bonehealthandosteoporosis.org/patients/what-is-osteoporosis/> (accessed 2023-07-21).
- (4) Antimicrobial resistance surveillance in Europe 2023–2021 data. *European Centre for Disease Prevention and Control and World Health Organization*. 2023. <https://www.ecdc.europa.eu/en/publications-data/antimicrobial-resistance-surveillance-europe-2023-2021-data> (accessed 2023-07-21).
- (5) Uskoković, V.; Janković-Častvan, I.; Wu, V. M. Bone mineral crystallinity governs the orchestration of ossification and resorption during bone remodeling. *ACS Biomaterials Science & Engineering* **2019**, *5* (7), 3483–3498.
- (6) Lin, X.; Patil, S.; Gao, Y. G.; Qian, A. The Bone Extracellular Matrix in Bone Formation and Regeneration. *Front. Pharmacol.* **2020**, *11*, No. 757, DOI: 10.3389/fphar.2020.00757.
- (7) Hu, C.; Ashok, D.; Nisbet, D. R.; Gautam, V. Bioinspired surface modification of orthopedic implants for bone tissue engineering. *Biomaterials* **2019**, *219*, 119366.
- (8) Ansari, M. Bone tissue regeneration: Biology, strategies and interface studies. *Progress in Biomaterials* **2019**, *8* (4), 223–237.
- (9) Zhu, Y. S.; Gu, Y.; Jiang, C.; Chen, L. Osteonectin regulates the extracellular matrix mineralization of osteoblasts through P38 signaling pathway. *Journal of Cellular Physiology* **2020**, *235* (3), 2220–2231.
- (10) Tzaphlidou, M. Bone architecture: collagen structure and calcium/phosphorus maps. *Journal of Biological Physics* **2008**, *34*, 39–49.
- (11) Garnero, P. The role of collagen organization on the properties of bone. *Calcified Tissue International* **2015**, *97*, 229–240.
- (12) Fernández-Tresguerres-Hernández-Gil, I.; Alobera-Gracia, M. A.; del-Canto-Pingarrón, M.; Blanco-Jerez, L. Physiological bases of bone regeneration I. Histology and physiology of bone tissue. *Med Oral Patol Oral Cir Bucal* **2006**, *11* (1), E47–E51.
- (13) Bailey, A.; Poundarik, A.; Sroga, G.; Vashishth, D. Structural role of osteocalcin and its modification in bone fracture. *Applied Physics Reviews* **2023**, *10*, 011410.
- (14) Manolagas, S. C. Osteocalcin promotes bone mineralization but is not a hormone. *PLoS Genetics* **2020**, *16* (6), e1008714.
- (15) Roach, H. Why does bone matrix contain non-collagenous proteins? The possible roles of osteocalcin, osteonectin, osteopontin and bone sialoprotein in bone mineralisation and resorption. *Cell Biol. Int.* **1994**, *18* (6), 617–628.
- (16) Hauschka, P. V.; Lian, J. B.; Cole, D. E.; Gundberg, C. M. Osteocalcin and matrix Gla protein: Vitamin K-dependent proteins in bone. *Physiol. Rev.* **1989**, *69* (3), 990–1047.
- (17) Hauschka, P. V.; Wians, F. H. Osteocalcin-hydroxyapatite interaction in the extracellular organic matrix of bone. *Anatomical Record* **1989**, *224* (2), 180–188.
- (18) Carvalho, M. S.; Cabral, J. M. S.; da Silva, C. L.; Vashishth, D. Synergistic effect of extracellularly supplemented osteopontin and osteocalcin on stem cell proliferation, osteogenic differentiation, and angiogenic properties. *Journal of Cellular Biochemistry* **2019**, *120*, 6555–6569.
- (19) Knepper-Nicolai, B.; Reinstorf, A.; Hofinger, I.; Flade, K.; Wenz, R.; Pompe, W. Influence of osteocalcin and collagen I on the mechanical and biological properties of Biocement D. *Biomolecular Engineering* **2002**, *19* (2–6), 227–231.
- (20) Rammelt, S.; Neumann, M.; Hanisch, U.; Reinstorf, A.; Pompe, W.; Zwipp, H.; Biewener, A. Osteocalcin enhances bone remodeling around hydroxyapatite/collagen composites. *J. Biomed. Mater. Res., Part A* **2005**, *73A* (3), 284–294.
- (21) Bradshaw, A. D. Diverse biological functions of the SPARC family of proteins. *International Journal of Biochemistry & Cell Biology* **2012**, *44* (3), 480–488.
- (22) Murphy-Ullrich, J. E.; Sage, E. H. Revisiting the matricellular concept. *Matrix Biology* **2014**, *37*, 1–14.
- (23) Termine, J. D.; Kleinman, H. K.; Whitson, S. W.; Conn, K. M.; McGarvey, M. L.; Martin, G. R. Osteonectin, a bone-specific protein linking mineral to collagen. *Cell* **1981**, *26* (1), 99–105.
- (24) Nakase, T.; Takaoka, K.; Hirakawa, K.; Hirota, S.; Takemura, T.; Onoue, H.; Takebayashi, K.; Kitamura, Y.; Nomura, S. Alterations in the expression of osteonectin, osteopontin and osteocalcin mRNAs during the development of skeletal tissues in vivo. *Bone and Mineral* **1994**, *26* (2), 109–122.
- (25) Bradshaw, A. D.; Sage, E. H. SPARC, a matricellular protein that functions in cellular differentiation and tissue response to injury. *J. Clin. Invest.* **2001**, *107* (9), 1049–1054.
- (26) Zhu, Y.; Wang, J.; Wu, J.; Zhang, J.; Wan, Y.; Wu, H. Injectable hydrogels embedded with alginate microspheres for controlled delivery of bone morphogenetic protein-2. *Biomedical Materials* **2016**, *11* (2), 025010.
- (27) Tamma, R.; Carbone, C.; Colucci, S. Bone matrix proteins and mineralization process. In *Imaging of prosthetic joints: A combined radiological and clinical perspective*; Albanese, C. V., Faletti, C., Eds.; Springer Milan; Milano, 2014; pp 15–25.
- (28) McKee, M. D.; Pedraza, C. E.; Kaartinen, M. T. Osteopontin and wound healing in bone. *Cells Tissues Organs* **2011**, *194* (2–4), 313–319.
- (29) Nikel, O.; Laurencin, D.; McCallum, S. A.; Gundberg, C. M.; Vashishth, D. NMR investigation of the role of osteocalcin and osteopontin at the organic-inorganic interface in bone. *Langmuir: The ACS Journal of Surfaces and Colloids* **2013**, *29* (45), 13873–13882.
- (30) Sun, Y.; Jiang, Y.; Liu, Q.; Gao, T.; Feng, J. Q.; Dechow, P.; D’Souza, R. N.; Qin, C.; Liu, X. Biomimetic engineering of nanofibrous gelatin scaffolds with noncollagenous proteins for enhanced bone regeneration. *Tissue Engineering. Part A* **2013**, *19* (15–16), 1754–1763.
- (31) Pountos, I.; Panteli, M.; Lampropoulos, A.; Jones, E.; Calori, G. M.; Giannoudis, P. V. The role of peptides in bone healing and regeneration: A systematic review. *BMC Medicine* **2016**, *14*, 103.

- (32) Wang, C.; Liu, Y.; Fan, Y.; Li, X. The use of bioactive peptides to modify materials for bone tissue repair. *Regenerative Biomaterials* **2017**, *4* (3), 191–206.
- (33) Falcigno, L.; D'Auria, G.; Calvanese, L.; Marasco, D.; Iacobelli, R.; Scognamiglio, P. L.; Brun, P.; Danesin, R.; Pasqualin, M.; Castagliuolo, I.; Dettin, M. Osteogenic properties of a short BMP-2 chimera peptide. *Journal of Peptide Science* **2015**, *21* (9), 700–709.
- (34) Reddi, A. H.; Reddi, A. Bone morphogenetic proteins (BMPs): From morphogens to metabologens. *Cytokine & Growth Factor Reviews* **2009**, *20* (5–6), 341–342.
- (35) Zhou, X.; Feng, W.; Qiu, K.; Chen, L.; Wang, W.; Nie, W.; Mo, X.; He, C. BMP-2 derived peptide and dexamethasone incorporated mesoporous silica nanoparticles for enhanced osteogenic differentiation of bone mesenchymal stem cells. *ACS Appl. Mater. Interfaces* **2015**, *7* (29), 15777–15789.
- (36) Li, R.; Zhou, C.; Chen, J.; Luo, H.; Li, R.; Chen, D.; Zou, X.; Wang, W. Synergistic osteogenic and angiogenic effects of KP and QK peptides incorporated with an injectable and self-healing hydrogel for efficient bone regeneration. *Bioact Mater* **2022**, *18*, 267–283.
- (37) Ross, A.; Sauce-Guevara, M. A.; Alarcon, E. I.; Mendez-Rojas, M. A. Peptide Biomaterials for Tissue Regeneration. *Front. Bioeng. Biotechnol.* **2022**, *10*, No. 893936.
- (38) Song, Y.; Wu, C.; Zhang, X.; Bian, W.; Liu, N.; Yin, S.; Yang, M. F.; Luo, M.; Tang, J.; Yang, X. A short peptide potentially promotes the healing of skin wound. *Biosci. Rep.* **2019**, *39* (3), No. BSR20181734.
- (39) Correa, R.; Arenas, J.; Montoya, G.; Hoz, L.; Lopez, S.; Salgado, F.; Arroyo, R.; Salmeron, N.; Romo, E.; Zeichner-David, M.; Arzate, H. Synthetic cementum protein 1-derived peptide regulates mineralization in vitro and promotes bone regeneration in vivo. *FASEB J.* **2019**, *33* (1), 1167–1178.
- (40) Bhatt, M. P.; Lim, Y. C.; Hwang, J. Y.; Na, S. H.; Kim, Y. M.; Ha, K. S. C-peptide prevents hyperglycemia-induced endothelial apoptosis through inhibition of reactive oxygen species-mediated transglutaminase 2 activation. *Diabetes* **2013**, *62* (1), 243–253.
- (41) Ma, Y.; Zhao, S.; Shen, S.; Fang, S.; Ye, Z.; Shi, Z.; Hong, A. A novel recombinant slow-release TNF α -derived peptide effectively inhibits tumor growth and angiogenesis. *Sci. Rep.* **2015**, *5*, No. 13595.
- (42) Landis, W. J.; Jacquet, R. Association of calcium and phosphate ions with collagen in the mineralization of vertebrate tissues. *Calcified Tissue International* **2013**, *93* (4), 329–337.
- (43) Tavafoghi, M.; Cerruti, M. The role of amino acids in hydroxyapatite mineralization. *Journal of the Royal Society, Interface* **2016**, *13* (123), 20160462.
- (44) Sinha, S.; Goel, S. C. Effect of amino acids lysine and arginine on fracture healing in rabbits: A radiological and histomorphological analysis. *Indian Journal of Orthopaedics* **2009**, *43* (4), 328–334.
- (45) Zhang, T.; Chen, S.; Zhang, Y.; Xiao, X. Application of amino acids in the modification of polylactic acid nanofiber scaffolds. *International Journal of Polymeric Materials and Polymeric Biomaterials* **2023**, *72* (2), 101–107.
- (46) Devescovi, V.; Leonardi, E.; Ciapetti, G.; Cenni, E. Growth factors in bone repair. *La Chirurgia degli Organi di Movimento* **2008**, *92* (3), 161–168.
- (47) Khan, S. N.; Bostrom, M. P. G.; Lane, J. M. Bone growth factors. *Orthopedic Clinics of North America* **2000**, *31* (3), 375–387.
- (48) Agarwal, A.; Singh, N.; Khan, M.; Nabi Khan, S. M.; Sahu, K.; Jadhav, S. Role of growth factors in bone regeneration. *International Journal of Preventive and Clinical Dental Research* **2020**, *7* (3), 69–71.
- (49) Nauth, A.; Ristevski, B.; Li, R.; Schemitsch, E. H. Growth factors and bone regeneration: How much bone can we expect? *Injury* **2011**, *42* (6), 574–579.
- (50) Reddi, A. H. BMPs: From bone morphogenetic proteins to body morphogenetic proteins. *Cytokine & Growth Factor Reviews* **2005**, *16* (3), 249–250.
- (51) Charoenlarp, P.; Rajendran, A. K.; Iseki, S. Role of fibroblast growth factors in bone regeneration. *Inflammation and Regeneration* **2017**, *37*, 10.
- (52) Barrientos, S.; Stojadinovic, O.; Golinko, M. S.; Brem, H.; Tomic-Canic, M. Growth factors and cytokines in wound healing. *Wound Repair and Regeneration* **2008**, *16* (5), 585–601.
- (53) Werner, S.; Grose, R. Regulation of wound healing by growth factors and cytokines. *Physiol Rev* **2003**, *83*, 835–870.
- (54) Ozturk, B. Y.; Inci, I.; Egri, S.; Ozturk, A. M.; Yetkin, H.; Goktas, G.; Elmas, C.; Piskin, E.; Erdogan, D. The treatment of segmental bone defects in rabbit tibiae with vascular endothelial growth factor (VEGF)-loaded gelatin/hydroxyapatite “cryogel” scaffold. *European Journal of Orthopaedic Surgery & Traumatology* **2013**, *23* (7), 767–774.
- (55) Chen, Y.; Wu, T.; Huang, S.; Suen, C. W. W.; Cheng, X.; Li, J.; Hou, H.; She, H.; Zhang, H.; Wang, H.; Zheng, X.; Zha, Z. Sustained release SDF-1 α /TGF- β 1-loaded silk fibroin-porous gelatin scaffold promotes cartilage repair. *ACS Appl. Mater. Interfaces* **2019**, *11* (16), 14608–14618.
- (56) Gimeno, E. J.; Muñoz-Torres, M.; Escobar-Jiménez, F.; Charneco, M. Q.; Castillo, J. D. L. D.; Oleà, N. Identification of metabolic bone disease in patients with endogenous hyperthyroidism: Role of biological markers of bone turnover. *Calcified Tissue International* **1997**, *61* (5), 370–376.
- (57) Canalis, E.; McCarthy, T. L.; Centrella, M. The role of growth factors in skeletal remodeling. *Endocrinology and Metabolism Clinics of North America* **1989**, *18* (4), 903–918.
- (58) Wojda, S. J.; Donahue, S. W. Parathyroid hormone for bone regeneration. *Journal of Orthopaedic Research* **2018**, *36* (10), 2586–2594.
- (59) Paridis, D.; Karachalios, T. Atrophic femoral bone nonunion treated with 1-84 PTH. *Journal of Musculoskeletal and Neuronal Interactions* **2011**, *11* (4), 320–323.
- (60) Fernández-Tresguerres-Hernández-Gil, I.; Alobera-Gracia, M. A.; del-Canto-Pingarrón, M.; Blanco-Jerez, L. Physiological bases of bone regeneration II. The remodeling process. *Med Oral Patol Oral Cir Buca* **2006**, *11* (2), E151–E157.
- (61) Tian, G.; Zhang, G.; Tan, Y. H. Calcitonin gene-related peptide stimulates BMP-2 expression and the differentiation of human osteoblast-like cells in vitro. *Acta Pharmacologica Sinica* **2013**, *34* (11), 1467–1474.
- (62) Raisz, L. G. Bone cell biology: New approaches and unanswered questions. *Journal of Bone and Mineral Research* **1993**, *8* (S2), S457–S465.
- (63) Hofbauer, L. C.; Khosla, S.; Dunstan, C. R.; Lacey, D. L.; Spelsberg, T. C.; Riggs, B. L. Estrogen stimulates gene expression and protein production of osteoprotegerin in human osteoblastic cells. *Endocrinology* **1999**, *140* (9), 4367–4370.
- (64) Kream, B. E.; Graves, L.; Lukert, B. P. Clinical and basic aspects of glucocorticoid action in bone A2. *Principles of Bone Biology (Second Edition)*; Elsevier: 2008; Chapter 41, pp 723–740. DOI: 10.1016/B978-012098652-1.50143-8
- (65) Ferron, M.; Wei, J.; Yoshizawa, T.; Del Fattore, A.; DePinho, R. A.; Teti, A.; Ducy, P.; Karsenty, G. Insulin signaling in osteoblasts integrates bone remodeling and energy metabolism. *Cell* **2010**, *142* (2), 296–308.
- (66) Klein, G. L. Insulin and bone: Recent developments. *World Journal of Diabetes* **2014**, *5* (1), 14–16.
- (67) Barbalho, S. M.; Araújo, A. C.; Detregiachi, C. R. P.; Buchaim, D. V.; Guiguer, É. L. The potential role of medicinal plants in bone regeneration. *Altern Ther Health Med* **2019**, *25* (4), 32–39.
- (68) Preethi Soundarya, S.; Sanjay, V.; Haritha Menon, A.; Dhivya, S.; Selvamurugan, N. Effects of flavonoids incorporated biological macromolecules based scaffolds in bone tissue engineering. *Int. J. Biol. Macromol.* **2018**, *110*, 74–87.
- (69) Han, Q. Q.; Du, Y.; Yang, P. S. The role of small molecules in bone regeneration. *Future Medicinal Chemistry* **2013**, *5* (14), 1671–1684.
- (70) Kuang, M. J.; Zhang, W. H.; He, W. W.; Sun, L.; Ma, J. X.; Wang, D.; Ma, X. L. Naringin regulates bone metabolism in glucocorticoid-induced osteonecrosis of the femoral head via the

Akt/Bad signal cascades. *Chemico-Biological Interactions* **2019**, *304*, 97–105.

(71) Peng, Z.; Dai, K. R.; Yan, S. G.; Yan, W. Q.; Chao, Z.; Chen, D. Q.; Xu, B.; Xu, Z. W. Effects of naringin on the proliferation and osteogenic differentiation of human bone mesenchymal stem cell. *Eur. J. Pharmacol.* **2009**, *607* (1–3), 1–5.

(72) Yang, X.; Almassri, H. N. S.; Zhang, Q.; Ma, Y.; Zhang, D.; Chen, M.; Wu, X. Electrospayed naringin-loaded microsphere/SAIB hybrid depots enhance bone formation in a mouse calvarial defect model. *Drug Delivery* **2019**, *26* (1), 137–146.

(73) Song, J. E.; Jeon, Y. S.; Tian, J.; Kim, W. K.; Choi, M. J.; Carlomagno, C.; Khang, G. Evaluation of silymarin/duck's feet-derived collagen/hydroxyapatite sponges for bone tissue regeneration. *Materials Science and Engineering: C* **2019**, *97*, 347–355.

(74) Bafna, P. S.; Patil, P. H.; Maru, S. K.; Mutha, R. E. Cissus quadrangularis L: A comprehensive multidisciplinary review. *Journal of Ethnopharmacology* **2021**, *279*, 114355.

(75) Parisuthiman, D.; Singhatanadgit, W.; Dechatiwongse, T.; Koontongkaew, S. Cissus quadrangularis extract enhances biomineralization through up-regulation of MAPK-dependent alkaline phosphatase activity in osteoblasts. *In Vitro Cellular & Developmental Biology - Animal* **2009**, *45* (3–4), 194–200.

(76) Soumya, S.; Sajesh, K. M.; Jayakumar, R.; Nair, S. V.; Chennazhi, K. P. Development of a phytochemical scaffold for bone tissue engineering using Cissus quadrangularis extract. *Carbohydr. Polym.* **2012**, *87* (2), 1787–1795.

(77) Suganya, S.; Venugopal, J.; Ramakrishna, S.; Lakshmi, B. S.; Giri Dev, V. R. Herbally derived polymeric nanofibrous scaffolds for bone tissue regeneration. *J. Appl. Polym. Sci.* **2014**, *131* (3), 39835.

(78) Abdul, Q. A.; Choi, R. J.; Jung, H. A.; Choi, J. S. Health benefit of fucosterol from marine algae: A review. *Journal of the Science of Food and Agriculture* **2016**, *96* (6), 1856–1866.

(79) Hannan, M. A.; Sohag, A. A. M.; Dash, R.; Haque, M. N.; Mohibullah, Md.; Oktaviani, D. F.; Hossain, M. T.; Choi, H. J.; Moon, I. S. Phytosterols of marine algae: Insights into the potential health benefits and molecular pharmacology. *Phytomedicine* **2020**, *69*, 153201.

(80) Lee, D. G.; Park, S. Y.; Chung, W. S.; Park, J. H.; Shin, H. S.; Hwang, E.; Kim, I. H.; Yi, T. H. The bone regenerative effects of fucosterol in vitro and in vivo models of postmenopausal osteoporosis. *Molecular Nutrition & Food Research* **2014**, *58* (6), 1249–1257.

(81) Yan, C. P.; Wang, X. K.; Jiang, K.; Yin, C.; Xiang, C.; Wang, Y.; Pu, C.; Chen, L.; Li, Y. L. β -Ecdysterone enhanced bone regeneration through the BMP-2/SMAD/RUNX2/osterix signaling pathway. *Frontiers in Cell and Developmental Biology* **2022**, *10*, 883228.

(82) Hokugo, A.; Sorice, S.; Parhami, F.; Yalom, A.; Li, A.; Zuk, P.; Jarrahy, R. A novel oxysterol promotes bone regeneration in rabbit cranial bone defects. *Journal of Tissue Engineering and Regenerative Medicine* **2016**, *10* (7), 591–599.

(83) Cui, Z. K.; Kim, S.; Baljon, J. J.; Doroudgar, M.; Lafleur, M.; Wu, B. M.; Aghaloo, T.; Lee, M. Design and characterization of a therapeutic non-phospholipid liposomal nanocarrier with osteoinductive characteristics to promote bone formation. *ACS Nano* **2017**, *11* (8), 8055–8063.

(84) Lee, J. S.; Kim, E. J.; Han, S.; Kang, K. L.; Heo, J. S. Evaluating the oxysterol combination of 22(S)-hydroxycholesterol and 20(S)-hydroxycholesterol in periodontal regeneration using periodontal ligament stem cells and alveolar bone healing models. *Stem Cell Research & Therapy* **2017**, *8* (1), 276.

(85) Kwon, I. K.; Lee, S. C.; Hwang, Y. S.; Heo, J. S. Mitochondrial function contributes to oxysterol-induced osteogenic differentiation in mouse embryonic stem cells. *Biochimica et Biophysica Acta (BBA)* **2015**, *1853* (3), 561–572.

(86) Aghaloo, T. L.; Amantea, C. M.; Cowan, C. M.; Richardson, J. A.; Wu, B. M.; Parhami, F.; Tetradis, S. Oxysterols enhance osteoblast differentiation in vitro and bone healing in vivo. *Journal of Orthopaedic Research* **2007**, *25* (11), 1488–1497.

(87) Johnson, J. S.; Meliton, V.; Kim, W. K.; Lee, K. B.; Wang, J. C.; Nguyen, K.; Yoo, D.; Jung, M. E.; Atti, E.; Tetradis, S.; Pereira, R. C.; Magyar, C.; Nargizyan, T.; Hahn, T. J.; Farouz, F.; Thies, S.; Parhami, F. Novel oxysterols have pro-osteogenic and anti-adipogenic effects in vitro and induce spinal fusion in vivo. *Journal of Cellular Biochemistry* **2011**, *112* (6), 1673–1684.

(88) Cottrill, E.; Lazzari, J.; Pennington, Z.; Ehresman, J.; Schilling, A.; Dirckx, N.; Theodore, N.; Sciubba, D.; Witham, T. Oxysterols as promising small molecules for bone tissue engineering: Systematic review. *World Journal of Orthopedics* **2020**, *11* (7), 328–344.

(89) Kang, M.; Lee, C. S.; Lee, M. Bioactive scaffolds integrated with liposomal or extracellular vesicles for bone regeneration. *Bioengineering (Basel, Switzerland)* **2021**, *8* (10), 137.

(90) Lee, C. S.; Kim, S.; Fan, J.; Hwang, H. S.; Aghaloo, T.; Lee, M. Smoothened agonist sterosome immobilized hybrid scaffold for bone regeneration. *Science Advances* **2020**, *6* (17), eaaz7822.

(91) Park, J.; Lutz, R.; Felszeghy, E.; Wiltfang, J.; Nkenke, E.; Neukam, F. W.; Schlegel, K. A. The effect on bone regeneration of a liposomal vector to deliver BMP-2 gene to bone grafts in peri-implant bone defects. *Biomaterials* **2007**, *28* (17), 2772–2782.

(92) Cheng, R.; Liu, L.; Xiang, Y.; Lu, Y.; Deng, L.; Zhang, H.; Santos, H. A.; Cui, W. Advanced liposome-loaded scaffolds for therapeutic and tissue engineering applications. *Biomaterials* **2020**, *232*, 119706.

(93) Montagnani, A.; Gonnelli, S.; Cepollaro, C.; Pacini, S.; Campagna, M. S.; Franci, M. B.; Lucani, B.; Gennari, C. Effect of simvastatin treatment on bone mineral density and bone turnover in hypercholesterolemic postmenopausal women: A 1-year longitudinal study. *Bone* **2003**, *32* (4), 427–433.

(94) Ayukawa, Y.; Okamura, A.; Koyano, K. Simvastatin promotes osteogenesis around titanium implants. A histological and histometrical study in rats. *Clinical Oral Implants Research* **2004**, *15* (3), 346–350.

(95) Wong, R. W. K.; Rabie, A. B. M. Early healing pattern of statin-induced osteogenesis. *British Journal of Oral and Maxillofacial Surgery* **2005**, *43* (1), 46–50.

(96) Wong, R. W. K.; Rabie, A. B. M. Histologic and ultrastructural study on statin graft in rabbit skulls. *Journal of Oral and Maxillofacial Surgery* **2005**, *63* (10), 1515–1521.

(97) Moriyama, Y.; Ayukawa, Y.; Ogino, Y.; Atsuta, I.; Todo, M.; Takao, Y.; Koyano, K. Local application of fluvastatin improves peri-implant bone quantity and mechanical properties: A rodent study. *Acta Biomaterialia* **2010**, *6* (4), 1610–1618.

(98) Masuzaki, T.; Ayukawa, Y.; Moriyama, Y.; Jinno, Y.; Atsuta, I.; Ogino, Y.; Koyano, K. The effect of a single remote injection of statin-impregnated poly (lactic-co-glycolic acid) microspheres on osteogenesis around titanium implants in rat tibia. *Biomaterials* **2010**, *31* (12), 3327–3334.

(99) Rakhmatia, Y. D.; Ayukawa, Y.; Furuhashi, A.; Koyano, K. Carbonate apatite containing statin enhances bone formation in healing incisal extraction sockets in rats. *Materials (Basel, Switzerland)* **2018**, *11* (7), 1201.

(100) Chamani, S.; Liberale, L.; Mobasher, L.; Montecucco, F.; Al-Rasadi, K.; Jamialahmadi, T.; Sahebkar, A. The role of statins in the differentiation and function of bone cells. *European Journal of Clinical Investigation* **2021**, *51* (7), e13534.

(101) Hernández-Arriaga, A. M.; Campano, C.; Rivero-Buceta, V.; Prieto, M. A. When microbial biotechnology meets material engineering. *Microbial Biotechnology* **2022**, *15* (1), 149–163.

(102) Moradali, M. F.; Rehm, B. H. A. Bacterial biopolymers: From pathogenesis to advanced materials. *Nature Reviews. Microbiology* **2020**, *18* (4), 195–210.

(103) Lahiri, D.; Nag, M.; Dutta, B.; Dey, A.; Sarkar, T.; Pati, S.; Edinur, H. A.; Kari, Z. A.; Noor, N. H. M.; Ray, R. R. Bacterial cellulose: Production, characterization, and application as antimicrobial agent. *International Journal of Molecular Sciences* **2021**, *22* (23), 12984.

(104) Thongwai, N.; Futui, W.; Ladpala, N.; Sirichai, B.; Weechan, A.; Kanklai, J.; Rungsirivanich, P. Characterization of bacterial

cellulose produced by komagataeibacter maltaceti P285 isolated from contaminated honey wine. *Microorganisms* **2022**, *10* (3), 528.

(105) Farnezi Bassi, A. P.; Bizelli, V. F.; Brasil, L. F. D. M.; Pereira, J. C.; Al-Sharani, H. M.; Momesso, G. A. C.; Faverani, L. P.; Lucas, F. d. A. Is the bacterial cellulose membrane feasible for osteopromotive property? *Membranes (Basel)* **2020**, *10* (9), 230.

(106) Huang, C.; Ye, Q.; Dong, J.; Li, L.; Wang, M.; Zhang, Y.; Zhang, Y.; Wang, X.; Wang, P.; Jiang, Q. Biofabrication of natural Au/bacterial cellulose hydrogel for bone tissue regeneration via in-situ fermentation. *Smart Materials in Medicine* **2023**, *4*, 1–14.

(107) Kheiry, E. V.; Parivar, K.; Baharara, J.; Bazzaz, B. S. F.; Iranbakhsh, A. The osteogenesis of bacterial cellulose scaffold loaded with fisetin. *Iran J Basic Med Sci* **2018**, *21* (9), 965–971.

(108) Saska, S.; Barud, H. S.; Gaspar, A. M. M.; Marchetto, R.; Ribeiro, S. J. L.; Messaddeq, Y. Bacterial cellulose-hydroxyapatite nanocomposites for bone regeneration. *Int J Biomater* **2011**, *2011*, 175362.

(109) Kumar, A.; Han, S. S. Efficacy of bacterial nanocellulose in hard tissue regeneration: A review. *Materials (Basel, Switzerland)* **2021**, *14* (17), 4777.

(110) Swingler, S.; Gupta, A.; Gibson, H.; Kowalczyk, M.; Heaselgrave, W.; Radecka, I. Recent advances and applications of bacterial cellulose in biomedicine. *Polymers* **2021**, *13* (3), 412.

(111) Bashir, K. M. I.; Choi, J. S. Clinical and physiological perspectives of β -glucans: The past, present, and future. *International Journal of Molecular Sciences* **2017**, *18* (9), 1906.

(112) Vlassopoulou, M.; Yannakoulia, M.; Pletsa, V.; Zervakis, G. I.; Kyriacou, A. Effects of fungal beta-glucans on health – a systematic review of randomized controlled trials. *Food & Function* **2021**, *12* (8), 3366–3380.

(113) Ariyoshi, W.; Hara, S.; Koga, A.; Nagai-Yoshioka, Y.; Yamasaki, R. Biological effects of β -glucans on osteoclastogenesis. *Molecules (Basel, Switzerland)* **2021**, *26* (7), 1982.

(114) Hara, S.; Nagai-Yoshioka, Y.; Yamasaki, R.; Adachi, Y.; Fujita, Y.; Watanabe, K.; Maki, K.; Nishihara, T.; Ariyoshi, W. Dectin-1-mediated suppression of RANKL-induced osteoclastogenesis by glucan from baker's yeast. *Journal of Cellular Physiology* **2021**, *236* (7), 5098–5107.

(115) Belcarz, A.; Ginalska, G.; Pycka, T.; Zima, A.; Ślósarczyk, A.; Polkowska, I.; Paszkiewicz, Z.; Piekarczyk, W. Application of β -1,3-glucan in production of ceramics-based elastic composite for bone repair. *Open Life Sciences* **2013**, *8* (6), 534–548.

(116) Borkowski, L.; Pawłowska, M.; Radzki, R. P.; Bieńko, M.; Polkowska, I.; Belcarz, A.; Karpiński, M.; Słowik, T.; Matuszewski, Ł.; Ślósarczyk, A.; Ginalska, G. Effect of a carbonated HAP/ β -glucan composite bone substitute on healing of drilled bone voids in the proximal tibial metaphysis of rabbits. *Materials Science and Engineering: C* **2015**, *53*, 60–67.

(117) Aquinas, N.; Bhat M, R.; Selvaraj, S. A review presenting production, characterization, and applications of biopolymer Curdlan in food and pharmaceutical sectors. *Polym. Bull.* **2022**, *79* (9), 6905–6927.

(118) Yamasaki, T.; Ariyoshi, W.; Okinaga, T.; Adachi, Y.; Hosokawa, R.; Mochizuki, S.; Sakurai, K.; Nishihara, T. The dectin 1 agonist Curdlan regulates osteoclastogenesis by inhibiting nuclear factor of activated T cells cytoplasmic 1 (NFATc1) through Syk kinase. *J. Biol. Chem.* **2014**, *289* (27), 19191–19203.

(119) Klimek, K.; Palka, K.; Truszkiewicz, W.; Douglas, T. E. L.; Nurzynska, A.; Ginalska, G. Could Curdlan/whey protein isolate/hydroxyapatite biomaterials be considered as promising bone scaffolds?-fabrication, characterization, and evaluation of cytocompatibility towards osteoblast cells in vitro. *Cells* **2022**, *11* (20), 3251.

(120) Przekora, A.; Palka, K.; Ginalska, G. Biomedical potential of chitosan/HA and chitosan/ β -1,3-glucan/HA biomaterials as scaffolds for bone regeneration — A comparative study. *Materials Science and Engineering: C* **2016**, *58*, 891–899.

(121) Toullec, C.; Le Bideau, J.; Geoffroy, V.; Halgand, B.; Buchtova, N.; Molina-Peña, R.; Garcion, E.; Avril, S.; Sindji, L.; Dube,

A.; Boury, F.; Jérôme, C. Curdlan-chitosan electrospun fibers as potential scaffolds for bone regeneration. *Polymers* **2021**, *13* (4), 526.

(122) Nadzir, M. M.; Nurhayati, R. W.; Idris, F. N.; Nguyen, M. H. Biomedical applications of bacterial exopolysaccharides: A review. *Polymers* **2021**, *13* (4), 530.

(123) Manda, M. G.; da Silva, L. P.; Cerqueira, M. T.; Pereira, D. R.; Oliveira, M. B.; Mano, J. F.; Marques, A. P.; Oliveira, J. M.; Correlo, V. M.; Reis, R. L. Gellan gum-hydroxyapatite composite spongy-like hydrogels for bone tissue engineering. *J. Biomed. Mater. Res., Part A* **2018**, *106* (2), 479–490.

(124) Lee, K. Y.; Mooney, D. J. Alginate: Properties and biomedical applications. *Prog. Polym. Sci.* **2012**, *37* (1), 106–126.

(125) Behzadi, P.; Baráth, Z.; Gajdács, M. It's not easy being green: A narrative review on the microbiology, virulence and therapeutic prospects of multidrug-resistant *Pseudomonas aeruginosa*. *Antibiotics (Basel, Switzerland)* **2021**, *10* (1), 42.

(126) Cavallini, C.; Vitiello, G.; Adinolfi, B.; Silvestri, B.; Armanetti, P.; Manini, P.; Pezzella, A.; d'Ischia, M.; Luciani, G.; Menichetti, L. Melanin and melanin-like hybrid materials in regenerative medicine. *Nanomaterials (Basel, Switzerland)* **2020**, *10* (8), 1518.

(127) Yoo, H. S.; Chung, K. H.; Lee, K. J.; Kim, D. H.; An, J. H. Melanin extract from *Gallus gallus domesticus* promotes proliferation and differentiation of osteoblastic MG-63 cells via bone morphogenetic protein-2 signaling. *Nutrition Research and Practice* **2017**, *11* (3), 190–197.

(128) Seeman, E.; Delmas, P. D. Bone quality — the material and structural basis of bone strength and fragility. *New England Journal of Medicine* **2006**, *354* (21), 2250–2261.

(129) Sowjanya, J. A.; Singh, J.; Mohita, T.; Sarvanan, S.; Moorthi, A.; Srinivasan, N.; Selvamurugan, N. Biocomposite scaffolds containing chitosan/alginate/nano-silica for bone tissue engineering. *Colloids Surf., B* **2013**, *109*, 294–300.

(130) Shen, F. H.; Samartzis, D.; An, H. S. Cell technologies for spinal fusion. *Spine Journal* **2005**, *5* (6), S231–S239.

(131) Kuboki, Y.; Jin, Q.; Kikuchi, M.; Mamood, J.; Takita, H. Geometry of artificial ECM: Sizes of pores controlling phenotype expression in BMP-induced osteogenesis and chondrogenesis. *Connective Tissue Research* **2002**, *43* (2), 529–534.

(132) Peter, M.; Binulal, N. S.; Nair, S. V.; Selvamurugan, N.; Tamura, H.; Jayakumar, R. Novel biodegradable chitosan–gelatin/nano-bioactive glass ceramic composite scaffolds for alveolar bone tissue engineering. *Chemical Engineering Journal* **2010**, *158* (2), 353–361.

(133) Bae, M. S.; Yang, D. H.; Lee, J. B.; Heo, D. N.; Kwon, Y.-D.; Youn, I. C.; Choi, K.; Hong, J. H.; Kim, G. T.; Choi, Y. S.; Hwang, E. H.; Kwon, I. K. Photo-cured hyaluronic acid-based hydrogels containing simvastatin as a bone tissue regeneration scaffold. *Biomaterials* **2011**, *32* (32), 8161–8171.

(134) Makvandi, P.; Ali, G. W.; Della Sala, F.; Abdel-Fattah, W. I.; Borzacchiello, A. Hyaluronic acid/corn silk extract based injectable nanocomposite: A biomimetic antibacterial scaffold for bone tissue regeneration. *Materials Science and Engineering: C* **2020**, *107*, 110195.

(135) Ber, S.; Köse, G. T.; Hasırcı, V. Bone tissue engineering on patterned collagen films: An in vitro study. *Biomaterials* **2005**, *26* (14), 1977–1986.

(136) Rodrigues, C. V. M.; Serricella, P.; Linhares, A. B. R.; Guerdes, R. M.; Borojevic, R.; Rossi, M. A.; Duarte, M. E. L.; Farina, M. Characterization of a bovine collagen–hydroxyapatite composite scaffold for bone tissue engineering. *Biomaterials* **2003**, *24* (27), 4987–4997.

(137) Ren, L.; Tsuru, K.; Hayakawa, S.; Osaka, A. Novel approach to fabricate porous gelatin–siloxane hybrids for bone tissue engineering. *Biomaterials* **2002**, *23* (24), 4765–4773.

(138) Torgbo, S.; Sukyai, P. Bacterial cellulose-based scaffold materials for bone tissue engineering. *Applied Materials Today* **2018**, *11*, 34–49.

(139) Sabir, M. I.; Xu, X.; Li, L. A review on biodegradable polymeric materials for bone tissue engineering applications. *J. Mater. Sci.* **2009**, *44* (21), 5713–5724.

- (140) Swetha, M.; Sahithi, K.; Moorthi, A.; Srinivasan, N.; Ramasamy, K.; Selvamurugan, N. Biocomposites containing natural polymers and hydroxyapatite for bone tissue engineering. *Int. J. Biol. Macromol.* **2010**, *47* (1), 1–4.
- (141) Luo, Z.; Pan, J.; Sun, Y.; Zhang, S.; Yang, Y.; Liu, H.; Li, Y.; Xu, X.; Sui, Y.; Wei, S. Injectable 3D porous micro-scaffolds with a bio-engine for cell transplantation and tissue regeneration. *Adv. Funct. Mater.* **2018**, *28* (41), 1804335.
- (142) Ju, J.; Peng, X.; Huang, K.; Li, L.; Liu, X.; Chitrakar, C.; Chang, L.; Gu, Z.; Kuang, T. High-performance porous PLLA-based scaffolds for bone tissue engineering: Preparation, characterization, and in vitro and in vivo evaluation. *Polymer* **2019**, *180*, 121707.
- (143) Lou, T.; Wang, X.; Song, G.; Gu, Z.; Yang, Z. Fabrication of PLLA/ β -TCP nanocomposite scaffolds with hierarchical porosity for bone tissue engineering. *Int. J. Biol. Macromol.* **2014**, *69*, 464–470.
- (144) Shor, L.; Güçeri, S.; Chang, R.; Gordon, J.; Kang, Q.; Hartsock, L.; An, Y.; Sun, W. Precision extruding deposition (PED) fabrication of polycaprolactone (PCL) scaffolds for bone tissue engineering. *Biofabrication* **2009**, *1* (1), 015003.
- (145) Yilgor, P.; Sousa, R. A.; Reis, R. L.; Hasirci, N.; Hasirci, V. 3D plotted PCL scaffolds for stem cell based bone tissue engineering. *Macromol. Symp.* **2008**, *269* (1), 92–99.
- (146) Wang, J. Z.; You, M. L.; Ding, Z. Q.; Ye, W. B. A review of emerging bone tissue engineering via PEG conjugated biodegradable amphiphilic copolymers. *Materials Science and Engineering: C* **2019**, *97*, 1021–1035.
- (147) Silva, J. C.; Udangawa, R. N.; Chen, J.; Mancinelli, C. D.; Garrudo, F. F. F.; Mikael, P. E.; Cabral, J. M. S.; Ferreira, F. C.; Linhardt, R. J. Kartogenin-loaded coaxial PGS/PCL aligned nanofibers for cartilage tissue engineering. *Materials Science & Engineering, C, Materials for Biological Applications* **2020**, *107*, 110291.
- (148) Mizumoto, S.; Inada, Y.; Weiland, A. Pre-formed vascularized bone grafts using polyethylene chambers. *Journal of Reconstructive Microsurgery* **1992**, *8* (4), 325–333.
- (149) Mizumoto, S.; Inada, Y.; Weiland, A. Fabrication of vascularized bone grafts using ceramic chambers. *Journal of Reconstructive Microsurgery* **1993**, *9* (6), 441–449.
- (150) Oliveira, J. M.; Rodrigues, M. T.; Silva, S. S.; Malafaya, P. B.; Gomes, M. E.; Viegas, C. A.; Dias, I. R.; Azevedo, J. T.; Mano, J. F.; Reis, R. L. Novel hydroxyapatite/chitosan bilayered scaffold for osteochondral tissue-engineering applications: Scaffold design and its performance when seeded with goat bone marrow stromal cells. *Biomaterials* **2006**, *27* (36), 6123–6137.
- (151) Venkatesan, J.; Kim, S. K. Nano-hydroxyapatite composite biomaterials for bone tissue engineering—a review. *Journal of Biomedical Nanotechnology* **2014**, *10* (10), 3124–3140.
- (152) Beck, G. R. Inorganic phosphate as a signaling molecule in osteoblast differentiation. *Journal of Cellular Biochemistry* **2003**, *90* (2), 234–243.
- (153) Zhang, P.; Hong, Z.; Yu, T.; Chen, X.; Jing, X. In vivo mineralization and osteogenesis of nanocomposite scaffold of poly(lactide-co-glycolide) and hydroxyapatite surface-grafted with poly(l-lactide). *Biomaterials* **2009**, *30* (1), 58–70.
- (154) Jones, J. R. Review of bioactive glass: From Hench to hybrids. *Acta Biomaterialia* **2013**, *9* (1), 4457–4486.
- (155) Piszko, P.; Kryszak, B.; Piszko, A.; Szustakiewicz, K. Brief review on poly(glycerol sebacate) as an emerging polyester in biomedical application: Structure, properties and modifications. *Polymers in Medicine* **2021**, *51* (1), 43–50.
- (156) Pomerantseva, I.; Krebs, N.; Hart, A.; Neville, C. M.; Huang, A. Y.; Sundback, C. A. Degradation behavior of poly (glycerol sebacate). *J. Biomed. Mater. Res., Part A* **2009**, *91A* (4), 1038–1047.
- (157) Yoshimoto, H.; Shin, Y. M.; Terai, H.; Vacanti, J. P. A biodegradable nanofiber scaffold by electrospinning and its potential for bone tissue engineering. *Biomaterials* **2003**, *24* (12), 2077–2082.
- (158) Jang, J. H.; Castano, O.; Kim, H. W. Electrospun materials as potential platforms for bone tissue engineering. *Adv. Drug Delivery Rev.* **2009**, *61* (12), 1065–1083.
- (159) Sill, T. J.; von Recum, H. A. Electrospinning: Applications in drug delivery and tissue engineering. *Biomaterials* **2008**, *29*, 1989–2006.
- (160) Agarwal, S.; Greiner, A. On the way to clean and safe electrospinning-green electrospinning: Emulsion and suspension electrospinning. *Polym. Adv. Technol.* **2011**, *22*, 372–378.
- (161) Nam, Y. S.; Park, T. G. Porous biodegradable polymeric scaffolds prepared by thermally induced phase separation. *J. Biomed. Mater. Res.* **1999**, *47* (1), 8–17.
- (162) Szustakiewicz, K.; Gazinska, M.; Kryszak, B.; Grzymajło, M.; Piękowski, J.; Węglusz, R.; Okamoto, M. The influence of hydroxyapatite content on properties of poly(L-lactide)/hydroxyapatite porous scaffolds obtained using thermal induced phase separation technique. *Eur. Polym. J.* **2019**, *113*, 313–320.
- (163) Huang, D.; Niu, L.; Li, J.; Du, J.; Wei, Y.; Hu, Y.; Lian, X.; Chen, W.; Wang, K. Reinforced chitosan membranes by microspheres for guided bone regeneration. *Journal of the Mechanical Behavior of Biomedical Materials* **2018**, *81*, 195–201.
- (164) Le Bolay, N.; Santran, V.; Dechambre, G.; Combes, C.; Drouet, C.; Lamure, A.; Rey, C. Production, by co-grinding in a media mill, of porous biodegradable polylactic acid-apatite composite materials for bone tissue engineering. *Powder Technol.* **2009**, *190* (1–2), 89–94.
- (165) Ge, M.; Xue, L.; Nie, T.; Ma, H.; Zhang, J. The precision structural regulation of PLLA porous scaffold and its influence on the proliferation and differentiation of MC3T3-E1 cells. *Journal of Biomaterials Science Polymer Edition* **2016**, *27* (17), 1685–1697.
- (166) Chen, V. J.; Ma, P. X. Nano-fibrous poly(l-lactic acid) scaffolds with interconnected spherical macropores. *Biomaterials* **2004**, *25* (11), 2065–2073.
- (167) He, L.; Zuo, Q.; Shi, Y.; Xue, W. Microstructural characteristics and crystallization behaviors of poly(l-lactide) scaffolds by thermally induced phase separation. *J. Appl. Polym. Sci.* **2014**, *131* (4), No. 39436.
- (168) Piszko, P.; Włodarczyk, M.; Zielińska, S.; Gazińska, M.; Płociński, P.; Rudnicka, K.; Szwed, A.; Krupa, A.; Grzymajło, M.; Sobczak-Kupiec, A.; Słota, D.; Kobielarz, M.; Wojtków, M.; Szustakiewicz, K. PGS/HAP Microporous Composite Scaffold Obtained in the TIPS-TCL-SL Method: An Innovation for Bone Tissue Engineering. *International Journal of Molecular Sciences* **2021**, *22* (16), 8587.
- (169) Kim, J. F.; Jung, J. T.; Wang, H. H.; Lee, S. Y.; Moore, T.; Sanguineti, A.; Drioli, E.; Lee, Y. M. Microporous PVDF membranes via thermally induced phase separation (TIPS) and stretching methods. *J. Membr. Sci.* **2016**, *509*, 94–104.
- (170) Zeinali, R.; Del Valle, L. J.; Torras, J.; Puiggali, J. Recent progress on biodegradable tissue engineering scaffolds prepared by thermally-induced phase separation (TIPS). *International Journal of Molecular Sciences* **2021**, *22*, 3504.
- (171) Ujčić, A.; Sobótka, M.; Šlouf, M.; Róžański, M.; Szustakiewicz, K. Structure-property relationships in PCL porous scaffolds obtained by means of the TIPS and TIPS-PL methods. *Polym. Test.* **2023**, *118*, 107906.
- (172) Zhou, W. Y.; Lee, S. H.; Wang, M.; Cheung, W. L.; Ip, W. Y. Selective laser sintering of porous tissue engineering scaffolds from poly(l-lactide)/carbonated hydroxyapatite nanocomposite microspheres. *J. Mater. Sci.: Mater. Med.* **2008**, *19* (7), 2535–2540.
- (173) Chen, G.; Chen, N.; Wang, Q. Fabrication and properties of poly(vinyl alcohol)/ β -tricalcium phosphate composite scaffolds via fused deposition modeling for bone tissue engineering. *Compos. Sci. Technol.* **2019**, *172*, 17–28.
- (174) Kao, C. T.; Lin, C. C.; Chen, Y. W.; Yeh, C. H.; Fang, H. Y.; Shie, M. Y. Poly(dopamine) coating of 3D printed poly(lactic acid) scaffolds for bone tissue engineering. *Materials Science and Engineering: C* **2015**, *56*, 165–173.
- (175) Ahmadifar, M.; Benfriha, K.; Shiribayan, M.; Tcharkhtchi, A. Additive Manufacturing of Polymer-Based Composites Using Fused Filament Fabrication (FFF): a Review. *Applied Composite Materials* **2021**, *28*, 1335–1380.

- (176) Maines, E.; Porwal, M.; Ellison, C.; Reineke, T. Sustainable advances in SLA/DLP 3D printing materials and processes. *Green Chem.* **2021**, *23*, 6863.
- (177) Mota, C.; Puppi, D.; Chiellini, F.; Chiellini, E. Additive manufacturing techniques for the production of tissue engineering constructs. *Journal of Tissue Engineering and Regenerative Medicine* **2015**, *9* (3), 174–190.
- (178) Rohner, D.; Huttmacher, D. W.; Cheng, T. K.; Oberholzer, M.; Hammer, B. In vivo efficacy of bone-marrow-coated polycaprolactone scaffolds for the reconstruction of orbital defects in the pig. *J. Biomed. Mater. Res.* **2003**, *66B* (2), 574–580.
- (179) Mazzoli, A.; Ferretti, C.; Gigante, A.; Salvolini, E.; Mattioli-Belmonte, M. Selective laser sintering manufacturing of polycaprolactone bone scaffolds for applications in bone tissue engineering. *Rapid Prototyping Journal* **2015**, *21* (4), 386–392.
- (180) Du, Y.; Liu, H.; Shuang, J.; Wang, J.; Ma, J.; Zhang, S. Microsphere-based selective laser sintering for building macroporous bone scaffolds with controlled microstructure and excellent biocompatibility. *Colloids Surf., B* **2015**, *135*, 81–89.
- (181) Duan, B.; Cheung, W. L.; Wang, M. Optimized fabrication of Ca–P/PHBV nanocomposite scaffolds via selective laser sintering for bone tissue engineering. *Biofabrication* **2011**, *3* (1), 015001.
- (182) Meneghello, G.; Parker, D. J.; Ainsworth, B. J.; Perera, S. P.; Chaudhuri, J. B.; Ellis, M. J.; De Bank, P. A. Fabrication and characterization of poly(lactic-co-glycolic acid)/polyvinyl alcohol blended hollow fibre membranes for tissue engineering applications. *J. Membr. Sci.* **2009**, *344* (1–2), 55–61.
- (183) Qu, H. Additive manufacturing for bone tissue engineering scaffolds. *Materials Today Communications* **2020**, *24*, 101024.
- (184) Shuai, C.; Mao, Z.; Lu, H.; Nie, Y.; Hu, H.; Peng, S. Fabrication of porous polyvinyl alcohol scaffold for bone tissue engineering via selective laser sintering. *Biofabrication* **2013**, *5* (1), 015014.
- (185) Moreno Madrid, A. P. M.; Vrech, S. M.; Sanchez, M. A.; Rodriguez, A. P. Advances in additive manufacturing for bone tissue engineering scaffolds. *Materials Science and Engineering: C* **2019**, *100*, 631–644.
- (186) Huttmacher, D. W.; Sittinger, M.; Risbud, M. V. Scaffold-based tissue engineering: Rationale for computer-aided design and solid free-form fabrication systems. *Trends Biotechnol.* **2004**, *22* (7), 354–362.
- (187) Cooke, M. N.; Fisher, J. P.; Dean, D.; Rimnac, C.; Mikos, A. G. Use of stereolithography to manufacture critical-sized 3D biodegradable scaffolds for bone ingrowth. *J. Biomed. Mater. Res.* **2003**, *64B* (2), 65–69.
- (188) Ray, S. S.; Okamoto, M. Polymer/layered silicate nanocomposites: A review from preparation to processing. *Prog. Polym. Sci.* **2003**, *28* (11), 1539–1641.
- (189) Silveira, Z. D. C.; Netto, J. M. J. On the design and technology of co-rotating twin screw extruders. Paper presented at the Anais do IX congresso brasileiro de engenharia de fabricação, Joinville, Santa Catarina, Brasil, 2017.
- (190) Tsiroidis, E.; Upadhyay, N.; Giannoudis, P. Molecular aspects of fracture healing: Which are the important molecules? *Injury* **2007**, *38* (1), S11–S25.
- (191) Baranowski, A.; Klein, A.; Ritz, U.; Ackermann, A.; Anthonissen, J.; Kaufmann, K. B.; Brendel, C.; Götz, H.; Rommens, P. M.; Hofmann, A. Surface functionalization of orthopedic titanium implants with bone sialoprotein. *PLoS One* **2016**, *11* (4), e0153978.
- (192) Goddard, J. M.; Hotchkiss, J. H. Polymer surface modification for the attachment of bioactive compounds. *Prog. Polym. Sci.* **2007**, *32* (7), 698–725.
- (193) Stewart, C.; Akhavan, B.; Wise, S. G.; Bilek, M. M. M. A review of biomimetic surface functionalization for bone-integrating orthopedic implants: Mechanisms, current approaches, and future directions. *Prog. Mater. Sci.* **2019**, *106*, 100588.
- (194) Xie, G.; Sun, J.; Zhong, G.; Liu, C.; Wei, J. Hydroxyapatite nanoparticles as a controlled-release carrier of BMP-2: Adsorption and release kinetics in vitro. *J. Mater. Sci.: Mater. Med.* **2010**, *21* (6), 1875–1880.
- (195) Zhou, P.; Wu, J.; Xia, Y.; Yuan, Y.; Zhang, H.; Xu, S.; Lin, K. Loading BMP-2 on nanostructured hydroxyapatite microspheres for rapid bone regeneration. *Int. J. Nanomed.* **2018**, *13*, 4083–4092.
- (196) Liu, T.; Fang, W.; Wu, G.; Li, Y.; Pathak, J. L.; Liu, Y. Low dose BMP2-doped calcium phosphate graft promotes bone defect healing in a large animal model. *Frontiers in Cell and Developmental Biology* **2021**, *8*, 613891.
- (197) Kämmerer, P. W.; Schiegnitz, E.; Palarie, V.; Dau, M.; Frerich, B.; Al-Nawas, B. Influence of platelet-derived growth factor on osseous remodeling properties of a variable-thread tapered dental implant in vivo. *Clinical Oral Implants Research* **2017**, *28* (2), 201–206.
- (198) Oest, M. E.; Dupont, K. M.; Kong, H. J.; Mooney, D. J.; Guldborg, R. E. Quantitative assessment of scaffold and growth factor-mediated repair of critically sized bone defects. *Journal of Orthopaedic Research* **2007**, *25* (7), 941–950.
- (199) Ozeki, K.; Aoki, H.; Fukui, Y. The effect of adsorbed vitamin D and K to hydroxyapatite on ALP activity of MC3T3-E1 cell. *J. Mater. Sci.: Mater. Med.* **2008**, *19* (4), 1753–1757.
- (200) Yoo, H. S.; Kim, T. G.; Park, T. G. Surface-functionalized electrospun nanofibers for tissue engineering and drug delivery. *Adv. Drug Delivery Rev.* **2009**, *61* (12), 1033–1042.
- (201) Zeng, S.; Ye, J.; Cui, Z.; Si, J.; Wang, Q.; Wang, X.; Peng, K.; Chen, W. Surface biofunctionalization of three-dimensional porous poly(lactic acid) scaffold using chitosan/OGP coating for bone tissue engineering. *Materials Science and Engineering: C* **2017**, *77*, 92–101.
- (202) Kandori, K.; Oda, S.; Tsuyama, S. Effects of pyrophosphate ions on protein adsorption onto calcium hydroxyapatite. *J. Phys. Chem. B* **2008**, *112* (8), 2542–2547.
- (203) Kandori, K.; Tsuyama, S.; Tanaka, H.; Ishikawa, T. Protein adsorption characteristics of calcium hydroxyapatites modified with pyrophosphoric acids. *Colloids Surf., B* **2007**, *58* (2), 98–104.
- (204) Ishihara, S.; Matsumoto, T.; Onoki, T.; Uddin, M. H.; Sohmura, T.; Nakahira, A. Regulation of the protein-loading capacity of hydroxyapatite by mercaptosuccinic acid modification. *Acta Biomaterialia* **2010**, *6* (3), 830–835.
- (205) Lee, W. H.; Loo, C. Y.; Van, K. L.; Zavgorodniy, A. V.; Rohanizadeh, R. Modulating protein adsorption onto hydroxyapatite particles using different amino acid treatments. *Journal of the Royal Society, Interface* **2012**, *9* (70), 918–927.
- (206) Boix, T.; Gómez-Morales, J.; Torrent-Burgués, J.; Monfort, A.; Puigdomènech, P.; Rodríguez-Clemente, R. Adsorption of recombinant human bone morphogenetic protein rhBMP-2m onto hydroxyapatite. *Journal of Inorganic Biochemistry* **2005**, *99* (5), 1043–1050.
- (207) Uludag, H.; D'Augusta, D.; Palmer, R.; Timony, G.; Wozney, J. Characterization of rhBMP-2 pharmacokinetics implanted with biomaterial carriers in the rat ectopic model. *J. Biomed. Mater. Res.* **1999**, *46* (2), 193–202.
- (208) Winn, S. R.; Uludag, H.; Hollinger, J. O. Carrier systems for bone morphogenetic proteins. *Clinical Orthopaedics and Related Research* **1999**, *367*, S95–S106.
- (209) Autefage, H.; Briand-Mésange, F.; Cazalbou, S.; Drouet, C.; Fourmy, D.; Gonçalves, S.; Salles, J. P.; Combes, C.; Swider, P.; Rey, C. Adsorption and release of BMP-2 on nanocrystalline apatite-coated and uncoated hydroxyapatite/ β -tricalcium phosphate porous ceramics. *Journal of Biomedical Materials Research Part B: Applied Biomaterials* **2009**, *91B* (2), 706–715.
- (210) Hanje, C.; Peter, T.; Cameron, C.; Sean, P. Effect of burst and/or sustained release of rhBMP-2 on bone formation in vivo. *Frontiers in Bioengineering and Biotechnology* **2016**, *4*. DOI: 10.3389/fbioe.2016.01.02728.
- (211) James, A. W.; LaChaud, G.; Shen, J.; Asatrian, G.; Nguyen, V.; Zhang, X.; Ting, K.; Soo, C. A review of the clinical side effects of bone morphogenetic protein-2. *Tissue Engineering. Part B, Reviews* **2016**, *22* (4), 284–297.
- (212) Heller, M.; Kumar, V. V.; Pabst, A.; Brieger, J.; Al-Nawas, B.; Kämmerer, P. W. Osseous response on linear and cyclic RGD-

- peptides immobilized on titanium surfaces in vitro and in vivo. *J. Biomed. Mater. Res., Part A* **2018**, *106* (2), 419–427.
- (213) Kim, S. E.; Song, S. H.; Yun, Y. P.; Choi, B. J.; Kwon, I. K.; Bae, M. S.; Moon, H. J.; Kwon, Y. D. The effect of immobilization of heparin and bone morphogenetic protein-2 (BMP-2) to titanium surfaces on inflammation and osteoblast function. *Biomaterials* **2011**, *32* (2), 366–373.
- (214) Sevilla, P.; Cirera, A.; Dotor, J.; Gil, F. J.; Galindo-Moreno, P.; Aparicio, C. In vitro cell response on CP-Ti surfaces functionalized with TGF- β 1 inhibitory peptides. *J. Mater. Sci.: Mater. Med.* **2018**, *29* (6), 73.
- (215) Biju, V. Chemical modifications and bioconjugate reactions of nanomaterials for sensing, imaging, drug delivery and therapy. *Chem. Soc. Rev.* **2014**, *43* (3), 744–764.
- (216) Maia, F. R.; Bidarra, S. J.; Granja, P. L.; Barrias, C. C. Functionalization of biomaterials with small osteoinductive moieties. *Acta Biomaterialia* **2013**, *9* (11), 8773–8789.
- (217) Zhang, Z.; Gupte, M. J.; Jin, X.; Ma, P. X. Injectable peptide decorated functional nanofibrous hollow microspheres to direct stem cell differentiation and tissue regeneration. *Adv. Funct. Mater.* **2015**, *25* (3), 350–360.
- (218) Przekora, A. Current trends in fabrication of biomaterials for bone and cartilage regeneration: Materials modifications and biophysical stimulations. *International Journal of Molecular Sciences* **2019**, *20* (2), 435.
- (219) Hu, Y.; Winn, S. R.; Krajchich, I.; Hollinger, J. O. Porous polymer scaffolds surface-modified with arginine-glycine-aspartic acid enhance bone cell attachment and differentiation in vitro. *J. Biomed. Mater. Res.* **2003**, *64A* (3), 583–590.
- (220) Rosenberg, M.; Shilo, D.; Galperin, L.; Capucha, T.; Tarabieh, K.; Rachmiel, A.; Segal, E. Bone morphogenetic protein 2-loaded porous silicon carriers for osteoinductive implants. *Pharmaceutics* **2019**, *11* (11), 602.
- (221) Oya, K.; Tanaka, Y.; Saito, H.; Kurashima, K.; Nogi, K.; Tsutsumi, H.; Tsutsumi, Y.; Doi, H.; Nomura, N.; Hanawa, T. Calcification by MC3T3-E1 cells on RGD peptide immobilized on titanium through electrodeposited PEG. *Biomaterials* **2009**, *30* (7), 1281–1286.
- (222) Kashiwagi, K.; Tsuji, T.; Shiba, K. Directional BMP-2 for functionalization of titanium surfaces. *Biomaterials* **2009**, *30* (6), 1166–1175.
- (223) Singh, S.; Wu, B. M.; Dunn, J. C. Y. The enhancement of VEGF-mediated angiogenesis by polycaprolactone scaffolds with surface cross-linked heparin. *Biomaterials* **2011**, *32* (8), 2059–2069.
- (224) Young, E. The anti-inflammatory effects of heparin and related compounds. *Thrombosis Research* **2008**, *122* (6), 743–752.
- (225) Singh, A.; Gill, G.; Kaur, H.; Amhmed, M.; Jakhu, H. Role of osteopontin in bone remodeling and orthodontic tooth movement: A review. *Progress in Orthodontics* **2018**, *19* (1), 18.
- (226) Verrier, S.; Pallu, S.; Bareille, R.; Jonczyk, A.; Meyer, J.; Dard, M.; Amédée, J. Function of linear and cyclic RGD-containing peptides in osteoprogenitor cells adhesion process. *Biomaterials* **2002**, *23* (2), 585–596.
- (227) Dang, M.; Saunders, L.; Niu, X.; Fan, Y.; Ma, P. X. Biomimetic delivery of signals for bone tissue engineering. *Bone Research* **2018**, *6*, 25.
- (228) Wright, T. A.; Page, R. C.; Konkolewicz, D. Polymer conjugation of proteins as a synthetic post-translational modification to impact their stability and activity. *Polym. Chem.* **2019**, *10* (4), 434–454.
- (229) Sunasee, R.; Narain, R. *Covalent and noncovalent bioconjugation strategies Chemistry of Bioconjugates: Synthesis, Characterization, and Biomedical Applications*; John Wiley & Sons, Inc.: 2014; pp 1–75.
- (230) Breinbauer, R.; Köhn, M. Azide-alkyne coupling: A powerful reaction for bioconjugate chemistry. *ChemBioChem.* **2003**, *4* (11), 1147–1149.
- (231) Baeza, A.; Izquierdo-Barba, I.; Vallet-Regí, M. Biotinylation of silicon-doped hydroxyapatite: A new approach to protein fixation for bone tissue regeneration. *Acta Biomaterialia* **2010**, *6* (3), 743–749.
- (232) Cheng, C. H.; Lai, Y. H.; Chen, Y. W.; Yao, C. H.; Chen, K. Y. Immobilization of bone morphogenetic protein-2 to gelatin/avidin-modified hydroxyapatite composite scaffolds for bone regeneration. *Journal of Biomaterials Applications* **2019**, *33* (9), 1147–1156.
- (233) Udomluck, N.; Lee, H.; Hong, S.; Lee, S. H.; Park, H. Surface functionalization of dual growth factor on hydroxyapatite-coated nanofibers for bone tissue engineering. *Appl. Surf. Sci.* **2020**, *520*, 146311.
- (234) Kämmerer, P. W.; Lehnert, M.; Al-Nawas, B.; Kumar, V. V.; Hagmann, S.; Alshihri, A.; Frerich, B.; Veith, M. Osseointegration of a specific streptavidin-biotin-fibronectin surface coating of biotinylated titanium implants - a rabbit animal study. *Clinical Implant Dentistry and Related Research* **2015**, *17*, e601–e612.
- (235) Jiskoot, W.; Randolph, T. W.; Volkin, D. B.; Russell Middaugh, C.; Schöneich, C.; Winter, G.; Friess, W.; Crommelin, D. J. A.; Carpenter, J. F. Protein instability and immunogenicity: Roadblocks to clinical application of injectable protein delivery systems for sustained release. *J. Pharm. Sci.* **2012**, *101* (3), 946–954.
- (236) Vugmeyster, Y.; Xu, X.; Theil, F. P.; Khawli, L. A.; Leach, M. W. Pharmacokinetics and toxicology of therapeutic proteins: Advances and challenges. *World Journal of Biological Chemistry* **2012**, *3* (4), 73–92.
- (237) Mariner, P. D.; Wudel, J. M.; Miller, D. E.; Genova, E. E.; Streubel, S. O.; Anseth, K. S. Synthetic hydrogel scaffold is an effective vehicle for delivery of INFUSE (rhBMP2) to critical-sized calvaria bone defects in rats. *Journal of Orthopaedic Research* **2013**, *31* (3), 401–406.
- (238) Geuze, R. E.; Theyse, L. F. H.; Kempen, D. H. R.; Hazewinkel, H. A. W.; Kraak, H. Y. A.; Öner, F. C.; Dhert, W. J. A.; Alblas, J. A. A differential effect of bone morphogenetic protein-2 and vascular endothelial growth factor release timing on osteogenesis at ectopic and orthotopic sites in a large-animal model. *Tissue Engineering. Part A* **2012**, *18* (19–20), 2052–2062.
- (239) Quinlan, E.; López-Noriega, A.; Thompson, E.; Kelly, H. M.; Cryan, S. A.; O'Brien, F. J. Development of collagen-hydroxyapatite scaffolds incorporating PLGA and alginate microparticles for the controlled delivery of rhBMP-2 for bone tissue engineering. *J. Controlled Release* **2015**, *198*, 71–79.
- (240) Saik, J. E.; Gould, D. J.; Watkins, E. M.; Dickinson, M. E.; West, J. L. Covalently immobilized platelet-derived growth factor-BB promotes angiogenesis in biomimetic poly(ethylene glycol) hydrogels. *Acta Biomaterialia* **2011**, *7* (1), 133–143.
- (241) Wei, G.; Pettway, G. J.; McCauley, L. K.; Ma, P. X. The release profiles and bioactivity of parathyroid hormone from poly(lactic-co-glycolic acid) microspheres. *Biomaterials* **2004**, *25* (2), 345–352.
- (242) Wei, G.; Jin, Q.; Giannobile, W. V.; Ma, P. X. The enhancement of osteogenesis by nano-fibrous scaffolds incorporating rhBMP-7 nanospheres. *Biomaterials* **2007**, *28* (12), 2087–2096.
- (243) Yilgor, P.; Hasirci, N.; Hasirci, V. Sequential BMP-2/BMP-7 delivery from polyester nanocapsules. *J. Biomed. Mater. Res., Part A* **2010**, *93* (2), 528–536.
- (244) Kupikowska-Stobba, B.; Kasprzak, M. Fabrication of nanoparticles for bone regeneration: new insight into applications of nanoemulsion technology. *J. Mater. Chem. B* **2021**, *9* (26), 5221–44.
- (245) Quinlan, E.; López-Noriega, A.; Thompson, E. M.; Hibbitts, A.; Cryan, S. A.; O'Brien, F. J. Controlled release of vascular endothelial growth factor from spray-dried alginate microparticles in collagen-hydroxyapatite scaffolds for promoting vascularization and bone repair. *Journal of Tissue Engineering and Regenerative Medicine* **2017**, *11* (4), 1097–1109.
- (246) Quinlan, E.; Thompson, E. M.; Matsiko, A.; O'Brien, F. J.; López-Noriega, A. Functionalization of a collagen-hydroxyapatite scaffold with osteostatin to facilitate enhanced bone regeneration. *Adv. Healthcare Mater.* **2015**, *4* (17), 2649–2656.
- (247) Wang, H.; Leeuwenburgh, S. C. G.; Li, Y.; Jansen, J. A. The use of micro- and nanospheres as functional components for bone tissue regeneration. *Tissue Engineering. Part B, Reviews* **2012**, *18* (1), 24–39.

- (248) Jin, Q.; Wei, G.; Lin, Z.; Sugai, J. V.; Lynch, S. E.; Ma, P. X.; Giannobile, W. V. Nanofibrous scaffolds incorporating PDGF-BB microspheres induce chemokine expression and tissue neogenesis in vivo. *PLoS One* **2008**, *3* (3), e1729.
- (249) Allison, S. D. Analysis of initial burst in PLGA microparticles. *Expert Opinion on Drug Delivery* **2008**, *5* (6), 615–628.
- (250) Kupikowska-Stobba, B.; Lewińska, D. Polymer microcapsules and microbeads as cell carriers for: In vivo biomedical applications. *Biomaterials Science* **2020**, *8* (6), 1536–1574.
- (251) Lewińska, D.; Grzechkowicz, M.; Kupikowska-Stobba, B. Influence of electric parameters on the alginate-polyethersulfone microcapsule structure. *Desalination and Water Treatment* **2017**, *64*, 400–408.
- (252) Kupikowska, B.; Lewińska, D.; Dudzinski, K.; Jankowska-Sliwińska, J.; Grzechkowicz, M.; Wojciechowski, C.; Chwojnowski, A. Influence of changes in composition of the membrane-forming solution on the structure of alginate-polyethersulfone microcapsules. *Biocybernetics and Biomedical Engineering* **2009**, *29*, 61–69.
- (253) Monteiro, N.; Martins, A.; Reis, R. L.; Neves, N. M. Liposomes in tissue engineering and regenerative medicine. *Journal of the Royal Society, Interface* **2014**, *11* (101), 20140459.
- (254) Wang, G.; Mostafa, N. Z.; Incani, V.; Kucharski, C.; Uludağ, H. Bisphosphonate-decorated lipid nanoparticles designed as drug carriers for bone diseases. *J. Biomed. Mater. Res., Part A* **2012**, *100A* (3), 684–693.
- (255) Düzgüneş, N.; Nir, S. Mechanisms and kinetics of liposome–cell interactions. *Adv. Drug Delivery Rev.* **1999**, *40* (1–2), 3–18.
- (256) Yadav, A.; Murthy, M.; Shete, A.; Sfurti, S. Stability aspects of liposomes. *Indian Journal of Pharmaceutical Research and Education* **2011**, *45* (4), 402–413.
- (257) Mumcuoglu, D.; Fahmy-Garcia, S.; Ridwan, Y.; Nicke, J.; Farrell, E.; Kluijtmans, S.; van Osch, G. Injectable BMP-2 delivery system based on collagen-derived microspheres and alginate induced bone formation in a time- and dose-dependent manner. *European Cells and Materials* **2018**, *35*, 242–254.
- (258) Xia, Y. J.; Wei, W.; Xia, H.; Ying, Q. S.; Yu, X.; Li, L. H.; Wang, J. H.; Zhang, Y. Effect of recombinant human bone morphogenetic protein delivered by chitosan microspheres on ectopic osteogenesis in rats. *Experimental and Therapeutic Medicine* **2019**, *17* (5), 3891–3898.
- (259) Whitely, M.; Rodriguez-Rivera, G.; Waldron, C.; Mohiuddin, S.; Cereceres, S.; Sears, N.; Ray, N.; Cosgriff-Hernandez, E. Porous PolyHIPE microspheres for protein delivery from an injectable bone graft. *Acta Biomaterialia* **2019**, *93*, 169–179.
- (260) Wang, X.; Wu, X.; Xing, H.; Zhang, G.; Shi, Q.; E, L.; Liu, N.; Yang, T.; Wang, D.; Qi, F.; Wang, L.; Liu, H. Porous nano-hydroxyapatite/collagen scaffolds loading insulin PLGA particles for restoration of critical size bone defect. *ACS Applied Materials & Interfaces* **2017**, *9* (13), 11380–11391.
- (261) Xia, P.; Wang, S.; Qi, Z.; Zhang, W.; Sun, Y. BMP-2-releasing gelatin microspheres/PLGA scaffolds for bone repairment of X-ray-radiated rabbit radius defects. *Artificial Cells, Nanomedicine, and Biotechnology* **2019**, *47* (1), 1662–1673.
- (262) Fahimipour, F.; Rasouljanboroujeni, M.; Dashtimoghadam, E.; Khoshroo, K.; Tahiri, M.; Bastami, F.; Lobner, D.; Tayebi, L. 3D printed TCP-based scaffold incorporating VEGF-loaded PLGA microspheres for craniofacial tissue engineering. *Dental Materials* **2017**, *33* (11), 1205–1216.
- (263) Xin, S.; Chimene, D.; Garza, J. E.; Gaharwar, A. K.; Alge, D. L. Clickable PEG hydrogel microspheres as building blocks for 3D bioprinting. *Biomaterials Science* **2019**, *7* (3), 1179–1187.
- (264) Wang, X.; Wenk, E.; Zhang, X.; Meinel, L.; Vunjak-Novakovic, G.; Kaplan, D. L. Growth factor gradients via microsphere delivery in biopolymer scaffolds for osteochondral tissue engineering. *J. Controlled Release* **2009**, *134* (2), 81–90.
- (265) Perets, A.; Baruch, Y.; Weisbuch, F.; Shoshany, G.; Neufeld, G.; Cohen, S. Enhancing the vascularization of three-dimensional porous alginate scaffolds by incorporating controlled release basic fibroblast growth factor microspheres. *J. Biomed. Mater. Res.* **2003**, *65A* (4), 489–497.
- (266) Wagner, E. R.; Parry, J.; Dadsetan, M.; Bravo, D.; Riestler, S. M.; Van Wijnen, A. J.; Yaszemski, M. J.; Kakar, S. VEGF-mediated angiogenesis and vascularization of a fumarate-crosslinked polycaprolactone (PCLF) scaffold. *Connective Tissue Research* **2018**, *59* (6), 542–549.
- (267) Cui, H.; Zhu, W.; Nowicki, M.; Zhou, X.; Khademhosseini, A.; Zhang, L. G. Hierarchical fabrication of engineered vascularized bone biphasic constructs via dual 3D bioprinting: Integrating regional bioactive factors into architectural design. *Adv. Healthcare Mater.* **2016**, *5* (17), 2174–2181.
- (268) Dang, M.; Koh, A. J.; Danciu, T.; McCauley, L. K.; Ma, P. X. Preprogrammed long-term systemic pulsatile delivery of parathyroid hormone to strengthen bone. *Adv. Healthcare Mater.* **2017**, *6* (3), 1600901.
- (269) Dang, M.; Koh, A. J.; Jin, X.; McCauley, L. K.; Ma, P. X. Local pulsatile PTH delivery regenerates bone defects via enhanced bone remodeling in a cell-free scaffold. *Biomaterials* **2017**, *114*, 1–9.
- (270) Grayson, A. C. R.; Choi, I. S.; Tyler, B. M.; Wang, P. P.; Brem, H.; Cima, M. J.; Langer, R. Multi-pulse drug delivery from a resorbable polymeric microchip device. *Nat. Mater.* **2003**, *2* (11), 767–772.
- (271) West, J. L. Pulsed polymers. *Nat. Mater.* **2003**, *2* (11), 709–710.
- (272) Kempen, D. H. R.; Lu, L.; Heijink, A.; Hefferan, T. E.; Creemers, L. B.; Maran, A.; Yaszemski, M. J.; Dhert, W. J. A. Effect of local sequential VEGF and BMP-2 delivery on ectopic and orthotopic bone regeneration. *Biomaterials* **2009**, *30* (14), 2816–2825.
- (273) Basmanav, F. B.; Kose, G. T.; Hasirci, V. Sequential growth factor delivery from complexed microspheres for bone tissue engineering. *Biomaterials* **2008**, *29* (31), 4195–4204.
- (274) Liu, X.; Pettway, G. J.; McCauley, L. K.; Ma, P. X. Pulsatile release of parathyroid hormone from an implantable delivery system. *Biomaterials* **2007**, *28* (28), 4124–4131.
- (275) Farra, R.; Sheppard, N. F.; McCabe, L.; Neer, R. M.; Anderson, J. M.; Santini, J. T.; Cima, M. J.; Langer, R. First-in-human testing of a wirelessly controlled drug delivery microchip. *Science Translational Medicine* **2012**, *4* (122), 122ra121.
- (276) Dempster, D. W.; Cosman, F.; Parisien, M. A. Y.; Shen, V.; Lindsay, R. Anabolic actions of parathyroid hormone on bone. *Endocrine Reviews* **1993**, *14* (6), 690–709.
- (277) Qin, L.; Raggatt, L. J.; Partridge, N. C. Parathyroid hormone: A double-edged sword for bone metabolism. *Trends in Endocrinology & Metabolism* **2004**, *15* (2), 60–65.
- (278) Yilgor, P.; Tuzlakoglu, K.; Reis, R. L.; Hasirci, N.; Hasirci, V. Incorporation of a sequential BMP-2/BMP-7 delivery system into chitosan-based scaffolds for bone tissue engineering. *Biomaterials* **2009**, *30* (21), 3551–3559.
- (279) Kim, S.; Kang, Y.; Krueger, C. A.; Sen, M.; Holcomb, J. B.; Chen, D.; Wenke, J. C.; Yang, Y. Sequential delivery of BMP-2 and IGF-1 using a chitosan gel with gelatin microspheres enhances early osteoblastic differentiation. *Acta Biomaterialia* **2012**, *8* (5), 1768–1777.
- (280) Subbiah, R.; Hwang, M. P.; Van, S. Y.; Do, S. H.; Park, H.; Lee, K.; Kim, S. H.; Yun, K.; Park, K. Osteogenic/angiogenic dual growth factor delivery microcapsules for regeneration of vascularized bone tissue. *Adv. Healthcare Mater.* **2015**, *4* (13), 1982–1992.
- (281) Freeman, I.; Cohen, S. The influence of the sequential delivery of angiogenic factors from affinity-binding alginate scaffolds on vascularization. *Biomaterials* **2009**, *30* (11), 2122–2131.
- (282) Dashtimoghadam, E.; Fahimipour, F.; Tongas, N.; Tayebi, L. Microfluidic fabrication of microcarriers with sequential delivery of VEGF and BMP-2 for bone regeneration. *Sci. Rep.* **2020**, *10* (1), 11764.
- (283) Perez, R. A.; Kim, J. H.; Buitrago, J. O.; Wall, I. B.; Kim, H. W. Novel therapeutic core–shell hydrogel scaffolds with sequential delivery of cobalt and bone morphogenetic protein-2 for synergistic bone regeneration. *Acta Biomaterialia* **2015**, *23*, 295–308.

- (284) Spiller, K. L.; Nassiri, S.; Witherell, C. E.; Anfang, R. R.; Ng, J.; Nakazawa, K. R.; Yu, T.; Vunjak-Novakovic, G. Sequential delivery of immunomodulatory cytokines to facilitate the M1-to-M2 transition of macrophages and enhance vascularization of bone scaffolds. *Biomaterials* **2015**, *37*, 194–207.
- (285) Lee, H. J.; Koh, W. G. Hydrogel micropattern-incorporated fibrous scaffolds capable of sequential growth factor delivery for enhanced osteogenesis of hMSCs. *ACS Appl. Mater. Interfaces* **2014**, *6* (12), 9338–9348.
- (286) El Bialy, I.; Jiskoot, W.; Reza Nejadnik, M. Formulation, delivery and stability of bone morphogenetic proteins for effective bone regeneration. *Pharm. Res.* **2017**, *34* (6), 1152–1170.
- (287) Wang, Y.; Shim, M. S.; Levinson, N. S.; Sung, H. W.; Xia, Y. Stimuli-responsive materials for controlled release of theranostic agents. *Adv. Funct. Mater.* **2014**, *24* (27), 4206–4220.
- (288) Kim, H. K.; Lee, J. S.; Kim, J. H.; Seon, J. K.; Park, K. S.; Jeong, M. H.; Yoon, T. R. Bone-forming peptide-2 derived from BMP-7 enhances osteoblast differentiation from multipotent bone marrow stromal cells and bone formation. *Experimental & Molecular Medicine* **2017**, *49* (5), e328.
- (289) Segredo-Morales, E.; García-García, P.; Reyes, R.; Pérez-Herrero, E.; Delgado, A.; Évora, C. Bone regeneration in osteoporosis by delivery BMP-2 and PRGF from tetrionic–alginate composite thermogel. *Int. J. Pharm.* **2018**, *543* (1–2), 160–168.
- (290) Gao, Z. G.; Fain, H. D.; Rapoport, N. Controlled and targeted tumor chemotherapy by micellar-encapsulated drug and ultrasound. *J. Controlled Release* **2005**, *102* (1), 203–222.
- (291) Nomikou, N.; Feichtinger, G. A.; Saha, S.; Nuernberger, S.; Heimel, P.; Redl, H.; McHale, A. P. Ultrasound-responsive gene-activated matrices for osteogenic gene therapy using matrix-assisted sonoporation. *Journal of Tissue Engineering and Regenerative Medicine* **2018**, *12* (1), e250–e260.
- (292) Wu, G.; Mikhailovsky, A.; Khant, H. A.; Fu, C.; Chiu, W.; Zasadzinski, J. A. Remotely triggered liposome release by near-infrared light absorption via hollow gold nanoshells. *J. Am. Chem. Soc.* **2008**, *130* (26), 8175–8177.
- (293) Ge, J.; Neofytou, E.; Cahill, T. J.; Beygui, R. E.; Zare, R. N. Drug release from electric-field-responsive nanoparticles. *ACS Nano* **2012**, *6* (1), 227–233.
- (294) Hu, S. H.; Liu, T. Y.; Liu, D. M.; Chen, S. Y. Controlled pulsatile drug release from a ferrogel by a high-frequency magnetic field. *Macromolecules* **2007**, *40* (19), 6786–6788.
- (295) Sanchez-Casanova, S.; Martin-Saavedra, F. M.; Escudero-Duch, C.; Falguera Uceda, M. I.; Prieto, M.; Arruebo, M.; Acebo, P.; Fabiilli, M. L.; Franceschi, R. T.; Vilaboa, N. Local delivery of bone morphogenetic protein-2 from near infrared-responsive hydrogels for bone tissue regeneration. *Biomaterials* **2020**, *241*, 119909.
- (296) Kim, M. K.; Lee, H. N.; Jenjob, R.; Lee, J.; Yang, S. G. Calcium-triggered pulsatile delivery of parathyroid hormone from microbeads for osteoporosis treatment. *Biomacromolecules* **2017**, *18* (10), 3099–3105.
- (297) Lutolf, M. P.; Lauer-Fields, J. L.; Schmoekel, H. G.; Metters, A. T.; Weber, F. E.; Fields, G. B.; Hubbell, J. A. Synthetic matrix metalloproteinase-sensitive hydrogels for the conduction of tissue regeneration: Engineering cell-invasion characteristics. *Proc. Natl. Acad. Sci. U.S.A.* **2003**, *100* (9), 5413–5418.
- (298) Seliktar, D.; Zisch, A. H.; Lutolf, M. P.; Wrana, J. L.; Hubbell, J. A. MMP-2 sensitive, VEGF-bearing bioactive hydrogels for promotion of vascular healing. *J. Biomed. Mater. Res.* **2004**, *68A* (4), 704–716.
- (299) Hsu, C. W.; Olabisi, R. M.; Olmsted-Davis, E. A.; Davis, A. R.; West, J. L. Cathepsin K-sensitive poly(ethylene glycol) hydrogels for degradation in response to bone resorption. *J. Biomed. Mater. Res., Part A* **2011**, *98A* (1), 53–62.
- (300) Wade, R. J.; Bassin, E. J.; Rodell, C. B.; Burdick, J. A. Protease-degradable electrospun fibrous hydrogels. *Nat. Commun.* **2015**, *6*, 6639.
- (301) Anjum, F.; Lienemann, P. S.; Metzger, S.; Biernaskie, J.; Kallos, M. S.; Ehrbar, M. Enzyme responsive GAG-based natural-synthetic hybrid hydrogel for tunable growth factor delivery and stem cell differentiation. *Biomaterials* **2016**, *87*, 104–117.
- (302) Holloway, J. L.; Ma, H.; Rai, R.; Hankenson, K. D.; Burdick, J. A. Synergistic effects of SDF-1 α and BMP-2 delivery from proteolytically degradable hyaluronic acid hydrogels for bone repair. *Macromol. Biosci.* **2015**, *15* (9), 1218–1223.
- (303) Bessa, P. C.; Machado, R.; Nürnbergger, S.; Dopler, D.; Banerjee, A.; Cunha, A. M.; Rodríguez-Cabello, J. C.; Redl, H.; van Griensven, M.; Reis, R. L.; Casal, M. Thermoresponsive self-assembled elastin-based nanoparticles for delivery of BMPs. *J. Controlled Release* **2010**, *142* (3), 312–318.
- (304) Chun, C. J.; Lim, H. J.; Hong, K. Y.; Park, K. H.; Song, S. C. The use of injectable, thermosensitive poly(organophosphazene)–RGD conjugates for the enhancement of mesenchymal stem cell osteogenic differentiation. *Biomaterials* **2009**, *30* (31), 6295–6308.
- (305) He, C.; Kim, S. W.; Lee, D. S. In situ gelling stimuli-sensitive block copolymer hydrogels for drug delivery. *J. Controlled Release* **2008**, *127* (3), 189–207.
- (306) Kim, M. S.; Kim, S. K.; Kim, S. H.; Hyun, H.; Khang, G.; Lee, H. B. In vivo osteogenic differentiation of rat bone marrow stromal cells in thermosensitive MPEG-PCL diblock copolymer gels. *Tissue Engineering* **2006**, *12* (10), 2863–2873.
- (307) Na, K.; Kim, S. w.; Sun, B. K.; Woo, D. G.; Yang, H. N.; Chung, H. M.; Park, K. H. Osteogenic differentiation of rabbit mesenchymal stem cells in thermo-reversible hydrogel constructs containing hydroxyapatite and bone morphogenetic protein-2 (BMP-2). *Biomaterials* **2007**, *28* (16), 2631–2637.
- (308) Patois, E.; Cruz, S. O. D.; Tille, J. C.; Walpoth, B.; Gurny, R.; Jordan, O. Novel thermosensitive chitosan hydrogels: In vivo evaluation. *J. Biomed. Mater. Res., Part A* **2009**, *91A* (2), 324–330.
- (309) Shi, J.; Liu, L.; Liu, X.; Sun, X.; Cao, S. Inorganic–organic hybrid alginate beads with LCST near human body temperature for sustained dual-sensitive drug delivery. *Polym. Adv. Technol.* **2008**, *19* (11), 1467–1473.
- (310) Adibfar, A.; Amoabediny, G.; Baghaban Eslaminejad, M.; Mohamadi, J.; Bagheri, F.; Zandieh Doulabi, B. VEGF delivery by smart polymeric PNIPAM nanoparticles affects both osteogenic and angiogenic capacities of human bone marrow stem cells. *Materials Science and Engineering: C* **2018**, *93*, 790–799.
- (311) Dutta, K.; Das, R.; Ling, J.; Monibas, R. M.; Carballo-Jane, E.; Kekec, A.; Feng, D. D.; Lin, S.; Mu, J.; Saklatvala, R.; Thayumanavan, S.; Liang, Y. In situ forming injectable thermoresponsive hydrogels for controlled delivery of biomacromolecules. *ACS Omega* **2020**, *5* (28), 17531–17542.
- (312) Santoveña, A.; Monzón, C.; Alvarez-Lorenzo, C.; del Rosario, C.; Delgado, A.; Évora, C.; Concheiro, A.; Llabrés, M.; Fariña, J. B. Structure-performance relationships of temperature-responsive PLGA-PEG-PLGA gels for sustained release of bone morphogenetic protein-2. *J. Pharm. Sci.* **2017**, *106* (11), 3353–3362.
- (313) Seo, B. B.; Choi, H.; Koh, J. T.; Song, S. C. Sustained BMP-2 delivery and injectable bone regeneration using thermosensitive polymeric nanoparticle hydrogel bearing dual interactions with BMP-2. *J. Controlled Release* **2015**, *209*, 67–76.
- (314) Vermonden, T.; Censi, R.; Hennink, W. E. Hydrogels for protein delivery. *Chem. Rev.* **2012**, *112* (5), 2853–2888.
- (315) Reyes-Ortega, F. pH-responsive polymers: Properties, synthesis and applications. In *Smart polymers and their applications*; Aguilar, M. R., Román, J. S., Eds.; Woodhead Publishing Ltd.: Cambridge, 2014; pp 45–92.
- (316) Banerjee, I.; Mishra, D.; Maiti, T. K. Wound pH-responsive sustained release of therapeutics from a poly(NIPAAm-co-AAc) hydrogel. *Journal of Biomaterials Science, Polymer Edition* **2012**, *23* (1–4), 111–132.
- (317) Tao, B.; Deng, Y.; Song, L.; Ma, W.; Qian, Y.; Lin, C.; Yuan, Z.; Lu, L.; Chen, M.; Yang, X.; Cai, K. BMP2-loaded titania nanotubes coating with pH-responsive multilayers for bacterial infections inhibition and osteogenic activity improvement. *Colloids Surf., B* **2019**, *177*, 242–252.

- (318) Gan, Q.; Zhu, J.; Yuan, Y.; Liu, H.; Qian, J.; Li, Y.; Liu, C. A dual-delivery system of pH-responsive chitosan-functionalized mesoporous silica nanoparticles bearing BMP-2 and dexamethasone for enhanced bone regeneration. *J. Mater. Chem. B* **2015**, *3* (10), 2056–2066.
- (319) Gan, Q.; Zhu, J.; Yuan, Y.; Liu, H.; Zhu, Y.; Liu, C. A proton-responsive ensemble using mesocellular foam supports capped with N,O-carboxymethyl chitosan for controlled release of bioactive proteins. *J. Mater. Chem. B* **2015**, *3* (11), 2281–2285.
- (320) Garbern, J. C.; Hoffman, A. S.; Stayton, P. S. Injectable pH- and temperature-responsive poly(N-isopropylacrylamide-co-propylacrylic acid) copolymers for delivery of angiogenic growth factors. *Biomacromolecules* **2010**, *11* (7), 1833–1839.
- (321) Kim, H. K.; Shim, W. S.; Kim, S. E.; Lee, K. H.; Kang, E.; Kim, J. H.; Kim, K.; Kwon, I. C.; Lee, D. S. Injectable in situ-forming pH/thermo-sensitive hydrogel for bone tissue engineering. *Tissue Engineering Part A* **2009**, *15* (4), 923–933.
- (322) Evans, C. H. Gene delivery to bone. *Adv. Drug Delivery Rev.* **2012**, *64* (12), 1331–1340.
- (323) Ranjbarnejad, F.; Khazaei, M.; Shahyari, A.; Khazaei, F.; Rezakhani, L. Recent advances in gene therapy for bone tissue engineering. *Journal of Tissue Engineering and Regenerative Medicine* **2022**, *16* (12), 1121–1137.
- (324) Levy, O.; Ruvinov, E.; Reem, T.; Granot, Y.; Cohen, S. Highly efficient osteogenic differentiation of human mesenchymal stem cells by eradication of STAT3 signaling. *International Journal of Biochemistry & Cell Biology* **2010**, *42* (11), 1823–1830.
- (325) Zhang, J.; Tu, Q.; Bonewald, L. F.; He, X.; Stein, G.; Lian, J.; Chen, J. Effects of miR-335-5p in modulating osteogenic differentiation by specifically downregulating Wnt antagonist DKK1. *Journal of Bone and Mineral Research* **2011**, *26* (8), 1953–1963.
- (326) Betz, O. B.; Betz, V. M.; Nazarian, A.; Pilapil, C. G.; Vrahas, M. S.; Boussein, M. L.; Gerstenfeld, L. C.; Einhorn, T. A.; Evans, C. H. Direct percutaneous gene delivery to enhance healing of segmental bone defects. *Journal of Bone & Joint Surgery* **2006**, *88* (2), 355–365.
- (327) Ishihara, A.; Shields, K. M.; Litsky, A. S.; Mattoon, J. S.; Weisbrode, S. E.; Bartlett, J. S.; Bertone, A. L. Osteogenic gene regulation and relative acceleration of healing by adenoviral-mediated transfer of human BMP-2 or -6 in equine osteotomy and ostectomy models. *Journal of Orthopaedic Research* **2008**, *26* (6), 764–771.
- (328) Liu, Y. G.; Zhou, Y.; Hu, X.; Fu, J. J.; Pan, Y.; Chu, T. W. Effect of vascular endothelial growth factor 121 adenovirus transduction in rabbit model of femur head necrosis. *Journal of Trauma: Injury, Infection & Critical Care* **2011**, *70* (6), 1519–1523.
- (329) Tarkka, T.; Sipola, A.; Jämsä, T.; Soini, Y.; Ylä-Herttua, S.; Tuukkanen, J.; Hautala, T. Adenoviral VEGF-A gene transfer induces angiogenesis and promotes bone formation in healing osseous tissues. *Journal of Gene Medicine* **2003**, *5* (7), 560–566.
- (330) Strohbach, C. A.; Rundle, C. H.; Wergedal, J. E.; Chen, S. T.; Linkhart, T. A.; Lau, K. H. W.; Strong, D. D. LMP-1 retroviral gene therapy influences osteoblast differentiation and fracture repair: A preliminary study. *Calcified Tissue International* **2008**, *83* (3), 202–211.
- (331) Rundle, C. H.; Strong, D. D.; Chen, S. T.; Linkhart, T. A.; Sheng, M. H. C.; Wergedal, J. E.; Lau, K. H. W.; Baylink, D. J. Retroviral-based gene therapy with cyclooxygenase-2 promotes the union of bony callus tissues and accelerates fracture healing in the rat. *Journal of Gene Medicine* **2008**, *10* (3), 229–241.
- (332) Sakai, S.; Tamura, M.; Mishima, H.; Kojima, H.; Uemura, T. Bone regeneration induced by adenoviral vectors carrying *til-1/Cbfa1* genes implanted with biodegradable porous materials in animal models of osteonecrosis of the femoral head. *Journal of Tissue Engineering and Regenerative Medicine* **2008**, *2* (2–3), 164–167.
- (333) Zhang, Y.; Song, J.; Shi, B.; Wang, Y.; Chen, X.; Huang, C.; Yang, X.; Xu, D.; Cheng, X.; Chen, X. Combination of scaffold and adenovirus vectors expressing bone morphogenetic protein-7 for alveolar bone regeneration at dental implant defects. *Biomaterials* **2007**, *28* (31), 4635–4642.
- (334) Baltzer, A. W. A.; Lattermann, C.; Whalen, J. D.; Braunstein, S.; Robbins, P. D.; Evans, C. H. A gene therapy approach to accelerating bone healing. *Evaluation of gene expression in a New Zealand white rabbit model. Knee Surgery, Sports Traumatology, Arthroscopy* **1999**, *7* (3), 197–202.
- (335) Alden, T. D.; Pittman, D. D.; Hankins, G. R.; Beres, E. J.; Engh, J. A.; Das, S.; Hudson, S. B.; Kerns, K. M.; Kallmes, D. F.; Helm, G. A. In vivo endochondral bone formation using a bone morphogenetic protein 2 adenoviral vector. *Hum. Gene Ther.* **1999**, *10* (13), 2245–2253.
- (336) Baltzer, A. W. A.; Lattermann, C.; Whalen, J. D.; Wooley, P.; Weiss, K.; Grimm, M.; Ghivizzani, S. C.; Robbins, P. D.; Evans, C. H. Genetic enhancement of fracture repair: Healing of an experimental segmental defect by adenoviral transfer of the BMP-2 gene. *Gene Ther.* **2000**, *7* (9), 734–739.
- (337) Thomas, C. E.; Ehrhardt, A.; Kay, M. A. Progress and problems with the use of viral vectors for gene therapy. *Nat. Rev. Genet.* **2003**, *4* (5), 346–358.
- (338) Bright, C.; Park, Y. S.; Sieber, A. N.; Kostuik, J. P.; Leong, K. W. In vivo evaluation of plasmid DNA encoding OP-1 protein for spine fusion. *Spine* **2006**, *31* (19), 2163–2172.
- (339) Remy, M. T.; Akkouch, A.; He, L.; Eliason, S.; Sweat, M. E.; Krongbaramee, T.; Fei, F.; Qian, F.; Amendt, B. A.; Song, X.; Hong, L. Rat Calvarial Bone Regeneration by 3D-Printed β -Tricalcium Phosphate Incorporating MicroRNA-200c. *ACS Biomaterials Science & Engineering* **2021**, *7* (9), 4521–4534.
- (340) Backstrom, K. C.; Bertone, A. L.; Wisner, E. R.; Weisbrode, S. E. Response of induced bone defects in horses to collagen matrix containing the human parathyroid hormone gene. *Am. J. Vet. Res.* **2004**, *65* (9), 1223–1232.
- (341) Keeney, M.; van den Beucken, J. J. P.; van der Kraan, P. M.; Jansen, J. A.; Pandit, A. The ability of a collagen/calcium phosphate scaffold to act as its own vector for gene delivery and to promote bone formation via transfection with VEGF165. *Biomaterials* **2010**, *31* (10), 2893–2902.
- (342) Fang, J.; Zhu, Y. Y.; Smiley, E.; Bonadio, J.; Rouleau, J. P.; Goldstein, S. A.; McCauley, L. K.; Davidson, B. L.; Roessler, B. J. Stimulation of new bone formation by direct transfer of osteogenic plasmid genes. *Proc. Natl. Acad. Sci. U.S.A.* **1996**, *93* (12), 5753–5758.
- (343) Itaka, K.; Ohba, S.; Miyata, K.; Kawaguchi, H.; Nakamura, K.; Takato, T.; Chung, U. I.; Kataoka, K. Bone regeneration by regulated in vivo gene transfer using biocompatible polyplex nanomicelles. *Molecular Therapy* **2007**, *15* (9), 1655–1662.
- (344) Zhang, X.; Li, Y.; Chen, Y. E.; Chen, J.; Ma, P. X. Cell-free 3D scaffold with two-stage delivery of miRNA-26a to regenerate critical-sized bone defects. *Nat. Commun.* **2016**, *7*, 10376.
- (345) Bonadio, J.; Smiley, E.; Patil, P.; Goldstein, S. Localized, direct plasmid gene delivery in vivo: Prolonged therapy results in reproducible tissue regeneration. *Nature Medicine* **1999**, *5* (7), 753–759.
- (346) Chew, S. A.; Kretlow, J. D.; Spicer, P. P.; Edwards, A. W.; Baggett, L. S.; Tabata, Y.; Kasper, F. K.; Mikos, A. G. Delivery of plasmid DNA encoding bone morphogenetic protein-2 with a biodegradable branched polycationic polymer in a critical-size rat cranial defect model. *Tissue Engineering. Part A* **2011**, *17* (5–6), 751–763.
- (347) Boden, S. D.; Titus, L.; Hair, G.; Liu, Y.; Viggswarapu, M.; Nanes, M. S.; Baranowski, C. 1998 Volvo award winner in basic sciences studies: Lumbar spine fusion by local gene therapy with a cDNA encoding a novel osteoinductive protein (LMP-1). *Spine* **1998**, *23* (23), 2486–2492.
- (348) Park, J.; Ries, J.; Gelse, K.; Kloss, F.; von der Mark, K.; Wiltfang, J.; Neukam, F. W.; Schneider, H. Bone regeneration in critical size defects by cell-mediated BMP-2 gene transfer: A comparison of adenoviral vectors and liposomes. *Gene Ther.* **2003**, *10* (13), 1089–1098.
- (349) Alshehri, A.; Grabowska, A.; Stolnik, S. Pathways of cellular internalisation of liposomes delivered siRNA and effects on siRNA

- engagement with target mRNA and silencing in cancer cells. *Sci. Rep.* **2018**, *8* (1), 3748.
- (350) Guo-Ping, W.; Xiao-Chuan, H.; Zhi-Hui, Y.; Li, G. Influence on the osteogenic activity of the human bone marrow mesenchymal stem cells transfected by liposome-mediated recombinant plasmid pIRES-hBMP2-hVEGF165 in vitro. *Annals of Plastic Surgery* **2010**, *65* (1), 80–84.
- (351) Zylberberg, C.; Gaskill, K.; Pasley, S.; Matosevic, S. Engineering liposomal nanoparticles for targeted gene therapy. *Gene Ther.* **2017**, *24* (8), 441–452.
- (352) Sun, X.; Wei, J.; Lyu, J.; Bian, T.; Liu, Z.; Huang, J.; Pi, F.; Li, C.; Zhong, Z. Bone-targeting drug delivery system of biomineral-binding liposomes loaded with icariin enhances the treatment for osteoporosis. *J. Nanobiotechnol.* **2019**, *17* (1), 10.
- (353) Rea, J. C.; Gibly, R. F.; Barron, A. E.; Shea, L. D. Self-assembling peptide-lipoplexes for substrate-mediated gene delivery. *Acta Biomaterialia* **2009**, *5* (3), 903–912.
- (354) Liu, L.; Xiang, Y.; Wang, Z.; Yang, X.; Yu, X.; Lu, Y.; Deng, L.; Cui, W. Adhesive liposomes loaded onto an injectable, self-healing and antibacterial hydrogel for promoting bone reconstruction. *NPG Asia Materials* **2019**, *11* (1), 81.
- (355) Mickova, A.; Buzgo, M.; Benada, O.; Rampichova, M.; Fisar, Z.; Filova, E.; Tesarova, M.; Lukas, D.; Amler, E. Core/shell nanofibers with embedded liposomes as a drug delivery system. *Biomacromolecules* **2012**, *13* (4), 952–962.
- (356) De Smedt, S. C.; Demeester, J.; Hennink, W. E. Cationic polymer based gene delivery systems. *Pharm. Res.* **2000**, *17* (2), 113–126.
- (357) Tiera, M. J.; Shi, Q.; Winnik, F. M.; Fernandes, J. C. Polycation-based gene therapy: Current knowledge and new perspectives. *Current Gene Therapy* **2011**, *11* (4), 288–306.
- (358) Stayton, P. S.; Hoffman, A. S.; Murthy, N.; Lackey, C.; Cheung, C.; Tan, P.; Klumb, L. A.; Chilkoti, A.; Willbur, F. S.; Press, O. W. Molecular engineering of proteins and polymers for targeting and intracellular delivery of therapeutics. *J. Controlled Release* **2000**, *65* (1–2), 203–220.
- (359) Hall, A.; Lächelt, U.; Bartek, J.; Wagner, E.; Moghimi, S. M. Polyplex evolution: Understanding biology, optimizing performance. *Molecular Therapy* **2017**, *25* (7), 1476–1490.
- (360) Gabrielson, N. P.; Pack, D. W. Acetylation of polyethylenimine enhances gene delivery via weakened polymer/DNA interactions. *Biomacromolecules* **2006**, *7* (8), 2427–2435.
- (361) Oskuee, R. K.; Dehshahri, A.; Shier, W. T.; Ramezani, M. Alkylcarboxylate grafting to polyethylenimine: A simple approach to producing a DNA nanocarrier with low toxicity. *Journal of Gene Medicine* **2009**, *11* (10), 921–932.
- (362) Cheng, R.; Yan, Y.; Liu, H.; Chen, H.; Pan, G.; Deng, L.; Cui, W. Mechanically enhanced lipo-hydrogel with controlled release of multi-type drugs for bone regeneration. *Applied Materials Today* **2018**, *12*, 294–308.
- (363) Kupikowska-Stobba, B.; Grzeczkwicz, M.; Lewińska, D. A one-step in vitro continuous flow assessment of protein release from core-shell polymer microcapsules designed for therapeutic protein delivery. *Biocybernetics and Biomedical Engineering* **2021**, *41* (4), 1347–1364.
- (364) Longoni, A.; Li, J.; Lindberg, G. C. J.; Rnjak-Kovacina, J.; Wise, L. M.; Hooper, G. J.; Woodfield, T. B. F.; Kieser, D. C.; Lim, K. S. Strategies for inclusion of growth factors into 3D printed bone grafts. *Essays in Biochemistry* **2021**, *65* (3), 569–585.
- (365) Raggatt, L. J.; Partridge, N. C. Cellular and molecular mechanisms of bone remodeling. *J. Biol. Chem.* **2010**, *285* (33), 25103–25108.
- (366) Bonewald, L. F. The amazing osteocyte. *Journal of Bone and Mineral Research* **2011**, *26* (2), 229–238.
- (367) Iseme, R. A.; McEvoy, M.; Kelly, B.; Agnew, L.; Walker, F. R.; Attia, J. Is osteoporosis an autoimmune mediated disorder? *Bone Reports* **2017**, *7*, 121–131.
- (368) Florencio-Silva, R.; Sasso, G. R. D. S.; Sasso-Cerri, E.; Simões, M. J.; Cerri, P. S. Biology of bone tissue: Structure, function, and factors that influence bone cells. *BioMed. Research International* **2015**, *2015*, 421746.
- (369) Meskinfam, M. Polymer scaffolds for bone regeneration. *Characterization of Polymeric Biomaterials* **2017**, 441–475.
- (370) Iolascon, G.; Napolano, R.; Gioia, M.; Moretti, A.; Riccio, I.; Gimigliano, F. The contribution of cortical and trabecular tissues to bone strength: Insights from denosumab studies. *Clinical Cases in Mineral and Bone Metabolism* **2013**, *10* (1), 47–51.
- (371) Hunter, D. J.; Sambrook, P. N. Bone loss. Epidemiology of bone loss. *Arthritis Research* **2000**, *2* (6), 441–445.
- (372) Pietschmann, P.; Mechtcheriakova, D.; Meshcheryakova, A.; Föger-Samwald, U.; Ellinger, I. Immunology of osteoporosis: A mini-review. *Gerontology* **2016**, *62* (2), 128–137.
- (373) Caetano-Lopes, J.; Canhão, H.; Fonseca, J. E. Osteoimmunology - the hidden immune regulation of bone. *Autoimmunity Reviews* **2009**, *8* (3), 250–255.
- (374) Bugatti, S.; Bogliolo, L.; Vitolo, B.; Manzo, A.; Montecucco, C.; Caporali, R. Anti-citrullinated protein antibodies and high levels of rheumatoid factor are associated with systemic bone loss in patients with early untreated rheumatoid arthritis. *Arthritis Research & Therapy* **2016**, *18* (1), 226.
- (375) Sokolove, J.; Pisetsky, D. Bone loss, pain and inflammation: Three faces of ACPA in RA pathogenesis. *Annals of the Rheumatic Diseases* **2016**, *75* (4), 637–639.
- (376) Amarasekara, D. S.; Yu, J.; Rho, J. Bone loss triggered by the cytokine network in inflammatory autoimmune diseases. *Journal of Immunology Research* **2015**, *2015*, 832127.
- (377) Boissier, M. C. Cell and cytokine imbalances in rheumatoid synovitis. *Joint Bone Spine* **2011**, *78* (3), 230–234.
- (378) Fischer, J. A. A.; Hueber, A. J.; Wilson, S.; Galm, M.; Baum, W.; Kitson, C.; Auer, J.; Lorenz, S.; Moelleken, J.; Bader, M.; Tissot, A. C.; Tan, S. L.; Seeber, S.; Schett, G. Combined inhibition of tumor necrosis factor α and interleukin-17 as a therapeutic opportunity in rheumatoid arthritis: Development and characterization of a novel bispecific antibody. *Arthritis & Rheumatology* **2015**, *67* (1), 51–62.
- (379) Wei, H.; Cui, J.; Lin, K.; Xie, J.; Wang, X. Recent advances in smart stimuli-responsive biomaterials for bone therapeutics and regeneration. *Bone Res.* **2022**, *10* (1), No. 17.
- (380) Chen, B.; Xiang, H.; Pan, S.; Yu, L.; Xu, T.; Chen, Y. Advanced theragenerative biomaterials with therapeutic and regeneration multifunctionality. *Adv. Funct. Mater.* **2020**, *30*, 2002621.
- (381) Zhang, J.; Zhao, S.; Zhu, M.; Zhu, Y.; Zhang, Y.; Liu, Z.; Zhang, C. 3D-printed magnetic Fe₃O₄/MBG/PCL composite scaffold with multifunctionality of bone regeneration, local anticancer drug delivery and hyperthermia. *J. Mater. Chem. B* **2014**, *2* (43), 7583.
- (382) Wang, D.; Peng, F.; Li, J.; Qiao, Y.; Li, Q.; Liu, X. Butyrate-inserted Ni–Ti layered double hydroxide film for H₂O₂-mediated tumor and bacteria killing. *Mater. Today* **2017**, *20* (5), 238–257.
- (383) Ma, H.; Li, T.; Huan, Z.; Zhang, M.; Yang, Z.; Wang, J.; Chang, J.; Wu, C. 3D printing of high-strength bioscaffolds for the synergistic treatment of bone cancer. *NPG Asia Materials* **2018**, *10* (4), 31–44.
- (384) Yin, S.; Zhang, W.; Zhang, Z.; Jiang, X. Recent advances in scaffold design and material for vascularized tissue-engineered bone regeneration. *Adv. Healthcare Mater.* **2019**, *8* (10), 1801433.
- (385) Bhatnagar, R. S.; Qian, J. J.; Wedrychowska, A.; Sadeghi, M.; Wu, Y. M.; Smith, N. Design of biomimetic habitats for tissue engineering with P-15, a synthetic peptide analogue of collagen. *Tissue Engineering* **1999**, *5* (1), 53–65.
- (386) Emam, H. A.; Behiri, G.; El-Alaily, M.; Sharawy, M. The efficacy of a tissue-engineered xenograft in conjunction with sodium hyaluronate carrier in maxillary sinus augmentation: A clinical study. *International Journal of Oral and Maxillofacial Surgery* **2015**, *44* (10), 1287–1294.
- (387) Nguyen, H.; Qian, J. J.; Bhatnagar, R. S.; Li, S. Enhanced cell attachment and osteoblastic activity by P-15 peptide-coated matrix in hydrogels. *Biochem. Biophys. Res. Commun.* **2003**, *311* (1), 179–186.

- (388) Yang, X. B.; Bhatnagar, R. S.; Li, S.; Oreffo, R. O. C. Biomimetic collagen scaffolds for human bone cell growth and differentiation. *Tissue Engineering* **2004**, *10* (7), 1148–1159.
- (389) Cakarar, S.; Olgac, V.; Aksakalli, N.; Tang, A.; Keskin, C. Acceleration of consolidation period by thrombin peptide 508 in tibial distraction osteogenesis in rats. *British Journal of Oral and Maxillofacial Surgery* **2010**, *48* (8), 633–636.
- (390) Huang, H.; Zhao, Y.; Liu, Z.; Zhang, Y.; Zhang, H.; Fu, T.; Ma, X. Enhanced osteoblast functions on RGD immobilized surface. *Journal of Oral Implantology* **2003**, *29* (2), 73–79.
- (391) Priddy, L. B.; Chaudhuri, O.; Stevens, H. Y.; Krishnan, L.; Uhrig, B. A.; Willett, N. J.; Guldberg, R. E. Oxidized alginate hydrogels for bone morphogenetic protein-2 delivery in long bone defects. *Acta Biomaterialia* **2014**, *10* (10), 4390–4399.
- (392) Rammelt, S.; Illert, T.; Bierbaum, S.; Scharnweber, D.; Zwipp, H.; Schneiders, W. Coating of titanium implants with collagen, RGD peptide and chondroitin sulfate. *Biomaterials* **2006**, *27* (32), 5561–5571.
- (393) Egusa, H.; Kaneda, Y.; Akashi, Y.; Hamada, Y.; Matsumoto, T.; Saeki, M.; Thakor, D. K.; Tabata, Y.; Matsuura, N.; Yatani, H. Enhanced bone regeneration via multimodal actions of synthetic peptide SVVYGLR on osteoprogenitors and osteoclasts. *Biomaterials* **2009**, *30* (27), 4676–4686.
- (394) Hamada, Y.; Yuki, K.; Okazaki, M.; Fujitani, W.; Matsumoto, T.; Hashida, M. K.; Harutsugu, K.; Nokihara, K.; Daito, M.; Matsuura, N.; Takahashi, J. Osteopontin-derived peptide SVVYGLR induces angiogenesis in vivo. *Dental Materials Journal* **2004**, *23* (4), 650–655.
- (395) Park, K. M.; Lee, Y.; Son, J. Y.; Bae, J. W.; Park, K. D. In situ SVVYGLR peptide conjugation into injectable gelatin-poly(ethylene glycol)-tyramine hydrogel via enzyme-mediated reaction for enhancement of endothelial cell activity and neo-vascularization. *Bioconjugate Chem.* **2012**, *23* (10), 2042–2050.
- (396) Mhanna, R.; Öztürk, E.; Vallmajo-Martin, Q.; Millan, C.; Müller, M.; Zenobi-Wong, M. GFOGER-modified MMP-sensitive polyethylene glycol hydrogels induce chondrogenic differentiation of human mesenchymal stem cells. *Tissue Engineering. Part A* **2014**, *20* (7–8), 1165–1174.
- (397) Reyes, C. D.; García, A. J. A2B1 integrin-specific collagen-mimetic surfaces supporting osteoblastic differentiation. *J. Biomed. Mater. Res., Part A* **2004**, *69A* (4), 591–600.
- (398) Reyes, C. D.; Petrie, T. A.; Burns, K. L.; Schwartz, Z.; García, A. J. Biomolecular surface coating to enhance orthopaedic tissue healing and integration. *Biomaterials* **2007**, *28* (21), 3228–3235.
- (399) Shekaran, A.; García, J. R.; Clark, A. Y.; Kavanaugh, T. E.; Lin, A. S.; Guldberg, R. E.; García, A. J. Bone regeneration using an alpha 2 beta 1 integrin-specific hydrogel as a BMP-2 delivery vehicle. *Biomaterials* **2014**, *35* (21), 5453–5461.
- (400) Lee, J. Y.; Choo, J. E.; Park, H. J.; Park, J. B.; Lee, S. C.; Jo, I.; Lee, S. J.; Chung, P. C.; Park, Y. J. Injectable gel with synthetic collagen-binding peptide for enhanced osteogenesis in vitro and in vivo. *Biochem. Biophys. Res. Commun.* **2007**, *357* (1), 68–74.
- (401) Shin, M. K.; Kim, M. K.; Bae, Y. S.; Jo, I.; Lee, S. J.; Chung, C. P.; Park, Y. J.; Min, D. S. A novel collagen-binding peptide promotes osteogenic differentiation via Ca²⁺/calmodulin-dependent protein kinase II/ERK/AP-1 signaling pathway in human bone marrow-derived mesenchymal stem cells. *Cellular Signalling* **2008**, *20* (4), 613–624.
- (402) Kim, Y. J.; Park, Y. J.; Lee, Y. M.; Rhyu, I. C.; Ku, Y. The biological effects of fibrin-binding synthetic oligopeptides derived from fibronectin on osteoblast-like cells. *Journal of Periodontal & Implant Science* **2012**, *42* (4), 113–118.
- (403) Lee, J. A.; Ku, Y.; Rhyu, I. C.; Chung, C. P.; Park, Y. J. Effects of fibrin-binding oligopeptide on osteopromotion in rabbit calvarial defects. *Journal of Periodontal & Implant Science* **2010**, *40* (5), 211–219.
- (404) Martino, M. M.; Tortelli, F.; Mochizuki, M.; Traub, S.; Ben-David, D.; Kuhn, G. A.; Müller, R.; Livne, E.; Eming, S. A.; Hubbell, J. A. Engineering the growth factor microenvironment with fibronectin domains to promote wound and bone tissue healing. *Science Translational Medicine* **2011**, *3* (100), 100ra189.
- (405) Zhang, X.; Guo, W. G.; Cui, H.; Liu, H. Y.; Zhang, Y.; Müller, W. E. G.; Cui, F. Z. In vitro and in vivo enhancement of osteogenic capacity in a synthetic BMP-2 derived peptide-coated mineralized collagen composite. *Journal of Tissue Engineering and Regenerative Medicine* **2016**, *10* (2), 99–107.
- (406) Chen, Y.; Liu, X.; Liu, R.; Gong, Y.; Wang, M.; Huang, Q.; Feng, Q.; Yu, B. Zero-order controlled release of BMP2-derived peptide P24 from the chitosan scaffold by chemical grafting modification technique for promotion of osteogenesis in vitro and enhancement of bone repair in vivo. *Theranostics* **2017**, *7* (5), 1072–1087.
- (407) Li, W.; Zheng, Y.; Zhao, X.; Ge, Y.; Chen, T.; Liu, Y.; Zhou, Y. Osteoinductive effects of free and immobilized bone forming peptide-1 on human adipose-derived stem cells. *PLoS One* **2016**, *11* (3), e0150294.
- (408) Lv, L.; Wang, Y.; Zhang, J.; Zhang, T.; Li, S. Healing of periodontal defects and calcitonin gene related peptide expression following inferior alveolar nerve transection in rats. *Journal of Molecular Histology* **2014**, *45* (3), 311–320.
- (409) Wang, Y. H.; Zhang, L.; Jia, L.; Liu, J.; Liu, K.; Feng, Q. Z.; Wang, Q. Calcitonin gene-related peptide in aerobic exercise induces collateral circulation development in rat ischemia myocardium. *Biomedicine & Pharmacotherapy* **2016**, *82*, 561–567.
- (410) Zhou, X. Y.; Xu, X. M.; Wu, S. Y.; Wang, F.; Yang, Y. L.; Li, M.; Wei, X. Z. Spatiotemporal changes of calcitonin gene-related peptide innervation in spinal fusion. *BioMed. Research International* **2016**, *2016*, 5872860.
- (411) Alkhiary, Y. M.; Gerstenfeld, L. C.; Krall, E.; Westmore, M.; Sato, M.; Mitlak, B. H.; Einhorn, T. A. Enhancement of experimental fracture-healing by systemic administration of recombinant human parathyroid hormone (PTH 1–34). *Journal of Bone & Joint Surgery* **2005**, *87* (4), 731–741.
- (412) Whitfield, J. F.; Morley, P.; Willick, G. E. Parathyroid hormone, its fragments and their analogs for the treatment of osteoporosis. *Treatments in Endocrinology* **2002**, *1* (3), 175–190.
- (413) An, G.; Xue, Z.; Zhang, B.; Deng, Q. K.; Wang, Y. S.; Lv, S. C. Expressing osteogenic growth peptide in the rabbit bone mesenchymal stem cells increased alkaline phosphatase activity and enhanced the collagen accumulation. *European Review for Medical and Pharmacological Sciences* **2014**, *18* (11), 1618–1624.
- (414) Fei, Q.; Guo, C.; Xu, X.; Gao, J.; Zhang, J.; Chen, T.; Cui, D. Osteogenic growth peptide enhances the proliferation of bone marrow mesenchymal stem cells from osteoprotegerin-deficient mice by CDK2/cyclin A. *Acta Biochimica et Biophysica Sinica* **2010**, *42* (11), 801–806.
- (415) Spreafico, A.; Frediani, B.; Capperucci, C.; Leonini, A.; Gambera, D.; Ferrata, P.; Rosini, S.; Di Stefano, A.; Galeazzi, M.; Marcolongo, R. Osteogenic growth peptide effects on primary human osteoblast cultures: Potential relevance for the treatment of glucocorticoid-induced osteoporosis. *Journal of Cellular Biochemistry* **2006**, *98* (4), 1007–1020.
- (416) Li, G.; Cui, Y.; McMurray, L.; Allen, W. E.; Wang, H. rhBMP-2, rhVEGF165, rhPTN and thrombin-related peptide, TPS08 induce chemotaxis of human osteoblasts and microvascular endothelial cells. *Journal of Orthopaedic Research* **2005**, *23* (3), 680–685.
- (417) Jimi, E.; Aoki, K.; Saito, H.; D'Acquisto, F.; May, M. J.; Nakamura, I.; Sudo, T.; Kojima, T.; Okamoto, F.; Fukushima, H.; Okabe, K.; Ohya, K.; Ghosh, S. Selective inhibition of NF-κB blocks osteoclastogenesis and prevents inflammatory bone destruction in vivo. *Nature Medicine* **2004**, *10* (6), 617–624.
- (418) Soysa, N. S.; Alles, N.; Shimokawa, H.; Jimi, E.; Aoki, K.; Ohya, K. Inhibition of the classical NF-κB pathway prevents osteoclast bone-resorbing activity. *Journal of Bone and Mineral Metabolism* **2009**, *27* (2), 131–139.
- (419) Jo, J.; Hong, S.; Choi, W. Y.; Lee, D. R. Cell-penetrating peptide (CPP)-conjugated proteins is an efficient tool for

manipulation of human mesenchymal stromal cells. *Sci. Rep.* **2014**, *4*, 4378.

(420) Karagiannis, E. D.; Urbanska, A. M.; Sahay, G.; Pelet, J. M.; Jhunjhunwala, S.; Langer, R.; Anderson, D. G. Rational design of a biomimetic cell penetrating peptide library. *ACS Nano* **2013**, *7* (10), 8616–8626.

(421) Hou, T.; Li, Z.; Luo, F.; Xie, Z.; Wu, X.; Xing, J.; Dong, S.; Xu, J. A composite demineralized bone matrix – Self assembling peptide scaffold for enhancing cell and growth factor activity in bone marrow. *Biomaterials* **2014**, *35* (22), 5689–5699.

(422) Flaig, F.; Ragot, H.; Simon, A.; Revet, G.; Kitsara, M.; Kitasato, L.; Hébraud, A.; Agbulut, O.; Schlatter, G. Design of functional electrospun scaffolds based on poly(glycerol sebacate) elastomer and poly(lactic acid) for cardiac tissue engineering. *ACS Biomaterials Science & Engineering* **2020**, *6* (4), 2388–2400.

(423) Prabhakaran, M. P.; Venugopal, J.; Ramakrishna, S. Electrospun nanostructured scaffolds for bone tissue engineering. *Acta Biomaterialia* **2009**, *5* (8), 2884–2893.

(424) Fakhrali, A.; Semnani, D.; Salehi, H.; Ghane, M. Electrospun PGS/PCL nanofibers: From straight to sponge and spring-like morphology. *Polym. Adv. Technol.* **2020**, *31* (12), 3134–3149.

(425) Blaker, J. J.; Maquet, V.; Jérôme, R.; Boccaccini, A. R.; Nazhat, S. N. Mechanical properties of highly porous PDLA/Bioglass® composite foams as scaffolds for bone tissue engineering. *Acta Biomaterialia* **2005**, *1* (6), 643–652.

(426) Huang, Y. X.; Ren, J.; Chen, C.; Ren, T. B.; Zhou, X. Y. Preparation and properties of poly(lactide-co-glycolide) (PLGA)/nano-hydroxyapatite (NHA) scaffolds by thermally induced phase separation and rabbit MSCs culture on scaffolds. *Journal of Biomaterials Applications* **2008**, *22* (5), 409–432.

(427) Grémare, A.; Guduric, V.; Bareille, R.; Heroguez, V.; Latour, S.; L'Heureux, N.; Fricain, J. C.; Catros, S.; Le Nihouannen, D. Characterization of printed PLA scaffolds for bone tissue engineering. *J. Biomed. Mater. Res., Part A* **2018**, *106* (4), 887–894.

(428) Du, Y.; Liu, H.; Yang, Q.; Wang, S.; Wang, J.; Ma, J.; Noh, I.; Mikos, A. G.; Zhang, S. Selective laser sintering scaffold with hierarchical architecture and gradient composition for osteochondral repair in rabbits. *Biomaterials* **2017**, *137*, 37–48.

(429) Duan, B.; Wang, M.; Zhou, W. Y.; Cheung, W. L.; Li, Z. Y.; Lu, W. W. Three-dimensional nanocomposite scaffolds fabricated via selective laser sintering for bone tissue engineering. *Acta Biomaterialia* **2010**, *6* (12), 4495–4505.

(430) Szustakiewicz, K.; Stępak, B.; Antończak, A. J.; Maj, M.; Gazińska, M.; Kryszak, B.; Pięłowski, J. Femtosecond laser-induced modification of PLLA/hydroxyapatite composite. *Polym. Degrad. Stab.* **2018**, *149*, 152–161.

(431) Kryszak, B.; Szustakiewicz, K.; Stępak, B.; Gazińska, M.; Antończak, A. J. Structural, thermal and mechanical changes in poly(l-lactide)/hydroxyapatite composite extruded foils modified by CO₂ laser irradiation. *Eur. Polym. J.* **2019**, *114*, 57–65.

(432) Szustakiewicz, K.; Kryszak, B.; Gazińska, M.; Chęcmanowski, J.; Stępak, B.; Grzymajło, M.; Antończak, A. The effect of selective mineralization of PLLA in simulated body fluid induced by ArF excimer laser irradiation: Tailored composites with potential in bone tissue engineering. *Compos. Sci. Technol.* **2020**, *197*, 108279.

(433) Smieszek, A.; Marycz, K.; Szustakiewicz, K.; Kryszak, B.; Targonska, S.; Zawisza, K.; Watras, A.; Wiglusz, R. J. New approach to modification of poly (l-lactic acid) with nano-hydroxyapatite improving functionality of human adipose-derived stromal cells (hASCs) through increased viability and enhanced mitochondrial activity. *Materials Science and Engineering: C* **2019**, *98*, 213–226.

**Podsumowanie prac
wchodzących w skład
rozprawy doktorskiej**

P.I.

In Vitro and *In Vivo* Biocompatibility of Natural and Synthetic *Pseudomonas aeruginosa* Pyomelanin for Potential Biomedical Applications

Urbaniak M. M., Gazińska M., Rudnicka K., Płociński P., Nowak M., Chmiela M.

International Journal of Molecular Sciences, 2023, 24, 7846.

DOI: 10.3390/ijms24097846

W pierwszym etapie badań wchodzących w skład publikacji **P.I.**, w celu nasilenia biosyntezy oraz efektywniejszej izolacji bakteryjnej PyoM z płynnych hodowli *P. aeruginosa* Mel+, opracowano dwa podłoża minimalne PMM (*pyomelanin minimal medium*) – podłoże PMM I składające się z glukozy, soli mineralnych (KH₂PO₄, NaCl, MgSO₄) i tyrozyny, będącej prekursorowym aminokwasem dla produkcji HGA i PyoM oraz podłoże PMM II, będące rozszerzoną wersją pożywki PMM I suplementowanej arabinozą i kwasem jabłkowym. W kolejnym kroku opracowano metodę otrzymywania i oczyszczania dwóch form bakteryjnej PyoM – rozpuszczalnej (PyoM_{sol}) lub nierozpuszczalnej w wodzie (PyoM_{insol}), a także syntetycznego odpowiednika tego bakteryjnego barwnika (sPyoM) otrzymanego w reakcji polimeryzacji HGA. Użycie podłoży PMM I lub PMM II oraz metody oczyszczania PyoM, z wykorzystaniem chromatografii powinowactwa i wirowania zatężającego, zwiększyło skuteczność izolacji barwnika na poziomie, odpowiednio 1,13 ± 0,12 g/L (PMM I) i 1,79 ± 0,18 g/L (PMM II) dla PyoM_{sol} oraz 0,71 ± 0,04 g/L (PMM I) i 1,22 ± 0,10 g/L (PMM II) dla PyoM_{insol}, w porównaniu do wydajności otrzymywania PyoM z hodowli *P. aeruginosa* w komercyjnym podłożu LB (odpowiednio PyoM_{sol} i PyoM_{insol}: 0,45 ± 0,14 g/L i 0,69 ± 0,15 g/L). Podczas syntezy chemicznej tego barwnika, w porównaniu do produkcji PyoM przez bakterie, otrzymano jedynie 0,077 ± 0,01g sPyoM z 1 g kwasu HGA.

W kolejnym etapie badań scharakteryzowano strukturę chemiczną uzyskanych wariantów PyoM z wykorzystaniem techniki FTIR oraz określono ich termostabilność przy użyciu metody TGA i DSC, aby wykluczyć możliwą degradację cieplną w procesie autoklawowania i przetwórstwa. W strukturze bakteryjnych PyoM wykazano ugrupowania charakterystyczne dla związków melaninowych wywodzących się z HGA tj. pierścienie

aromatyczne, grupy karboksylowe oraz grupy hydroksylowe. Analiza wyników badań uzyskanych metodami TGA i DCS wykazała, że najwyższą stabilnością termiczną charakteryzuje się PyoM_{insol} (196,4°C) a najniższą sPyoM (158,0°C), co może wskazywać na większy udział ugrupowań aromatycznych lub innych sprzężonych wiązań nienasyconych w łańcuchach bakteryjnych PyoM_{insol}.

W ostatniej części pracy scharakteryzowano uzyskane warianty PyoM pod względem cytokompatybilności, na modelu *in vitro* referencyjnych fibroblastów L929 myszy i monocytów THP-1 człowieka, oraz określono bezpieczeństwo biologiczne *in vivo* na modelu larw *Galleria mellonella* z wyznaczeniem wskaźnika HISS. Ponadto oceniono zdolność PyoM do aktywacji czynnika transkrypcyjnego NF-κB, kluczowego w rozwoju reakcji odpornościowych i procesów regeneracji uszkodzonych tkanek. Wykazano, że bakteryjne piomelaniny, PyoM_{sol} i PyoM_{insol}, są wysoce cytokompatybilne wobec fibroblastów L929 i monocytów THP-1, spełniając założenia normy ISO 10993-5:2009 (Biologiczna ocena wyrobów medycznych – Część 5: Testy cytotoksyczności *in vitro*). Oba warianty naturalnej PyoM *P. aeruginosa* były cytozgodne w zakresie stężeń 1 – 1024 µg/ml, w przeciwieństwie do formy syntetycznej, która nie wykazywała działania cytotoksycznego jedynie w zakresie stężeń 1–32 µg/ml względem fibroblastów myszy i w zakresie stężeń 1–16 µg/ml wobec monocytów człowieka. W badaniu z wykorzystaniem reporterowych monocytów THP1-Blue™ NF-κB wykazano istotne różnice w aktywacji czynnika transkrypcyjnego NF-κB przez badane PyoM. Czynniki NF-κB był najsilniej aktywowany w hodowlach monocytów stymulowanych PyoM_{sol} (aktywacja zależna od dawki w zakresie 1–1024 µg/ml). Natomiast po traktowaniu komórek reporterowych PyoM_{insol} lub sPyoM wykazano aktywację czynnika NF-κB w zakresie stężeń, odpowiednio 64–1024 µg/ml lub 1–64 µg/ml. Wyniki biokompatybilności uzyskane na modelu *in vivo* były spójne z wynikami eksperymentów komórkowych *in vitro*. Nie wykazano objawów toksyczności układowej dwóch wariantów bakteryjnej PyoM po 0, 12, 24, 48, 72, 96 i 120 godzinach od wstrzyknięcia barwnika larwom. Całkowita punktacja HISS u larw traktowanych PyoM_{sol} lub PyoM_{insol} była zbliżona do wskaźnika HISS u larw kontrolnych nastrzykniętych solą fizjologiczną buforowaną fosforanami (PBS, *phosphate buffered saline*), który wynosił 9,0. Sumaryczny wskaźnik HISS u larw nastrzykniętych sPyoM był niższy (7,79–3,58), w porównaniu do HISS u larw, którym podano naturalne warianty PyoM lub PBS.

P.II.

Can Pyomelanin Produced by *Pseudomonas aeruginosa* Promote the Regeneration of Gastric Epithelial Cells and Enhance *Helicobacter pylori* Phagocytosis?

Urbaniak M. M., Rudnicka K., Gościński G., Chmiela M.

International Journal of Molecular Sciences, 2023, 24, 13911.

DOI: 10.3390/ijms241813911

Celem drugiego etapu badań, na podstawie którego powstała praca **P.II.** było określenie przeciwdrobnoustrojowego działania bakteryjnych PyoM_{sol} i PyoM_{insol} wobec pałeczek *H. pylori* oraz hamowania działania cytotoksycznego LPS tych bakterii, które jest powiązane z nasileniem stresu oksydacyjnego i apoptozy, na modelu fibroblastów L929, monocytów THP-1 oraz komórek nabłonka żołądka AGS. Ponadto celem badań była weryfikacja zdolności tych barwników do wspomagania procesu regeneracji komórek nabłonkowych żołądka i nasilania fagocytozy *H. pylori* przez komórki żerne *in vitro*.

W pierwszym kroku scharakteryzowano właściwości przeciwbakteryjne wariantów PyoM w teście redukcji resazuryiny z wyznaczeniem najniższego stężenia hamującego (MIC, *minimum inhibitory concentration*) wzrost referencyjnych i klinicznych szczepów *H. pylori*. Wartości MIC₅₀ i MIC₉₉ zdefiniowano jako najniższe stężenie PyoM, przy którym żywotność bakterii ulegała obniżeniu, odpowiednio o 50% lub 99%. Wykazano, że PyoM_{sol} i PyoM_{insol} istotnie hamowały żywotność referencyjnych i klinicznych szczepów *H. pylori*. MIC₅₀ PyoM_{sol} wobec szczepu *H. pylori* CCUG 17784 wynosił 14,5 µg/ml, natomiast wobec szczepów klinicznych M91 i M102 odpowiednio, 19,5 µg/ml i 18,6 µg/ml. Wartości MIC₅₀ dla PyoM_{insol} wynosiły odpowiednio, 7,2 µg/ml, 18,4 µg/ml i 15,5 µg/ml. Wartość MIC₉₉ PyoM_{sol} w stosunku do badanych szczepów *H. pylori* mieściła się w zakresie 31,7–34,2 µg/ml, natomiast dla PyoM_{insol} w zakresie 19,3–29,0 µg/ml.

W kolejnym etapie badań oceniono właściwości cytoprotekcyjne i przeciwapoptotyczne badanych form PyoM, w środowisku referencyjnego LPS *E. coli* lub LPS *H. pylori*, odpowiednio w teście redukcji MTT i TUNEL. Wykazano, że PyoM_{sol}

i PyoM_{insol}, w badanych stężeniach (1 µg/ml lub 16 µg/ml), nie wpływały na żywotność fibroblastów L-929, monocytów THP-1 i komórek nabłonka żołądka AGS. W hodowlach komórkowych traktowanych LPS *H. pylori* lub LPS *E. coli* odsetek żywych komórek istotnie zmniejszył się, natomiast po kostymulacji komórek PyoM i LPS *H. pylori* lub LPS *E. coli* ich żywotność była zbliżona do żywotności komórek nietraktowanych, co sugeruje, że bakteryjne PyoM neutralizowały cytotoksyczne działanie LPS. Takie działanie PyoM stało się przesłanką do zbadania, czy wykazanemu efektowi cytoprotekcji towarzyszy także hamowanie apoptozy komórek. Same bakteryjne PyoM nie indukowały apoptozy w badanych komórkach. Wykazano, że w środowisku PyoM_{sol}, proces apoptozy komórek w hodowlach komórek nabłonka żołądka, fibroblastów lub monocytów traktowanych LPS *H. pylori*, lub LPS *E. coli*, był istotnie statystycznie ograniczony w porównaniu do hodowli komórkowych nie zawierających PyoM. PyoM_{insol} wywoływała efekt przeciwapoptyczny jedynie w stężeniu 1 µg/ml, na modelu komórek AGS lub THP-1 kostymulowanych LPS *H. pylori*.

Mając na uwadze, iż stres oksydacyjny jest jednym z kluczowych czynników warunkujących uszkodzenie materiału genetycznego, a w jego następstwie apoptozę komórek, w celu weryfikacji przeciw-oksydacyjnego działania bakteryjnych PyoM, w komórkach nabłonka żołądka AGS eksponowanych na LPS *H. pylori* wykorzystano fluorymetryczną sondę H₂DCFDA, umożliwiającą ocenę aktywności wewnątrzkomórkowych ROS. Wykazano, że w środowisku LPS *H. pylori* lub referencyjnego LPS *E. coli* poziom ROS w komórkach AGS, po 30 minutach lub 24 godzinach ekspozycji był istotnie podwyższony, w porównaniu z komórkami nietraktowanymi LPS. Oba warianty PyoM znacząco redukowały poziom ROS, w hodowlach komórkowych kostymulowanych PyoM i LPS *H. pylori* lub LPS *E. coli*, w porównaniu z komórkami traktowanymi samym LPS.

W kolejnym etapie badań oceniono zdolność komórek AGS, stymulowanych PyoM lub kostymulowanych PyoM i LPS *H. pylori*, lub LPS *E. coli*, do migracji w tzw. „teście gojenia rany” *in vitro*. Wykazano, że PyoM_{sol} i PyoM_{insol} istotnie stymulowały migrację komórek po 24 i 48 godzinach, w przeciwieństwie do obu LPS bakteryjnych, które ograniczały ten proces, w porównaniu do komórek nietraktowanych. Kostymulacja komórek AGS PyoM_{sol} i LPS *H. pylori*, lecz nie LPS *E. coli*, skutkowała bardziej efektywną migracją komórek po 24, 48 i 72 godzinach, w porównaniu do intensywności migracji komórek w środowisku samego LPS. Dla porównania PyoM_{insol} jedynie w kostymulacji z LPS *E. coli* zwiększała szybkość zamykania uszkodzonej strefy bez komórek po 24 i 48 godzinach.

Ostatnia część pracy dotyczyła zbadania wpływu bakteryjnych PyoM na intensywność pochłaniania przez monocyty THP-1 referencyjnych pałeczek *E. coli* (pHrodo™ Green *E. coli* BioParticles™) lub fluorescencyjnie znakowanych *H. pylori* w środowisku LPS. Stymulacja monocytów PyoM_{sol} lub PyoM_{insol} skutkowała istotnym nasileniem pochłaniania referencyjnych pałeczek *E. coli*, natomiast taka aktywność monocytów w obecności LPS *H. pylori* w hodowli była znacząco słabsza, w porównaniu z aktywnością komórek nietraktowanych LPS. Wykazano także, że kostymulacja monocytów THP-1 PyoM_{sol} (1 i 16 µg/ml) lub PyoM_{insol} (1 µg/ml) i LPS *H. pylori* skutkowała przywróceniem aktywności fagocytarnej monocytów, zahamowanej przez ten LPS. W przypadku żywych, znakowanych fluorescencyjnie *H. pylori*, PyoM_{sol} w stężeniu 1 µg/ml lub 16 µg/ml istotnie nasilała pochłanianie tych bakterii przez monocyty, w porównaniu do intensywności pochłaniania w hodowli nie zawierającej PyoM. PyoM_{insol} wykazywała podobne działanie, jednak wyłącznie w stężeniu 1 µg/ml.

P.III.

Manuskrypt w recenzji

Exploring the Osteoinductive Potential of Bacterial Pyomelanin Derived from *Pseudomonas aeruginosa* on Human Osteoblasts Model

Urbaniak M. M., Rudnicka K., Płociński P., Chmiela M.

International Journal of Biological Macromolecules

Celem ostatniej pracy oryginalnej wchodzącej w skład niniejszej rozprawy doktorskiej było określenie potencjału osteoindukcyjnego i osteokondukcyjnego bakteryjnych PyoM, a także ich właściwości proregeneracyjnych na modelu osteoblastów człowieka i aktywności przeciwbakteryjnej przeciwko klinicznym szczepom *Staphylococcus* sp. wyizolowanym z zakażonej tkanki kostnej.

Cytokompatybilność i właściwości przeciwapoptotyczne bakteryjnych PyoM zweryfikowano na modelu osteoblastów człowieka hFOB 1.19 odpowiednio, w teście redukcji MTT lub w teście TUNEL. Wykazano, że PyoM_{sol} nie wpływała na żywotność badanych komórek w zakresie stężeń 1–1024 µg/ml, spełniając wymagania cytozgodności według normy ISO 10993-5-2009. Podobny efekt wykazano dla PyoM_{insol}, jednakże w stężeniu 1024 µg/ml ten wariant PyoM powodował istotny spadek żywotności osteoblastów w porównaniu z żywotnością komórek w hodowlach nie zawierających PyoM. Wykazano także, że obie formy bakteryjnych PyoM nie indukowały apoptozy osteoblastów hFOB 1.19, w przeciwieństwie do DOX (kontrola pozytywna w teście apoptozy; cytostatyk stosowany w leczeniu nowotworów kości). W środowisku PyoM_{sol} lub PyoM_{insol}, apoptoza indukowana DOX była słabiej wyrażona, przy czym PyoM_{sol} skuteczniej znosiła proapoptotyczne działanie DOX niż PyoM_{insol}.

W teście gojenia rany PyoM_{sol} efektywnie stymulowała migrację osteoblastów po 24, 48 i 72 godzinach. Podobne wyniki uzyskano dla komórek kościotwórczych traktowanych PyoM_{insol}. Wykazano również, że osteoblasty ekspozycje na PyoM_{sol} jedynie po 24 godz. stymulacji migrowały efektywniej niż komórki traktowane PyoM_{insol}.

W kolejnym etapie badań, na podstawie analizy transkryptomicznej wykazano, że osteoblasty hodowane w warunkach osteoindukcyjnych traktowane PyoM_{sol} różnicują się wydajniej niż komórki w hodowlach nie zawierających PyoM. Wykazano więcej zmian w transkryptomie osteoblastów stymulowanych PyoM_{sol} niż nietraktowanych. Zmiany transkryptomyczne obejmowały m.in. istotny wzrost ekspresji czynnika BMP-2 i tendencję nasiloną ekspresji niespecyficznego tkankowo fosfatazy alkalicznej (TNSALP, *tissue-nonspecific alkaline phosphatase*) związanej z dojrzewaniem komórek kostnych, a także wzrost ekspresji 3-kinazy fosfatydyloinozytolu – kinazy serynowo/treoninowej (PI3K-Akt) i zależnych od wapnia szlaków sygnałowych zaangażowanych w proliferację i różnicowanie osteoblastów.

Proliferację osteoblastów w długoterminowych hodowlach osteoindukcyjnych oceniano na podstawie ilościowego oznaczenia DNA za pomocą testu CyQUANT™. Wykazano, że liczba osteoblastów w hodowlach stymulowanych PyoM_{sol} lub PyoM_{insol} była istotnie wyższa w porównaniu do liczby komórek w hodowlach bez PyoM. W 7 dniu hodowli osteoindukcyjnej w środowisku PyoM_{sol} więcej było osteoblastów niż w pierwszym dniu hodowli. Ponadto stymulacja osteoblastów PyoM_{sol} lub PyoM_{insol} prowadziła do istotnego wzrostu aktywności ALP, w porównaniu do hodowli komórek nietraktowanych, osiągając w 28 dniu hodowli stężenie, odpowiednio $6,67 \pm 0,35$ IU/ml, $5,61 \pm 0,26$ IU/ml lub $4,70 \pm 0,29$ IU/ml. Stężenie OC w supernatantach z hodowli osteoblastów stymulowanych PyoM_{sol} istotnie wzrastało przez cały czas trwania hodowli, osiągając odpowiednio $901,0 \pm 85,3$ pg/ml w dniu 7 oraz $2440,2 \pm 128,3$ pg/ml w dniu 28. Istotne różnice w wydzielaniu OC wykazano także po 21 dniach hodowli osteoblastów stymulowanych PyoM_{insol}, w porównaniu z komórkowymi niestymulowanymi. Podobnie do OC, stężenie IL-6 istotnie wzrastało przez cały czas trwania hodowli osteoblastów traktowanych PyoM_{sol}, osiągając $291,5 \pm 6,0$ pg/ml w 28 dniu, w porównaniu do komórek nietraktowanych ($58,0 \pm 10,4$ pg/ml). Wykazano także tendencję wzrostową w wydzielaniu IL-6, w hodowlach komórkowych traktowanych PyoM_{insol}, różnica była istotna statystycznie od 14 dnia hodowli. Podobny był profil wydzielania IL-10. Maksymalne stężenie tej cytokiny wykazano w 14 dniu hodowli osteoblastów stymulowanych bakteryjnymi PyoM. Stężenie IL-10 w hodowlach komórkowych eksponowanych na PyoM_{insol} malało z czasem, natomiast w hodowlach komórkowych traktowanych PyoM_{sol} wykazano ponowny wzrost wytwarzania IL-10 od 25 do 28 dnia hodowli. W punkcie końcowym hodowli stężenie IL-10 w supernatantach pochodzących z osteoblastów stymulowanych PyoM_{sol} lub PyoM_{insol} było istotnie wyższe,

w porównaniu ze stężeniem tej cytokiny w supernatantach z hodowli komórek nietraktowanych PyoM. Ponadto wykazano istotnie wyższe stężenie TNF- α w supernatantach z hodowli osteoblastów po stymulacji PyoM_{sol} lub PyoM_{insol}, w 28 dniu, które wynosiło odpowiednio, $391,2 \pm 28,2$ pg/ml i $517,0 \pm 38,5$ pg/ml, w porównaniu do hodowli komórek niestymulowanych ($55,5 \pm 14,7$ pg/ml).

W ostatnim etapie badań oceniono w teście redukcji resazury w właściwości przeciwbakteryjne PyoM wobec klinicznych szczepów *Staphylococcus* spp. wyizolowanych z zakażonej tkanki kostnej. Wykazano, że obie formy PyoM istotnie zmniejszały żywotność zarówno szczepów referencyjnych jak i klinicznych *Staphylococcus* spp. Najniższy MIC₅₀ ($57,6$ μ g/ml) PyoM_{sol} wykazano dla klinicznego szczepu *S. aureus* MRSA, natomiast najwyższy MIC₅₀ ($153,1$ μ g/ml) dla referencyjnego szczepu *S. aureus* ATCC 29213. PyoM_{insol} również hamowała aktywność metaboliczną *S. aureus*, jakkolwiek słabiej niż PyoM_{sol}.

P.IV.

Bioactive Materials for Bone Regeneration: Biomolecules and Delivery Systems

Szwed-Georgiou A., Płociński P., Kupikowska-Stobba B., Urbaniak M. M., Rusek-Wala P., Szustakiewicz K., Piszko P., Krupa A., Biernat M., Gazińska M., Kasprzak M., Nawrotek K., Mira N. P., Rudnicka K.

ACS Biomaterials Science & Engineering, 2023, 9, 5222–5254

DOI: 10.1021/acsbmaterials.3c00609

W artykule dokonano przeglądu najnowszych badań *in vitro* i *in vivo* dotyczących cząsteczek bioaktywnych, platform ich dostarczania, metod wytwarzania materiałów polimerowych oraz możliwości zastosowania biomateriałów i substancji biologicznie aktywnych w celowanej regeneracji tkanki kostnej.

W publikacji scharakteryzowano bioaktywne komponenty, które wspierają osteoindukcję, osteokondukcję i regenerację kości m. in. składniki macierzy zewnątrzkomórkowej kości, hormony, flawonoidy i sterole pochodzenia roślinnego, a także peptydy, aminokwasy i polimery wytwarzane przez drobnoustroje. Zaprezentowano również wybrane metody wytwarzania materiałów i rusztowań, w tym polimerów i wypełniaczy nieorganicznych wspomagających procesy regeneracyjne kości, a także metody dostarczania biologicznie aktywnych substancji. Ponadto wskazano wyzwania i możliwe rozwiązania w projektowaniu i zastosowaniu biomateriałów w inżynierii tkanki kostnej.

Diskusja

Bakterie należą do unikalnych źródeł pozyskiwania związków o potencjale terapeutycznym, wykazujących aktywność przeciwdrobnoustrojową, cytoprotekcyjną lub immunomodulacyjną, a także zdolność stymulowania procesów regeneracji uszkodzonych tkanek [P.IV].^{195–197} W niniejszej rozprawie doktorskiej scharakteryzowano PyoM wyizolowaną z Gram-ujemnych pałeczek *P. aeruginosa*, pod względem fizykochemicznym oraz właściwości biologicznych wobec komórek bariery nabłonkowej żołądka i komórek kościotwórczych, a także w kierunku działania przeciwbakteryjnego przeciwko pałeczkom *H. pylori* i ziarniakom z rodzaju *Staphylococcus* mając na uwadze pooperacyjne powikłania wywoływane przez gronkowce.

W badaniach użyto trzy warianty PyoM; naturalnie wytwarzaną przez *P. aeruginosa*, w formie rozpuszczalnej (PyoM_{sol}) lub nierozpuszczalnej w wodzie (PyoM_{insol}) oraz PyoM syntetyczną (sPyoM), aby wyłonić preparat o najlepszych właściwościach biologicznych. Wydajność syntezy naturalnej PyoM zwiększono dzięki zastosowaniu opracowanego w ramach niniejszej pracy podłoża PMM I i II, w którym rolę składników stymulujących syntezę bakteryjnego barwnika wykazywały L-tyrozyna, arabinoza i kwas jabłkowy [P.I.].

Substancje pochodzenia bakteryjnego badane w kierunku przyszłego biomedycznego zastosowania muszą wykazywać się cyto- i biokompatybilnością. W pracach oryginalnych P.I.–III. wykazano bezpieczeństwo na poziomie *in vitro* bakteryjnych PyoM, w szerokim zakresie stężeń, względem fibroblastów, monocytów, komórek nabłonka żołądka oraz osteoblastów. W przeciwieństwie do wysokiej cytotoksyczności sPyoM, bakteryjne PyoM_{sol} i PyoM_{insol} [P.II.–III.] nie indukowały apoptozy i nie powodowały toksyczności układowej *in vivo* na modelu *Galleria mellonella* [P.I.]. Toksyczność sPyoM może wynikać z niepełnej polimeryzacji HGA w cząsteczkach tego wariantu barwnika. Profile bezpieczeństwa *in vitro* i *in vivo* pozwoliły wyselekcjonować oba warianty bakteryjnej piomelaniny, PyoM_{sol} i PyoM_{insol}, do dalszych badań biologicznych i wykluczyć wariant syntetycznej PyoM. Uzyskane wyniki są zgodne z wcześniejszymi doniesieniami literaturowymi wskazującymi na wysoką cytokompatybilność bakteryjnych melanin wobec keratynocytów człowieka HaCaT i HEKn oraz fibroblastów hFB.^{198–200} Ferraz i wsp. wykazali brak cytotoksyczności PyoM izolowanej z *P. putida* względem komórek nabłonka skóry A-375, komórek nabłonkowych szyjki macicy HeLa, komórek nabłonkowych wątroby HEPG2 i komórek nabłonkowych okrężnicy Caco-2.²⁰¹

Monocyty odgrywają kluczową rolę w rozwoju odpowiedzi zapalnej, która determinuje eliminację czynników zakaźnych, indukcję nabytej odpowiedzi odpornościowej oraz regenerację uszkodzonych tkanek.²⁰² Poziom aktywacji monocytów może różnić się w zależności od interakcji komórkowych w niszy zapalnej oraz struktury chemicznej i pochodzenia substancji bioaktywnej działającej na te komórki. W odpowiedzi na uszkodzenie tkanek, monocyty i makrofagi produkują cytokiny prozapalne, w tym chemokiny, które ułatwiają rekrutację komórek immunokompetentnych i usuwanie przez nie resztek tkankowych, co jest warunkiem pomyślnego gojenia. W kolejnych etapach regeneracji tkanek monocyty i makrofagi mogą redukować stan zapalny poprzez wydzielanie cytokin przeciwzapalnych, kontrolować różnicowanie komórek macierzystych i regulować angiogenezę.²⁰³ Inicjacja regeneracji tkanek, w tym nabłonka żołądka lub kości, oraz jej efektywny postęp zależne są od aktywacji jądrowego czynnika transkrypcyjnego NF- κ B.²⁰⁴ W pracy **P.I.** wykazano, że PyoM_{sol} i PyoM_{insol} aktywują szlak NF- κ B i mogą stanowić modulator odpowiedzi odpornościowej i regeneracji, jednakże potrzebne są dalsze badania umożliwiające scharakteryzowanie mechanizmu ich działania. W przyszłych badaniach należy uwzględnić m.in. profil cytokin prozapalnych i/lub przeciwzapalnych oraz czynników wzrostowych wytwarzanych przez monocyty/makrofagi, a także nasilenie ich wytwarzania, aby wykluczyć możliwość indukowania przez badane PyoM nadmiernej reakcji zapalnej, która mogłaby nasilać proces chorobowy w nabłonku żołądka podczas zakażenia *H. pylori* lub po zabiegach operacyjnych na tkance kostnej.

Migracja komórek jest jednym z kluczowych fizjologicznych procesów komórkowych, niezbędnym do prawidłowego rozwoju organizmu podczas embriogenezy, tworzenia złożonej architektury przestrzennej tkanek i narządów, jak również regeneracji uszkodzonych tkanek.^{205,206} W tym ostatnim przypadku migrujące komórki bardzo szybko zasklepiają ubytki tkanki, co pozwala na stworzenie środowiska do drugiego etapu regeneracji, który wiąże się z nasileniem proliferacji komórek. W pracach **P.II.** i **P.III.** wykazano, w tzw. „teście gojenia rany”, że bakteryjne PyoM stymulują komórki nabłonka żołądka lub osteoblasty do migracji, co skutkuje zasklepieniem uszkodzenia monowarstwy komórek. Podczas zakażenia *H. pylori* komponenty uwalniane z tych bakterii uszkadzają komórki nabłonkowe w sposób bezpośredni, a także w wyniku nasilenia stresu oksydacyjnego. Takie działanie wykazuje LPS *H. pylori*, co potwierdzono zarówno na modelach komórkowych *in vitro*, jak i na modelu eksperymentalnego zakażenia *H. pylori* u kawii domowej (*Caviae porcellus*).¹⁶³ Efektem nadmiernego stresu oksydacyjnego jest

nasilenie procesu apoptozy i dezintegracji zespolonych komórek.^{163,207} We wcześniejszych badaniach wykazano, że komponenty *H. pylori* uszkodzają komórki śródbłonka naczyniowego.²⁰⁸ Natomiast w obecnej pracy wykazano, że migracja komórek nabłonkowych żołądka zahamowana przez LPS *H. pylori* była przywracana w środowisku PyoM. **[P.II.]** Efekt ten jest bardzo istotny, ponieważ uszkodzenie ciągłości bariery nabłonkowej żołądka może ułatwiać przenikanie do krwioobiegu i ogólnoustrojową dystrybucję cytotoksycznych składników *H. pylori*, w szczególności gdy postępujące zakażenie przyczynia się do zmniejszenia aktywności proregeneracyjnej komórek nabłonkowych żołądka i nasila apoptozę komórek poprzez generowanie nadmiernej produkcji ROS.^{163,208} Biorąc pod uwagę właściwości przeciwoksydacyjne piomelaniny można sądzić, iż to zdolność PyoM_{sol} do neutralizacji ROS skutkuje ograniczeniem apoptozy i zachowaniem integralności komórek, która została zaburzona przez LPS *H. pylori*, co wykazano w publikacji **P.II**.

Wzrastająca lekooporność pałeczek *H. pylori* na powszechnie stosowane antybiotyki oraz unikanie wrodzonych komórkowych mechanizmów odpornościowych przez te bakterie, w tym fagocytozy, a także hamowanie aktywności limfocytów, stanowią przesłanki do poszukiwania nowych substancji wspomagających eradykację tych bakterii umożliwiając rozpoczęcie procesów naprawczych tkanki żołądka.^{157,166–168,209} W publikacji **P.II** wykazano, że bakteryjne PyoM ograniczały żywotność referencyjnych i klinicznych wielolekoopornych szczepów *H. pylori*, a także istotnie nasilały zdolność pochłaniania przez monocyty wyznakowanych fluorescencyjnie referencyjnych pałeczek *E. coli* lub żywych *H. pylori*. Ta aktywność fagocytów była istotnie osłabiona w środowisku LPS *H. pylori*. W publikacji **P.III** wykazano, że oba warianty PyoM zmniejszyły żywotność gronkowców *S. aureus* oraz *S. felis* wyizolowanych z zakażonej tkanki kostnej, przy czym PyoM_{sol} efektywniej ograniczała aktywność metaboliczną tych bakterii w porównaniu do PyoM_{insol}. Wynik ten pozwala sugerować, że PyoM może być rozważana jako substancja ograniczająca ryzyko wystąpienia zakażenia pooperacyjnego związanego z implantacją lub wystąpieniem złamań otwartych wymagających interwencji chirurgicznej.^{210,211} Uzyskane wyniki badań są zgodne z doniesieniami innych autorów na temat przeciwbakteryjnych właściwości melanin wytwarzanych przez inne gatunki drobnoustrojów. Vasanthabharathi i wsp. wykazali, że melanina wyizolowana z morskiego szczepu *Streptomyces* sp. hamuje wzrost *E. coli* i *Lactobacillus vulgaris*²¹², natomiast wg. Zerrad i wsp. PyoM *Pseudomonas balearica* wykazuje działanie przeciwbakteryjne przeciwko *S. aureus* i *E. coli* wywołującym zakażenia u ludzi, a także wobec fitopatogenom *Erwinia chrysanthemi* i *E. carotovora*.²¹³ Xu i wsp.

sugerują, że toksyczność melanin drobnoustrojowych wobec *Vibrio parahaemolyticus* lub *S. aureus* związana jest z przerwaniem ciągłości bakteryjnej błony komórkowej.²¹⁴

Skuteczność przebudowy tkanki kostnej i jej regeneracji zależy od efektywności podziałów komórek progenitorowych i długości życia osteoblastów.²¹⁵ W publikacji **P.III.** wykazano, że w hodowlach osteoblastów prowadzonych przez 28 dni w podłożu hodowlanym zawierającym PyoM_{sol} lub PyoM_{insol} było więcej komórek niż w hodowlach bez PyoM. Może to wynikać z hamowania przez PyoM apoptozy osteoblastów, co wykazano w eksperymencie, w którym proces ten był indukowany przez DOX [**P.III.**]. W fizjologicznym procesie dojrzewania osteoblastów, część komórek ulega apoptozie. PyoM może ograniczać ten proces poprzez neutralizację stresu oksydacyjnego lub poprzez nasilenie wytwarzania IL-6, przyczyniając się do efektywniejszej osteoindukcji i osteokondukcji komórek kościotwórczych.^{171,174} W prezentowanej pracy, w 7 dniu hodowli osteoblastów, wykazano nasiloną proliferację komórek w środowisku PyoM_{sol}, co może wskazywać na bezpośredni lub pośredni wpływ PyoM na cykl komórkowy. Jakkolwiek poznanie potencjalnych mechanizmów wspomaganie wzrostu osteoblastów przez PyoM wymaga dalszych badań.

Obecność w środowisku komórek kościotwórczych cytokin i czynników wzrostowych, w tym IL-6, IL-10, TNF- α lub TGF- β , zapewnia kontrolowaną regenerację tkanki kostnej.^{216,217} Wykazano, że PyoM jako biomimetyk złogów ochronotycznych powstających w AKU, stymuluje osteoblasty do nasilenia syntezy czynników dojrzewania i mineralizacji tkanki kostnej tj. ALP, OC, IL-6, IL-10 i TNF- α , co pozwala sugerować możliwość wykorzystania tego bakteryjnego barwnika jako potencjalnego stymulatora procesów osteoindukcji i osteokondukcji [**P.III.**]. Wzrost aktywności ALP w środowisku PyoM może zwiększać biodostępność nieorganicznych fosforanów, które są prekursorami HA niezbędnego do mineralizacji macierzy kostnej.^{174,177} Obie formy PyoM istotnie stymulowały sekrecję OC, kluczowego markera kostnienia odpowiedzialnego za wiązanie i stabilizację jonów wapnia w HA, co warunkuje mechaniczną wytrzymałość tkanki kostnej.²¹⁸ Wiadomo, że IL-6 sprzyja tworzeniu kości poprzez zwiększenie różnicowania prekursorów osteoblastów i ochronę komórek kościotwórczych przed apoptozą.^{219,220} Cytokina ta stymuluje także wytwarzanie ALP, OC i sialoproteiny kostnej przyczyniając się do mineralizacji macierzy pozakomórkowej.²²¹ Ponadto, IL-6 może chronić tkankę kostną przed nadmierną resorpcją poprzez zmniejszenie ekspresji RANKL w osteoklastach i stymulację produkcji cytokin przeciwosteoklastogennych tj. IL-4 i IL-10.²²² W publikacji **P.III.** wykazano, że stymulacja osteoblastów PyoM_{sol} lub PyoM_{insol} istotnie zwiększa

wydzielanie przez nie IL-10, która bierze udział w procesie kościotwórczym poprzez szlak sygnałowy MAPK.²²³ Ponadto IL-10 hamuje wczesną fazę różnicowania komórek progenitorowych osteoklastów do prekursorów osteoklastów, a także ogranicza różnicowanie osteoklastów poprzez nasilenie wytwarzania białka OPG hamującego ekspresję RANKL.^{224,225} W prezentowanych badaniach wzięto pod uwagę wpływ PyoM na wytwarzanie przez komórki kościotwórcze TNF- α , który indukuje resorpcję kości i tworzenie osteoklastów z makrofagów szpikowych.^{226,227} TNF- α inicjuje i aktywuje osteoklasty resorbujące kości, co może korzystnie wpłynąć na kształtowanie się kości podczas procesu gojenia. Wpływ TNF- α na funkcję osteoblastów może być zależny od dawki. Wykazano, że cytokina ta w niskich stężeniach stymuluje mezenchymalne komórki prekursorowe do różnicowania się w osteoblasty, natomiast w wysokich stężeniach TNF- α hamuje tworzenie kości.^{228,229} Stężenie TNF- α w hodowlach osteoblastów traktowanych bakteryjnymi PyoM było wyższe niż w hodowlach komórek kontrolnych hodowanych w samym podłożu. Poziom TNF- α był wyższy w hodowlach osteoblastów stymulowanych PyoM_{insol} niż PyoM_{sol}. Biorąc pod uwagę rolę TNF- α w wywoływaniu odpowiedzi zapalnej, słabsze pobudzenie przez PyoM_{sol} niż PyoM_{insol} wydzielania TNF- α może być korzystne dla procesu tworzenia kości, ze względu na mniejsze ryzyko nadmiernej reakcji zapalnej.

Podsumowując, w modelu *in vitro* komórek nabłonkowych żołądka wykazano działanie przeciwbakteryjne PyoM wobec pałeczek *H. pylori*, wywołujących przewlekłe zapalenie błony śluzowej żołądka lub dwunastnicy. Ponadto wykazano neutralizację stresu oksydacyjnego indukowanego przez komponenty tych bakterii w hodowli komórek nabłonkowych żołądka, ograniczenie zależnej od reaktywnych form tlenu apoptozy i nasilenie zdolności komórek do migracji, co sugeruje działanie proregeneracyjne tego bakteryjnego barwnika. PyoM nasilała również zdolność pochłaniania *H. pylori* przez monocyty i aktywowała czynnik transkrypcyjny NF- κ B, który moduluje wiele efektorowych funkcji komórkowych. Można przypuszczać, że *in vivo* działając w powyższy sposób PyoM może hamować rozwój zakażenia *H. pylori* i neutralizować jego skutki. Potwierdzenie takiego działania PyoM wymaga dalszych badań na modelu eksperymentalnego zakażenia *H. pylori* u podatnych na takie zakażenie zwierząt doświadczalnych. Sugerowanym modelem jest kawia domowa, jako dobrze scharakteryzowany model zwierzęcy pod względem przebiegu zakażenia *H. pylori* oraz rozwoju reakcji zapalnej i odpornościowej.^{163,208,230}

W drugim modelu badawczym, w którym wykorzystano komórki kościotwórcze wykazano, że oba warianty bakteryjnej PyoM zapobiegają apoptozie tych komórek

co powoduje, że więcej komórek może osiągnąć stan dojrzałości podczas procesów wymagających regeneracji kości. Oba warianty PyoM powodują nasilenie wydzielania przez komórki kościotwórcze mediatorów rozpuszczalnych będących markerami ich dojrzewania. Ponadto wstępne wyniki badań wskazują, że PyoM_{sol} stymuluje proliferację osteoblastów, co pozwala sądzić, że może wpływać zarówno na wzrost jak i dojrzewanie komórek kostnych. Wyniki te stanowią przesłankę do opracowania biokompozytów modyfikowanych PyoM i ich wykorzystanie w badaniach *in vivo* na dedykowanym modelu zwierzęcym z ubytkami kostnymi.

Wnioski szczegółowe i wniosek końcowy

W przeprowadzonych badaniach wykazano:

- użyteczność podłoży PMM I i PMM II do hodowli bakterii *P. aeruginosa* i izolacji PyoM_{sol} i PyoM_{insol},
- obecność grup funkcyjnych (hydroksylowej i karboksylowej) w cząsteczkach PyoM_{sol}, PyoM_{insol} i sPyoM charakterystycznych dla melanin będących pochodnymi HGA,
- wysoką termoodporność PyoM,
- wysoką cytokompatybilność PyoM_{sol} i PyoM_{insol}, w przeciwieństwie do sPyoM, wobec fibroblastów myszy, monocytów człowieka, komórek nabłonka żołądka i osteoblastów człowieka, w hodowlach *in vitro*, oraz bezpieczeństwo powyższych wariantów PyoM *in vivo* na modelu *Galleria mellonella*.
- aktywację przez PyoM_{sol} czynnika transkrypcyjnego NF-κB monocytów, w hodowlach *in vitro*,
- cytoprotekcyjne i przeciwapoptotyczne działanie bakteryjnych PyoM, wobec komórek nabłonkowych żołądka, w hodowlach *in vitro*, w kostymulacji z LPS *H. pylori* lub *E. coli*,
- nasilenie pochłaniania pałeczek *H. pylori* przez monocyty w środowisku hodowlanym z PyoM_{sol},
- wspomaganie migracji komórek nabłonka żołądka i osteoblastów, w hodowlach *in vitro*, w środowisku PyoM,
- przeciwbakteryjne właściwości PyoM przeciwko referencyjnym i klinicznym szczepom *H. pylori* oraz *Staphylococcus* sp,
- wspomaganie przez PyoM dojrzewania osteoblastów w hodowlach *in vitro*, poprzez nasilenie aktywności ALP i sekrecji OC, IL-6, IL-10 oraz TNF-α.

Wniosek końcowy:

Uzyskane wyniki badań wskazują, że naturalne PyoM produkowane przez *P. aeruginosa* posiadają szereg właściwości biologicznych, które pozwalają wstępnie typować te polimery pochodzenia bakteryjnego o działaniu przeciwbakteryjnym, proregeneracyjnym i immunomodulacyjnym, jako potencjalne związki do zastosowań medycznych.

Literatura

- (1) Girard, L.; Lood, C.; Höfte, M.; Vandamme, P.; Rokni-Zadeh, H.; van Noort, V.; Lavigne, R.; De Mot, R. The Ever-Expanding *Pseudomonas* Genus: Description of 43 New Species and Partition of the *Pseudomonas* Putida Group. *Microorganisms*. 2021, 9 (8), 1766. DOI: 10.3390/microorganisms9081766.
- (2) Palleroni, N. J. The *Pseudomonas* Story. *Environmental Microbiology*. 2010, 12 (6), 1377–1383. DOI: 10.1111/j.1462-2920.2009.02041.x.
- (3) Diggle, S. P.; Whiteley, M. Microbe Profile: *Pseudomonas aeruginosa*: Opportunistic Pathogen and Lab Rat. *Microbiology*. 2020, 166 (1), 30–33. DOI:10.1099/mic.0.000860.
- (4) Sanya, D. R. A.; Onésime, D.; Vizzarro, G.; Jacquier, N. Recent Advances in Therapeutic Targets Identification and Development of Treatment Strategies towards *Pseudomonas aeruginosa* Infections. *BMC Microbiology*. 2023, 23, 86. DOI:10.1186/s12866-023-02832-x.
- (5) Jain, R.; Behrens, A. J.; Kaefer, V.; Kazmierczak, B. I. Type IV Pilus Assembly in *Pseudomonas aeruginosa* over a Broad Range of Cyclic Di-GMP Concentrations. *J. Bacteriol.* 2012, 194 (16), 4285–4294. DOI:10.1128/JB.00803-12.
- (6) Kazmierczak, B. I.; Schniederberend, M.; Jain, R. Cross-Regulation of *Pseudomonas* Motility Systems: The Intimate Relationship between Flagella, Pili and Virulence. *Curr. Opin. Microbiol.* 2015, 28, 78–82. DOI:10.1016/j.mib.2015.07.017.
- (7) LaBauve, A. E.; Wargo, M. J. Growth and Laboratory Maintenance of *Pseudomonas aeruginosa*. *Curr. Protoc. Microbiol.* 2012, 25, 1-7. DOI:10.1002/9780471729259.mc06e01s25.
- (8) Saati-Santamaría, Z.; Peral-Aranega, E.; Velázquez, E.; Rivas, R.; García-Fraile, P. Phylogenomic Analyses of the Genus *Pseudomonas* Lead to the Rearrangement of Several Species and the Definition of New Genera. *Biology*. 2021, 10 (8), 782. DOI:10.3390/biology10080782.
- (9) Ozer, E. A.; Allen, J. P.; Hauser, A. R. Characterization of the Core and Accessory Genomes of *Pseudomonas aeruginosa* Using Bioinformatic Tools Spine and AGEnt. *BMC Genomics* 2014, 15 (1), 737. DOI:10.1186/1471-2164-15-737.
- (10) Liao, C.; Huang, X.; Wang, Q.; Yao, D.; Lu, W. Virulence Factors of *Pseudomonas aeruginosa* and Antivirulence Strategies to Combat Its Drug Resistance. *Front. Cell. Infect.* 2022, 12, 926758. DOI:10.3389/fcimb.2022.926758.
- (11) Kessler, C.; Mhatre, E.; Cooper, V.; Kim, W. Evolutionary Divergence of the Wsp Signal Transduction Systems in *Beta*- and *Gammaproteobacteria*. *Appl. Environ. Microbiol.* 2021, 87 (22), 130621. DOI: 10.1128/AEM.01306-21.
- (12) Arai, H. Regulation and Function of Versatile Aerobic and Anaerobic Respiratory Metabolism in *Pseudomonas aeruginosa*. *Front Microbiol.* 2011, 2, 103. DOI:10.3389/fmicb.2011.00103.

- (13) Filiatrault, M. J.; Picardo, K. F.; Ngai, H.; Passador, L.; Iglewski, B. H. Identification of *Pseudomonas aeruginosa* Genes Involved in Virulence and Anaerobic Growth. *Infect. Immun.* 2006, 74 (7), 4237–4245. DOI:10.1128/IAI.02014-05.
- (14) Xu, K. D.; Stewart, P. S.; Xia, F.; Huang, C.; Mcfeters, G. A. Spatial Physiological Heterogeneity in *Pseudomonas aeruginosa* Biofilm is Determined by Oxygen Availability. *Appl. Environ. Microbiol.* 1998, 64 (10), 4035–4039. DOI: 10.1128/aem.64.10.4035-4039.1998.
- (15) Hassett, D. J.; Cuppoletti, J.; Trapnell, B.; Lyman, S. V.; Rowe, J. J.; Yoon, S. S.; Hilliard, G. M.; Parvatiyar, K.; Kamani, M. C.; Wozniak, D. J.; Hwang, S.-H.; Mcdermott, T. R.; Ochsner, U. A. A. Anaerobic Metabolism and Quorum Sensing by *Pseudomonas aeruginosa* Biofilms in Chronically Infected Cystic Fibrosis Airways: Rethinking Antibiotic Treatment Strategies and Drug Targets. *Adv. Drug. Deliv. Rev.* 2002, 54(11), 1425-1443. DOI:10.1016/s0169-409x(02)00152-7.
- (16) Stover, C. K.; Pham, X. Q.; Erwin, A. L.; Mizoguchi, S. D.; Warrenner, P.; Hickey, M. J.; Brinkman, F. S. L.; Hufnagle, W. O.; Kowalik, D. J.; Lagrou, M.; Garber, R. L.; Goltry, L.; Tolentino, E.; Westbrook-Wadman, S.; Yuan, Y.; Brody, L. L.; Coulter, S. N.; Folger, K. R.; Kas, A.; Larbig, K.; Lim, R.; Smith, K.; Spencer, D.; Wong, S.; Wu, Z.; Paulsen, I. T.; Reizer, J.; Saier, M. H.; Hancock, R. E. W.; Lory, S.; Olson, M. V. Complete Genome Sequence of *Pseudomonas aeruginosa* PAO1, an Opportunistic Pathogen. *Nature.* 2000, 406, 959–964. DOI: 10.1038/35023079.
- (17) Sathe, N.; Beech, P.; Croft, L.; Suphioglu, C.; Kapat, A.; Athan, E. *Pseudomonas aeruginosa*: Infections and Novel Approaches to Treatment “Knowing the Enemy” the Threat of *Pseudomonas aeruginosa* and Exploring Novel Approaches to Treatment. *Infectious Medicine.* 2023, 2 (3), 178–194. DOI:10.1016/j.imj.2023.05.003.
- (18) Wolfmeier, H.; Wardell, S. J. T.; Liu, L. T.; Falsafi, R.; Draeger, A.; Babiychuk, E. B.; Pletzer, D.; Hancock, R. E. W. Targeting the *Pseudomonas aeruginosa* Virulence Factor Phospholipase C with Engineered Liposomes. *Front. Microbiol.* 2022, 13, 867449. DOI:10.3389/fmicb.2022.867449.
- (19) Douraghi, M.; Ghasemi, F.; Soltan Dallal, M. M.; Rahbar, M.; Rahimiforushani, A. Molecular Identification of *Pseudomonas aeruginosa* Recovered from Cystic Fibrosis Patients. *J. Prev. Med. Hyg.* 2014, 55 (2), 50-53.
- (20) Bai, S.; Chen, H.; Zhu, L.; Liu, W.; Yu, H. D.; Wang, X.; Yin, Y. Comparative Study on the *in vitro* Effects of *Pseudomonas aeruginosa* and Seaweed Alginates on Human Gut Microbiota. *PLoS One.* 2017, 12(2), 171576. DOI:10.1371/journal.pone.0171576.
- (21) Valentine, M. E.; Kirby, B. D.; Withers, T. R.; Johnson, S. L.; Long, T. E.; Hao, Y.; Lam, J. S.; Niles, R. M.; Yu, H. D. Generation of a Highly Attenuated Strain of *Pseudomonas aeruginosa* for Commercial Production of Alginate. *Microb. Biotechnol.* 2020, 13 (1), 162–175. DOI:10.1111/1751-7915.13411.
- (22) Franklin, M. J.; Nivens, D. E.; Weadge, J. T.; Lynne Howell, P. Biosynthesis of the *Pseudomonas aeruginosa* Extracellular Polysaccharides, Alginate, Pel, and Psl. *Front. Microbiol.* 2011, 2, 167. DOI:10.3389/fmicb.2011.00167.

- (23) Boyd, A.; Chakrabarty, A. M. *Pseudomonas aeruginosa* Biofilms: Role of the Alginate Exopolysaccharide. *J. Ind. Microbiol.* 1995, 15 (3), 162-168. DOI:10.1007/BF01569821.
- (24) Spoială, A.; Ilie, C. I.; Fikai, D.; Fikai, A.; Andronescu, E. From Biomedical Applications of Alginate towards CVD Implications Linked to COVID-19. *Pharmaceutics.* 2022, 15 (3), 318. DOI:10.3390/ph15030318.
- (25) Ahmad Raus, R.; Wan Nawawi, W. M. F.; Nasaruddin, R. R. Alginate and Alginate Composites for Biomedical Applications. *Asian J. Pharm. Sci.* 2021, 16 (3), 280–306. DOI:10.1016/j.ajps.2020.10.001.
- (26) Froelich, A.; Jakubowska, E.; Wojtyłko, M.; Jadach, B.; Gackowski, M.; Gadziński, P.; Napierała, O.; Ravliv, Y.; Osmałek, T. Alginate-Based Materials Loaded with Nanoparticles in Wound Healing. *Pharmaceutics.* 2023, 15(4), 1142. DOI:10.3390/pharmaceutics15041142.
- (27) Tomić, S. L.; Babić Radić, M. M.; Vuković, J. S.; Filipović, V. V.; Nikodinovic-Runic, J.; Vukomanović, M. Alginate-Based Hydrogels and Scaffolds for Biomedical Applications. *Mar. Drugs.* 2023, 21 (3), 177. <https://doi.org/10.3390/md21030177>.
- (28) Lee, K. Y.; Mooney, D. J. Alginate: Properties and Biomedical Applications. *Prog. Polym. Sci.* 2012, 37 (1), 106–126. DOI:10.1016/j.progpolymsci.2011.06.003.
- (29) Kapsetaki, S. E.; Tzelepis, I.; Avgousti, K.; Livadaras, I.; Garantonakis, N.; Varikou, K.; Apidianakis, Y. The Bacterial Metabolite 2-Aminoacetophenone Promotes Association of Pathogenic Bacteria with Flies. *Nat. Commun.* 2014, 5, 4401. DOI:10.1038/ncomms5401.
- (30) DeBritto, S.; Gajbar, T. D.; Satapute, P.; Sundaram, L.; Lakshmikantha, R. Y.; Jogaiah, S.; Ito, S. Isolation and Characterization of Nutrient Dependent Pyocyanin from *Pseudomonas aeruginosa* and its Dye and Agrochemical Properties. *Sci. Rep.* 2020, 10 (1), 1542. DOI:10.1038/s41598-020-58335-6.
- (31) Abdelaziz, A. A.; Kamer, A. M. A.; Al-Monofy, K. B.; Al-Madboly, L. A. *Pseudomonas aeruginosa*'s Greenish-Blue Pigment Pyocyanin: Its Production and Biological Activities. *Microb. Cell Factories.* 2023, 22, 110. DOI:10.1186/s12934-023-02122-1.
- (32) Hense, B. A.; Schuster, M. Core Principles of Bacterial Autoinducer Systems. *Microbiol. Mol. Biol. Rev.* 2015, 79 (1), 153–169. DOI:10.1128/mubr.00024-14.
- (33) Marrez, D. A. Biological Activity and Applications of Pyocyanin Produced by *Pseudomonas aeruginosa*. *Open Acc. J. Biomed. Sci.* 2020, 1 (4), 133. DOI:10.38125/oajbs.000133.
- (34) Price-Whelan, A.; Dietrich, L. E. P.; Newman, D. K. Rethinking “Secondary” Metabolism: Physiological Roles for Phenazine Antibiotics. *Nat. Chem. Biol.* 2006, 2, 71–78. DOI:10.1038/nchembio764.
- (35) Ramos, I.; Dietrich, L. E. P.; Price-Whelan, A.; Newman, D. K. Phenazines Affect Biofilm Formation by *Pseudomonas aeruginosa* in Similar Ways at Various Scales. *Res. Microbiol.* 2010, 161 (3), 187–191. DOI:10.1016/j.resmic.2010.01.003.

- (36) Das, T.; Kutty, S. K.; Kumar, N.; Manefield, M. Pyocyanin Facilitates Extracellular DNA Binding to *Pseudomonas aeruginosa* Influencing Cell Surface Properties and Aggregation. PLoS One. 2013, 8 (3), 58299. DOI:10.1371/journal.pone.0058299.
- (37) Nawas, T. Extraction and Purification of Pyocyanin: A Simpler and More Reliable Method. MOJ Toxicol. 2018, 4 (6), 417–422. DOI:10.15406/mojt.2018.04.00139.
- (38) Finlayson, E. A.; Brown, P. D. Comparison of Antibiotic Resistance and Virulence Factors in Pigmented and Non-Pigmented *Pseudomonas aeruginosa*. West Indian Med. J. 2011, 60 (1), 24-32.
- (39) Managò, A.; Becker, K. A.; Carpinteiro, A.; Wilker, B.; Soddemann, M.; Seitz, A. P.; Edwards, M. J.; Grassmé, H.; Szabò, I.; Gulbins, E. *Pseudomonas aeruginosa* Pyocyanin Induces Neutrophil Death via Mitochondrial Reactive Oxygen Species and Mitochondrial Acid Sphingomyelinase. Antioxid. Redox Signal. 2015, 22 (13), 1097–1110. DOI:10.1089/ars.2014.5979.
- (40) Meirelles, L. A.; Newman, D. K. Both Toxic and Beneficial Effects of Pyocyanin Contribute to the Lifecycle of *Pseudomonas aeruginosa*. Mol. Microbiol. 2018, 110 (6), 995–1010. DOI:10.1111/mmi.14132.
- (41) Usher, L. R.; Lawson, R. A.; Geary, I.; Taylor, C. J.; Bingle, C. D.; Taylor, G. W.; Whyte, M. K. B. Induction of Neutrophil Apoptosis by the *Pseudomonas aeruginosa* Exotoxin Pyocyanin: A Potential Mechanism of Persistent Infection. J. Immun. 2002, 168 (4), 1861–1868. DOI:10.4049/jimmunol.168.4.1861.
- (42) Mavrodi, D. V.; Bonsall, R. F.; Delaney, S. M.; Soule, M. J.; Phillips, G.; Thomashow, L. S. Functional Analysis of Genes for Biosynthesis of Pyocyanin and Phenazine-1-Carboxamide from *Pseudomonas aeruginosa* PAO1. J. Bacteriol. 2001, 183 (21), 6454–6465. DOI:10.1128/JB.183.21.6454-6465.2001.
- (43) Ulmer, A. J.; Pryjma, J.; Tarnok, Z.; Ernst, M.; Flad, H.D. Inhibitory and Stimulatory Effects of *Pseudomonas aeruginosa* Pyocyanine on Human T and B Lymphocytes and Human Monocytes. Infect. Immun. 1990, 58 (3), 808–815.
- (44) Jayaseelan, S.; Ramaswamy, D.; Dharmaraj, S. Pyocyanin: Production, Applications, Challenges and New Insights. World J. Microbiol. Biotechnol. 2014, 30 (4), 1159-1168. DOI:10.1007/s11274-013-1552-5.
- (45) Hamad, M. N. F.; Marrez, D. A.; El-Sherbieny, S. M. R. Toxicity Evaluation and Antimicrobial Activity of Purified Pyocyanin from *Pseudomonas aeruginosa*. Biointerface Res. Appl Chem. 2020, 10 (6), 6974–6990. DOI:10.33263/BRIAC106.69746990.
- (46) Darwesh, O. M.; Barakat, K. M.; Mattar, M. Z.; Sabae, S. Z.; Hassan, S. H. Production of Antimicrobial Blue Green Pigment Pyocyanin by Marine *Pseudomonas aeruginosa*. Biointerface Res. Appl Chem. 2019, 9 (5), 4334-4339. DOI:10.33263/BRIAC95.334339.
- (47) Abdul-Hussein, Z. R.; Atia, S. S. Antimicrobial Effect of Pyocyanin Extracted from *Pseudomonas aeruginosa*. Eur. J. Exp. Bio. 2016, 1, 1-4.
- (48) Patil, S.; Nikam, M.; Anokhina, T.; Kochetkov, V.; Chaudhari, A. Multi-Stress Tolerant Plant Growth Promoting *Pseudomonas* spp. MCC 3145 Producing Cytostatic and

- Fungicidal Pigment. *Biocatal. Agric. Biotechnol.* 2017, 10, 53–63. DOI:10.1016/j.bcab.2017.02.006.
- (49) Zhao, J.; Wu, Y.; Alfred, A. T.; Wei, P.; Yang, S. Anticancer Effects of Pyocyanin on HepG2 Human Hepatoma Cells. *Lett. Appl. Microbiol.* 2014, 58 (6), 541–548. DOI:10.1111/lam.12224.
- (50) Moayedi, A.; Nowroozi, J.; Akhavan Sepahy, A. Cytotoxic Effect of Pyocyanin on Human Pancreatic Cancer Cell Line (Panc-1). *Iran. J. Basic. Med. Sci.* 2018, 21 (8), 794–799. DOI:10.22038/ijbms.2018.27865.6799.
- (51) Hall, S.; McDermott, C.; Anoopkumar-Dukie, S.; McFarland, A. J.; Forbes, A.; Perkins, A. V.; Davey, A. K.; Chess-Williams, R.; Kiefel, M. J.; Arora, D.; Grant, G. D. Cellular Effects of Pyocyanin, a Secreted Virulence Factor of *Pseudomonas aeruginosa*. *Toxins*. 2016, 8 (8), 236. DOI:10.3390/toxins8080236.
- (52) McDermott, C.; Chess-Williams, R.; Mills, K. A.; Kang, S. H.; Farr, S. E.; Grant, G. D.; Perkins, A. V.; Davey, A. K.; Anoopkumar-Dukie, S. Alterations in Acetylcholine, PGE2 and IL-6 Release from Urothelial Cells Following Treatment with Pyocyanin and Lipopolysaccharide. *Toxicol. In Vitro*. 2013, 27 (6), 1693–1698. DOI:10.1016/j.tiv.2013.04.015.
- (53) Kang, D.; Revtovich, A. V.; Chen, Q.; Shah, K. N.; Cannon, C. L.; Kirienko, N. V. Pyoverdine-Dependent Virulence of *Pseudomonas aeruginosa* Isolates from Cystic Fibrosis Patients. *Front. Microbiol.* 2019, 10, 2048. DOI:10.3389/fmicb.2019.02048.
- (54) Bonneau, A.; Roche, B.; Schalk, I. J. Iron Acquisition in *Pseudomonas aeruginosa* by the Siderophore Pyoverdine: An Intricate Interacting Network Including Periplasmic and Membrane Proteins. *Sci. Rep.* 2020, 10 (1), 120. DOI:10.1038/s41598-019-56913-x.
- (55) Imperi, F.; Tiburzi, F.; Visca, P.; Greenberg, E. P. Molecular Basis of Pyoverdine Siderophore Recycling in *Pseudomonas aeruginosa*. *PNAS*. 2009, 106 (48), 20440-20445. DOI:10.1073/pnas.09087601
- (56) Ezraty, B.; Barras, F. The “liaisons Dangereuses” between Iron and Antibiotics. *FEMS Microbiol. Rev.* 2016, 40 (3) 418-435. DOI:10.1093/femsre/fuw004.
- (57) Oglesby-Sherrouse, A. G.; Djapagne, L.; Nguyen, A. T.; Vasil, A. I.; Vasil, M. L. The Complex Interplay of Iron, Biofilm Formation, and Mucoidy Affecting Antimicrobial Resistance of *Pseudomonas aeruginosa*. *Pathog. Dis.* 2014, 70 (3), 307–320. DOI:10.1111/2049-632X.12132.
- (58) Cézard, C.; Farvacques, N.; Sonnet, P. Chemistry and Biology of Pyoverdines, *Pseudomonas* Primary Siderophores. *Curr. Med. Chem.* 2015, 22 (2), 165-186. 10.2174/0929867321666141011194624.
- (59) Meyer, J. M.; Neely, A.; Stintzi, A.; Georges, C.; Holder, I. A. Pyoverdin Is Essential for Virulence of *Pseudomonas aeruginosa*. *Infect. Immun.* 1996, 64 (2), 518-23. DOI:10.1128/iai.64.2.518-523.1996.

- (60) Behzadi, P.; Baráth, Z.; Gajdács, M. It's Not Easy Being Green: A Narrative Review on the Microbiology, Virulence and Therapeutic Prospects of Multidrug-Resistant *Pseudomonas aeruginosa*. *Antibiotics*. 2021, 10 (1), 42. DOI:10.3390/antibiotics10010042.
- (61) Orlandi, V. T.; Bolognese, F.; Chiodaroli, L.; Tolker-Nielsen, T.; Barbieri, P. Pigments Influence the Tolerance of *Pseudomonas aeruginosa* PAO1 to Photodynamically Induced Oxidative Stress. *Microbiology*, 2015, 161 (12), 2298–2309. DOI:10.1099/mic.0.000193.
- (62) Alba, L. D.; Shawkey, M. D. Melanosomes: Biogenesis, Properties, and Evolution of an Ancient Organelle. *Physiol. Rev.* 2019, 99, 1–19. DOI: 10.1152/physrev.00059.2017.
- (63) Cao, W.; Zhou, X.; McCallum, N. C.; Hu, Z.; Ni, Q. Z.; Kapoor, U.; Heil, C. M.; Cay, K. S.; Zand, T.; Mantanona, A. J.; Jayaraman, A.; Dhinojwala, A.; Deheyn, D. D.; Shawkey, M. D.; Burkart, M. D.; Rinehart, J. D.; Gianneschi, N. C. Unraveling the Structure and Function of Melanin through Synthesis. *J. Am. Chem. Soc.* 2021, 143 (7), 2622–2637. DOI:10.1021/jacs.0c12322.
- (64) Pavan, M. E.; López, N. I.; Pettinari, M. J. Melanin Biosynthesis in Bacteria, Regulation and Production Perspectives. *Appl. Microbiol. Biotechnol.* 2020, 104, 1357–1370. DOI:10.1007/s00253-019-10245-y.
- (65) Mostert, A. B. Melanin, the What, the Why and the How: An Introductory Review for Materials Scientists Interested in Flexible and Versatile Polymers. *Polymers*. 2021, 13 (10), 1670. DOI:10.3390/polym13101670.
- (66) Meredith, P.; Sarna, T. The Physical and Chemical Properties of Eumelanin. *Pigment Cell Res.* 2006, 19 (6), 572–594. DOI:10.1111/j.1600-0749.2006.00345.x.
- (67) Ito, S.; Sugumaran, M.; Wakamatsu, K. Chemical Reactivities of Ortho-Quinones Produced in Living Organisms: Fate of Quinonoid Products Formed by Tyrosinase and Phenoloxidase Action on Phenols and Catechols. *Int. J. Mol. Sci.* 2020, 21 (17), 6080, DOI:10.3390/ijms21176080.
- (68) Suthar, M.; Dufossé, L.; Singh, S. K. The Enigmatic World of Fungal Melanin: A Comprehensive Review. *J. Fungi.* 2023, 9 (9), 891. DOI:10.3390/jof9090891
- (69) Martínez, L. M.; Martínez, A.; Gosset, G. Production of Melanins with Recombinant Microorganisms. *Front. Bioeng. Biotechnol.* 2019, 7, 285. DOI:10.3389/fbioe.2019.00285.
- (70) Tran-Ly, A. N.; Reyes, C.; Schwarze, F. W. M. R.; Ribera, J. Microbial Production of Melanin and Its Various Applications. *World J. Microbiol. Biotechnol.* 2020, 36, 170. DOI:10.1007/s11274-020-02941-z.
- (71) Yang, X.; Tang, C.; Zhao, Q.; Jia, Y.; Qin, Y.; Zhang, J. Melanin: A Promising Source of Functional Food Ingredient. *J. Funct. Foods.* 2023, 105, 105574. DOI:10.1016/j.jff.2023.105574.
- (72) Park, J.; Moon, H.; Hong, S. Recent Advances in Melanin-like Nanomaterials in Biomedical Applications: A Mini Review. *Biomater. Res.* 2019, 23, 24. DOI:10.1186/s40824-019-0175-9.

- (73) ElObeid, A. S.; Kamal-Eldin, A.; Abdelhalim, M. A. K.; Haseeb, A. M. Pharmacological Properties of Melanin and Its Function in Health. *Basic. Clin. Pharmacol. Toxicol.* 2017, 120 (6), 515-522. DOI:10.1111/bcpt.12748.
- (74) El-Naggar, N. E. A.; Saber, W. I. A. Natural Melanin: Current Trends, and Future Approaches, with Especial Reference to Microbial Source. *Polymers.* 2022, 14 (7), 1339. DOI:10.3390/polym14071339.
- (75) Silva, C.; Santos, A.; Salazar, R.; Lamilla, C.; Pavez, B.; Meza, P.; Hunter, R.; Barrientos, L. Evaluation of Dye Sensitized Solar Cells Based on a Pigment Obtained from Antarctic *Streptomyces fildesensis*. *Sol. Energy.* 2019, 181, 379–385. DOI:10.1016/j.solener.2019.01.035.
- (76) Fischer, F. Photoelectrode, Photovoltaic and Photosynthetic Microbial Fuel Cells. *Renew. Sustain. Energy Rev.* 2018, 90, 16–27. DOI:10.1016/j.rser.2018.03.053.
- (77) Xu, R.; Gouda, A.; Caso, M. F.; Soavi, F.; Santato, C. Melanin: A Greener Route to Enhance Energy Storage under Solar Light. *ACS Omega* 2019, 4 (7), 12244–12251. DOI:10.1021/acsomega.9b01039.
- (78) Bolognese, F.; Scanferla, C.; Caruso, E.; Orlandi, V. T. Bacterial Melanin Production by Heterologous Expression of 4 hydroxyphenylpyruvate Dioxygenase from *Pseudomonas aeruginosa*. *Int. J. Biol. Macromol.* 2019, 133, 1072–1080. DOI:10.1016/j.ijbiomac.2019.04.061.
- (79) Yabuuchi, E.; Ohyama, A. Characterization of “Pyomelanin” Producing Strains of *Pseudomonas aeruginosa*. *Int. J. Syst. Evol. Microbiol.* 1972, 22 (2), 53-64. DOI:10.1099/00207713-22-2-53
- (80) Lorquin, F.; Piccerelle, P.; Orneto, C.; Robin, M.; Lorquin, J. New Insights and Advances on Pyomelanin Production: From Microbial Synthesis to Applications. *J. Ind. Microbiol. Biotechnol.* 2022, 49 (4), 13. DOI:10.1093/jimb/kuac013.
- (81) Liebgott, P. P.; Labat, M.; Amouric, A.; Tholozan, J. L.; Lorquin, J. Tyrosol Degradation via the Homogentisic Acid Pathway in a Newly Isolated *Halomonas* Strain from Olive Processing Effluents. *J. Appl. Microbiol.* 2008, 105 (6), 2084–2095. DOI:10.1111/j.1365-2672.2008.03925.x.
- (82) Ketelboeter, L. M.; Potharla, V. Y.; Bardy, S. L. NTBC Treatment of the Pyomelanogenic *Pseudomonas aeruginosa* Clinical Isolate PA1111 Inhibits Pigment Production and Increases Sensitivity to Oxidative Stress. *Curr. Microbiol.* 2014, 69 (3), 343–348. DOI:10.1007/s00284-014-0593-9.
- (84) Ketelboeter, L. M.; Bardy, S. L. Characterization of 2-(2-Nitro-4-Trifluoromethylbenzoyl)-1,3-Cyclohexanedione Resistance in Pyomelanogenic *Pseudomonas aeruginosa* DKN343. *PLoS One.* 2017, 12 (6), 178084. DOI:10.1371/journal.pone.0178084.
- (85) Turick, C. E.; Tisa, L. S.; Caccavo, F. Melanin Production and Use as a Soluble Electron Shuttle for Fe(III) Oxide Reduction and as a Terminal Electron Acceptor by *Shewanella* Algae BrY. *Appl. Environ. Microbiol.* 2002, 68 (5), 2436–2444. DOI:10.1128/AEM.68.5.2436-2444.2002.

- (86) Schmalzer-Ripcke, J.; Sugareva, V.; Gebhardt, P.; Winkler, R.; Kniemeyer, O.; Heinekamp, T.; Brakhage, A. A. Production of Pyomelanin, a Second Type of Melanin, via the Tyrosine Degradation Pathway in *Aspergillus fumigatus*. *Appl. Environ. Microbiol.* 2009, 75 (2), 493–503. DOI:10.1128/AEM.02077-08.
- (87) Turick, C. E.; Beliaev, A. S.; Zakrajsek, B. A.; Reardon, C. L.; Lowy, D. A.; Poppy, T. E.; Maloney, A.; Ekechukwu, A. A. The Role of 4-Hydroxyphenylpyruvate Dioxygenase in Enhancement of Solid-Phase Electron Transfer by *Shewanella oneidensis* MR-1. *FEMS Microbiol. Ecol.* 2009, 68 (2), 223–225. DOI:10.1111/j.1574-6941.2009.00670.x.
- (88) Li, Y.; Ye, Z.; Lu, P.; Lu, L. Pyomelanin Produced by *Streptomyces* sp. ZL-24 and Its Protective Effects against SH-SY5Y Cells Injury Induced by Hydrogen Peroxide. *Sci. Rep.* 2021, 11 (1), 16649. <https://doi.org/10.1038/s41598-021-94598-3>.
- (89) Ahmad, S.; Lee, S. Y.; Kong, H. G.; Jo, E. J.; Choi, H. K.; Khan, R.; Lee, S. W. Genetic Determinants for Pyomelanin Production and Its Protective Effect against Oxidative Stress in *Ralstonia solanacearum*. *PLoS One* 2016, 11 (8), 160845. DOI:10.1371/journal.pone.0160845.
- (90) Seo, D.; Choi, K. Y. Heterologous Production of Pyomelanin Biopolymer Using 4-Hydroxyphenylpyruvate Dioxygenase Isolated from *Ralstonia pickettii* in *Escherichia coli*. *Biochem. Eng. J.* 2020, 157 (15), 107548. DOI:10.1016/j.bej.2020.107548.
- (91) Andrews, S. C.; Robinson, A. K.; Rodríguez-Quñones, F. Bacterial Iron Homeostasis. *FEMS Microbiol. Rev.* 2003, 27 (2), 215–237. DOI:10.1016/S0168-6445(03)00055-X.
- (92) Turick, C. E.; Caccavo, F.; Tisa, L. S. Pyomelanin Is Produced by *Shewanella* Algae BrY and Affected by Exogenous Iron. *Can. J. Microbiol.* 2008, 54 (4), 334–339. DOI:10.1139/W08-014.
- (93) Zheng, H.; Chatfield, C. H.; Liles, M. R.; Cianciotto, N. P. Secreted Pyomelanin of *Legionella pneumophila* Promotes Bacterial Iron Uptake and Growth under Iron-Limiting Conditions. *Infect. Immun.* 2013, 81 (11), 4182–4191. DOI:10.1128/IAI.00858-13.
- (94) Hong, L.; Simon, J. D. Current Understanding of the Binding Sites, Capacity, Affinity, and Biological Significance of Metals in Melanin. *J. Phys. Chem. B.* 2007, 111 (28), 7938–7947. DOI:10.1021/jp071439h.
- (95) Sarna, T.; Swartz, H. M.; Żądło, A. Interaction of Melanin with Metal Ions Modulates Their Cytotoxic Potential. *Appl. Magn. Reson.* 2022, 53, 105–121. DOI:10.1007/s00723-021-01386-3.
- (96) Di Mauro, E.; Xu, R.; Soliveri, G.; Santato, C. Natural Melanin Pigments and Their Interfaces with Metal Ions and Oxides: Emerging Concepts and Technologies. *MRS Commun.* 2017, 7 (2), 141–151. DOI:10.1557/mrc.2017.33.
- (97) Nosanchuk, J. D.; Casadevall, A. Impact of Melanin on Microbial Virulence and Clinical Resistance to Antimicrobial Compounds. *Antimicrob. Agents Chemother.* 2006, 50 (11), 3519–3528. DOI:10.1128/AAC.00545-06.

- (98) Noorian, P.; Hu, J.; Chen, Z.; Kjelleberg, S.; Wilkins, M. R.; Sun, S.; McDougald, D. Pyomelanin Produced by *Vibrio cholerae* Confers Resistance to Predation by *Acanthamoeba castellanii*. *FEMS Microbiol. Ecol.* 2017, 93 (12), 147. DOI:10.1093/femsec/fix147.
- (99) Chatfield, C. H.; Cianciotto, N. P. The Secreted Pyomelanin Pigment of *Legionella pneumophila* Confers Ferric Reductase Activity. *Infect. Immun.* 2007, 75 (8), 4062–4070. DOI:10.1128/IAI.00489-07.
- (100) Valeru, S. P.; Rompikuntal, P. K.; Ishikawa, T.; Vaitkevicius, K.; Sjöling, Å.; Dolganov, N.; Zhu, J.; Schoolnik, G.; Wai, S. N. Role of Melanin Pigment in Expression of *Vibrio cholerae* Virulence Factors. *Infect. Immun.* 2009, 77 (3), 935–942. DOI:10.1128/IAI.00929-08.
- (101) Fonseca, É.; Freitas, F.; Caldart, R.; Morgado, S.; Vicente, A. C. Pyomelanin Biosynthetic Pathway in Pigment-Producer Strains from the Pandemic *Acinetobacter baumannii* IC-5. *Mem. Inst. Oswaldo. Cruz.* 2020, 115 (10), 1–6. DOI:10.1590/0074-02760200371.
- (102) Liu, L.; Xu, H.; Gao, L.; Zhao, Y.; Wang, H.; Shi, N.; Guo, L.; Liu, P. Application of Melanin as Biological Functional Material in Composite Film Field. *Sci. Eng. Compos. Mater.* 2022, 126–139. DOI:10.1515/secm-2022-0013.
- (103) Singh, S.; Nimse, S. B.; Mathew, D. E.; Dhimmar, A.; Sahastrabudhe, H.; Gajjar, A.; Ghadge, V. A.; Kumar, P.; Shinde, P. B. Microbial Melanin: Recent Advances in Biosynthesis, Extraction, Characterization, and Applications. *Biotechnol. Adv.* 2021, 53, 107773. DOI:10.1016/j.biotechadv.2021.107773.
- (104) Xu, C.; Li, J.; Yang, L.; Shi, F.; Yang, L.; Ye, M. Antibacterial Activity and a Membrane Damage Mechanism of *Lachnum* YM30 Melanin against *Vibrio parahaemolyticus* and *Staphylococcus aureus*. *Food Control* 2017, 73, 1445–1451. DOI:10.1016/j.foodcont.2016.10.048.
- (105) Sivaperumal, P.; Kamala, K.; Rajaram, R. Bioactive DOPA Melanin Isolated and Characterised from a Marine Actinobacterium *Streptomyces* Sp. MVCS6 from Versova Coast. *Nat. Prod. Res.* 2015, 29 (22), 2117–2121. DOI:10.1080/14786419.2014.988712.
- (106) El-Naggar, N. E. A.; Saber, W. I. A. Natural Melanin: Current Trends, and Future Approaches, with Especial Reference to Microbial Source. *Polymers.* 2022, 14 (7), 1339. DOI:10.3390/polym14071339.
- (107) Manivasagan, P.; Venkatesan, J.; Senthilkumar, K.; Sivakumar, K.; Kim, S. K. Isolation and Characterization of Biologically Active Melanin from *Actinoalloteichus* sp. MA-32. *Int. J. Biol. Macromol.* 2013, 58, 263–274. DOI:10.1016/j.ijbiomac.2013.04.041.
- (108) Arun, G.; Eyini, M.; Gunasekaran, P. Characterization and Biological Activities of Extracellular Melanin Produced by *Schizophyllum* Commune (Fries). *Indian J. Exp. Biol.* 2015, 53 (6), 380–387.
- (109) El-Bialy, H. A.; El-Gamal, M. S.; Elsayed, M. A.; Saudi, H. A.; Khalifa, M. A. Microbial Melanin Physiology under Stress Conditions and Gamma Radiation Protection Studies. *Radiat. Phys. Chem.* 2019, 162, 178–186. DOI:10.1016/j.radphyschem.2019.05.002.

- (110) Marcovici, I.; Coricovac, D.; Pinzaru, I.; Macasoi, I. G.; Popescu, R.; Chioibas, R.; Zupko, I.; Dehelean, C. A. Melanin and Melanin-Functionalized Nanoparticles as Promising Tools in Cancer Research - A Review. *Cancers*. 2022, 14 (7), 1838. DOI:10.3390/cancers14071838.
- (111) Cuzzubbo, S.; Carpentier, A. F.; Pshezhetskiy, D.; Panyam, J. Applications of Melanin and Melanin-Like Nanoparticles in Cancer Therapy: A Review of Recent Advances. *Cancers*. 2021, 13 (6), 1463. DOI:10.3390/cancers.
- (112) Kurian, N. K.; Nair, H. P.; Bhat, S. G. Evaluation of Anti-Inflammatory Property of Melanin from Marine *Bacillus* spp. Btcz31. *Asian J. Pharm. Clin. Res.* 2015, 8 (3), 251-255.
- (113) Amal, A. M.; Abeer, K. A.; Samia, H. M.; El-Nasser Nadia, A. H. Selection of Pigment (Melanin) Production in *Streptomyces* and Their Application in Printing and Dyeing of Wool Fabrics. *Res. J. Chem. Sci.* 2011, 1 (5), 22-28.
- (114) Liu, Y.; Zhang, Y.; Yu, Z.; Qi, C.; Tang, R.; Zhao, B.; Wang, H.; Han, Y. Microbial Dyes: Dyeing of Poplar Veneer with Melanin Secreted by *Lasiodiplodia theobromae* Isolated from Wood. *Appl. Microbiol. Biotechnol.* 2020, 104 (8), 3367–3377. DOI:10.1007/s00253-020-10478-2.
- (115) Kurian, N. K.; Bhat, S. G. Food, Cosmetic and Biological Applications of Characterized DOPA-Melanin from *Vibrio alginolyticus* Strain BTKKS3. *Appl. Biol. Chem.* 2018, 61 (2), 163–171. DOI:10.1007/s13765-018-0343-y.
- (116) Guo, L.; Li, W.; Gu, Z.; Wang, L.; Guo, L.; Ma, S.; Li, C.; Sun, J.; Han, B.; Chang, J. Recent Advances and Progress on Melanin: From Source to Application. *Int. J. Mol. Sci.* 2023, 24 (5), 4360; DOI:10.3390/ijms24054360.
- (117) Methneni, N.; Morales-González, J. A.; Jaziri, A.; Mansour, H. Ben; Fernandez-Serrano, M. Persistent Organic and Inorganic Pollutants in the Effluents from the Textile Dyeing Industries: Ecotoxicology Appraisal via a Battery of Biotests. *Environ. Res.* 2021, 196, 110956. DOI:10.1016/j.envres.2021.110956.
- (118) Bala, S.; Garg, D.; Thirumalesh, B. V.; Sharma, M.; Sridhar, K.; Inbaraj, B. S.; Tripathi, M. Recent Strategies for Bioremediation of Emerging Pollutants: A Review for a Green and Sustainable Environment. *Toxics*. 2022, 10 (8), 484. DOI:10.3390/toxics10080484.
- (119) Azubuiké, C. C.; Chikere, C. B.; Okpokwasili, G. C. Bioremediation Techniques—Classification Based on Site of Application: Principles, Advantages, Limitations and Prospects. *World J. Microbiol. Biotechnol.* 2016, 32, 180. DOI:10.1007/s11274-016-2137-x.
- (120) Ayilara, M. S.; Babalola, O. O. Bioremediation of Environmental Wastes: The Role of Microorganisms. *Fron. Agron.* 2023, 5, 1183691. DOI:10.3389/fagro.2023.1183691.
- (121) Turick, C. E.; Knox, A. S.; Leverette, C. L.; Kritzas, Y. G. In Situ Uranium Stabilization by Microbial Metabolites. *J. Environ. Radioact.* 2008, 99 (6), 890–899. DOI:10.1016/j.jenvrad.2007.11.020.

- (122) Shatila, M.; Thomas, A. S. Current and Future Perspectives in the Diagnosis and Management of *Helicobacter pylori* Infection. *J. Clin. Med.* 2022, 11 (17), 5086. DOI:10.3390/jcm11175086.
- (123) Guevara, B.; Cogdill, A. G. *Helicobacter pylori*: A Review of Current Diagnostic and Management Strategies. *Dig. Dis. Sci.* 2020, 65 (7), 1917–1931. DOI:10.1007/s10620-020-06193-7.
- (124) Hooi, J. K. Y.; Lai, W. Y.; Ng, W. K.; Suen, M. M. Y.; Underwood, F. E.; Tanyingoh, D.; Malfertheiner, P.; Graham, D. Y.; Wong, V. W. S.; Wu, J. C. Y.; Chan, F. K. L.; Sung, J. J. Y.; Kaplan, G. G.; Ng, S. C. Global Prevalence of *Helicobacter pylori* Infection: Systematic Review and Meta-Analysis. *Gastroenterology*, 2017, 153 (2), 420–429. DOI:1053/j.gastro.2017.04.022.
- (125) Dunne, C.; Dolan, B.; Clyne, M. Factors That Mediate Colonization of the Human Stomach by *Helicobacter pylori*. *World J. Gastroenterol.* 2014, 20 (19), 5610–5624. DOI:10.3748/wjg.v20.i19.5610.
- (126) Pop, R.; Tăbăran, A. F.; Ungur, A. P.; Negoescu, A.; Cătoi, C. *Helicobacter pylori*-Induced Gastric Infections: From Pathogenesis to Novel Therapeutic Approaches Using Silver Nanoparticles. *Pharmaceutics*. 2022, 14 (7), 1463. DOI:10.3390/pharmaceutics14071463.
- (127) Testerman, T. L.; Morris, J. Beyond the Stomach: An Updated View of *Helicobacter pylori* Pathogenesis, Diagnosis, and Treatment. *World J. Gastroenterol.* 2014, 20 (36), 12781–12808. DOI:10.3748/wjg.v20.i36.12781.
- (128) Correa, P.; Piazuelo, M. B. Evolutionary History of the *Helicobacter pylori* Genome: Implications for Gastric Carcinogenesis. *Gut Liver*. 2012, 6 (1), 21–28. DOI:10.5009/gnl.2012.6.1.21.
- (129) Kodaman, N.; Pazos, A.; Schneider, B. G.; Blanca Piazuelo, M.; Mera, R.; Sobota, R. S.; Sicinski, L. A.; Shaffer, C. L.; Romero-Gallo, J.; De Sablet, T.; Harder, R. H.; Bravo, L. E.; Peek, R. M.; Wilson, K. T.; Cover, T. L.; Williams, S. M.; Correa, P. Human and *Helicobacter pylori* Coevolution Shapes the Risk of Gastric Disease. *PNAS*. 2014, 111 (4), 1455–1460. <https://doi.org/10.1073/pnas.1318093111>.
- (130) Ahmed, N. 23 Years of the Discovery of *Helicobacter pylori*: Is the Debate Over? *Ann Clin Microbiol Antimicrob.* 2005; 4, 17. DOI:10.1186/1476-0711-4-17.
- (131) Moss, S. F. The Rediscovery of *H. pylori* Bacteria in the Gastric Mucosa by Robin Warren, and Implications of This Finding for Human Biology and Disease. *Dig. Dis. Sci.* 2013, 58 (11), 3072–3078. DOI:10.1007/s10620-013-2863-y.
- (132) Krzyżek, P.; Gościński, G. Morphology of *Helicobacter pylori* as a Result of Peptidoglycan and Cytoskeleton Rearrangements. *Prz. Gastroenterol.* 2018; 13(3), 182–195. DOI:10.5114/pg.2018.78284.
- (133) Ierardi, E.; Losurdo, G.; Mileti, A.; Paolillo, R.; Giorgio, F.; Principi, M.; Di Leo, A. The Puzzle of Coccoid Forms of *Helicobacter pylori*: Beyond Basic Science. *Antibiotics*. 2020, 9 (6), 293. DOI:10.3390/antibiotics9060293.

- (134) Hirukawa, S.; Sagara, H.; Kaneto, S.; Kondo, T.; Kiga, K.; Sanada, T.; Kiyono, H.; Mimuro, H. Characterization of Morphological Conversion of *Helicobacter pylori* under Anaerobic Conditions. *Microbiol. Immunol.* 2018, 62 (4), 221–228. DOI:10.1111/1348-0421.12582.
- (135) Cover, T. L. Perspectives on Methodology for *in vitro* Culture of *Helicobacter pylori*. *Methods Mol. Biol.* 2012, 921, 11–15. DOI:10.1007/978-1-62703-005-2_3.
- (136) Zullo, A.; De Francesco, V.; Gatta, L. *Helicobacter pylori* Culture: From Bench to Bedside. *Ann. Gastroenterol.* 2022, 35 (3), 243–248. DOI:10.20524/aog.2022.0703.
- (137) Henriksen, T. H.; Brorson, O.; Schøyen, R.; Thoresen, T.; Setegn, D.; Madebo, T. Rapid Growth of *Helicobacter pylori*. *Eur. J. Clin. Microbiol. Infect. Dis.* 1995, 14 (11), 1008–1011. DOI:10.1007/BF01691385.
- (138) Fischer, W.; Breithaupt, U.; Kern, B.; Smith, S. I.; Spicher, C.; Haas, R. A Comprehensive Analysis of *Helicobacter pylori* Plasticity Zones Reveals That They are Integrating Conjugative Elements with Intermediate Integration Specificity. *BMC Genomics.* 2014, 15 (1), 310. DOI:10.1186/1471-2164-15-310.
- (139) Lara-Ramírez, E. E.; Segura-Cabrera, A.; Guo, X.; Yu, G.; García-Pérez, C. A.; Rodríguez-Pérez, M. A. New Implications on Genomic Adaptation Derived from the *Helicobacter pylori* Genome Comparison. *PLoS One.* 2011, 6 (2), 17300. DOI:10.1371/journal.pone.0017300.
- (140) Hessey, S. J.; Spencer, J.; Wyatt, J. I.; Sobala, G.; Rathbone, B. J.; Axon, A. T. R.; Dixon, M. F.; Leeds, L. S. J. H. J. S. J. I.; Sobala, B. W. G.; Rathbone, J.; Axon, A. R. Bacterial Adhesion and Disease Activity in *Helicobacter* Associated Chronic Gastritis. *Gut.* 1990, 31(2), 134–138.
- (141) De Brito, B. B.; Da Silva, F. A. F.; Soares, A. S.; Pereira, V. A.; Cordeiro Santos, M. L.; Sampaio, M. M.; Moreira Neves, P. H.; De Melo, F. F. Pathogenesis and Clinical Management of *Helicobacter pylori* Gastric Infection. *World J. Gastroenterol.* 2019, 25 (37), 5578–5589. DOI:10.3748/wjg.v25.i37.5578.
- (142) Celli, J. P.; Turner, B. S.; Afdhal, N. H.; Keates, S.; Ghiran, I.; Kelly, C. P.; Ewoldt, R. H.; McKinley, G. H.; So, P.; Erramilli, S.; Bansil, R. *Helicobacter pylori* Moves through Mucus by Reducing Mucin Viscoelasticity. *PNAS.* 2009, 106 (34), 14321–14326. DOI:10.1073/pnas.0903438106
- (143) Celli, J. P.; Turner, B. S.; Afdhal, N. H.; Ewoldt, R. H.; McKinley, G. H.; Bansil, R.; Erramilli, S. Rheology of Gastric Mucin Exhibits a PH-Dependent Sol-Gel Transition. *Biomacromolecules.* 2007, 8 (5), 1580–1586. DOI:10.1021/bm0609691.
- (144) Hage, N.; Howard, T.; Phillips, C.; Brassington, C.; Overman, R.; Debreczeni, J.; Gellert, P.; Stolnik, S.; Winkler, G. S.; Falcone, F. H. Structural Basis of Lewis b Antigen Binding by the *Helicobacter pylori* Adhesin BabA. *Sci. Adv.* 2015, 1 (7), 1500315. DOI:10.1126/sciadv.1500315.
- (145) Aspholm, M.; Olfat, F. O.; Nordén, J.; Sondén, B.; Lundberg, C.; Sjöström, R.; Altraja, S.; Odenbreit, S.; Haas, R.; Wadström, T.; Engstrand, L.; Semino-Mora, C.; Liu, H.; Dubois, A.; Teneberg, S.; Arnqvist, A.; Borén, T. SabA Is the *H. pylori* Hemagglutinin and

Is Polymorphic in Binding to Sialylated Glycans. *PLoS Pathog.* 2006, 2 (10), 989–1001. DOI:10.1371/journal.ppat.0020110.

(146) Jones, K. R.; Whitmire, J. M.; Merrell, D. S. A. Tale of Two Toxins: *Helicobacter pylori* CagA and VacA Modulate Host Pathways That Impact Disease. *Front. Microbiol.* 2010, 1, 115. DOI:10.3389/fmicb.2010.00115.

(147) Wang, H.; Zhao, M.; Shi, F.; Zheng, S.; Xiong, L.; Zheng, L. A. Review of Signal Pathway Induced by Virulent Protein CagA of *Helicobacter pylori*. *Front. Cell Infect. Microbiol.* 2023, 13, 1062803. DOI:10.3389/fcimb.2023.1062803.

(148) Hatakeyama, M. Structure and Function of *Helicobacter pylori* Caga, the First-Identified Bacterial Protein Involved in Human Cancer. *Proc. Jpn. Acad. Ser. B Phys. Biol. Sci.* 2017, 93 (4), 196–219. DOI: 10.2183/pjab.93.013.

(149) Keikha, M.; Sahebkar, A.; Yamaoka, Y.; Karbalaeei, M. *Helicobacter pylori* CagA Status and Gastric Mucosa-Associated Lymphoid Tissue Lymphoma: A Systematic Review and Meta-Analysis. *J. Health Popul. Nutr.* 2022, 41 (1), 2. DOI:10.1186/s41043-021-00280-9.

(150) Takahashi-Kanemitsu, A.; Knight, C. T.; Hatakeyama, M. Molecular Anatomy and Pathogenic Actions of *Helicobacter pylori* CagA That Underpin Gastric Carcinogenesis. *Cell. Mol. Immunol.* 2020, 17 (1), 50-63. DOI:10.1038/s41423-019-0339-5.

(151) Stein, M.; Ruggiero, P.; Rappuoli, R.; Bagnoli, F. *Helicobacter pylori* CagA: From Pathogenic Mechanisms to Its Use as an Anti-Cancer Vaccine. *Front. Immunol.* 2013, 4, 328. DOI:10.3389/fimmu.2013.00328.

(152) Trang, T. T. H.; Binh, T. T.; Yamaoka, Y. Relationship between VacA Types and Development of Gastroduodenal Diseases. *Toxins.* 2016, 8 (6), 182. DOI:10.3390/toxins8060182.

(153) Cover, T. L.; Blanke, S. R. *Helicobacter pylori* VacA, a Paradigm for Toxin Multifunctionality. *Nat. Rev. Microbiol.* 2005, 3 (4), 320-332. DOI:10.1038/nrmicro1095.

(154) Palframan, S. L.; Kwok, T.; Gabriel, K. Vacuolating Cytotoxin A (VacA), a Key Toxin for *Helicobacter pylori* Pathogenesis. *Front. Cell. Infect. Microbiol.* 2012, 12 (2), 92. DOI: 10.3389/fcimb.2012.00092.

(155) Foegeding, N. J.; Caston, R. R.; McClain, M. S.; Ohi, M. D.; Cover, T. L. An Overview of *Helicobacter pylori* VacA Toxin Biology. *Toxins.* 2016, 8 (6), 173. DOI:10.3390/toxins8060173.

(156) Salama, N. R.; Hartung, M. L.; Müller, A. Life in the Human Stomach: Persistence Strategies of the Bacterial Pathogen *Helicobacter pylori*. *Nat. Rev. Microbiol.* 2013, 11(6), 385–399. DOI:10.1038/nrmicro3016.

(157) Chmiela, M.; Miszczyk, E.; Rudnicka, K. Structural Modifications of *Helicobacter pylori* Lipopolysaccharide: An Idea for How to Live in Peace. *World J. Gastroenterol.* 2014, 20 (29), 9882–9897. DOI:10.3748/wjg.v20.i29.9882.

(158) Grebowska, A.; Moran, A.P.; Matusiak, A.; Bak-Romaniszyn, L.; Czkwianianc, E.; Rechciński, T.; Walencka, M.; Płaneta-Małecka, I.; Rudnicka, W.; Chmiela, M. Anti-

- Phagocytic Activity of *Helicobacter pylori* Lipopolysaccharide (LPS)-Possible Modulation of the Innate Immune Response to These Bacteria. *Pol. J. Microbiol.* 2008, 57 (3), 185-192.
- (159) Wessler, S.; Backert, S. Molecular Mechanisms of Epithelial-Barrier Disruption by *Helicobacter pylori*. *Trends Microbiol.* 2008, 16 (8), 397-405. DOI:10.1016/j.tim.2008.05.005.
- (160) Miller, S. I.; Ernst, R. K.; Bader, M. W. LPS, TLR4 and Infectious Disease Diversity. *Nat. Rev. Microbiol.* 2005, 3 (1), 36-46. DOI:10.1038/nrmicro1068.
- (161) Kusters, J. G.; Van Vliet, A. H. M.; Kuipers, E. J. Pathogenesis of *Helicobacter pylori* Infection. *Clin. Microbiol. Rev.* 2006, 19 (3), 449–490. DOI:10.1128/CMR.00054-05.
- (162) Handa, O.; Naito, Y.; Yoshikawa, T. Redox Biology and Gastric Carcinogenesis: The Role of *Helicobacter pylori*. *Redox Rep.* 2011, 16 (1), 1-7. DOI:10.1179/174329211X12968219310756.
- (163) Gonciarz, W.; Krupa, A.; Hinc, K.; Obuchowski, M.; Moran, A. P.; Gajewski, A.; Chmiela, M. The Effect of *Helicobacter pylori* Infection and Different *H. pylori* Components on the Proliferation and Apoptosis of Gastric Epithelial Cells and Fibroblasts. *PLoS One.* 2019, 14 (8), 220636. DOI:10.1371/journal.pone.0220636.
- (164) Wang, D.; Guo, Q.; Yuan, Y.; Gong, Y. The Antibiotic Resistance of *Helicobacter pylori* to Five Antibiotics and Influencing Factors in an Area of China with a High Risk of Gastric Cancer. *BMC Microbiol.* 2019, 19 (1), 152. DOI:10.1186/s12866-019-1517-4.
- (165) Krzyżek, P.; Pawełka, D.; Iwańczak, B.; Kempniński, R.; Leśniakowski, K.; Mégraud, F.; Łaczmański, Ł.; Biernat, M.; Gościński, G. High Primary Antibiotic Resistance of *Helicobacter pylori* Strains Isolated from Pediatric and Adult Patients in Poland during 2016–2018. *Antibiotics* 2020, 9 (5), 228. DOI:10.3390/antibiotics9050228.
- (166) Ayala, G.; Escobedo-Hinojosa, W. I.; de La Cruz-Herrera, C. F.; Romero, I. Exploring Alternative Treatments for *Helicobacter pylori* Infection. *World J. Gastroenterol.* 2014, 20 (6), 1450–1469. DOI:10.3748/wjg.v20.i6.1450.
- (167) Sukri, A.; Hanafiah, A.; Patil, S.; Lopes, B. S. The Potential of Alternative Therapies and Vaccine Candidates against *Helicobacter pylori*. *Pharmaceuticals.* 2023, 16 (4), 552. DOI:10.3390/ph16040552.
- (168) Tshibangu-Kabamba, E.; Yamaoka, Y. *Helicobacter pylori* Infection and Antibiotic Resistance — from Biology to Clinical Implications. *Nat. Rev. Gastroenterol. Hepatol.* 2021, 18 (9), 613-629. DOI:10.1038/s41575-021-00449-x.
- (169) Su, N.; Yang, J.; Xie, Y.; Du, X.; Chen, H.; Zhou, H.; Chen, L. Bone Function, Dysfunction and Its Role in Diseases Including Critical Illness. *Int. J. Biol. Sci.* 2019, 15 (4), 776–787. DOI:10.7150/ijbs.27063.
- (170) Han, Y.; You, X.; Xing, W.; Zhang, Z.; Zou, W. Paracrine and Endocrine Actions of Bone - The Functions of Secretory Proteins from Osteoblasts, Osteocytes, and Osteoclasts. *Bone Res.* 2018, 24 (6), 16. DOI:10.1038/s41413-018-0019-6.
- (171) Clarke, B. Normal Bone Anatomy and Physiology. *Clin. J. Am. Soc. Nephrol.* 2008. 3 (3), 131–139. DOI:10.2215/CJN.04151206.

- (172) Bolamperti, S.; Villa, I.; Rubinacci, A. Bone Remodeling: An Operational Process Ensuring Survival and Bone Mechanical Competence. *Bone Res.* 2022, 10, 48. DOI:10.1038/s41413-022-00219-8.
- (173) Capulli, M.; Paone, R.; Rucci, N. Osteoblast and Osteocyte: Games without Frontiers. *Archives of Biochemistry and Biophysics. Arch. Biochem. Biophys.* 2014, 561, 3-12. DOI: 10.1016/j.abb.2014.05.003.
- (174) Schini, M.; Vilaca, T.; Gossiel, F.; Salam, S.; Eastell, R. Bone Turnover Markers: Basic Biology to Clinical Applications. *Endocr. Rev.* 2023, 44 (3), 417-473. DOI:10.1210/endrev/bnac031.
- (175) Blair, H. C.; Larrouture, Q. C.; Li, Y.; Lin, H.; Beer-Stoltz, D.; Liu, L.; Tuan, R. S.; Robinson, L. J.; Schlesinger, P. H.; Nelson, D. J. Osteoblast Differentiation and Bone Matrix Formation *in Vivo* and *in Vitro*. *Tissue Eng. Part. B Rev.* 2017, 23 (3), 268-280. DOI: 10.1089/ten.TEB.2016.0454.
- (176) Langdahl, B.; Ferrari, S.; Dempster, D. W. Bone Modeling and Remodeling: Potential as Therapeutic Targets for the Treatment of Osteoporosis. *Ther. Adv. Musculoskelet. Dis.* 2016, 8 (6), 225-235. DOI:10.1177/1759720X16670154.
- (177) Šromová, V.; Sobola, D.; Kaspar, P. A Brief Review of Bone Cell Function and Importance. *Cells.* 2023, 12 (21), 2576. DOI:10.3390/cells12212576.
- (178) Lin, X.; Patil, S.; Gao, Y. G.; Qian, A. The Bone Extracellular Matrix in Bone Formation and Regeneration. *Front. Pharmacol.* 2020, 11, 757. DOI:10.3389/fphar.2020.00757.
- (179) Florencio-Silva, R.; Sasso, G. R. D. S.; Sasso-Cerri, E.; Simões, M. J.; Cerri, P. S. Biology of Bone Tissue: Structure, Function, and Factors That Influence Bone Cells. *BioMed. Res. Int.* 2015, 421746. DOI:10.1155/2015/421746.
- (180) McDonald, M. M.; Kim, A. S.; Mulholland, B. S.; Rauner, M. New Insights Into Osteoclast Biology. *JBMR Plus.* 2021, 5 (9), 0539. DOI:10.1002/jbm4.10539.
- (181) Long, F. Building Strong Bones: Molecular Regulation of the Osteoblast Lineage. *Nat. Rev. Mol. Cell. Biol.* 2011, 13 (1), 27-38. DOI:10.1038/nrm3254.
- (182) Tsukasaki, M.; Takayanagi, H. Osteoclast Biology in the Single-Cell Era. *Inflamm. Regen.* 2022, 42 (1), 27. DOI:10.1186/s41232-022-00213-x.
- (183) Blumer, M. J. F. Bone Tissue and Histological and Molecular Events during Development of the Long Bones. *Ann. Anat.* 2021, 235, 151704. DOI:10.1016/j.aanat.2021.151704
- (184) Berendsen, A. D.; Olsen, B. R. Bone Development. *Bone.* 2015, 80, 14–18. DOI:10.1016/j.bone.2015.04.035.
- (185) Dimitriou, R.; Jones, E.; McGonagle, D.; Giannoudis, P. V. Bone Regeneration: Current Concepts and Future Directions. *BMC Medicine.* 2011, 9, 66. DOI:10.1186/1741-7015-9-66.

- (186) Wu, A. M.; Bisignano, C.; James, S. L.; Abady, G. G.; Abedi, A.; Abu-Gharbieh, E.; Alhassan, R. K.; Alipour, V.; Arabloo, J.; Asaad, M.; Asmare, W. N.; Awedew, A. F.; Banach, M.; Banerjee, S. K.; Bijani, A.; Birhanu, T. T. M.; Bolla, S. R.; Cámera, L. A.; Chang, J. C.; Cho, D. Y.; Chung, M. T.; Couto, R. A. S.; Dai, X.; Dandona, L.; Dandona, R.; Farzadfar, F.; Filip, I.; Fischer, F.; Fomenkov, A. A.; Gill, T. K.; Gupta, B.; Haagsma, J. A.; Haj-Mirzaian, A.; Hamidi, S.; Hay, S. I.; Ilic, I. M.; Ilic, M. D.; Ivers, R. Q.; Jürisson, M.; Kalhor, R.; Kanchan, T.; Kavetsky, T.; Khalilov, R.; Khan, E. A.; Khan, M.; Kneib, C. J.; Krishnamoorthy, V.; Kumar, G. A.; Kumar, N.; Laloo, R.; Lasrado, S.; Lim, S. S.; Liu, Z.; Manafi, A.; Manafi, N.; Menezes, R. G.; Meretoja, T. J.; Miazgowski, B.; Miller, T. R.; Mohammad, Y.; Mohammadian-Hafshejani, A.; Mokdad, A. H.; Murray, C. J. L.; Naderi, M.; Naimzada, M. D.; Nayak, V. C.; Nguyen, C. T.; Nikbakhsh, R.; Olagunju, A. T.; Otstavnov, N.; Otstavnov, S. S.; Padubidri, J. R.; Pereira, J.; Pham, H. Q.; Pinheiro, M.; Polinder, S.; Pourchamani, H.; Rabiee, N.; Radfar, A.; Rahman, M. H. U.; Rawaf, D. L.; Rawaf, S.; Saeb, M. R.; Samy, A. M.; Sanchez Riera, L.; Schwebel, D. C.; Shahabi, S.; Shaikh, M. A.; Soheili, A.; Tabarés-Seisdedos, R.; Tovani-Palone, M. R.; Tran, B. X.; Travillian, R. S.; Valdez, P. R.; Vasankari, T. J.; Velazquez, D. Z.; Venketasubramanian, N.; Vu, G. T.; Zhang, Z. J.; Vos, T. Global, Regional, and National Burden of Bone Fractures in 204 Countries and Territories, 1990–2019: A Systematic Analysis from the Global Burden of Disease Study 2019. *Lancet Healthy Longev.* 2021, 2 (9), 580–592. DOI:10.1016/S2666-7568(21)00172-0.
- (187) Szwed-Georgiou, A.; Płociński, P.; Kupikowska-Stobba, B.; Urbaniak, M. M.; Rusek-Wala, P.; Szustakiewicz, K.; Piszko, P.; Krupa, A.; Biernat, M.; Gazińska, M.; Kasprzak, M.; Nawrotek, K.; Mira, N. P.; Rudnicka, K. Bioactive Materials for Bone Regeneration: Biomolecules and Delivery Systems. *ACS Biomater. Sci. Eng.* 2023, 9 (9), 5222–5254. DOI:10.1021/acsbomaterials.3c00609.
- (188) Kemmak, A. R.; Rezapour, A.; Jahangiri, R.; Nikjoo, S.; Farabi, H.; Soleimanpour, S. Economic Burden of Osteoporosis in the World: A Systematic Review. *Med. J. Islam. Repub. Iran.* 2020, 12 (34), 154. DOI:10.34171/mjiri.34.154.
- (189) Weycker, D.; Li, X.; Barron, R.; Bornheimer, R.; Chandler, D. Hospitalizations for Osteoporosis-Related Fractures: Economic Costs and Clinical Outcomes. *Bone Rep.* 2016, 5, 186–191. DOI:10.1016/j.bonr.2016.07.005.
- (190) Kazimierczak, P.; Przekora, A. Osteoconductive and Osteoinductive Surface Modifications of Biomaterials for Bone Regeneration: A Concise Review. *Coatings.* 2020, 10 (10), 971. DOI:10.3390/coatings10100971.
- (191) Taylor, A. M.; Hsueh, M. F.; Ranganath, L. R.; Gallagher, J. A.; Dillon, J. P.; Huebner, J. L.; Catterall, J. B.; Kraus, V. B. Cartilage Biomarkers in the Osteoarthropathy of Alkaptonuria Reveal Low Turnover and Accelerated Ageing. *Rheumatology.* 2017, 56 (1), 156–164. DOI:10.1093/rheumatology/kew355.
- (192) Davison, A. S.; Hughes, A. T.; Milan, A. M.; Sireau, N.; Gallagher, J. A.; Ranganath, L. R. Alkaptonuria – Many Questions Answered, Further Challenges Beckon. *Ann. Clin. Biochem.* 2020, 57 (2), 106-120. DOI:10.1177/0004563219879957.
- (193) Chow, Y.; Norman, B. P.; Roberts, N. B.; Ranganath, L. R.; Teutloff, C.; Bittl, R.; Duer, M. J.; Gallagher, J. A.; Oschkinat, H. Fibrous Proteins Hot Paper Pigmentation

Chemistry and Radical-Based Collagen Degradation in Alkaptonuria and Osteoarthritic Cartilage. *Angew. Chem. Int. Ed. Engl.* 2020, 59 (29), 11937–11942. DOI:10.26434/chemrxiv.11590950.

(194) Roberts, N. B.; Curtis, S. A.; Milan, A. M.; Ranganath, L. R. The Pigment in Alkaptonuria Relationship to Melanin and Other Coloured Substances: A Review of Metabolism, Composition and Chemical Analysis. *JIMD Rep.* 2015, 24, 51-66. DOI: 10.1007/8904_2015_453.

(195) Abdel-Razek, A. S.; El-Naggar, M. E.; Allam, A.; Morsy, O. M.; Othman, S. I. Microbial Natural Products in Drug Discovery. *Processes.* 2020, 8 (4), 470. DOI:10.3390/PR8040470.

(196) Atanasov, A. G.; Zotchev, S. B.; Dirsch, V. M.; Orhan, I. E.; Banach, M.; Rollinger, J. M.; Barreca, D.; Weckwerth, W.; Bauer, R.; Bayer, E. A.; Majeed, M.; Bishayee, A.; Bochkov, V.; Bonn, G. K.; Braidy, N.; Bucar, F.; Cifuentes, A.; D'Onofrio, G.; Bodkin, M.; Diederich, M.; Dinkova-Kostova, A. T.; Efferth, T.; El Bairi, K.; Arkells, N.; Fan, T. P.; Fiebich, B. L.; Freissmuth, M.; Georgiev, M. I.; Gibbons, S.; Godfrey, K. M.; Gruber, C. W.; Heer, J.; Huber, L. A.; Ibanez, E.; Kijjoo, A.; Kiss, A. K.; Lu, A.; Macias, F. A.; Miller, M. J. S.; Mocan, A.; Müller, R.; Nicoletti, F.; Perry, G.; Pittalà, V.; Rastrelli, L.; Ristow, M.; Russo, G. L.; Silva, A. S.; Schuster, D.; Sheridan, H.; Skalicka-Woźniak, K.; Skaltsounis, L.; Sobarzo-Sánchez, E.; Brecht, D. S.; Stuppner, H.; Sureda, A.; Tzvetkov, N. T.; Vacca, R. A.; Aggarwal, B. B.; Battino, M.; Giampieri, F.; Wink, M.; Wolfender, J. L.; Xiao, J.; Yeung, A. W. K.; Lizard, G.; Popp, M. A.; Heinrich, M.; Berindan-Neagoe, I.; Stadler, M.; Daglia, M.; Verpoorte, R.; Supuran, C. T. Natural Products in Drug Discovery: Advances and Opportunities. *Nat. Rev. Drug. Discov.* 2021, 20 (3), 200-216. DOI:10.1038/s41573-020-00114-z.

(197) Demain, A. L.; Sanchez, S. Microbial Drug Discovery: 80 Years of Progress. *J. Antibiot.* 2009, 62 (1), 5-16. DOI:10.1038/ja.2008.16.

(198) Oh, J. J.; Kim, J. Y.; Son, S. H.; Jung, W. J.; Kim, D. H.; Seo, J. W.; Kim, G. H. Fungal Melanin as a Biocompatible Broad-Spectrum Sunscreen with High Antioxidant Activity. *RSC Adv.* 2021, 11 (32), 19682–19689. DOI:10.1039/d1ra02583j.

(199) Lorquin, F.; Ziarelli, F.; Amouric, A.; Di Giorgio, C.; Robin, M.; Piccerelle, P.; Lorquin, J. Production and Properties of Non-Cytotoxic Pyomelanin by Laccase and Comparison to Bacterial and Synthetic Pigments. *Sci. Rep.* 2021, 11 (1), 8538. DOI:10.1038/s41598-021-87328-2.

(200) Eskandari, S.; Etemadifar, Z. Biocompatibility and Radioprotection by Newly Characterized Melanin Pigment and Its Production from *Dietzia Schimae* NM3 in Optimized Whey Medium by Response Surface Methodology. *Ann. Microbiol.* 2021, 71 (1). DOI:10.1186/s13213-021-01628-6.

(201) Ferraz, A. R.; Pacheco, R.; Vaz, P. D.; Pintado, C. S.; Ascensão, L.; Serralheiro, M. L. Melanin: Production from Cheese Bacteria, Chemical Characterization, and Biological Activities. *Int. J. Environ. Res. Public Health* 2021, 18 (20), 10562. DOI:10.3390/ijerph182010562.

- (202) Ogle, M. E.; Segar, C. E.; Sridhar, S.; Botchwey, E. A. Monocytes and Macrophages in Tissue Repair: Implications for Immunoregenerative Biomaterial Design. *Exp. Biol. Med.* 2016, 241 (10), 1084-1097. DOI:10.1177/1535370216650293.
- (203) Oishi, Y.; Manabe, I. Macrophages in Inflammation, Repair and Regeneration. *Int. Immunol.* 2018, 30 (11), 511–528. DOI:10.1093/intimm/dxy054.
- (204) Lin, T. H.; Pajarinen, J.; Lu, L.; Nabeshima, A.; Cordova, L. A.; Yao, Z.; Goodman, S. B. NF-KB as a Therapeutic Target in Inflammatory-Associated Bone Diseases. *Adv. Protein Chem. Struct. Biol.* 2017, 107, 117-154. DOI:10.1016/bs.apcsb.2016.11.002.
- (205) Myat, M. M.; Louis, D.; Mavrommatis, A.; Collins, L.; Mattis, J.; Ledru, M.; Vergheze, S.; Su, T. T. Regulators of Cell Movement during Development and Regeneration in *Drosophila*. *Open Biol.* 2019, 9 (5), 180245. DOI:10.1098/rsob.180245.
- (206) Friedl, P.; Gilmour, D. Collective Cell Migration in Morphogenesis, Regeneration and Cancer. *Nat. Rev. Mol. Cell Biol.* 2009, 10 (7), 445-457. DOI:10.1038/nrm2720.
- (207) Mnich, E.; Kowalewicz-Kulbat, M.; Sicinska, P.; Hinc, K.; Obuchowski, M.; Gajewski, A.; Moran, A. P.; Chmiela, M. Impact of *Helicobacter pylori* on the Healing Process of the Gastric Barrier. *World. J. Gastroenterol.* 2016, 22 (33), 7536–7558. DOI:10.3748/wjg.v22.i33.7536.
- (208) Gajewski, A.; Gawrysiak, M.; Krupa, A.; Rechciński, T.; Chałubiński, M.; Gonciarz, W.; Chmiela, M. Accumulation of Deleterious Effects in Gastric Epithelial Cells and Vascular Endothelial Cells In Vitro in the Milieu of *Helicobacter pylori* Components, 7-Ketocholesterol and Acetylsalicylic Acid. *Int. J. Mol. Sci.* 2022, 23 (11), 6355. DOI:10.3390/ijms23116355.
- (209) Chmiela, M.; Kupcinkas, J. Review: Pathogenesis of *Helicobacter pylori* Infection. *Helicobacter.* 2019, 24 (S1). DOI:10.1111/hel.12638.
- (210) Thomas, M. V.; Puleo, D. A. Infection, Inflammation, and Bone Regeneration: A Paradoxical Relationship. *J. Dent. Res.* 2011, 90 (9), 1052-1061. DOI: 10.1177/0022034510393967.
- (211) Birt, M. C.; Anderson, D. W.; Bruce Toby, E.; Wang, J. Osteomyelitis: Recent Advances in Pathophysiology and Therapeutic Strategies. *J. Orthop.* 2017, 14 (1), 45–52. DOI:10.1016/j.jor.2016.10.004.
- (212) Vasanthabharathi, V.; Lakshminarayanan, R.; Jayalakshmi, S. Melanin Production from Marine *Streptomyces*. *Afr. J. Biotechnol.* 2011, 10 (54), 11224–11234. DOI:10.5897/ajb11.296.
- (213) Zerrad, A.; Anissi, J.; Ghanam, J.; Sendide, K.; El Hassouni, M. Antioxidant and Antimicrobial Activities of Melanin Produced by *Pseudomonas balearica* Strain. *J. Biot. Lett.* 2014, 5 (1), 87-94.
- (214) Xu, C.; Li, J.; Yang, L.; Shi, F.; Yang, L.; Ye, M. Antibacterial Activity and a Membrane Damage Mechanism of Lachnum YM30 Melanin against *Vibrio parahaemolyticus* and *Staphylococcus aureus*. *Food Control.* 2017, 73, 1445–1451. DOI:10.1016/j.foodcont.2016.10.048.

- (215) Jilka, R.; Weinstein, R.; Bellido, T.; Roberson, P.; Parfitt, A.; Manolagas, S. Increased Bone Formation by Prevention of Osteoblast Apoptosis with Parathyroid Hormone. *J. Clin. Invest.* 1999, 104 (4), 439-446. DOI:10.1172/JCI6610.
- (216) Amarasekara, D. S.; Kim, S.; Rho, J. Regulation of Osteoblast Differentiation by Cytokine Networks. *Int. J. Mol. Sci.* 2021, 22 (6), 2851. DOI:10.3390/ijms22062851.
- (217) Xu, J.; Yu, L.; Liu, F.; Wan, L.; Deng, Z. The Effect of Cytokines on Osteoblasts and Osteoclasts in Bone Remodeling in Osteoporosis: A Review. *Front. Immunol.* 2023, 5 (14), 1222129. DOI:10.3389/fimmu.2023.1222129.
- (218) Zoch, M. L.; Clemens, T. L.; Riddle, R. C. New Insights into the Biology of Osteocalcin. *Bone.* 2016, 82, 42–49. DOI:10.1016/j.bone.2015.05.046.
- (219) Jilka, R. L.; Weinstein, R. S.; Bellido, T.; Parfitt, A. M.; Manolagas, S. C. Osteoblast Programmed Cell Death (Apoptosis): Modulation by Growth Factors and Cytokines. *J. Bone Miner. Res.* 1998, 13 (5), 793-802. DOI:10.1359/jbmr.1998.13.5.793.
- (220) Blanchard, F.; Duplomb, L.; Baudhuin, M.; Brounais, B. The Dual Role of IL-6-Type Cytokines on Bone Remodeling and Bone Tumors. *Cytokine Growth Factor Rev.* 2009, 20 (1), 19-28. DOI:10.1016/j.cytogfr.2008.11.004.
- (221) Itoh, S.; Udagawa, N.; Takahashi, N.; Yoshitake, F.; Narita, H.; Ebisu, S.; Ishihara, K. A Critical Role for Interleukin-6 Family-Mediated Stat3 Activation in Osteoblast Differentiation and Bone Formation. *Bone.* 2006, 39 (3), 505–512. DOI:10.1016/j.bone.2006.02.074.
- (222) Yoshitake, F.; Itoh, S.; Narita, H.; Ishihara, K.; Ebisu, S. Interleukin-6 Directly Inhibits Osteoclast Differentiation by Suppressing Receptor Activator of NF- κ B Signaling Pathways. *J. Biol. Chem.* 2008, 283 (17), 11535–11540. DOI:10.1074/jbc.M607999200.
- (223) Chen, E.; Liu, G.; Zhou, X.; Zhang, W.; Wang, C.; Hu, D.; Xue, D.; Pan, Z. Concentration-Dependent, Dual Roles of IL-10 in the Osteogenesis of Human BMSCs via P38/MAPK and NF- κ B Signaling Pathways. *FASEB.* 2018, 32 (9), 4917–4929. DOI:10.1096/fj.201701256RRR.
- (224) Liu, D.; Yao, S.; Wise, G. E. Effect of Interleukin-10 on Gene Expression of Osteoclastogenic Regulatory Molecules in the Rat Dental Follicle. *Eur. J. Oral. Sci.* 2006, 114 (1), 42-49. DOI:10.1111/j.1600-0722.2006.00283.x.
- (225) Xin, L. X.; Kukita, T.; Kukita, A.; Otsuka, T.; Niho, Yosh.; Iijima, T. Interleukin-10 Selectively Inhibits Osteoclastogenesis by Inhibiting Differentiation of Osteoclast Progenitors into Preosteoclast-Like Cells in Rat Bone Marrow Culture System. *J. Cell Physiol.* 1995, 165 (3), 624-629. DOI:10.1002/jcp.1041650321.
- (226) Kobayashi, K.; Takahashi, N.; Jimi, E.; Udagawa, N.; Takami, M.; Kotake, S.; Nakagawa, N.; Kinoshita, M.; Yamaguchi, K.; Shima, N.; Yasuda, H.; Morinaga, T.; Higashio, K.; Martin, T. J.; Suda, T. Tumor Necrosis Factor Stimulates Osteoclast Differentiation by a Mechanism Independent of the ODF/RANKL-RANK Interaction. *J. Exp. Med.* 2000, 191 (2), 275-286. DOI:10.1084/jem.191.2.275.

- (227) Yang, N.; Liu, Y. The Role of the Immune Microenvironment in Bone Regeneration. *Int. J. Med. Sci.* 2021, 18 (16), 3697-3707. DOI:10.7150/ijms.61080.
- (228) Osta, B.; Benedetti, G.; Miossec, P. Classical and Paradoxical Effects of TNF- α on Bone Homeostasis. *Front. Immunol.* 2014, 13 (5), 48. DOI:10.3389/fimmu.2014.00048.
- (229) Kitaura, H.; Marahleh, A.; Ohori, F.; Noguchi, T.; Nara, Y.; Pramusita, A.; Kinjo, R.; Ma, J.; Kanou, K.; Mizoguchi, I. Role of the Interaction of Tumor Necrosis Factor- α and Tumor Necrosis Factor Receptors 1 and 2 in Bone-Related Cells. *Int. J. Mol. Sci.* 2022, 23 (3), 1481. DOI:10.3390/ijms23031481.
- (230) Walencka, M.; Gonciarz, W.; Mnich, E.; Gajewski, A.; Stawerski, P.; Knapik-Dabrowicz, A.; Chmiela, M. The Microbiological, Histological, Immunological and Molecular Determinants of *Helicobacter pylori* Infection in Guinea Pigs as a Convenient Animal Model to Study Pathogenicity of These Bacteria and the Infection Dependent Immune Response of the Host. *Acta Biochim. Pol.* 2015, 62 (4), 697–706. DOI:10.18388/abp.2015_1110.

**Oświadczenia
współautorów o udziale
w publikacjach**

Łódź, dn. 23 marca 2024 r.

Mgr Mateusz M. Urbaniak

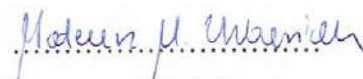
Katedra Immunologii i Biologii Infekcyjnej
Wydział Biologii i Ochrony Środowiska
Uniwersytet Łódzki
Banacha 12/16, 90-237 Łódź

OŚWIADCZENIE

1. Oświadczam, że w pracy:

Urbaniak M. M., Gazińska M., Rudnicka K., Płociński P., Nowak M., Chmiela M. *In Vitro and In Vivo* Biocompatibility of Natural and Synthetic *Pseudomonas aeruginosa* Pyomelanin for Potential Biomedical Applications. 2023. *International Journal of Molecular Sciences*, 2023, 24, 7846. DOI: 10.3390/ijms24097846

mój udział polegał na: opracowaniu koncepcji pracy i układów doświadczalnych, opracowaniu podłoży Pyomelanin Minimal Medium (PMM) do hodowli *Pseudomonas aeruginosa* i metod otrzymania piomelaniny rozpuszczalnej (PyoM_{sol}), nierozpuszczalnej w wodzie (PyoM_{insol}) oraz syntetycznej (sPyoM), izolacji i oczyszczeniu bakteryjnych PyoM, przeprowadzeniu oceny cytotoksyczności PyoM na modelu fibroblastów L929 i monocytów THP-1, toksyczności *in vivo* na modelu *Galleria mellonella* oraz aktywacji szlaku NF-κB na modelu monocytów THP-1 NF-κB Blue, interpretacji uzyskanych danych, przygotowaniu analizy statystycznej, abstraktu graficznego i wizualizacji uzyskanych wyników (tab.1, ryc. 4-7), przygotowaniu manuskryptu i redakcji treści odpowiedzi na recenzje.

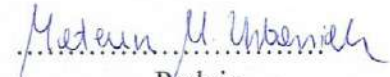

Podpis

2. Oświadczam, że w pracy:

Urbaniak M. M., Rudnicka K., Gościński G., Chmiela M. Can Pyomelanin Produced by *Pseudomonas aeruginosa* Promote the Regeneration of Gastric Epithelial Cells and Enhance *Helicobacter pylori* Phagocytosis? 2023. *International Journal of Molecular Sciences*, 24, 13911. DOI: 10.3390/ijms241813911

Oświadczenie współautora o udziale w publikacji

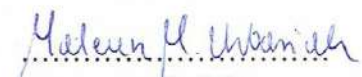
mój udział polegał na: opracowaniu koncepcji pracy i układów doświadczalnych, pozyskaniu finansowania (Inkubator Innowacyjności+), izolacji i oczyszczeniu bakteryjnych PyoM, przeprowadzeniu analizy żywotności bakterii *Helicobacter pylori* w środowisku PyoM, wykonaniu obliczeń minimalnego stężenia hamującego MIC₅₀ i MIC₉₉, ocenie żywotności i apoptozy fibroblastów L929, monocytów THP-1 i komórek nabłonka żołądka AGS traktowanych PyoM lub PyoM i lipopolisacharydami (LPS) bakteryjnymi, ocenie wydzielania reaktywnych form tlenu i migracji komórek nabłonka żołądka AGS stymulowanych PyoM lub PyoM i LPS, wykonaniu testów oceniających pochłanianie referencyjnych pałeczek *E. coli* pHrodo™ lub żywych znakowanych fluorescencyjnie *H. pylori* na modelu monocytów THP-1, interpretacji uzyskanych danych, przygotowaniu analizy statystycznej, abstraktu graficznego i wizualizacji uzyskanych wyników (ryc. 1-7), przygotowaniu manuskryptu i redakcji treści odpowiedzi na recenzje, a także pełnieniu roli autora korespondującego (wspólnie z prof. dr hab. Magdaleną Mikołajczyk-Chmielą).


Podpis

3. Oświadczam, że w pracy:

Urbaniak M. M., Rudnicka K., Płociński P., Chmiela M. Exploring the Osteoinductive Potential of Bacterial Pyomelanin Derived from *Pseudomonas aeruginosa* on Human Osteoblasts Model. 2024. International Journal of Biological Macromolecules – manuskrypt w recenzji

mój udział polegał na: opracowaniu koncepcji pracy i układów doświadczalnych, izolacji i oczyszczeniu bakteryjnych PyoM, ocenie żywotności i apoptozy osteoblastów hFOB 1.19 traktowanych PyoM lub PyoM i doksorobicyną, wykonaniu testu migracji osteoblastów hFOB 1.19 stymulowanych PyoM, ocenie aktywności markerów kostnienia (fosfatazy alkalicznej, interleukiny (IL)-6, IL-10, osteokalcyny, czynnika martwicy guza- α oraz liczby żywych osteoblastów hFOB 1.19 w długoterminowych hodowlach osteoindukcyjnych traktowanych PyoM, przeprowadzeniu analizy żywotności bakterii *Staphylococcus* sp. izolowanych z zakażonej tkanki kostnej w środowisku PyoM, wykonaniu obliczeń minimalnego stężenia hamującego MIC₅₀, interpretacji uzyskanych danych, przygotowaniu analizy statystycznej, abstraktu graficznego i wizualizacji uzyskanych wyników (ryc. 1,2, 4-6), przygotowaniu manuskryptu, a także pełnieniu roli autora korespondującego (wspólnie z prof. dr hab. Magdaleną Mikołajczyk-Chmielą).

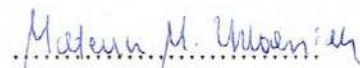

Podpis

Oświadczenie współautora o udziale w publikacji

4. Oświadczam, że w pracy:

Szwed-Georgiou A., Płociński P., Kupikowska-Stobba B., **Urbaniak M. M.**, Rusek-Wala P., Szustakiewicz K., Piszko P., Krupa A., Biernat M., Gazińska M., Kasprzak M., Nawrotek K., Mira N. P., Rudnicka K. 2023. Bioactive Materials for Bone Regeneration: Biomolecules and Delivery Systems. ACS Biomaterials Science & Engineering, 2023, 9, 5222–5254. DOI: 10.1021/acsbomaterials.3c00609

mój udział polegał na: przeprowadzeniu przeglądu literatury naukowej, napisaniu podrozdziału *Microbial Biopolymers*, przygotowaniu abstraktu graficznego i rycin (1 i 3), korekcie językowej i redakcyjnym przygotowaniu manuskryptu.


.....
Podpis

Łódź, dn. 25 marca 2024 r.

Prof. dr hab. Magdalena Mikołajczyk-Chmiela

Katedra Immunologii i Biologii Infekcyjnej
Wydział Biologii i Ochrony Środowiska
Uniwersytet Łódzki
Banacha 12/16, 90-237 Łódź

OŚWIADCZENIE

1. Oświadczam, że w pracy:

Urbaniak M. M., Gazińska M., Rudnicka K., Płociński P., Nowak M., **Chmiela M.** *In Vitro* and *In Vivo* Biocompatibility of Natural and Synthetic *Pseudomonas aeruginosa* Pyomelanin for Potential Biomedical Applications. 2023. *International Journal of Molecular Sciences*, 2023, 24, 7846. DOI: 10.3390/ijms24097846

mój udział polegał na: współudziale w tworzeniu koncepcji pracy, nadzorze nad realizacją badań, oceną postępów pracy i uczestnictwie w przygotowaniu manuskryptu.



Podpis

2. Oświadczam, że w pracy:

Urbaniak M. M., Rudnicka K., Gościński G., **Chmiela M.** Can Pyomelanin Produced by *Pseudomonas aeruginosa* Promote the Regeneration of Gastric Epithelial Cells and Enhance *Helicobacter pylori* Phagocytosis? 2023. *International Journal of Molecular Sciences*, 24, 13911. DOI: 10.3390/ijms241813911

mój udział polegał na: współudziale w tworzeniu koncepcji pracy, nadzorze nad realizacją badań, oceną postępów pracy i uczestnictwie w przygotowaniu manuskryptu.



Podpis

3. Oświadczam, że w pracy:

Urbaniak M. M., Rudnicka K., Płociński P., **Chmiela M.** Exploring the Osteoinductive Potential of Bacterial Pyomelanin Derived from *Pseudomonas aeruginosa* on Human Osteoblasts Model. 2024. International Journal of Biological Macromolecules – manuskrypt w recenzji

mój udział polegał na: współudziale w tworzeniu koncepcji pracy, nadzorze nad realizacją badań, oceną postępów pracy i uczestnictwie w przygotowaniu manuskryptu.

A handwritten signature in blue ink, appearing to read 'M. Chmiela', written over a dotted line.

Podpis

Oświadczenie współautora o udziale w publikacji

Łódź, dn. 23 marca 2024 r.

dr Karolina Rudnicka, prof. UŁ

Katedra Immunologii i Biologii Infekcyjnej
Wydział Biologii i Ochrony Środowiska
Uniwersytet Łódzki
Banacha 12/16, 90-237 Łódź

OŚWIADCZENIE

1. Oświadczam, że w pracy:

Urbaniak M. M., Gazińska M., **Rudnicka K.**, Płociński P., Nowak M., Chmiela M. *In Vitro* and *In Vivo* Biocompatibility of Natural and Synthetic *Pseudomonas aeruginosa* Pyomelanin for Potential Biomedical Applications. 2023. *International Journal of Molecular Sciences*, 2023, 24, 7846. DOI: 10.3390/ijms24097846

mój wkład polegał na: udziale w opracowaniu koncepcji pracy i przygotowaniu manuskryptu, pozyskaniu finansowania na badania eksperymentalne, monitorowaniu postępów pracy.



.....
Podpis

2. Oświadczam, że w pracy:

Urbaniak M. M., **Rudnicka K.**, Gościński G., Chmiela M. Can Pyomelanin Produced by *Pseudomonas aeruginosa* Promote the Regeneration of Gastric Epithelial Cells and Enhance *Helicobacter pylori* Phagocytosis? 2023. *International Journal of Molecular Sciences*, 24, 13911. DOI: 10.3390/ijms241813911

mój wkład polegał na: udziale w opracowaniu koncepcji pracy i przygotowaniu manuskryptu, pozyskaniu finansowania na badania eksperymentalne, monitorowaniu postępów pracy.



.....
Podpis

Oświadczenie współautora o udziale w publikacji

3. Oświadczam, że w pracy:

Urbaniak M. M., **Rudnicka K.**, Płociński P., Chmiela M. Exploring the Osteoinductive Potential of Bacterial Pyomelanin Derived from *Pseudomonas aeruginosa* on Human Osteoblasts Model. 2024. International Journal of Biological Macromolecules – manuskrypt w recenzji

mój wkład polegał na: udziale w opracowaniu koncepcji pracy i przygotowaniu manuskryptu, pozyskaniu finansowania na badania eksperymentalne, monitorowaniu postępów pracy.



.....
Podpis

4. Oświadczam, że w pracy:

Szwed-Georgiou A., Płociński P., Kupikowska-Stobba B., Urbaniak M. M., Rusek-Wala P., Szustakiewicz K., Piszko P., Krupa A., Biernat M., Gazińska M., Kasprzak M., Nawrotek K., Mira N. P., **Rudnicka K.** 2023. Bioactive Materials for Bone Regeneration: Biomolecules and Delivery Systems. ACS Biomaterials Science & Engineering, 2023, 9, 5222–5254. DOI: 10.1021/acsbmaterials.3c00609

mój wkład polegał na: opracowaniu koncepcji pracy, pozyskaniu finansowania, monitorowaniu postępów w przygotowaniu manuskryptu, przygotowaniu wstępnej recenzji manuskryptu, opracowaniu strategii publikacyjnej i prowadzeniu korespondencji z recenzentami.



.....
Podpis

Łódź, dn. 21 marca 2024 r.

Dr Przemysław Płociński


Katedra Immunologii i Biologii Infekcyjnej
Wydział Biologii i Ochrony Środowiska
Uniwersytet Łódzki
Banacha 12/16, 90-237 Łódź

OŚWIADCZENIE

1. Oświadczam, że w pracy:

Urbaniak M. M., Gazińska M., Rudnicka K., **Płociński P.**, Nowak M., Chmiela M. *In Vitro* and *In Vivo* Biocompatibility of Natural and Synthetic *Pseudomonas aeruginosa* Pyomelanin for Potential Biomedical Applications. 2023. *International Journal of Molecular Sciences*, 2023, 24, 7846. DOI: 10.3390/ijms24097846

mój udział polegał na: współdziałanie w tworzeniu koncepcji pracy, współdziałanie w analizie wyników i uczestnictwie w przygotowaniu manuskryptu.



.....

Podpis

2. Oświadczam, że w pracy:

Urbaniak M. M., Rudnicka K., **Płociński P.**, Chmiela M. Exploring the Osteoinductive Potential of Bacterial Pyomelanin Derived from *Pseudomonas aeruginosa* on Human Osteoblasts Model. 2024. *International Journal of Biological Macromolecules* – manuskrypt w recenzji

mój udział polegał na: współdziałanie w tworzeniu koncepcji pracy, przeprowadzeniu izolacji RNA i analiz transkryptomycznych, opracowaniu graficznym i statystycznym wyników transkryptomycznych (ryc. 3) i uczestnictwie w przygotowaniu manuskryptu.


.....

Podpis

3. Oświadczam, że w pracy:

Szwed-Georgiou A., **Płociński P.**, Kupikowska-Stobba B., Urbaniak M. M., Rusek-Wala P., Szustakiewicz K., Piszko P., Krupa A., Biernat M., Gazińska M., Kasprzak M., Nawrotek K., Mira N. P., Rudnicka K. 2023. Bioactive Materials for Bone Regeneration: Biomolecules and Delivery Systems. ACS Biomaterials Science & Engineering, 2023, 9, 5222–5254. DOI: 10.1021/acsbomaterials.3c00609

mój udział polegał na: współudziale w tworzeniu koncepcji pracy i uczestnictwo w przygotowaniu i edycji manuskryptu



.....
Podpis

Wrocław, dn. 26 marca 2024 r.

Dr inż. Małgorzata Gazińska

Katedra Inżynierii i Technologii Polimerów
Wydział Chemiczny
Politechnika Wrocławska
Smoluchowskiego 25, 50-372 Wrocław

OŚWIADCZENIE

1. Oświadczam, że w pracy:

Urbaniak M. M., **Gazińska M.**, Rudnicka K., Płociński P., Nowak M., Chmiela M. *In Vitro and In Vivo* Biocompatibility of Natural and Synthetic *Pseudomonas aeruginosa* Pyomelanin for Potential Biomedical Applications. 2023. *International Journal of Molecular Sciences*, 2023, 24, 7846. DOI: 10.3390/ijms24097846

mój wkład w przygotowanie powyższej publikacji polegał na: charakterystyce chemicznej piomelaniny (PyoM_{sol}, PyoM_{insol}, sPyoM) metodami FT-IR, TGA i DSC, opracowaniu uzyskanych wyników pod względem technicznym i graficznym oraz opisanu części wynikowej dotyczącej powyższego zakresu prac (ryc. 1-3, tab. 2) i udziale w przygotowaniu manuskryptu.



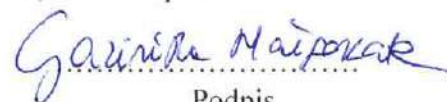
Podpis

2. Oświadczam, że w pracy:

Szwed-Georgiou A., Płociński P., Kupikowska-Stobba B., Urbaniak M. M., Rusek-Wala P., Szustakiewicz K., Piszko P., Krupa A., Biernat M., **Gazińska M.**, Kasprzak M., Nawrotek K., Mira N. P., Rudnicka K. 2023. Bioactive Materials for Bone Regeneration: Biomolecules and Delivery Systems. *ACS Biomaterials Science & Engineering*, 2023, 9, 5222–5254. DOI: 10.1021/acsbmaterials.3c00609

mój udział polegał na:

weryfikacji poprawności tekstu w sekcji Polymers, Inorganic Fillers, and Composites.



Podpis

Łódź, dn. 29 marca 2024 r.

Dr Monika Nowak

Katedra Immunologii i Biologii Infekcyjnej
Wydział Biologii i Ochrony Środowiska
Uniwersytet Łódzki
Banacha 12/16, 90-237 Łódź

OŚWIADCZENIE

Oświadczam, że w pracy:

Urbaniak M. M., Gazińska M., Rudnicka K., Płociński P., **Nowak M.**, Chmiela M. *In Vitro* and *In Vivo* Biocompatibility of Natural and Synthetic *Pseudomonas aeruginosa* Pyomelanin for Potential Biomedical Applications. 2023. *International Journal of Molecular Sciences*, 2023, 24, 7846. DOI: 10.3390/ijms24097846

mój udział polegał na: charakterystyce PyoM_{sol}, PyoM_{insol}, sPyoM metodą FT-IR.

Potwierdzam zgodność

KIEROWNIK

Katedry Immunologii i Biologii Infekcyjnej UŁ

M. P. Chmiela
prof. dr hab. Magdalena Mikolajczyk-Chmiela

.....
Podpis Promotora

M. Urbaniak
.....
Podpis Doktoranta

Oświadczenie współautora o udziale w publikacji

Wrocław, dn. 25 marca 2024 r.

Prof. dr hab. Grażyna Gościńskiak

Katedra i Zakład Mikrobiologii

Wydział Lekarski

Uniwersytet Medyczny im. Piastów Śląskich we Wrocławiu

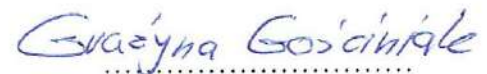
Chałubińskiego 4, 50-368 Wrocław

OŚWIADCZENIE

Oświadczam, że w pracy:

Urbaniak M. M., Rudnicka K., **Gościńskiak G.**, Chmiela M. Can Pyomelanin Produced by *Pseudomonas aeruginosa* Promote the Regeneration of Gastric Epithelial Cells and Enhance *Helicobacter pylori* Phagocytosis? 2023. International Journal of Molecular Sciences, 24, 13911. DOI: 10.3390/ijms241813911

mój udział polegał na: izolacji, charakterystyce i udostępnieniu klinicznych szczepów *Helicobacter pylori* M91 i M102.



.....
Podpis

Łódź, dn. 26 marca 2024 r.


Dr Aleksandra Szwed-Georgiou
Katedra Immunologii i Biologii Infekcyjnej
Wydział Biologii i Ochrony Środowiska
Uniwersytet Łódzki
Banacha 12/16, 90-237 Łódź

OŚWIADCZENIE

Oświadczam, że w pracy:

Szwed-Georgiou A., Płociński P., Kupikowska-Stobba B., Urbaniak M. M., Rusek-Wala P., Szustakiewicz K., Piszko P., Krupa A., Biernat M., Gazińska M., Kasprzak M., Nawrotek K., Mira N. P., Rudnicka K. 2023. Bioactive Materials for Bone Regeneration: Biomolecules and Delivery Systems. ACS Biomaterials Science & Engineering, 2023, 9, 5222–5254. DOI: 10.1021/acsbomaterials.3c00609

mój udział polegał na konceptualizacji, wyszukiwaniu literatury, przygotowaniu oraz napisaniu oryginalnego projektu manuskryptu oraz jego redagowaniu.



.....
Podpis

Warszawa, dn. 22 marca 2024 r.

Dr inż. Barbara Kupikowska – Stobba
Zakład Biosystemów i Miękkiej Materii
Instytut Podstawowych Problemów Techniki PAN
Pawińskiego 5B, 02-106 Warszawa

OŚWIADCZENIE

Oświadczam, że w pracy:

Szwed-Georgiou A., Płociński P., **Kupikowska-Stobba B.**, Urbaniak M. M., Rusek-Wala P., Szustakiewicz K., Piszko P., Krupa A., Biernat M., Gazińska M., Kasprzak M., Nawrotek K., Mira N. P., Rudnicka K. 2023. Bioactive Materials for Bone Regeneration: Biomolecules and Delivery Systems. ACS Biomaterials Science & Engineering, 2023, 9, 5222–5254. DOI: 10.1021/acsbmaterials.3c00609

mój udział polegał na: współtworzeniu koncepcji pracy, przeprowadzeniu przeglądu literatury naukowo-badawczej, pisaniu manuskryptu, przygotowaniu rycin, nanoszeniu poprawek i edycji pracy.


.....
Podpis

Łódź, dn. 20 marca 2024 r.

Mgr Paulina Rusek-Wala
Katedra Immunologii i Biologii Infekcyjnej
Wydział Biologii i Ochrony Środowiska
Uniwersytet Łódzki
Banacha 12/16, 90-237 Łódź

OŚWIADCZENIE

Oświadczam, że w pracy:

Szwed-Georgiou A., Płociński P., Kupikowska-Stobba B., Urbaniak M. M., **Rusek-Wala P.**, Szustakiewicz K., Piszko P., Krupa A., Biernat M., Gazińska M., Kasprzak M., Nawrotek K., Mira N. P., Rudnicka K. 2023. Bioactive Materials for Bone Regeneration: Biomolecules and Delivery Systems. ACS Biomaterials Science & Engineering, 2023, 9, 5222–5254. DOI: 10.1021/acsbmaterials.3c00609

mój udział polegał na: napisaniu podrozdziałów Plant sterols, Oxysterols, Liposomes oraz Statins; przygotowaniu ryciny 2 i redakcyjnym przygotowaniu manuskryptu.



Podpis

Łódź, dn. 23 marca 2024 r.

Dr hab. Agnieszka Krupa, prof. UŁ
Katedra Immunologii i Biologii Infekcyjnej
Wydział Biologii i Ochrony Środowiska
Uniwersytet Łódzki
Banacha 12/16, 90-237 Łódź

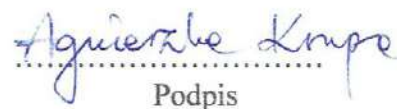
OŚWIADCZENIE

Oświadczam, że w pracy:

Szwed-Georgiou A., Płociński P., Kupikowska-Stobba B., Urbaniak M. M., Rusek-Wala P., Szustakiewicz K., Piszko P., **Krupa A.**, Biernat M., Gazińska M., Kasprzak M., Nawrotek K., Mira N. P., Rudnicka K. 2023. Bioactive Materials for Bone Regeneration: Biomolecules and Delivery Systems. ACS Biomaterials Science & Engineering, 2023, 9, 5222–5254. DOI: 10.1021/acsbomaterials.3c00609

mój udział polegał na:

redagowaniu rozdziału „Biomolecules used for bone regeneration” / Peptides / Amino Acids


.....
Podpis

Warszawa, dn. 22 marca 2024 r.

Dr inż. Monika Biernat

Grupa Badawcza Biomateriały

Łukasiewicz - Instytut Ceramiki i Materiałów Budowlanych

Cementowa 8, 31-983 Kraków

OŚWIADCZENIE

Oświadczam, że w pracy:

Szwed-Georgiou A., Płociński P., Kupikowska-Stobba B., Urbaniak M. M., Rusek-Wala P., Szustakiewicz K., Piszko P., Krupa A., **Biernat M.**, Gazińska M., Kasprzak M., Nawrotek K., Mira N. P., Rudnicka K. 2023. Bioactive Materials for Bone Regeneration: Biomolecules and Delivery Systems. ACS Biomaterials Science & Engineering, 2023, 9, 5222–5254. DOI: 10.1021/acsbomaterials.3c00609

mój udział polegał na: nadzorze procesu pisania, odpowiedzi na recenzje treści manuskryptu związanych z dostarczaniem substancji aktywnych do regeneracji tkanki kostnej.



Podpis

Warszawa, dn. 22 marca 2024 r.

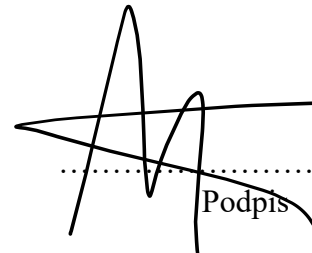
Dr inż. Mirosław Kasprzak
Katedra Przetwórstwa Produktów Zwierzęcych
Wydział Technologii Żywności
Uniwersytet Rolniczy im. Hugona Kołłątaja
Ul. Balicka 122, 30-149 Kraków

OŚWIADCZENIE

Oświadczam, że w pracy:

Szwed-Georgiou A., Płociński P., Kupikowska-Stobba B., Urbaniak M. M., Rusek-Wala P., Szustakiewicz K., Piszko P., Krupa A., Biernat M., Gazińska M., **Kasprzak M.**, Nawrotek K., Mira N. P., Rudnicka K. 2023. Bioactive Materials for Bone Regeneration: Biomolecules and Delivery Systems. ACS Biomaterials Science & Engineering, 2023, 9, 5222–5254. DOI: 10.1021/acsbomaterials.3c00609

mój udział polegał na: częściowym opracowaniu metod dostarczenia substancji aktywnych podczas regeneracji kości - do pierwszej wersji manuskryptu.



Podpis

Wrocław, dn. 26 marca 2024 r.

Dr hab. inż. Konrad Szustakiewicz, prof. PWr
Katedra Inżynierii i Technologii Polimerów
Wydział Chemiczny
Politechnika Wrocławska
Wybrzeże Wyspiańskiego 42, 50-370 Wrocław

OŚWIADCZENIE

Oświadczam, że w pracy:

Szwed-Georgiou A., Płociński P., Kupikowska-Stobba B., Urbaniak M. M., Rusek-Wala P., **Szustakiewicz K.**, Piszko P., Krupa A., Biernat M., Gazińska M., Kasprzak M., Nawrotek K., Mira N. P., Rudnicka K. 2023. Bioactive Materials for Bone Regeneration: Biomolecules and Delivery Systems. ACS Biomaterials Science & Engineering, 2023, 9, 5222–5254. DOI: 10.1021/acsbomaterials.3c00609

mój udział polegał na: przygotowaniu przeglądu literatury i opisaniu części technik wytwarzania rusztowań polimerowych w rozdziale „Pathways to Obtain BTE Composite Scaffolds”. W publikacji brałem również udział w tworzeniu koncepcji w/w rozdziału oraz w korekcie językowej.



Podpis

Wrocław, dn. 22 marca 2024 r.

Dr Paweł Piszko

Katedra Inżynierii i Technologii Polimerów

Wydział Chemiczny

Politechnika Wrocławska

Wybrzeże Wyspiańskiego 42, 50-370 Wrocław

OŚWIADCZENIE

Oświadczam, że w pracy:

Szwed-Georgiou A., Płociński P., Kupikowska-Stobba B., Urbaniak M. M., Rusek-Wala P., Szustakiewicz K., **Piszko P.**, Krupa A., Biernat M., Gazińska M., Kasprzak M., Nawrotek K., Mira N. P., Rudnicka K. 2023. Bioactive Materials for Bone Regeneration: Biomolecules and Delivery Systems. ACS Biomaterials Science & Engineering, 2023, 9, 5222–5254. DOI: 10.1021/acsbomaterials.3c00609

mój udział polegał na:

- Przeglądzie literatury związanej ze stanem wiedzy o biomateriałach polimerowych i kompozytowych wykorzystywanych w inżynierii tkanki kostnej, z uwzględnieniem technik ich wytwarzania
- Redakcji oraz weryfikacji merytorycznej podrozdziałów publikacji dotyczących wytwarzania biomateriałów oraz *scaffoldów* do zastosowania w inżynierii tkanki kostnej
- Zestawieniu oraz opisie technik wytwarzania biomateriałów do zastosowania w inżynierii tkankowej kości



.....
Podpis